

**Universität
Rostock**



Traditio et Innovatio

**Agrobiotechnology and Risk Assessment of Bio- and Gene Technology
Faculty of Agriculture and Environmental Science**

**Establishing the greenhouse-production of FGF21-Transferrin in
tobacco seeds and leaves for oral treatment of non-alcoholic
steatosis hepatis NASH**

Dissertation

submitted for the Degree of

Doctor of Agricultural Science (doctor agriculturæ, Dr. agr.)

Faculty of Agriculture and Environmental Science

University of Rostock

Submitted by

Hsuan-Wu Hou, M.Sc.

Rostock, 2024

Reviewer:

Dr. Henrik Nausch

Fraunhofer-Institut für Molekularbiologie und Angewandte Ökologie IME,
Abt. Bioprozessentwicklung

em. Prof. Dr. Inge Broer

Universität Rostock, AUF, Agrobiotechnologie

Prof. Dr. Susanne Klaus

Deutsches Institut für Ernährungsforschung Potsdam-Rehbrücke (DIfE),
Abt. Physiologie des Energiestoffwechsels

Dr. Rima Menassa

University of Western Ontario,
Biology Department / London Research and Development Centre,
Agriculture and Agri-Food Canada

Year of Submission: 2023

Year of Disputation: 2024

**Universität
Rostock**



Traditio et Innovatio

**Professur für Agrobiotechnologie und Begleitforschung zur Bio-und Gentechnologie
Der Agrar- und Umweltwissenschaftlichen Fakultät**

**Etablierung der Gewächshausproduktion von FGF21-Transferrin
in Tabaksamen und -blättern zur oralen Behandlung der
nichtalkoholische Steatohepatitis NASH**

Dissertation

zur Erlangung des akademischen Grades

Doktor der Agrarwissenschaften (doctor agriculturae, (Dr. agr.))

an der Agrar und Umweltwissenschaftlichen Fakultät

der Universität Rostock.

Vorgelegt von

Hsuan-Wu Hou, M.Sc.

Rostock, 2024

Gutachter:

Dr. Henrik Nausch

Fraunhofer-Institut für Molekularbiologie und Angewandte Ökologie IME,
Abt. Bioprozessentwicklung

em. Prof. Dr. Inge Broer

Universität Rostock, AUF, Agrobiotechnologie

Prof. Dr. Susanne Klaus

Deutsches Institut für Ernährungsforschung Potsdam-Rehbrücke (DIfE),
Abt. Physiologie des Energiestoffwechsels

Dr. Rima Menassa

University of Western Ontario,
Biology Department / London Research and Development Centre,
Agriculture and Agri-Food Canada

Jahr der Einreichung: 2023

Jahr der Verteidigung: 2024

Personal Acknowledgements

The thesis was completed in a blink of an eye. I am very grateful to those who encouraged me, cared about me, and helped me. They made my study in Germany the most precious and unforgettable time.

Frau Yueh-Hoh Chou Liu, I want to thank fate for allowing me to meet you and for allowing me to become a student in your German class. It was you who started my path to study in Germany.

Prof. Ching-Chuan Liu, I want to thank you for allowing me to meet Prof. Henning Bombeck from the University of Rostock in Taiwan. It is you who connected me with Germany.

Prof. Henning Bombeck, thank you for your internal recommendation that Inge gave me the opportunity to interview and further gave me the opportunity to visit her laboratory.

Inge, I want to thank you for giving me the opportunity to prove myself during my two months in Germany and for being willing to accept me from Taiwan. Thank you for your initial commitment to my PhD position. After waiting for three years in Taiwan, I finally returned to Germany to start my PhD studies.

Henrik, I am particularly grateful for the care and help you have given me in both research and life. You are a very scientifically talented person who is willing to share his experience selflessly. I have learned a lot from you. I am honored to be your doctoral student and friend.

Sonja and Kerstin, I want to thank you for giving me so much warmth. With your company, I am not alone in Germany! I like talking and laughing with you, and being around you makes me feel at ease.

Finally, I want to thank my family, because of your understanding and support, I was able to pursue my PhD without any worries.

“God helps those who help themselves”

For some things, you don't persist because you see hope;
it's because you persist that you see hope.

This work was funded by the German Research Federation DFG and was done both at the University of Rostock in Rostock and Fraunhofer Institute for Molecular Biology and Applied Ecology IME in Aachen. Also, this work was carried out in collaboration with the Department of Physiology of Energy Metabolism at the German Institute for Human Nutrition in Potsdam-Rehbrücke.

Content

Personal Acknowledgements	5
Abbreviations	11
Summary (Englisch).....	17
Summary (German).....	19
I. Introduction.....	22
I.1. A quarter of the world population suffer from liver diseases	22
I.2. <i>In vivo</i> studies indicated that FGF21 might be a drug candidate to cure liver diseases.	22
I.2.1. FGF21 signaling relies on its C-terminus and the β -Klotho co-receptor KLB to establish high-affinity binding to the FGF receptor FGF1c	23
I.2.2. FGF21 mediates the glucose and lipid metabolism under starvation	26
I.2.3. FGF21 shows dual glucose-and lipid-lowering effects but also reduced the bone mass in pre-clinical trials.....	27
I.2.4. Long-acting FGF21 analogues alleviated hepatic steatosis but also caused bone mass loss in clinical trial	28
I.3. Transferrin and furin cleavage site can be used to target orally administrated FGF21 to the liver.....	32
I.3.1. N-terminal domain of transferrin is essential for binding to the transferrin receptor and its transport from the intestine to the blood stream	33
I.3.2. Fusion of proteins to transferrin enables transfer from the small intestine to the portal vein but prolongs serum half-life in pre-clinical trials.....	35
I.3.3. Furin cleavage site can be used to separate FGF21 and transferrin after transfer from the small intestine to the portal vein.....	36
I.3.4. A fusion protein of FGF21-Transferrin and furin cleavage site can be used to target the liver by oral delivery	37
I.4. <i>In planta</i> encapsulation enables oral delivery of recombinant proteins through the stomach to the small intestine	38
I.4.1. Leaves can be used for oral delivery but are affected by proteolytic degradation of the target protein after harvest.....	39
I.4.2. Seeds can be used oral delivery and typically do not display a proteolytic degradation of the target protein	40
I.4.3. The <i>N. tabacum</i> cultivar SL632 might be used for seed-based oral delivery due its high yield of nicotine-free seeds	41

I.5. Recombinant proteins can be directly produced in plants	42
I.5.1. Recombinant proteins can be expressed in plants by either stable or transient transformation	43
I.5.1.1. Stable transformation expression system can produce recombinant proteins in leaves and seeds but is time-consuming.....	44
I.5.1.2. Transient expression system can rapidly produce recombinant proteins in leaves but requires downstream purification.....	49
I.5.2. Downstream processing of protein drug from plant tissue requires extraction, clarification/filtration and purification but might not be necessary for seed-produced protein drugs.....	52
I.6. Aim of the thesis	54
I.6.1. Optimization tobacco seed yield in contained greenhouses	54
I.6.2. Stable FGF21-F-Tf expression in seeds of <i>N. tabacum</i> SL632	54
I.6.3. Transient FGF21-F-Tf expression in leaves of <i>N. benthamiana</i>	54
I.6.4. Purification of nTf338-FGF21-PLUS for proof-of-concept bioavailability and bioactivity studies.....	55
II. Materials and Methods	58
II.1. Preface	58
II.2. Materials	58
II.3. Methods	67
II.3.1. Plant expression vectors	67
II.3.2. <i>Agrobacterium tumefaciens</i> culture.....	68
II.3.3. Plant <i>in vitro</i> tissue culture	69
II.3.4. Stable transformation.....	69
II.3.5. Segregation analysis	70
II.3.6. Plant cultivation in the greenhouse.....	70
II.3.7. Transient transformation.....	70
II.3.8. Protein extraction.....	70
II.3.9. Turbidity measurement.....	71
II.3.10. Protein purification using immobilized metal ion affinity chromatography	71
II.3.11. Protein quantification	71
II.3.12. TCA protein precipitation.....	72
II.3.14. Coomassie-staining.....	72
II.3.15. Western blot analysis.....	72

II.3.16. Densitometric analysis.....	73
II.3.17. FGF21 ELISA.....	73
II.3.18. 3D Structure analysis.....	73
II.3.19. DoE model building.....	73
II.3.20. Statistical analysis.....	73
III. Results	76
III.1. Optimization tobacco seed yield in contained greenhouses	107
III.1.1. Seed-rich cultivar SL632 was selected for seed production in the greenhouse .	107
III.1.2. Greenhouse cultivation strategies for tobacco focus on leaf production	109
III.1.3. For tobacco seed production, a nitrogen-rich fertilizer is optimal	113
III.1.4. Seed production can be increased in principle via topping and cutting	115
III.1.4.1. Seed yield of 1× top SL632 was ~4-fold higher compared to 1× top VG but inflorescences grew into the lights and leaves could not be harvested in parallel	115
III.1.4.2. Cutting can be used to limit the plant height.....	117
III.1.5. The cost for seed production were 11- to 36-fold higher compared to the leaf production, but this might be compensated by the fact that no processing of seeds is required for oral delivery.....	124
III.2. Stable FGF21-Transferrin expression in seeds of <i>N. tabacum</i> SL632	127
III.2.1. An FGF21-F-Tf fusion protein with a molecular mass of 100 kDa was designed with no steric hindrance between the fusion partners	127
III.2.2. <i>In vitro</i> plant tissue culture of SL632 is limited by rapid flowering	128
III.2.3. Stable transformation efficacy of FGF21-F-Tf in SL632 was similar to VG	129
III.2.4. FGF21-F-Tf accumulation in stably transformed SL632 and VG	130
III.2.4.1. Intact FGF21-F-Tf accumulation in seeds achieved to 6.7 mg kg ⁻¹ SDM..	131
III.2.4.2. Transgenic FGF21-F-Tf transformants were events with multiple integrations but showed normal seed viability (multi-copy-events).....	137
III.2.4.3. FGF21-F-Tf degradation was less in leaves than in seeds and degradation occurred during plant production	138
III.2.4.4. FGF21-F-Tf degradation occurs <i>in planta</i> and not during extraction.....	139
III.3. Transient FGF21-F-Tf expression in leaves of <i>N. benthamiana</i>	141
III.3.1. Transient expression of FGF21-F-Tf using magnICON vector system.....	141
III.3.2. Transient expression of FGF21-F-Tf using pTRAc vector system.....	144
III.3.3. Optimization of FGF21-F-Tf to improve accumulation and stability	147

III.3.3.1. FGF21 fused to full-length Tf without furin cleavage site reduced the amount of degradation products.....	147
III.3.3.2. FGF21 fused to the C-terminal domain of nTf338 without furin cleavage site had substantial impact	149
III.4. Purification of nTf338-FGF21-PLUS for proof-of-concept bioavailability and bioactivity studies.....	152
III.4.1. nTf338-FGF21-PLUS was stable in crude extract for 6 h at 20 °C	152
III.4.2. Large-scale purification of nTf338-FGF21-PLUS was impacted by substantial loss during depth filtrations.....	157
IV. Discussion	164
IV.1. Optimization tobacco seed yield in contained greenhouses yielded a competitive production platform.....	164
IV.2. Stable FGF21-Transferrin expression in seeds of <i>N. tabacum</i> SL632 was impacted by the instability of the fusion protein.....	166
IV.3. Protein engineering of FGF21-Transferrin via transient expression in leaves of <i>N. benthamiana</i> produced a stabilized FGF21-Transferrin variant nTf338-FGF21-PLUS that can be used for stable expression in seeds	170
IV.4. A purification method for nTf338-FGF21-PLUS was established that enabled pre-clinical proof-of-concept bioavailability and bioactivity studies	173
V. Conclusion.....	176
VI. References	180
Acknowledgements	209
Declaration of independence / Eidesstattliche Erklärung	210
Curriculum Vitae.....	211
List of publications in scientific journals and presentations at conferences	213

Abbreviations

(m v ⁻¹)	mass per volume
AA	amino acid
ADA	anti-drug antibody
AEX	anion exchange
AFLD	alcoholic fatty liver disease
AKT	protein kinase B (PKB)
ALP	alkaline phosphatase
ALT	alanine aminotransaminase
ANOVA	analysis of variance
AP	alkaline phosphatase
AST	aspartate aminotransaminase
<i>A. tumefaciens</i>	<i>Agrobacterium tumefaciens</i> (renamed to <i>R. radiobacter</i>)
BAT	brown adipose tissue
BCIP	5-bromo-4-chloro-3-indolyl-phosphate
BMI	body mass index
BHK	baby hamster kidney cells
BMS	BMS-986036, Pegbelfermin
BSA	bovine serum albumin
C	weeks post seeding of cutting
cv	cultivar
CaMV	cauliflower mosaic virus
CAPEX	capital investment
CEX	cation exchange
CHO	chinese hamster ovary cells
CNS	central nervous system
CREB	cAMP response element-binding protein
cr-TMV/TVCV	crucifer-infecting tobamovirus/ turnip vein-clearing virus
CPMV	cowpea mosaic virus
CTX	C-terminal telopeptide
CTB	cholera toxin β subunit
CTB-F-FIX	cholera toxin β subunit-furin cleavage site-coagulation factor IX
CTB-Pins	cholera toxin B subunit-human proinsulin
CSP	circumsporozoite protein
db/db mice	diabetic mice
DE	diatomaceous earth
DK linker	enterokinase cleavable linker, DDDDK
DMF	N, N-dimethylformamide
DMSO	dimethyl sulfoxide
DNA	deoxyribonucleic acid
DoE	design of experiments
dps	days post seeding
dpi	days post infiltration
DSP	downstream processing

E. coli *Escherichia coli*
 ECM extracellular matrix
 ECD extracellular domain
 EDTA ethylenediaminetetraacetic acid
 EK linker rigid linker, (LEA(EAAAK)₄AEAE(EAAAK)₄AE
 ELISA enzyme-linked immunosorbent assay
 ER endoplasmatic reticulum (bio-)
 ERK1/2 extracellular signal-regulated kinase 1 and 2
 Ex-4-Tf extendin-4-transferrin
 Extra extraction buffer

F weeks post seeding of flowering
 F site furin protease cleavage site
 Fab fragment antigen-binding
 FAP fibroblast activation protein
 Fc fragment crystallizable domain of human IgG1
 FDA food and drug administration
 FGFs fibroblast growth factors
 FGF21 fibroblast growth factor 21
 FGFR FGF receptor
 FGFR1c FGF receptor 1c
 FGF21-Fc Fc fused the C-terminus of FGF21
 Fc-FGF21 Fc was fused to the N-terminus of FGF21
 FGF21-Tc FGF21 transgenic
 FGF21-KO FGF21 knockout
 FGF21-Tf FGF21-transferrin
 FGF21-F-Tf FGF21-transferrin with furin cleavage site
 FIX coagulation factor IX
 FIX-Tf coagulation factor IX-Tf
 FM fresh mass
 Furin furin protease

G-CSF-Tf granulocyte colony-stimulating factor-transferrin
 GLP-1 glucagon-like peptide-1
 GOI gene of interest
 GRAS generally recognized as safe
 GS linker flexible linker, (GGGGS)₃

h hour(s)
 H weeks post seeding of harvest
 2xHis double-His₆ tag
 HCC hepatocellular carcinoma
 HCP host cell protein
 HDL-C high density lipoprotein-cholesterol
 HEK293 human embryonic kidney 293 cells
 HepG2 hepatoblastoma cell line
 HFD mice high-fat diet mice
 HFHC high-fat/high-carbohydrate
 hGH human growth hormone
 HS heparan sulfate

IEX	ion exchange
Ig	immunoglobulin
IgA	immunoglobulin A
IgE	immunoglobulin E
IgG	immunoglobulin G
IgG1	immunoglobulin G1
IME	Fraunhofer IME
IMAC	immobilized metal affinity chromatography
INS-Tf	insulin-Tf
IntN and IntC	DnaB intein fragments
IV	intravenous injection
K	potassium
KDEL	sequence for protein retention in the ER
KLA	α -Klotho
KLB	β -Klotho
Km	kanamycin
LB	lysogeny broth
LDL-C	low density lipoprotein-cholesterol
LDS	lithium dodecyl sulfate
LDS-PAGE	lithium dodecyl sulfate polyacrylamide gel electrophoresis
LE linker	dipeptide linker, LE
LFM	leaf fresh mass
LDM	leaf dry mass
LST	Linsmaier and Skoog medium for tobacco
LY	LY2405319
MAPK	mitogen-activated protein kinase pathway
MES	2-(N-morpholino)-ethanesulfonic acid
min	minute(s)
MS	Murashige & Skoog
MWCO	molecular weight cut-off
N	nitrogen
na	not applicable
NAFLD	non-alcoholic fatty liver disease
NASH	non-alcoholic steatohepatitis
<i>N. benthamiana</i>	<i>Nicotiana benthamiana</i>
NBT	nitro blue tetrazolium
NHP	non-human-primate
NIC	near-isogenic control
nm	nano meter
<i>nptII</i>	neomycin phosphotransferase II selectable marker gene
NPK	nitrogen, phosphorus and potassium
<i>N. tabacum</i>	<i>Nicotiana tabacum</i>
nTf338	N-terminal domain of mature Tf protein, position 1-338
NTU	nephelometric turbidity units
ob/ob mice	obese mice
OD	optical density

OPEX	operating expenses
P.....	phosphorus
P(tray).....	weeks post seeding of of plant growing tray
P(pot2).....	weeks post seeding of 5-L pot
p19.....	viral suppressor of RNA silencing
p35S.....	CaMV 35S promoter with duplicated transcriptional enhancer
pA35S.....	CaMV 35S polyadenylation signal
PAM	peptone agrobacterium medium
PBS.....	phosphate buffered saline
PCR	polymerase chain reaction
pCon	β -conglycinin α -subunit promoter
PD.....	protein drug
PD linker	non-helical polypeptide linker, (PEAPTD) ₂
Petunia	<i>Petunia parodii</i>
pEAQ.....	plasmid easy and quick
PEG	polyethylene glycol
PEGylated.....	polyethylene glycol-modified
pEx-4-Tf.....	purified Ex-4-TF
PF	PF-05231023
pGlo1	<i>Avena sativa</i> Globulin 1 promoter
pGt1	<i>Oryza sativa</i> seed storage protein glutelin 1 promoter
PI3K	phosphoinositide 3-kinase
PKB	protein kinase B (AKT)
PLC γ	phospholipase C γ
PLUS	liver-targeting peptide CSP, position 82-100
pLeb4.....	<i>Vicia faba</i> Legumin B4 promotor of the 11S globulin
PMP.....	plant-made (bio-)pharmaceutical
PMF	plant molecular farming
P1NP.....	procollagen type 1 N-terminal pro-peptide
PPAR α	peroxisome proliferator-activated receptor alpha
PPAR γ	peroxisome proliferator-activated receptor gamma
pPhas	<i>Phaseolus vulgaris</i> promoter of the 7S globulin
pPsbA	chloroplast psbA promoter
ProINS.....	proinsulin
ProINS-Tf.....	proinsulin-transferrin
PRO-C3	pro-peptide of type III collagen
pRbcS-3C	leaf specific tomato Rubisco small subunit promoter
pUbi.....	<i>Zea mays</i> upquitin 1 promoter
pUSP.....	<i>Vicia faba</i> unknown seed protein promoter
PVX.....	potato virus X
PVX-CP.....	PVX subgenomic viral coat protein promoter
PVX-SgPr.....	PVX subgenomic promoter
PVX-Sgt	PVX subgenomic terminator
RdRP	RNA-dependent RNA polymerase
RNA	ribonucleic acid
RT.....	room temperature
rpm	round per minute
<i>R. radiobacter</i>	<i>Rhizobium radiobacter</i> (formerly named as <i>A. tumefaciens</i>)

s	second(s)
S(pot1)	weeks post seeding of 2.2-L pot or 1.7-L pot
S(TCP)	weeks post seeding of tissue culture MS plate
SAR	scaffold attachment region of the tobacco Rb7 gene
SC	subcutaneous injection
SD	standard deviation
SDM	seed dry mass
SDS	sodium dodecyl sulfate
SEKDEL	ER-retention signal
SgPr	subgenomic promoter
Sgt	subgenomic terminator
SL	<i>N. tabacum</i> cv. SL632
SL632	<i>N. tabacum</i> cv. SL632
SM	seed mass
SP	signal peptide
STAT	signal transducer and activator of transcription
STAT 3	signal transducer and activator of transcription 3
STAT 5	signal transducer and activator of transcription 5
T	weeks post seeding of topping
t7-t5	T7-T5 terminators
t35S	CaMV 35S terminator
tArc	<i>Phaseolus vulgaris</i> terminator of the arcelin 5-I seed storage
tCon	β -conglycinin α -subunit terminator
TBSV	tomato bushy stunt virus
TCA	trichloroacetic acid
TCP	tissue culture MS plate
T2D	type 2 diabetes
T-DNA	transfer DNA
Tf	transferrin
TfR	transferrin receptor
TfR1	transferrin receptor 1
TG	triglyceride
Ti	tumor inducing
TMV	tobacco mosaic virus
TMV-SgPr	TMV subgenomic promoter
TMV-Sgt	TMV subgenomic terminator
tNos	<i>Agrobacterium tumefaciens</i> nopaline synthase terminator
tPhas	<i>Phaseolus vulgaris</i> terminator of the 7S globulin
tPinII	<i>Solanum tuberosum</i> potato proteinase inhibitor II terminator
tPsbA	chloroplast psbA terminator
TSP	total soluble protein
TVCV	turnip vein-clearing virus
UR	University of Rostock
USP	upstream processing
5' UTR	5' untranslated region
(v m ⁻¹)	volume per mass
VG	<i>N. tabacum</i> cv. VG
vir	virulence

VTEC verocytotoxic-producing *E. coli*

WAT white adipose tissue

WB Western blot

wps weeks post seeding

WT wild-type

YEB yeast extract broth

ZDF rat zucker diabetic fatty rat

Summary (Englisch)

The non-alcoholic steatohepatitis (NASH) is a prevalent disease in the developed countries with no effective medication available. The human fibroblast growth factor (FGF21) can reverse the liver dysfunction in pre-clinical trials, but it has a negative impact on other organs and thus requires exclusive delivery to the liver. Since oral administration allows direct targeting of the liver and since edible seeds can be used for oral administration, the production of FGF21 in seeds of commercial *Nicotiana tabacum* (*N. tabacum*) cultivars in the greenhouse have been established and compared to the conventional production in leaves in a greenhouse setting.

The seed production was maximized by repeated cutting and the subsequent induction of side branches, leading to a yield of $380 \text{ g m}^{-2} \text{ a}^{-1}$ and calculated manufacturing costs of 1.64 € g^{-1} compared to $11,170 \text{ g m}^{-2} \text{ a}^{-1}$ and 0.14 € g^{-1} for leaves.

For stable transformation, FGF21 was fused to transferrin (Tf) via a furin cleavage site (F), promoting the uptake from the intestine to the blood. The fusion protein accumulated with 9.1 mg kg^{-1} seed dry mass (SDM) and 6.2 mg kg^{-1} leave fresh mass (LFM) in the transgenic plants, whereby the accumulation seemed to be limited by *in planta* cleavage, which was more pronounced in seeds compared to leaves with 26-67 % and 8-41 % cleavage fragments, which might be the reason why the accumulation in leaves was in the similar range as in seeds.

To stabilize the fusion protein and to increase the accumulation level, the fusion protein was optimized via transient transformation in *Nicotiana benthamiana* (*N. benthamiana*). Removal of the furin site and introducing of the PLUS peptide reduced the amount of degradation fragments and doubled the accumulation level, while truncation of Tf (nTf338) and reversing the order of FGF21 and Tf in the fusion protein further decreased the degradation products down to 7-9 %, but had no substantial impact on the accumulation level. Nevertheless, might the optimized nTf338-FGF21-PLUS be used to achieve higher accumulation levels in transgenic *N. tabacum* seeds and/or leaves.

In vitro with liver cells (hepatoblastoma cell line, HepG2) and primary cells from wild type as well as FGF21 knock out mice) and *in vivo* with mice (wild type and FGF21 knock out mice) trials of the cooperation partner DIfE with the recombinant nTf338-FGF21-PLUS protein, partially purified via His-Tag and Immobilized Metal Affinity Chromatography (IMAC),

demonstrated that the partially purified nTf338-FGF21-PLUS could induce the expression of target genes at the mRNA level in HepG2 cells and that the fusion protein was transferred from the intestine to the blood when fed in an oil-matrix as surrogate for seeds to mice.

Hence, the medication of NASH via oral delivery nTf338-FGF21-PLUS containing seeds is in principle possible.

Summary (German)

Die nichtalkoholische Steatohepatitis (NASH) ist eine in den Industrieländern weit verbreitete Leber-Krankheit, für die keine wirksamen Medikamente verfügbar sind. Obschon der menschliche Fibroblasten-Wachstumsfaktor (fibroblast growth factor, FGF21) in präklinischen Studien die Leberfunktion wieder herstellen konnte, beeinträchtigte FGF21 jedoch andere Organe, weshalb das Protein für eine systemische Gabe z.B. durch Injektion ins Blut ungeeignet ist. Da die orale Verabreichung einen direkten Transport des Wirkstoffs zu Leber ermöglicht und essbare Samen für die orale Verabreichung verwendet werden können, wurde die Produktion von FGF21 in Samen kommerzieller *Nicotiana tabacum* (*N. tabacum*)-Sorten im Gewächshaus etabliert.

Der Samenertrag konnte durch wiederholtes Schneiden der Pflanzen und die dadurch ausgelöste Bildung von Seitentrieben mit jeweils eigenem Blütenstand auf $380 \text{ g m}^{-2} \text{ a}^{-1}$ gesteigert sowie die berechneten Herstellungskosten auf $1,64 \text{ € g}^{-1}$ gesenkt werden, wogegen der Blattertrag bei $11.170 \text{ g m}^{-2} \text{ a}^{-1}$ lag und sich die berechneten Herstellungskosten auf $0,14 \text{ € g}^{-1}$ beliefen.

Für die stabile Transformation der Pflanzen wurde FGF21 über eine Furin-Spaltungsstelle (F) mit Transferrin (Tf) fusioniert, dass zu einer Aufnahme vom Darm ins Blut führt. Das Fusionsprotein reicherte sich mit $9,1 \text{ mg kg}^{-1}$ Samentrockenmasse (SDM) sowie $6,2 \text{ mg kg}^{-1}$ Blattfrischmasse (LFM) an, wobei die Anreicherung durch die Spaltung des Fusionsproteins beeinträchtigt wurde, die in Samen mit einem Anteil von 26-67 % an Spaltfragmenten am Gesamt-Fusionsprotein im Vergleich zu Blättern mit einem Anteil 8-41 % stärker ausgeprägt war, was der Grund dafür sein könnte, dass die Akkumulation in Blättern in einem ähnlichen Bereich lag wie in Samen.

Zur Stabilisierung des Fusionsproteins und Steigerung der Proteinausbeute wurde das Fusionsprotein mittels transienter Transformation in *Nicotiana benthamiana* (*N. benthamiana*) angepasst. Die Entfernung der Furin-Stelle und die Einführung des PLUS Peptids wurde die Menge an Spaltfragmenten verringert und die Anreicherung verdoppelt, während die Verkürzung von Tf (nTf338) und die Umkehrung der Reihenfolge von FGF21 und Tf im Fusionsprotein die Abbauprodukte weiter auf 7-9 % reduzierte, jedoch keinen Einfluss auf die Ausbeute hatte. Nichtsdestotrotz könnte das optimierte nTf338-FGF21-PLUS dazu verwendet werden, um höhere Ausbeuten in transgenen *N. tabacum* Samen und/oder Blättern zu erreichen.

In-vitro-Untersuchungen an Leberzellen (Hepatoblastom-Zelllinie, HepG2) und Primärzellen vom Wildtyp sowie FGF21-Knockout-Mäusen) und *in-vivo*-Studien Mäusen (Wildtyp- und FGF21-Knockout-Mäuse), die von dem Kooperationspartner DIfE mit über einen His-Tag und Ionenaustauschchromatographie (IMAC) teilaufgereinigte nTf338-FGF21-PLUS-Protein durchgeführt wurden, zeigten, dass das teilaufgereinigte nTf338-FGF21-PLUS die Expression von Zielgenen auf der mRNA-Ebene in HepG2-Zellen steigern konnte und dass das Fusionsprotein in Mäusen vom Darm ins Blut aufgenommen würde, wenn das Fusionsprotein in einer den Samen ähnlichen Ölmatrix an Mäuse verfüttert wurde.

Daher ist die Behandlung von NASH durch orale Verabreichung von nTf338-FGF21-PLUS-haltigen Samen grundsätzlich möglich.

I. Introduction

I. Introduction

I.1. A quarter of the world population suffer from liver diseases

Liver diseases account for approximately 2 million deaths per year worldwide (Asrani et al., 2019), and viral hepatitis, alcoholic fatty liver disease (AFLD), non-alcoholic fatty liver disease (NAFLD) currently are the most common causative factors, whereby NAFLD is becoming more common due to high-fat, high-calorie diets, and lack of exercise. Epidemiological studies indicated that the global prevalence of NAFLD is around 25 %, affecting about 2 billion adults worldwide. By region of the world, the highest prevalence of NAFLD was in the Middle East (31.8 %) and South America (30.5 %), following by Asia (27.4 %), North America (24.1 %), Europe (23.7 %), and Africa (13.5 %) (Younossi et al., 2019).

NAFLD is a progressive condition that starts with the accumulation of fat in the liver (>5 %), which is often associated with metabolic diseases like obesity and type 2 diabetes (T2D) (Estes et al., 2018; Suzuki and Diehl, 2017). NAFLD can progress to non-alcoholic steatohepatitis (NASH), which is the more severe form of NAFLD. NASH is characterized by cell inflammation and necrosis, leading to liver fibrosis that eventually progresses to cirrhosis and hepatocellular carcinoma (HCC) (LaBrecque et al., 2014). The global prevalence of NASH is estimated to be around 5 %, affecting approximately 375 million people worldwide (Estes et al., 2018; Younossi et al., 2016).

Currently, there has not yet approved a drug for NASH available (Albhaisi and Sanyal, 2021; Moustafa et al., 2016; Mullard, 2020). Existing medications primarily aim to mitigate the symptoms, with the only curative option being a liver transplantation (Sharma et al., 2021).

I.2. *In vivo* studies indicated that FGF21 might be a drug candidate to cure liver diseases

In human studies, elevated circulating serum fibroblast growth factor 21 (FGF21) levels were observed in obese patients (Dushay et al., 2010; Zhang et al., 2010), as well as in patients with T2D (Cheng et al., 2011), NAFLD (Dushay et al., 2010), or NASH (Woo et al., 2013). These patients showed FGF21 levels ranging from 292-402 pg mL⁻¹, in contrast to the range of 199-213 pg mL⁻¹ in healthy subjects (Li et al., 2010; Mraz et al., 2009; Xie and Leung, 2017;

Zhang et al., 2008).

Furthermore, the FGF21 mRNA expression and serum FGF21 concentration correlated with increased degree of increased intrahepatic triglyceride (TG) and hepatic steatosis in NASH patients (Dushay et al., 2010; Li et al., 2010; Tanaka et al., 2015; Yilmaz et al., 2010).

These data could be explained by a FGF21-mediated compensatory response, meaning that supraphysiological doses of FGF21 are used to restore the normal physiology of the liver, e.g., to reduce fat content in obese, T2D and NAFLD patients and/or inflammation in NASH patients.

I.2.1. FGF21 signaling relies on its C-terminus and the β -Klotho co-receptor KLB to establish high-affinity binding to the FGF receptor FGF1c

FGF21 is a member of the fibroblast growth factors (FGFs) family, which comprises 22 members identified in both mice and humans (Oulion et al., 2012). These FGFs can be categorized into 3 subfamilies (Itoh et al., 2016).

The first family is the intracellular FGF11 subfamily, which includes FGFs such as FGF11, FGF12, FGF13, FGF14. These FGFs act as non-signaling proteins and are not secreted from the cell due to lack of signal peptides. Instead, they remain in the cytosol, where they function as cofactors of voltage-gated sodium channels, regulating the activity of neurons and cardiomyocytes (Itoh et al., 2016; Wang et al., 2011a).

The second family is the secreted canonical FGF family (also known as paracrine FGF), which is divided sequentially into the FGF1, FGF4, FGF7, FGF8, and FGF9 classes. Examples include FGF1 and FGF2 (FGF1 subfamily), FGF4, FGF5, and FGF6 (FGF4 subfamily), FGF3, FGF7, FGF10, and FGF22 (FGF7 subfamily), FGF8, FGF17, and FGF18 (FGF8 subfamily), and FGF9, FGF16, and FGF20 (FGF9 subfamily). These FGFs exhibit a high binding capacity for heparin/heparan sulfate (HS), which in turn stabilizes the binding to FGF receptors (FGFRs). The essential functions of the FGF-FGFR-HS complex regulate cell survival, growth, migration, differentiation and angiogenesis (Giralt et al., 2015; Perrimon and Bernfield, 2000). These FGFs act in an autocrine and/or paracrine manner by binding to HS on the surface of secreting cells or nearby cells, which limits the diffusion of FGFs through the extracellular matrix (ECM) (Ahmad et al., 2012; Itoh et al., 2016). The FGF-FGFR-HS complex induces FGFR dimerization, which in turn trans-phosphorylates the tyrosine kinase domain of FGFR, triggering intracellular signaling, including RAS-mitogen-activated protein kinase (MAPK), phosphoinositide 3-kinase (PI3K)-protein kinase B (PKB or

AKT), phospholipase C γ (PLC γ) and signal transducer and activator of transcription (STAT) pathways for cell survival, growth, migration, differentiation and angiogenesis (Beenken and Mohammadi, 2009; Knights and Cook, 2010; Pacini et al., 2021; Yun et al., 2010).

The third family is the endocrine FGF15/19 subfamily, which includes FGF15 (mouse)/FGF19 (human), FGF21, and FGF23. These FGFs have a low heparin/heparan sulfate binding capacity (Giralt et al., 2015; Perrimon and Bernfield, 2000), which allows them to diffuse from the surface of secreting cells into the bloodstream. They act on distant target cells/tissues/organs and bind to co-receptors α -Klotho (KLA) or β -Klotho (KLB) to stabilize their binding to FGFR. They act in an endocrine manner and play essential roles in metabolic processes such as bile acid metabolism (FGF15/19), glucose and lipid metabolism (FGF21), and phosphate and vitamin D metabolism (FGF23) (Goetz et al., 2007; Itoh et al., 2016; Meng et al., 2021). The FGF-FGFR-Klotho complex triggers FGFR phosphorylation and subsequent activation of intracellular signaling (Goetz and Mohammadi, 2013; Ornitz and Itoh, 2015). While FGFRs are widely expressed in various tissues, KLA coreceptor expression is primarily in the kidney and parathyroid glands (Li et al., 2004; Zhao et al., 2019), and KLB coreceptor expression is restricted to the liver, white adipose tissue (WAT), brown adipose tissue (BAT), pancreas and the central nervous system (CNS) (Ito et al., 2000; Kharitonov et al., 2007; Kurosu et al., 2007). The selective expression of Klotho determines the tissue specificity of the FGF15/FGF19 subfamily. In humans, KLA serves as a coreceptor for FGF23 (Kurosu et al., 2006), while KLB acts as a coreceptor for FGF19 and FGF21 (Ding et al., 2012; Kurosu et al., 2007).

Human FGF21

MDSDETGFEHSGLWVSVLAGLLLGACOAHPIDSSPLLQFGGQVRQRYLYTDDAQQTAEHLEIREDGTVGGAADQ
SPESLLQLKALKPGVIQILGVKTSRFLQRPDGALYGSLHFDPEACSFRELLLEDGYNVYQSEAHGLPLHLPGNK
SPHRDPAPRGPAPFLPLPGLPPALPEPPGILAPQPPDVGSDDLPMVGPSQGRSPSYAS

Figure 1. Schematic illustration of human FGF21 amino acid sequence. *Blue* – ER-targeting signal peptide (position 1-28 of FGF21 precursor); *Yellow* – FGF21 mature protein (181 AA, position 1-181 of mature FGF21 protein) has one intramolecular disulfide bond at Cys75 and Cys93; *Red* – FGF21 mature protein has one N-glycosylation site at Asn121 (NKS); *Green* – FGF21 mature protein has one O-glycosylation site at Ser167. ER – endoplasmic reticulum.

Human FGF21 is produced as a precursor consisting of 209 amino acids (AA) and has a molecular mass of ~20 kDa (Figure 1). The FGF21 precursor includes a 28 AA N-terminal endoplasmic reticulum (ER)-targeting signal peptide and a 181 AA mature FGF21. The mature FGF21 has as post-translational modifications (PTMs) an intramolecular disulfide

bond (Cys75-Cys93) and its C-terminal domain contains an N-glycosylation site at Asn121 as well as an O-glycosylation site at Ser167 (Kharitononkov et al., 2013; Kharitononkov and Adams, 2014; Sonoda et al., 2017).

FGF21 is a circulating hormone mainly produced by the liver and secreted into the blood circulation (Nishimura et al., 2000), and it may also be produced and released by other tissues/organs, e.g., WAT, BAT, pancreas, skeletal muscle, kidney, and cardiac endothelial (Anuwatmatee et al., 2019; Dolegowska et al., 2019; Gómez-Sámano et al., 2017). The main effector of FGF21 are the FGFRs. In the FGFR family, seven isoform tyrosine kinase receptors (FGFR1b, FGFR1c, FGFR2b, FGFR2c, FGFR3b, FGFR3c, and FGFR4) are encoded by four genes (FGFR1, FGFR2, FGFR3 and FGFR4). The extracellular region of FGFRs contains 3 immunoglobulin (Ig)-like domains: D1, D2, and D3, and structural studies have showed that ligand-receptor interactions occur in the D2-D3 region (Chen et al., 2023). These FGFRs are expressed on the cell surface of various studies, e.g., gallbladder (bile acid metabolism), liver (glucose and lipid metabolism), WAT (glucose and lipid metabolism), skeletal muscle (phosphate and vitamin D metabolism) (Kurosu et al., 2007). However, for action the coreceptor KLB is required (Suzuki et al., 2008). The FGF-FGFR-Klotho complex triggers FGFR phosphorylation and subsequent activation of intracellular signaling (Goetz and Mohammadi, 2013; Ornitz and Itoh, 2015). Through FGFR-KLB interaction, FGF21 primarily affects the liver and adipose tissue. The main impact of FGF21 on these 2 organs is to mediate glucose and lipid metabolism (Ito et al., 2000; Kurosu et al., 2007; Ogawa et al., 2007). In the liver, FGF21 increases fatty acid oxidation, gluconeogenesis and ketogenesis. In WAT, FGF21 increases glucose uptake, lipolysis, beta-oxidation, adiponectin (Salgado et al., 2021).

Previous studies have shown that FGF21 had a preference for the FGFR1c-KLB complex (Adams et al., 2012; Fisher and Maratos-Flier, 2016; Itoh and Ornitz, 2011; Kurosu et al., 2007; Ogawa et al., 2007). The C-terminus of FGF21 binds to the extracellular domain of KLB with high affinity (Gimeno and Moller, 2014; Kharitononkov et al., 2008; Ogawa et al., 2007). Binding to KLB allows the N-terminal domain of FGF21 to interact with the D2-D3 domains of FGFR1c to induce receptor dimerization, autophosphorylation and MAPK activation. MAPK induces extracellular signal-regulated kinase 1 and 2 (ERK1/2), which enter the nucleus and stimulate transcription of target genes such as the transcription factors signal transducer and activator of transcription 3 (STAT3) and cAMP response element-binding protein (CREB) for cell survival, cell proliferation and cell differentiation (Gimeno and Moller, 2014; Itoh, 2014; Kharitononkov et al., 2005; Mantamadiotis et al., 2012; Sonoda

et al., 2017; Wente et al., 2006; Xin et al., 2020).

In a previous study aimed at using FGF21 as a therapeutic drug, the fragment crystallizable domain (Fc) of human immunoglobulin G1 (IgG1) was fused to FGF21, resulting in 2 Fc fusions proteins named Fc-FGF21 and FGF21-Fc. The authors observed that FGF21 was active when Fc was fused to the N-terminus of FGF21 (Fc-FGF21) and had similar *in vitro* and *in vivo* activities to native FGF21 because Fc-FGF21 retained KLB binding affinity. However, when Fc was fused to the C-terminus of FGF21 (FGF21-Fc), FGF21 was inactive, suggesting that the C-terminus of FGF21 is critical (Hecht et al., 2012).

Furthermore, the C-terminus of FGF21 is easily processed by the serum endopeptidase fibroblast activation protein (FAP), leading to rapid removal of FGF21 (Coppage et al., 2016; Hecht et al., 2012; Sonoda et al., 2017; Zhen et al., 2016). The rapid C-terminal degradation is further enhanced by rapid N-terminal degradation, promoted by the four N-terminal AAs His-Pro-Ile-Pro (HPIP). Both C- and N-terminal degradation limit the half-life of FGF21 in blood to 1-2 h (Gimeno and Moller, 2014; Kharitononkov et al., 2005; Sonoda et al., 2017; Zhen et al., 2016).

Taken together, the rapid proteolytic degradation limits the use of FGF21 as a therapeutic protein drug (PD), with a critical emphasis on the C-terminus.

1.2.2. FGF21 mediates the glucose and lipid metabolism under starvation

FGF21 has been observed in human subjects, non-human primates (NHP), and rodents. It is induced in healthy subjects during periods of nutrient deprivation, starvation, and fasting to regulate glucose and lipid metabolism.

In wild-type (WT) mice, FGF21 is mainly expressed in the liver (Nishimura et al., 2000), and it triggers glucose uptake by stimulating the expression of the glucose transporter GLUT1 in adipocytes (Kharitononkov et al., 2005). Under normal conditions, when mice are fed *ad libitum*, serum FGF21 concentrations are typically in the range of 100-1,000 pg mL⁻¹ and can vary based on age and different inbred mouse lines (Fisher et al., 2010; Staiger et al., 2017). In contrast, after a 24-h fast, mouse serum FGF21 concentrations increase to levels of 2,500-3,500 pg mL⁻¹ (Markan et al., 2014).

In humans, serum concentrations of FGF21 in healthy individuals' of 199-213 pg mL⁻¹ are typical, but can have a range of 5-5,000 pg mL⁻¹ due to individual variability (Fazeli et al., 2015; Gälman et al., 2008; Li et al., 2009; Markan et al., 2014; Staiger et al., 2017; Zhang et al., 2008). Nevertheless, studies with humans have shown that FGF21 levels are positively

correlated with body mass index (BMI). For example, in these studies, healthy, lean human subjects (BMI 21-28 kg m⁻²) had FGF21 levels in the range of 250-4,000 pg mL⁻¹, compared to FGF21 levels of 2,000-5,000 pg mL⁻¹ in overweight or obese human subjects (BMI 28-39 kg m⁻²), and despite the variation, the difference was significant (Dushay et al., 2010). These results were further evidenced in fasting studies with humans. Human serum FGF21 concentrations averaged 188 ± 46 pg mL⁻¹ on day 0 and 799 ± 189 pg mL⁻¹ on day 10 of fasting (Fazeli et al., 2015).

The fasting-induced activation of hepatic FGF21 by peroxisome proliferator-activated receptor alpha (PPAR α) reduces TG level by downregulating hepatic lipogenesis and upregulating hepatic fatty acid oxidation (Badman et al., 2007; Feingold et al., 2012; Lundåsen et al., 2007; Woo et al., 2013). In adipose tissue, FGF21 further enhances insulin sensitivity of WAT to promote glucose utilization. Peroxisome proliferator-activated receptor gamma (PPAR γ) is highly expressed in WAT and is required for adipocyte differentiation. FGF21 induces WAT browning and activates BAT, thereby promoting thermogenesis and increasing energy expenditure (Douris et al., 2015; Owen et al., 2014; Rosen et al., 1999; Salgado et al., 2021; Szczepańska and Gietka-Czernel, 2022).

Taken together, FGF21 may be used as a therapeutic PD for the treatment of human metabolic diseases.

I.2.3. FGF21 shows dual glucose-and lipid-lowering effects but also reduced the bone mass in pre-clinical trials

The first pre-clinical study of therapeutic administration of FGF21 focused on obese and diabetic mice and involved the injection of native FGF21, which led to observed reductions in blood glucose and TG levels to near normal levels (Berglund et al., 2009).

In more detail, these pre-clinical experiments demonstrated that systemic administration of supraphysiological doses of FGF21 to various animal models, including obese (ob/ob) mice, diabetic (db/db) mice, high-fat diet (HFD) fed mice, obese Zucker diabetic obese (ZDF) rats, and diabetic rhesus monkeys, resulted in a substantial increase in plasma FGF21 concentrations after injection. These concentrations reached levels of 13,333-16,667 pg mL⁻¹ (Coskun et al., 2008; Laeger et al., 2017), 6,667-8,333 pg mL⁻¹ (Ying et al., 2019), 3,333-4,167 pg mL⁻¹ (Silva et al., 2019; Wang et al., 2008), 142,857-181,818 pg mL⁻¹ (Ghasemi et al., 2021; Giragossian et al., 2015), and 4,638-129,870 pg mL⁻¹ (Kharitononkov et al., 2007), respectively. These concentrations were notably higher than the typical range of 100-1,000 pg

mL⁻¹ observed in WT mice. This significant increase in FGF21 concentrations resulted in marked reductions in adiposity, blood glucose, and triglyceride levels, along with improvements in insulin sensitivity in these animal models.

In HFD-induced obese mice, FGF21 demonstrated the ability to reverse hepatic steatosis by reducing hepatic TG and cholesterol levels in the liver, as indicated by several studies (Jimenez et al., 2018; Keinicke et al., 2020; Kharitononkov and DiMarchi, 2017; Xu et al., 2009). This effect was accompanied by a reduction in plasma markers of liver dysfunction, such as aspartate aminotransferase (AST), alanine aminotransferase (ALT), and alkaline phosphatase (ALP) levels (Xu et al., 2009).

Consistent with this, in FGF21 knockout (FGF21-KO) mice, a chronic obesogenic diet promoted fatty liver excess (Badman et al., 2007; Badman et al., 2009), leading to progressive fibrosis, and 78 % of mice developed HCC (Singhal et al., 2018). Notably, FGF21-KO mice also showed increased bone mass compared to WT mice (Wei et al., 2012).

Conversely, FGF21 overexpressing transgenic (FGF21-TG) mice (with plasma FGF21 concentrations in FGF21-TG mice of ~22,000 pg mL⁻¹ compared to ~1,000 pg mL⁻¹ in WT mice) displayed resistance to high-fat/high-carbohydrate (HFHC) diet-induced obesity (Kharitononkov et al., 2008). Notably, the FGF21 levels in FGF21-TG mice were also higher after fasting, similar to those in WT mice (with ~21,000 pg mL⁻¹ and ~5,000 pg mL⁻¹ in fasted FGF21-TG and WT mice) (Inagaki et al., 2007). However, in the FGF21-TG mice, stable overexpression of FGF21 inhibited signal transducer and activator of transcription 5 (STAT5), a major mediator of growth hormone action, and resulted in growth retardation. For example, weight loss and bone mass loss (Inagaki et al., 2008; Wei et al., 2012).

Taken together, the pre-clinical studies demonstrating that FGF21 can potentially reverse hepatic steatosis suggest that FGF21 could be a potential therapeutic PD candidate not only for obesity and T2D but also for NAFLD and NASH, particularly if FGF21 can be specifically targeted to the liver.

I.2.4. Long-acting FGF21 analogues alleviated hepatic steatosis but also caused bone mass loss in clinical trial

Pre-clinical studies have shown that injection of FGF21 in mice improves glucose and lipid metabolism. However, using native FGF21 as a therapeutic PD faces several challenges, including: 1) Its short half-life in blood, which is about 1-2 h (Chapter I.2.1.) due to rapid hydrolysis of its C-terminal peptide by FAP. This requires daily or twice-daily injections

(Sonoda et al., 2017; Zhen et al., 2016). 2) Its low molecular mass of ~20 kDa, leading to rapid clearance by the kidneys in rodents (1 h) and NHPs (0.5-2 h) (Hecht et al., 2012; Kharitononkov et al., 2007; Sonoda et al., 2017). 3) FGF21's high tendency to aggregate *in vitro* in the presence of phenolic preservatives like m-cresol, rendering it inactive (Kharitononkov et al., 2013; Maa and Hsu, 1996).

Native FGF21 is not suitable for human drug therapy due to its instability in the bloodstream. As a result, pharmaceutical companies are concentrating on the development of stable FGF21 analogues with enhanced pharmacokinetic properties. Out of these, 3 FGF21 analogues have entered clinical trials (Table 1).

Table 1. Only 3 FGF21 analogues that have entered clinical trials are listed. Phase I, a trial to study the safety, tolerability and pharmacokinetics; Phase IIa, a trial to evaluate the safety, pharmacokinetics and pharmacodynamics.

Company	FGF21 analogue	FGF21 modification	Half-life	ClinicalTrials.gov ID	Injection dosage and duration	Positive effect (Change from the baseline)	Off-target effect
Eli Lilly and Company	LY2405319 (Gaich et al., 2013; Gimeno and Moller, 2014)	N-terminal 4 AA deletion, No O-glycosylation Disulfide bond	1.5-3 h	Phase I, NCT01869959, Obese-T2D (n=15)	SC, 20 mg daily, 4 weeks	Fasting insulin (-41 %) LDL-C (-20 %) HDL-C (20 %) Triglycerides (-45 %) Total cholesterol (-15 %) Adiponectin (83 %) Body weight (-2 %)	87 % ADA-positive, at 8 weeks & drop in blood pressure, urticaria and pruritus due to ADA (n=1)
						HDL-C (25 %) Triglycerides (-50 %) Total cholesterol (-14 %) Adiponectin (2,000 %) Body weight (-6 %) CTX (0.1 %) Osteocalcin (-3 %) PINP (-7 %)	changes in markers of bone turnover
Pfizer	PF-05231023 (Huang et al., 2013; Talukdar et al., 2016)	N-terminal 1 AA deletion, Disulfide bond Scaffold antibody	10-98 h	Phase I, NCT01396187, Obese-T2D (n=10)	IV, 100 mg 2x per week, 4 weeks		
Bristol-Myers Squibb	BMS-986036 (Charles et al., 2019; Sanyal et al., 2019)	PEGylation	19-24 h	Phase IIa, NCT02097277, Obese-T2D (n=24)	SC, 20 mg daily, 12 weeks	HDL-C (15 %) Triglycerides (-20 %) Adiponectin (35 %) PRO-C3 (-20 %)	83 % ADA-positive, at 18 weeks
						Hepatic fat fraction (-5 %) Liver stiffness (-15 %)	63 % ADA-positive, at 20 weeks

Abbreviations: AA – amino acid; ADA – anti-drug antibody; CTX – C-terminal telopeptide; HDL-C – high density lipoprotein-cholesterol; IV – intravenous injection; LDL-C – low density lipoprotein-cholesterol; NASH – non-alcoholic steatohepatitis; PEGylated – polyethylene glycol-modified; PINP – procollagen type 1 N-terminal pro-peptide; PRO-C3 – pro-peptide of type III collagen; SC – subcutaneous injection; T2D – type 2 diabetes.

The short-acting FGF21 analog LY2405319 (LY) was developed by Eli Lilly. This analog involved the elimination of O-glycosylation as a PTM by introducing the Ser167Ala mutation. This modification aimed to generate a homogenous protein that could be produced in yeast (*Pichia pastoris*) (Kharitononkov et al., 2013). Additionally, to improve the formulation stability and reduce aggregation, Eli Lilly introduced additional disulfide bonds (Leu118Cys and Ala134Cys) to stabilize the loops of the C-terminal domain of FGF21 (Huang et al., 2013; Kharitononkov et al., 2013). Lastly, to decrease the proteolytic degradation and increase the serum half-life, Eli Lilly deleted the four N-terminal AAs His-Pro-Ile-Pro (HPIP) (Kharitononkov et al., 2013). However, despite the improved stability of the modified FGF21, LY was quickly cleared by the kidneys (<3 h) due to its low molecular mass, which is similar to that of native FGF21 (~20 kDa) (Gimeno and Moller, 2014; Sonoda et al., 2017). Importantly, systemic LY clinical trials did not result in significant effects on blood sugar levels but did lead to significant changes in blood lipids (Gaich et al., 2013) (Table 1).

To prolong the circulating half-life of FGF21, one approach is to increase its molecular mass. To achieve this, Bristol-Myers Squibb developed a long-acting FGF21 analog known as BMS-986036 (BMS), also referred to as Pegbelfermin or ARX618. In BMS, a 30 kDa PEG was fused to the N-terminus of native FGF21 (PEG-FGF21) to increase its molecular mass from ~20 kDa to ~50 kDa (Sanyal et al., 2019). This modification significantly extended its half-life from 1-2 h to 98 h (Sonoda et al., 2017; Verzijl et al., 2020). Systemic long-lasting BMS has successfully completed 2 Phase 2a studies, showing improvements in obesity for individuals with T2D and NASH (Charles et al., 2019; Verzijl et al., 2020). Currently, 2 Phase 2b studies are being evaluated in patients with NASH and fibrosis, as well as in patients with NASH and cirrhosis, respectively (FALCON 1 and FALCON 2, ClinicalTrials.gov Identifiers: NCT03486899 and NCT03486912). Hence, BMS has confirmed the results obtained with LY, indicating that FGF21 primarily affects lipid metabolism rather than glucose metabolism (Table 1).

Another long-acting FGF21 analog was Pfizer's PF-05231023 (PF), also known as CVX343. PF was composed of 2 modified FGF21 molecules (Δ His1, Ala129Cys) linked at the N-terminus to the fragment antigen-binding (Fab) region of the scaffold antibody CVX-2000. PF had a molecular mass of ~190 kDa and a half-life of 24 h (Huang et al., 2013; Sonoda et al., 2017). Clinical trials with systemically applied PF resulted in changes in blood lipids. However, PF levels were associated with increased bone resorption and decreased bone

formation (Talukdar et al., 2016), similar to pre-clinical trials in transgenic mice (Chapter I.2.3.). As a result, PF did not undergo a phase 2 study (Talukdar et al., 2016; Verzijl et al., 2020) (Table 1).

Taken together, systemic long-acting FGF21 analogues used in clinical applications have demonstrated beneficial effects on lipid-related liver diseases. However, they have also been associated with off-target effects due to their extended half-life and direct injection into the bloodstream, leading to systemic distribution.

I.3. Transferrin and furin cleavage site can be used to target orally administrated FGF21 to the liver

FGF21 is a potential PD candidate for the treatment of NAFLD and NASH, but systemic FGF21 application of FGF21 had off-target effects, such as reducing bone mass in mice and bone turnover in humans (Chapters I.2.3. and I.2.4.). If FGF21 could be specifically targeted to the liver, off-target effects could be prevented, while enabling the positives effects of FGF21. This can be achieved by oral administration, whereby FGF21 enters the liver directly from the small intestine before entering the blood system (Figure 2).

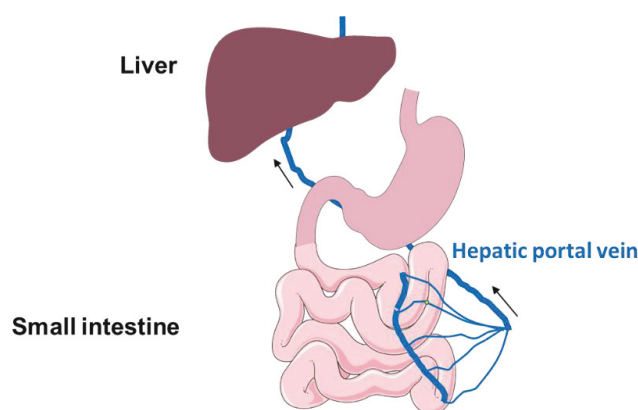


Figure 2. Schematic illustration of liver-specific targeting. Specific targeting of the liver is achieved by oral administration because the portal vein enters the liver directly from the small intestine before entering the blood system. Parts of the figure were drawn by using pictures from Servier Medical Art. Servier Medical Art by Servier is licensed under a Creative Commons Attribution 3.0 Unported License (<https://creativecommons.org/licenses/by/3.0/>).

One possibility to achieve this is the fusion of FGF21 to transferrin (Tf). Tf regulates cellular iron uptake into the cell layer by binding to transferrin receptor (TfR). Mediating the endocytosis in the intestinal epithelium (Banerjee et al., 1986; Li and Qian, 2002; Widera et al., 2003; Yong et al., 2019) (Figure 3).

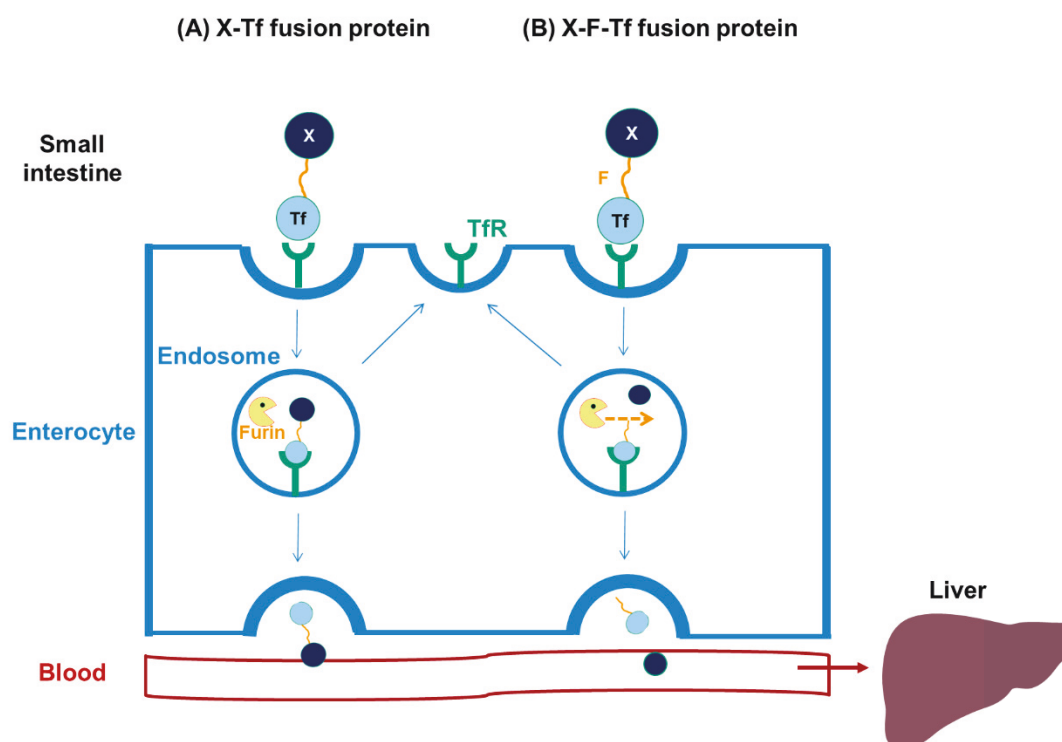


Figure 3. Schematic illustration of transferrin fusion protein with and without furin cleavage site via transferrin receptor-mediated cellular uptake. (A) X-Tf fusion protein, and (B) X-F-Tf fusion protein are taken up by cell surface TfR from the small intestine into enterocytes through the Tf-TfR system. After furin protease processing in the endosome, intact X-Tf fusion protein, furin protease-cleaved F-Tf protein and X passenger protein enter the liver through the portal vein. X – passenger protein; F – furin cleavage site; Furin – furin protease; Tf – transferrin; TfR – transferrin receptor; ER – endoplasmic reticulum. Parts of the figure were drawn by using pictures from Servier Medical Art. Servier Medical Art by Servier is licensed under a Creative Commons Attribution 3.0 Unported License (<https://creativecommons.org/licenses/by/3.0/>).

I.3.1. N-terminal domain of transferrin is essential for binding to the transferrin receptor and its transport from the intestine to the blood stream

Tf is a glycoprotein and a blood siderophore protein. It is primarily produced in the liver (Huggenvik et al., 1989), and its primary physiological function is to participate in iron metabolism by binding iron ions (Fe^{3+}) and transporting them to various cells. Tf is taken up by cells through transferrin receptor (TfR)-mediated transcytosis (Huggenvik et al., 1989; Mason et al., 1996; Thevis et al., 2003; Yu et al., 2020). Within the cell, Tf releases the iron ions. Its extended serum half-life of 8-10 days enhances the effectiveness of Tf as an iron carrier.

The Tf precursor, consisting of 698 AA, has a molecular mass of ~80 kDa. It comprises a 19 AA ER-targeting signal peptide and a 679 AA mature full-length Tf. The mature Tf protein

(position 1-679) has 19 intramolecular disulfide bonds and folds into 2 similar domains, the N-terminal domain (N-lobe, position 1-331 of Tf mature protein) and C-terminal domain (C-lobe, position 339-679 of Tf mature protein), each with an iron-binding site (Hall et al., 2002; Mason et al., 2009; Parkkinen et al., 2002; Steinlein et al., 1995; Wally et al., 2006). These 2 domains are connected by a 7 AA hinge region (position 332-338 of Tf mature protein), flanked by 19 intramolecular disulfide bonds, including two pairs of crucial disulfide bonds: Cys137-Cys331 in the N-terminal domain and Cys339-Cys596 in the C-terminal domain (Wally et al., 2006) (Figure 4).

Human Tf

MRLAVGALLVCAVLGICLAVPDKTVRWCAVSEHEATKQSFDRDHMKSVIPSDGPSVACVKKASYLDICIRATAANE
ADAVTLDAGLVYDAYLAPNNLKPVVAEFYGSKEDPQTFYYAVAVVKKDSGFQMNQLRGKKSCHTGLGRSAGWNIP
IGLLYCDLPEPRKPLEKAVANFFSGSCAPCADGTDFPOLCOLCPGCGCSTLNOYFGYSGAFKCLKDGAGDVAFAVK
HSTIFENLANKADRDOYELLCLDNTRKPVDEYKCHLAQVPSHTVVARSIGGKEDLIWELLNOAEHFGKDKSKE
FOLFSSPHGKDLLFKDSAAGFLKVPPRMDAKMYLGYEYVTAIRNLREGTCEAPTDECKPVKWCALSHHERLKCD
EWSVNSVGKIECVSAETTEDCIAKIMNGEADAMSLDGGFVYIAGKCGLVPVLAENYNKSDNCEDTPGAGYFAVAV
VKKSASDLTWDNLKGKKSCHTAVGRTAGWNIPMGLLYNKINHCRFDEFFSEGCAPGSKKDSSLCKLCMGSGLNLC
EPNNKEGYGYGTGAFRCLVEKGDVAFAVKHQTVPONTGGKNPDPAKKNLNEKDYELLCLDGTRKPVVEEYANCHLAR
APNHAVVTRKDKEACVHKILRQOHLFGSNVTDCSGNFCFLFRSETKDLLFRDDTVCLAKLHNRNTYEKYLGEYV
KAVGNLRKCTSSLLAEACTFRRP

Figure 4. Schematic illustration of human Tf amino acid sequence. *Blue* – ER-targeting signal peptide (position 1-19 of Tf precursor); *Thick bottom line* – N-terminal domain of mature Tf (position 1-331 of Tf mature protein); *Pink* –hinge region of Tf, 7 AA PEAPTDE (position 332-338 of Tf mature protein); *Dotted line* – C-terminal domain of mature Tf (position 339-674 of Tf mature protein); *Yellow* – Tf mature protein has 19 intramolecular disulfide bonds; *Red* – Tf mature protein has 2 N-glycosylation sites at C-terminal end (NKS, NVT). ER – endoplasmic reticulum.

Disulfide bond formation is crucial for Tf's biological function but not for glycosylation. For example, *Escherichia coli* (*E. coli*)-derived Tf was biologically inactive due to the absence of intramolecular disulfide bond formation (Hoefkens et al., 1996), while Tf produced in mammalian cells (e.g., baby hamster kidney (BHK) cells) (Mason et al., 1993) and rice (*Oryza sativa*) (Zhang et al., 2010) produced Tfs with disulfide bonds, and both Tfs retained their biological activity. In addition to the intramolecular disulfide bond, mature Tf has 2 N-glycosylation sites at Asn413 and Asn611 (Parkkinen et al., 2002). However, the biological significance of glycosylation in Tf function is not fully understood (Brown et al., 2012).

The major receptor for Tf is the transferrin receptor-1 (TfR1). TfR1 is a homodimeric type II membrane glycoprotein consisting of extracellular domain (ECD), transmembrane domain and intracellular domain, with a molecular mass of ~95 kDa. The EDC of TfR1 is composed of apical, helical, and protease-like domains (Hentze et al., 2004). Structure analysis of the Tf-

TfR1 complex showed that the N-terminal domain of Tf contacts the protease-like domain of TfR1, while the C-terminal domain of Tf interacts with the helical domain of TfR1 (Giannetti et al., 2003; Lawrence et al., 1999; Wessling-Resnick, 2018). The formed Tf-TfR1 complex facilitates entry of its ligand into cells for iron delivery (Hentze et al., 2004).

Most importantly, a previous study expressing the N-terminal domain of Tf in yeast (*Pichia pastoris*) showed that it was correctly folded and retained the ability to bind iron and the receptors, mediating cellular uptake (Mason et al., 2009). Apart from the liver, TfR1 is also expressed in human gastrointestinal epithelial cells, and it regulates intestinal epithelial endocytosis by binding to the iron-uptake cell layer of TfR1 cells (Banerjee et al., 1986; Li and Qian, 2002; Widera et al., 2003; Yong et al., 2019). Hence, Tf also mediates the uptake of iron from the intestine and its transport into the blood.

Taken together, considering disulfide bond formation is essential for biologically active Tf, recombinant Tf needs to be produced in eukaryotic cells such as yeast, mammals, or plants. In terms of the biological function of Tf, its N-terminal domain is crucial for the binding to TfR and its biological activity, including the transport of iron from the intestine into the blood.

I.3.2. Fusion of proteins to transferrin enables transfer from the small intestine to the portal vein but prolongs serum half-life in pre-clinical trials

Tf transports iron from the intestine to the blood stream, and this capability has been exploited for the oral delivery of PD into the bloodstream. In pre-clinical trials, oral administration of partially purified/purified Tf fusion proteins from different production platforms has shown enhanced oral bioavailability. These proteins can be transported by enterocytes from the small intestine to the blood and eventually reach the liver via TfR-mediated transcytosis (Figure 3).

In mouse trials, oral administration of recombinant plant-produced partially purified granulocyte colony-stimulating factor-transferrin (G-CSF-Tf) was used for medication of neutropenia (Bai et al., 2005). Similarly, plant-produced partially purified proinsulin-transferrin (ProINS-Tf) and extendin-4-transferrin (Ex-4-Tf) were used to treat T2D (Wang et al., 2014a). Partially purified Ex-4-TF lowered blood sugar levels by 33 %, whereas commercially purified Ex-4 lowered blood sugar levels by 11 %. Consequently, Ex-4-Tf was found to be 22 % more effective than Ex-4 (Choi et al., 2014).

In addition to improving the oral bioavailability, Tf can also stabilize the target protein to extend its half-life, as Tf itself has a half-life of 7-17 days (Kim et al., 2010). For example, in rabbits (*Oryctolagus cuniculus*), the half-life of plant-produced glucagon-like peptide 1 (GLP-

1) was increased from minutes to 27 h when fused to Tf (Hui et al., 2002; Matsubara et al., 2011). In mice, proinsulin (ProINS) increased half-life from 2 h to 48 h when fused to Tf (Wang et al., 2014a).

Taken together, oral administration of Tf fusion proteins offers the potential for enhanced oral bioavailability by facilitating the translocation of the fusion partners from the small intestine to the bloodstream or portal vein, respectively. However, it is crucial to note that the half-life of the Tf fusion protein is significantly longer than that of the unfused target protein when administered orally. This difference in half-life should be taken into account when developing therapeutic strategies involving Tf fusion proteins, especially when dealing with PD with a shorter half-life.

I.3.3. Furin cleavage site can be used to separate FGF21 and transferrin after transfer from the small intestine to the portal vein

While Tf enhances the uptake of fusion partners from the intestine into the bloodstream after oral administration, it is important to note that Tf also prolongs the serum half-life of the passenger protein, promoting its systemic distribution in the blood. In the case of FGF21, this extended half-life, facilitated by Tf, may give rise to off-target effects (Chapters I.2.3. and I.2.4.). Therefore, after transcytosis, the separation of Tf and FGF21 becomes necessary, and this can be achieved through the use of a furin cleavage site (F).

Furin is a mammalian protease belonging to the subtilisin-like proprotein convertase family. It is primarily located in the trans-Golgi network and can be transferred from the cell membrane to the endosome by endocytosis (Gendron et al., 2006; Seidah and Chrétien, 1999; Shapiro et al., 1997). Furin is present in all mammalian cells and tissue types and is responsible for the post-translational cleavage of precursor proteins into their biologically active form when secreted through the secretory pathway. This includes hormones, receptors, growth factors, adhesion molecules or metalloproteases (Braun and Sauter, 2019; Fuller et al., 1989; Steiner, 1998).

Notably, the furin cleavage site (Arg-Arg-Lys-Arg, RRKR) is cleaved without leaving any additional AA on the fused protein (Duckert et al., 2004; Nakayama, 1997; Seidah and Chrétien, 1999). However, in fusion proteins, typically 2 AA Ser-Val (SV) have been added after the furin cleavage site (RRKR). This addition enhances the efficiency of the furin cleavage site recognition (Boyhan and Daniell, 2011; Duckert et al., 2004; Kwon et al., 2018).

Oral administration of recombinant proteins containing a furin cleavage site in pre-clinical trials has demonstrated that the furin cleavage site is efficiently cleaved, releasing a functional target protein into the bloodstream (Boyhan and Daniell, 2011; Kohli et al., 2014; Kwon et al., 2013; Shenoy et al., 2014; Shil et al., 2014; Su et al., 2015b; Su et al., 2015a; Verma et al., 2010). For example, hemophilia B mice were orally gavaged with cholera toxin β subunit-furin cleavage site-coagulation factor IX (CTB-F-FIX) fusion protein (Su et al., 2015b; Verma et al., 2010). In terms of bioavailability, CTB-F-FIX crossed the epithelial cell barrier by binding to the receptor GM1 but did not co-localize with FIX in the bloodstream due to efficient furin cleavage between FIX and CTB in the epithelial cells (Su et al., 2015b; Verma et al., 2010; Wang et al., 2015). Consequently, liver staining showed positive labeling for FIX but not CTB. In terms of biological activity, CTB-F-FIX-fed mice prevented the formation of FIX inhibitors and immunoglobulin E (IgE) formation, thereby mitigating allergic reactions (Verma et al., 2010).

Notably, the furin protease is produced in mammals, but it is absent in non-mammalian cells such as plants (Schaller and Ryan, 1994). Previous studies have shown that recombinant proteins with furin cleavage sites were not cleaved when produced in plants that were heterologous host for recombinant protein production (Boyhan and Daniell, 2011; Kang et al., 2018; Kwon et al., 2013; Mamedov et al., 2019; Margolin et al., 2020; Verma et al., 2010).

Taken together, the furin cleavage site can be used to separate FGF21 and transferrin, allowing FGF21 to be released from small intestine to bloodstream. However, this fusion protein containing the furin cleavage site needs to be produced in non-mammalian hosts, such as plants.

I.3.4. A fusion protein of FGF21-Transferrin and furin cleavage site can be used to target the liver by oral delivery

The oral uptake of PD, such as FGF21, into the blood can be achieved by fusion with Tf, which induces transcytosis from the intestine to the portal vein (Chapter I.3.1.). Since Tf requires a disulfide bridge for its folding and biological function, the FGF21-Tf fusion protein needs to be targeted to the ER. This can be achieved by adding an ER targeting signal peptide and an ER retention signal to the C-terminal AA sequence of Tf (Chapter I.3.1.).

However, Tf also prolongs the half-life of the fusion protein, which might not be suitable for PD that require a short serum half-life, including FGF21. To address this, separation of the PD from Tf is needed during or after translocation (Chapter I.3.2.), and this can be achieved

by inserting the furin cleavage site (F) (Chapter I.3.3.). Since ER-targeted F-Tf remains in enterocytes, free PD is secreted into the portal vein and transported directly to the liver, where it is taken up. Notably, the short half-life of free FGF21, combined with the rapid degradation of FGF21 (Chapter I.2.1.) that is not absorbed by the liver, can reduce off-target effects of FGF21.

I.4. *In planta* encapsulation enables oral delivery of recombinant proteins through the stomach to the small intestine

Oral delivery of PD from the intestine to the blood stream is in principle possible (Chapter I.3.2.), but for real oral administration PD passes the stomach, where PD may be denatured by low pH of 1.0-3.0 and proteases in the stomach. Therefore, orally PD are typically encapsulated as tablets, mediating a targeted release in the small intestine where it is taken up. However, when PD is produced recombinantly in plants as heterologous host, the plant host itself might serve as protection (Figure 5).

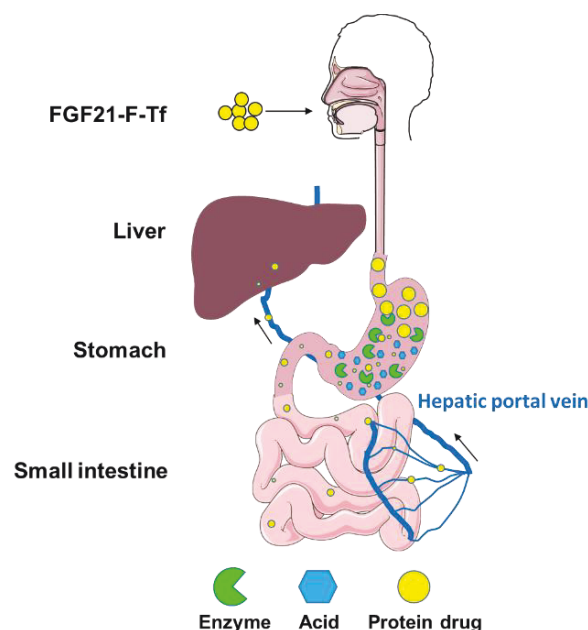


Figure 5. Schematic illustration of oral administration of FGF21-F-Tf. FGF21-F-Tf as a protein drug and it needs to be protected from the acidic and enzymatic conditions in the stomach and then transported into the liver from small intestine to portal vein. Parts of the figure were drawn by using pictures from Servier Medical Art. Servier Medical Art by Servier is licensed under a Creative Commons Attribution 3.0 Unported License (<https://creativecommons.org/licenses/by/3.0/>).

Plant cell walls containing lignin and cellulose can protect PD from digestive acids/enzymes via bio-encapsulation, which is called *in planta* encapsulation. Subsequently, PD can be

released into the small intestine when the glycosidic bonds of plant cell walls are broken down by gut commensal microbiota (Khan and Daniell, 2021; Kwon and Daniell, 2015, 2016).

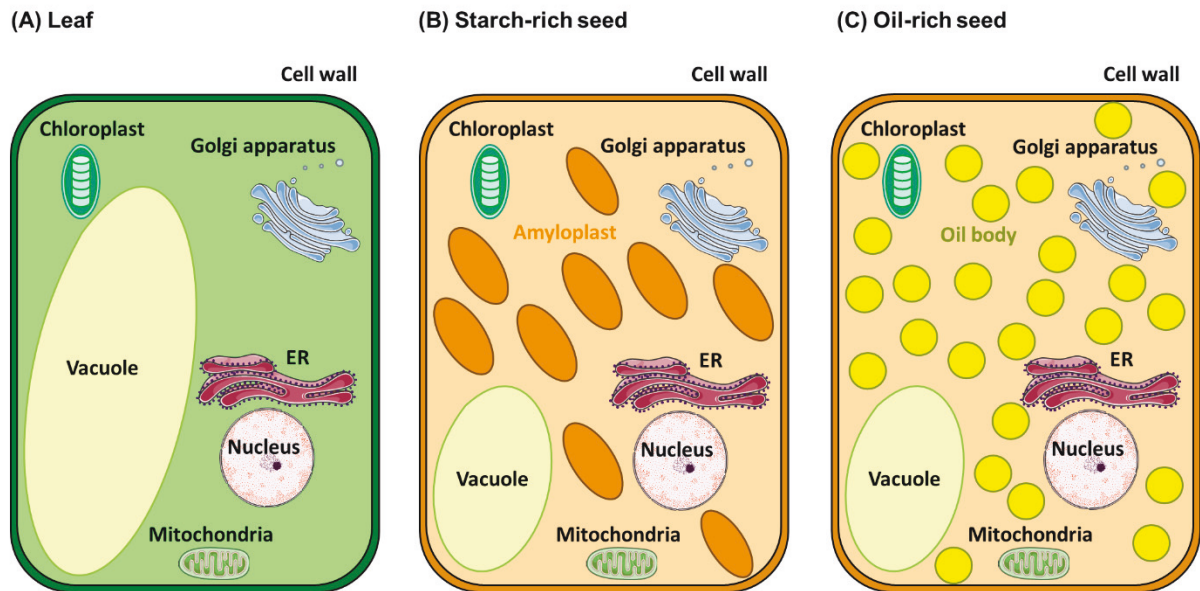


Figure 6. Schematic illustration of *in planta* bioencapsulation. (A) Leaf, (B) starch-rich seed, and (C) oil-rich seed. Plant matrices like cell walls in leaves and seeds, as well as structures such as amyloplasts or oil bodies within seeds, can serve as effective carriers or vehicles for the oral delivery of protein drugs. ER – endoplasmic reticulum. Parts of the figure were drawn by using pictures from Servier Medical Art. Servier Medical Art by Servier is licensed under a Creative Commons Attribution 3.0 Unported License (<https://creativecommons.org/licenses/by/3.0/>).

I.4.1. Leaves can be used for oral delivery but are affected by proteolytic degradation of the target protein after harvest

The cell walls of the leaves can provide a vehicle for the oral delivery of PD (Figure 6A). Lettuce is an ideal candidate for PD due to its edible leaves, established generally recognized as safe (GRAS) status, and well-developed chloroplast transformation system for PD expression (Boyhan and Daniell, 2011; Ruhlman et al., 2007; Su et al., 2015b). Previous studies have shown that freeze-dried lettuce cells did not lose protein activity when stored at ambient temperature for up to 24 months (Herzog et al., 2017).

In addition to edible lettuce, many pre-clinical studies were conducted using non-edible tobacco plants, such as leaf material from tobacco chloroplasts and transgenic tobacco plants. For example, cholera toxin B subunit-human proinsulin (CTB-Pins) fusion protein was expressed in tobacco chloroplasts, and it was orally administered to mice by gavaging frozen

leaf powder, which was resuspended in sterile phosphate-buffered saline (PBS) buffer. In CTB-Pins treated mice, the development of insulinitis in non-obese diabetic mice was prevented (Ruhlman et al., 2007). Another example is the oral administration of transgenic freeze-dried and powdered leaves expressing the bacterial ApxIIA toxin, which induced a protective immune response in mice infected with *Actinobacillus pleuropneumoniae* (Lee et al., 2006).

However, leaf proteins undergo rapid proteolytic degradation after leave harvesting and require immediate freezing and freeze-drying or transport in a frozen state. This complicates their application for oral administration (Basaran and Rodríguez-Cerezo, 2008).

I.4.2. Seeds can be used oral delivery and typically do not display a proteolytic degradation of the target protein

Compared to leaves for oral delivery (Chapter I.4.1.), seeds offer several advantages, particularly if they have GRAS status: 1) Long-term storage stability at ambient temperature: Mature seeds have no relevant proteolytic activity, allowing for long-term storage at ambient temperature (Benchabane et al., 2008; Boothe et al., 2010; Cunha et al., 2011). For example, a study stored transgenic soybean seeds containing human growth hormone (hGH) for 6 years with no detectable loss of activity at low water content in dormant seeds (Cunha et al., 2011). 2) Higher recombinant protein levels: Seeds may accumulate higher levels of recombinant proteins compared to leaves, as they typically contain about 25-38% of endogenous protein, whereas leaves contain only 1-2% (Frega et al., 1991). 3) Oral delivery without further purification: If they are edible and have GRAS status, seeds can be taken orally without the need for additional protein purification. 4) Additional nutritional value: Seeds not only provide a substantial amount of protein when ingested orally but are also rich in starch and oil, making them a valuable source of nutrients.

Seeds are divided into two categories: 1) Starch-rich seeds: The seed matrix consists of cell walls and amyloplast (starch-based matrix) (Figure 6B). 2) Oil-rich seeds: The seed matrix is composed of cell walls and oil bodies (oil-based matrix) (Figure 6C).

Plants with starch-rich seeds include rice (Fukuda et al., 2018; Nochi et al., 2007; Yuki et al., 2013), barley (Hensel et al., 2015; Zimmermann et al., 2009), pea (Zimmermann et al., 2009), and maize (Feng et al., 2017; Hayden et al., 2012; Nahampun et al., 2015). In the case of starch-rich seeds, transgenic rice MucoRice-CTB has been used as an edible plant vaccine in mice, which effectively induced serum CTB-specific immunoglobulin G (IgG) and fecal immunoglobulin A (IgA) antibody responses and provided gut immunity against diarrhea

(Nochi et al., 2007; Tokuhara et al., 2010; Yuki et al., 2013). Notably, in 2021, the oral MucoRice-CTB vaccine completed a phase 1 study to assess safety and microbiota-dependent immunogenicity (Yuki et al., 2021).

Plants with oil-rich seeds include tobacco (Rossi et al., 2013; Rossi et al., 2014), soybean (Moravec et al., 2007), and rapeseed (Lee et al., 2011). For oil-rich seeds, the oral administration of transgenic tobacco seeds in mice and piglets protected against the verocytotoxic-producing *E. coli* (VTEC) strain and showed a significant increase in fecal IgA antibody response (Rossi et al., 2013; Rossi et al., 2014).

In addition to oil-rich seeds, oil formulation matrices have been used to encapsulate PD within an oral delivery system. Previous findings demonstrated that mixing freeze-dried plant material with an oil-based emulsion (peanut oil: water = 62.5 %: 37.5 %) as an oral plant vaccine elicited mucosal and systemic immune responses in mice and sheep.

Taken together, starch- and oil-rich seeds have been demonstrated to provide gastric protection for PD when administered orally, but release PD enzymatically in the small intestine (Xiao et al., 2016). Therefore, edible seeds rich in both starch and oil provide suitable vehicles for oral delivery of PD.

I.4.3. The *N. tabacum* cultivar SL632 might be used for seed-based oral delivery due its high yield of nicotine-free seeds

N. tabacum cultivar SL632 (Sunchem N.L., Netherlands) was bred from *N. tabacum* cultivar Solaris (international patent PCT/IB/2007/053412), with oil content up to 45 %, protein content up to 28 %, seed yield 9 tons ha⁻¹ a⁻¹ (Fatica et al., 2019; Grisan et al., 2016). Due to its high seed yield, SL632 is termed as seed-rich tobacco cultivar. Furthermore, due to its nicotine content <5 µg kg⁻¹ leaf dry mass (LDM) compared to smoking tobacco varieties containing 3-30 mg kg⁻¹ nicotine, SL632 is also termed as nicotine-free cultivar.

Taken together, seed-enriched SL632 is suitable for oral administration due to its high protein content, promoting a high accumulation of PD. Additionally, its elevated seed oil content provides a matrix for the *in planta* encapsulation (Chapter I.4.). Moreover, the absence of detectable nicotine levels further enhances its suitability for effective oral delivery of therapeutic agents.

I.5. Recombinant proteins can be directly produced in plants

PD, also termed as biopharmaceuticals, are currently predominantly produced in microbes (e.g., bacteria like *E. coli* or yeasts like *Saccharomyces cerevisiae* or *P. pastoris*), if they do not require complex PTM, or mammalian cell cultures (chinese hamster ovary cells, CHO or human embryonic kidney 293 cells, HEK293) in case of proteins with a sophisticated disulfide and glycosylation pattern or in case of multimeric proteins (Kesik-Brodacka, 2018).

However, for upstream processing (USP), microbes and mammalian cell cultures require large capital-intensive facilities for bioreactor-based fermentation systems as well as expensive media and absolute sterility due to the risk of contamination with human pathogens like bacteria and viruses (Chen and Davis, 2016), while for downstream processing (DSP), they require thorough protein purification to remove bacterial endotoxins (Zeltins, 2013) and animal viruses (Kesik-Brodacka, 2018), increasing the overall production costs (Chapter I.5.2.).

Therefore, the production of PD in plants has been established, termed as plant-made (bio-)pharmaceuticals (PMPs), with the advantages of low production costs and high safety (Arntzen, 2015). Plants can be grown for PD production in simple contained greenhouse or vertical farm facilities, which is substantially lower with regard to the resource- and energy-consumption, and can be grown in simple inexpensive media, using soil as substrate and light as energy source (Holtz et al., 2015; Ma et al., 2015; Stoger et al., 2014). Moreover, in terms of safety, human pathogens do not replicate in plants, while plants introduce few pathogens and plant viruses which do not infect human cells. This reduces the risk of contamination when producing PD so that there is no need for absolute sterility, facilitating both USP and DSP (Kusnadi et al., 1997; Lico et al., 2008).

Due to the greenhouse cultivation and no need for absolute sterility, the plant-based production system is also easier to scale-up compared to the bioreactor-based infrastructure for microbes and mammalian cells, offering additional benefits in terms of scalability for PD that are required in huge amounts, e.g., for the treatment of diabetes and obesity (Castilho et al., 2014). Case studies shown that plant-based platforms had average production costs of 100-1000 € g⁻¹ protein, while bioreactor-based platforms had average production costs of 500-2.000 € g⁻¹ protein (Knödler et al., 2023; Ridgley et al., 2023; Tusé et al., 2014; Yuki et al., 2021).

Among plant-based production platforms, Common tobacco (*Nicotiana tabacum*) and Australian tobacco (*Nicotiana benthamiana*) are currently the main hosts for PD/PMP production, due to the high leaf biomass yield per time and area, but seeds of pea, soybean, maize, barley, rice and tobacco are also used. While in case of tobacco leaves, due to the presence of alkaloids like nicotine, the PD needs to be purified before it can be applied (Buyel et al., 2015c; Buyel and Fischer, 2014a), plant seeds used for PD production are edible and essentially free of toxic metabolites, so they can be directly orally administered without purification. This also includes tobacco seeds.

I.5.1. Recombinant proteins can be expressed in plants by either stable or transient transformation

The PD/PMP are typically produced in plant either by stable or transient expression, using the *Agrobacterium tumefaciens* (recently renamed to *Rhizobium radiobacter*) as vector for gene transfer. *A. tumefaciens* is a Gram-negative soil bacterium that can infect wound plant tissue and plant cells by nature and that is capable of transferring DNA fragments (transfer DNA, T-DNA) carrying functional genes into the host plant genome. After the T-DNA is transported into the plant cell, it is integrated into the plant nuclear genome with the help of a set of virulence proteins (vir proteins). The T-DNA is located on a tumor-inducing (Ti) plasmid in *A. tumefaciens* and naturally contains genes that induce the formation of crown galls and the production of nopaline- and octopine-type sugars in the crown galls which are then used as carbon and energy source by *Agrobacterium* (Chilton et al., 1977; Gelvin, 2003; Zupan et al., 2000).

A previous study has demonstrated that one or more T-DNA sequences are present in the sequences of all cultivated sweet potato germplasm but not in related wild relatives, suggesting that T-DNA is transferred to sweet potato progeny affecting plant traits. Hence, genetic modifications of the plant genome via the *Agrobacterium* and the T-DNA are a natural phenomenon, and sweet potatoes are naturally genetically modified plants (Kyndt et al., 2015). For PD/PMP production in plants, the Ti genes were replaced by the gene-of-interest (GOI) for PD, which is then integrated into the plant genome without inducing the formation of crown galls, and selection marker for selection of stably transformed plant cells from non-transformed ones. A typical plant expression vector is the pLH9000 (Hausmann and Töpfer, 1999) or the pTRA plasmid (Maclean et al., 2007).

This process can be used both for stable and transient transformation in *N. tabacum* and *N. benthamiana* while for seeds only stable transformation is possible.

I.5.1.1. Stable transformation expression system can produce recombinant proteins in leaves and seeds but is time-consuming

Stable transformation can be divided into nuclear transformation (stable integration into the plant nuclear genome) and chloroplast transformation (stable integration into the plant plastid genome). Both for stable and chloroplast transformation, tobacco is a widely used crop for PD production.

Chloroplast transformation is a method for producing transgenic plants by integrating the GOI into the plastid genome (Ozyigit and Yucebilgili Kurtoglu, 2020). In contrast to stable transformation, chloroplast transformation does not rely on *A. tumefaciens* but instead relies on biolistic transformation via particle bombardment, where the T-DNA is introduced using tungsten or gold particles. The most striking feature of the chloroplast genome is its high copy number, which may contain as many as 10,000 chloroplast genes per plant cell (Boyhan and Daniell, 2011). This enables chloroplast transformation to express high levels of exogenous proteins, accounting for >70 % total soluble protein (TSP) (Adem et al., 2017; Ruhlman et al., 2010) or 20 mg - 2.9 g kg⁻¹ leaf fresh mass (LFM), respectively (Table 2). For example, the green fluorescent protein-fibroblast growth factor 21 (GFP-FGF21) fusion protein has been expressed at 1.9 g kg⁻¹ LFM in transplastomic tobacco (Wang et al., 2023). However, due to the bacterial origin, transplastomic plants are unable to produce complex PD, unlike stably nuclear transformed plants such as Transferrin (Table 3).

In nuclear transformation, T-DNA is typically integrated into the plant genome by *Agrobacterium*-mediated transformation for inheritance to the next generation (Verwoerd et al., 1989) (Chapter I.5.1.). The *Agrobacterium*-mediated transformation protocol for stable transformation (Horsch et al., 1985): 1) Plant seeds are sterilized for *in vitro* culture. 2) Leaves from sterile plants are cut into leaf discs, and the leaf discs are wounded. In the case of cereals, embryos prepared from sterilized seeds are used instead of leaf discs. 3) For leaf/embryo transformation, leaf discs are co-cultured with *Agrobacterium* containing the recombinant expression vector. In addition to the GOI, the T-DNA also contains an antibiotic or herbicide resistance marker (e.g., kanamycin or phosphinothricin) for the selection of transformed and non-transformed cells. 4) During single-cell selection, plate infected leaf discs on agar plates containing transformation medium (e.g., ACB medium) and antibiotics or herbicides until callus formation and shoot development. At this stage, an antibiotic for

inhibiting *Agrobacterium* growth needs to be added as well. 5) Transfer newly developed shoots to agar plates containing cultivation medium (e.g., MS or LS medium) and antibiotics. 6) Confirm the positive transformants using polymerase chain reaction (PCR) to verify the presence of the GOI in each transformant. 7) Transfer the T0 plant transgene to the soil in the greenhouse for cultivation and leave or seed production.

The PD in leaves under nuclear transformation yielded 3.0 mg - 1.0 g kg⁻¹ LFM (Table 2). For example, Transferrin has been produced at 37 mg kg⁻¹ LFM in stably transformed transgenic tobacco leaves (Choi et al., 2014). However, the production of PD in transgenic leaves requires immediate freezing, lyophilization, or purification due to the rapid degradation of leaf proteins after harvest (Basaran and Rodríguez-Cerezo, 2008). Additionally, leaves like those of tobacco contain toxic alkaloids such as nicotine, which makes them unsuitable for oral application unless they are purified before administration (Chapter I.5.2.). For this reason, PD produced in leaves of stably transformed tobacco was calculated at a cost of 500-1,000 € g⁻¹ protein for moderate accumulation levels <100 mg kg⁻¹ LFM (Tusé et al., 2014). In contrast, transgenic seeds can be stored under ambient conditions for at least 6 years after harvest (Benchabane et al., 2008; Boothe et al., 2010; Coskun et al., 2008; Cunha et al., 2011), thereby reducing production costs downstream of the cold chain (Chapter I.4.2.). Since the DSP makes up to 80 % of the total costs (Wilken et al., 2012), the costs for seed-based PD production might be below 100 € g⁻¹.

For transgenic seeds, starch-rich crops have been commonly used to produce recombinant proteins, yielding 160 mg - 15.0 g kg⁻¹ seed dry mass (SDM). Among them, the yield of Tf expression in rice was as high as 10.0 g kg⁻¹ SDM (Table 3). Notably, rice seeds have been used in oral vaccination trials (Chapter I.4.2.). Additionally, oil-rich tobacco seeds have been used for the production of recombinant proteins, yielding 30.4 mg - 6.5 g kg⁻¹ SDM (Table 3). Consequently, oil-rich tobacco seeds had a similar range compared to starch-rich crops and were therefore equally suitable. Notably, tobacco seeds lack alkaloids such as nicotine and are thus edible. Previous studies have shown the use of tobacco seeds in piglet oral vaccine trials (Chapter I.4.2.). Hence, tobacco seeds may be a suitable platform for the seed-based oral delivery of PD such as FGF21-F-Tf.

However, PD needs to be produced in a contained environment such as a greenhouse and the seed production in greenhouses has to be established. This has already been done for barley (ORF Genetics, Island) and rice seeds (Ventria Bioscience, USA) in greenhouses. Notably, in a clinical study involving the use of rice seeds for an oral vaccine, the cost of PD in a

greenhouse production is calculated at 0.08 € g⁻¹ SDM. This cost corresponds to 28 € g⁻¹ PD for high accumulation levels of 3 g kg⁻¹ SDM (Yuki et al., 2021), which is 18- to 36-fold lower compared to the cost of PD purified from transgenic leaves.

Taken together, stable transformation is very time-consuming, and it takes a lot of time to produce transgenic plants for leave production (1-2 years) or seed production (2-3 years) (Hernández-Velázquez et al., 2015) as shown for tobacco as model plant for PD/PMP production.

Table 2. Yield of recombinant proteins in transgenic leaves of *N. tabacum*.

Genome-based expression	Recombinant protein	Promoter/Terminator	Protein accumulation in transgenic leaves [mg kg ⁻¹ LFM]	Reference
Tobacco Nuclear	FGF21-F-Tf	p35S/t35S	6.7 ± 0.2 (T2)	This study
	Major ampullate spidroin protein 2	p35S/tNos	3.05	(Menassa et al., 2004)
	Erythropoietin	p35S/tNos	8	(Conley et al., 2011)
	Complement factor 5a	p35S/t35S	11.2	(Nausch et al., 2012a)
	Transferrin	p35S/tNos	37	(Choi et al., 2014)
	Interleukin 10	p35S/tNos	64	(Conley et al., 2011)
	Interleukin 6	p35S/t35S	112	(Nausch et al., 2012b)
	Endoglucanase E1	pRbcS-3C/t7-t5	140	(Dai et al., 2000)
	Hyperthermostable α-amylase from <i>Pyrococcus furiosus</i>	p35S/tNos	200	(Conley et al., 2011)
	Human papillomavirus type 16 L1 capsid protein	p35S/t35S	650	(Maclean et al., 2007)
Tobacco Chloroplast	Synthetic antibody against <i>Pseudomonas aeruginosa</i>	p35S/tNos	1,000	(Conley et al., 2011)
	Coagulation factor IX fused with cholera toxin β-subunit (without a furin cleavage site)	pPsbA/tPsbA	20	(Verma et al., 2010)
	Coagulation factor IX fused with cholera toxin β-subunit (with a furin cleavage site)	pPsbA/tPsbA	400	(Verma et al., 2010)
	Exendin-4 fused with cholera toxin β-subunit	pPsbA/tPsbA	500	(Kwon et al., 2013)
	Proinsulin fused with cholera toxin β-subunit (with 3 furin cleavage sites)	pPsbA/tPsbA	2,920	(Boyhan and Daniell, 2011)
	GFP-FGF21	pPrn/tTrps16	1,923	(Wang et al., 2023)

LFM – leaf fresh mass; p35S – CaMV promoter with duplicated transcriptional enhancer; pRbcS-3C – leaf specific tomato Rubisco small subunit promoter; pPsbA – chloroplast psbA promoter; pPrn – plastid rRNA operon promoter; tNos – *Agrobacterium tumefaciens* nopal synthase terminator; t35S – CaMV terminator; t7-t5 – T7-T5 terminators; tPsbA – chloroplast psbA terminator; tTrps16 – plastid rps16 terminator; CaMV – cauliflower mosaic virus.

Table 3. Yield of recombinant proteins in transgenic seeds of different crops. Numbers represent mean \pm standard deviation.

Plant	Recombinant protein	Promoter/Terminator	Protein accumulation in transgenic seed [mg kg ⁻¹ SDM]	Reference
Tobacco	FGF21-F-Tf	p35S/t35S	6.7 \pm 0.2 (T1)	This study
	Complement factor 5a	p35S/t35S	35.8 (T1); 30.4 (T2)	(Nausch et al., 2012a)
	FLAG multimeric protein	pUSP/t35S	190	(Weichert et al., 2016)
	scFv antibody	pLeb4/t35S	230	(Fiedler and Conrad, 1995)
	Interleukin 6	p35S/t35S	273.6 (T1); 303.1 (T2)	(Nausch et al., 2012b)
	Insulin-like growth factor binding protein-3	pPhas/tPhas	800	(Cheung et al., 2009)
	Hemagglutinin	pPhas/tArc	3,000	(Ceballo et al., 2017)
	Anti-hepatitis B surface antigen antibody	pPhas/tArc	6,500	(Hernández-Velázquez et al., 2015)
Barley	Anti-HIV antibody	pGlo1/tNos	160	(Hensel et al., 2015)
	GFP	pGlo1/tNos	1,200	(Hensel et al., 2015)
Maize	β -glucuronidase	pUbi/tPinII	1,300	(Kusnadi et al., 1997)
Pea	Anti-Eimeria antibody	pUSP/t35S	1,800	(Zimmermann et al., 2009)
Soybean	Bone morphogenetic proteins 2	pCon/tCon	9,300	(Queiroz et al., 2019)
Rice	Transferrin	pGt1/tNos	10,000	(Zhang et al., 2010)
Arabidopsis	Murine single chain variable fragment G4	pPhas/tArc	10,000-15,000	(Jaeger et al., 2002)

SDM – seed dry mass; p35S – CaMV 35S promoter; pCon – β -conglycinin α -subunit promoter; pGlo1 – *Avena sativa* Globulin 1 promoter; pGt1 – *Oryza sativa* seed storage protein glutelin 1 promoter; pLeb4 – *Vicia faba* Legumin B4 promoter of the 11S globulin; pPhas – *Phaseolus vulgaris* promoter of the 7S globulin; pUbi – *Zea mays* upquitin 1 promoter; pUSP – *Vicia faba* unknown seed protein promoter; t35S – CaMV 35S terminator; tArc – *Phaseolus vulgaris* terminator of the arcilin 5-I seed storage protein; tCon – β -conglycinin α -subunit terminator; tNos – *Agrobacterium tumefaciens* nopal synthase terminator; tPhas – *Phaseolus vulgaris* terminator of the 7S globulin; tPinII – *Solanum tuberosum* potato proteinase inhibitor II terminator; CaMV – cauliflower mosaic virus.

I.5.1.2. Transient expression system can rapidly produce recombinant proteins in leaves but requires downstream purification

Stable transformation is time-consuming, and it takes a substantial amount of time to generate transgenic plants (1-2 years) (Chapter I.5.1.1.). Compared to stable transformation, transient expression can provide relevant quantities within weeks, but is restricted to leaf tissue of *N. benthamiana*.

Transient transformation also relies on *A. tumefaciens* and exploits the fact that during the process of T-DNA transfer and genome integration, there is a transient high number of T-DNAs present in the nucleus of >1,000 copies. Due to the high copy number, it results in relatively high expression levels shortly after infection within 1-2 days. After 3-14 days the expression level drops because only 1-10 copies are integrated into the plant genome, and all T-DNAs that are not integrated into the genome are degraded. By this time, the plant biomass is harvested (Gelvin, 2000). Transient transformation omits the clone selection (e.g., selection of individual transgenic plant cells that are regenerated to whole plants) required for the stable transformation and allows the production of the target protein within 1 week from WT plants. Moreover, due to the above-mentioned mode of action, transient expression usually yields substantially more recombinant protein or PD compared to stable transformed plant cells.

Transient transformation is typically achieved at large-scale by vacuum infiltration (Gengenbach et al., 2018; Giritch et al., 2006; Shamloul et al., 2014): 1) Plant seeds of *N. benthamiana* are grown in rockwool or soil pots for 4-9 weeks. 2) *Agrobacterium* containing the recombinant expression vector are grown in bioreactors for 1 day and then an infiltration solution, containing the *Agrobacteria*, prepared. 3) The 4-9-week-old plants are put upside down and immersed in the *Agrobacterium* infiltration solution for vacuum infiltration. A vacuum is applied to force the gases out of the intercellular space between the plant cells in the leaves, and then pressure is equalized to ambient conditions to infuse *Agrobacterium* suspension into the intercellular space of the plant leaves. 4) Transfer the infiltrated plants to the original plant growth environment and continue culturing for 2-7 days.

For transient expression, the same T-DNA vector is used as in stable transformation, such as the pLH9000 or pTRA plasmids (Chapter I.5.1.2.). However, transient transformation systems can also utilize elements of viral replicons, inducing either hyper-replication of the episomal T-DNA, such as the geminivirus systems (Yamamoto et al., 2018), hyper-transcription of the mRNA such as magnICON (Marillonnet et al., 2005) and TRBO (Lindbo, 2007), or hyper-translation of the mRNA, such as pEAQ (Sainsbury et al., 2009). Due to the excessive

expression of the genes on the T-DNA cassette, endogenous proteins are not produced, which are essential for the plant cell survival, and the cells die within 10-14 days, causing the GOI expression to stop as well. However, replicating RNA viral vectors are limited by the size of the insert (maximum size of DNA length of 2 kb) unlike standard vectors such as pLH9000 or pTRA (Gleba et al., 2005; Marillonnet et al., 2005). For larger GOIs, the transgene needs to be split into different fragments and co-expressed by different viral vectors (Giritch et al., 2006) (Table 4).

The PD production of both standard and viral vectors can be further boosted by the co-expression of p19 RNA silencing suppressor of tomato bushy stunt virus (TBSV) that inhibits the post-transcriptional gene silencing pathway (Voinnet et al., 1999). However, stable expression of the p19 protein in transgenic plants can have phenotypic and thus deleterious effects on the plant. For example, in transgenic *N. benthamiana*, the p19 gene caused curved flower bases, blistered leaf cuticles, or hairy, serrated leaves, while in transgenic tobacco, the p19 gene caused severely misshapen flowers. For this reason, the inhibitory effect of p19 on post-transcriptional gene silencing is limited to transient expression (Siddiqui et al., 2008).

For transient expression, *N. benthamiana* is commonly used as a plant model because it lacks an RNA-dependent RNA polymerase (RdRP)-based pathogen defense mechanism and is therefore immunocompromised (Yang et al., 2004). Since *N. benthamiana* plants only need 4-9 weeks of growth to be infected by *A. tumefaciens* and 1 week for transient expression, PD can be produced in 2-3 months in relevant amounts.

Typical accumulation levels of PD can reach up to 6 g kg⁻¹ LFM (Castilho et al., 2014) (Table 4). For example, FG21 and a GFP-FGF21 fusion have been expressed at 5 mg kg⁻¹ LFM and 450 mg kg⁻¹ LFM via transient expression (Fu et al., 2011).

However, plant transient transformation also has some disadvantages. First, transient transformation via vacuum infiltration is not as scalable as the cultivation of stably transformed plants due to the need for cultivating *Agrobacterium* in bioreactors and using the vacuum infiltration device, making it less suitable for the mass production of PD for the treatments such as obesity or diabetes (Commandeur and Twyman, 2004). Second, *N. benthamiana* leaves contain nicotine, and the use of *Agrobacterium* may introduce bacterial endotoxins, making them unsuitable for oral delivery and requiring thorough downstream purification (Chapter I.5.2.). For example, purified PD from transiently transformed leaves cost 100-500 € g⁻¹ PD (Knödler et al., 2023; Ridgley et al., 2023; Tusé et al., 2014), which is 4- to 18-fold higher compared to the 28 € g⁻¹ PD for transgenic rice seeds (Yuki et al., 2021).

Table 4. Yield of recombinant proteins in transient leaves of *N. benthamiana* under 2 transient expression vectors. MagnICON: replicating viral vector; pTRAc: non-replicating viral vector.

Vector system	Recombinant protein	Promoter/Terminator	Protein accumulation in transient leaves [mg kg ⁻¹ LFM]	Reference
MagnICON (TMV/PVX)	FGF21	PVX-SgPr/PVX-Sgt	5	(Fu et al., 2011)
	Glutamic acid decarboxylase	TMV-SgPr/TMV-Sgt	227	(Merlin et al., 2016)
	smGFP-hFGF21	PVX-SgPr/PVX-Sgt	450	(Fu et al., 2011)
	Full-size IgG antibodies (TMV and PVX co-expression)	TMV-SgPr/TMV-Sgt PVX-SgPr/PVX-Sgt	500	(Giritch et al., 2006)
	Complement factor 5a	PVX-SgPr/PVX-Sgt	559	(Nausch et al., 2012a)
	GFP	TMV-SgPr/TMV-Sgt	4,000	(Marillonnet et al., 2005)
	Colicin-M-like Klebsiella protein	TMV-SgPr/TMV-Sgt	4,448	(Denkovskienė et al., 2019)
	α 1-antitrypsin	TMV-SgPr/TMV-Sgt	6,000	(Castilho et al., 2014)
pTRA	Viscumin	p35S/t35S	3	(Gengenbach et al., 2019)
	Secretory immunoglobulin A	p35S/t35S	500	(Ma et al., 1995)
	Human papillomavirus L1 protein	p35S/t35S	533	(Maclean et al., 2007)
	Chimeric M12-4E10 antibody	p35S/t35S	250-2,500	(Zischewski et al., 2016)

LFM – leaf fresh mass; TMV-SgPr – TMV subgenomic promoter; PVX-SgPr – PVX subgenomic promoter; p35S – CaMV 35S promoter with duplicated transcriptional enhancer; TMV-Sgt – TMV subgenomic terminator; PVX-Sgt – PVX subgenomic terminator; t35S – CaMV 35S terminator; TMV – tobacco mosaic virus; PVX – potato virus X; SgPr – subgenomic promoter; Sgt – subgenomic terminator; CaMV – cauliflower mosaic virus.

I.5.2. Downstream processing of protein drug from plant tissue requires extraction, clarification/filtration and purification but might not be necessary for seed-produced protein drugs

Since tobacco is widely used for PD production (Chapters I.4.1. and I.4.2.), but requires the purification of PD due to the presence of alkaloids like nicotine (Chapter I.5.), DSP methods have been specially developed for the purification of tobacco leaf recombinant proteins. These methods can be divided into extraction, clarification and filtration, purification.

During extraction, harvested tobacco leaves are added to a suitable extraction buffer and mechanically homogenized via rotating blade systems, bead mills, and other systems (Menkhaus et al., 2004; Wang et al., 2008; Wilken and Nikolov, 2012). For the most efficient protein extraction, extraction buffers often contain phosphate and salt to stabilize pH and improve protein solubilization, e.g., PBS (Hassan et al., 2008; Wilken and Nikolov, 2012). Additionally, the addition of detergents (e.g., SDS, NP-40 and Triton X-100) (Kumar et al., 2021), phenolic binding agents (e.g., polyvinylpolypyrrolidone (PVPP)) (Holler et al., 2007; Holler and Zhang, 2008), and antioxidants (e.g., β -2-mercaptoethanol (BME) or dithiothreitol (DTT)) (Holler et al., 2007; Holler and Zhang, 2008) to the extraction buffer can also improve the solubility of the extracted protein and prevent protein oxidation. However, detergents and antioxidants may interfere with purification (Fischer et al., 2004; Holler et al., 2007; Holler and Zhang, 2008).

Leaf homogenization produces a large amount of process-related impurity particles in the crude extract, which need to be removed by clarification and filtration before purification. For example, plant fibers, cell debris, host cell proteins (HCP), and secondary metabolites, etc. (Menkhaus et al., 2004; Wilken and Nikolov, 2012).

Preliminary particle removal during clarification can be achieved by: 1) flocculants with different ionic charges for adsorption deposition (Barany and Szepesszentgyörgyi, 2004; Buyel et al., 2015b; Gregory and Barany, 2011), and/or 2) heat and pH treatment for the precipitation of HCP (Buyel and Fischer, 2014b; Menzel et al., 2016; Opdensteinen et al., 2021b).

The crude extract is then clarified through a combination of filters of different materials and pore sizes. For example, sequential filtration from large to small pore sizes to retain particles, such as bag filter (e.g., 1-800 μ m), depth filter (e.g., 6-15 μ m), and sterile filter (e.g.,

membrane filters 0.22 and 0.45 μm) (Buyel et al., 2015a; Buyel and Fischer, 2014b; Knödler et al., 2023; Rühl et al., 2018).

The content of the particles is monitored via nephelometric turbidity units (NTU). While the crude extract typically has 10,000-40,000 NTU, the clarified extract after sterile filtration usually has 1-10 NTU. To prevent clogging of the filter, filter aids like cellulose or diatomaceous earth (DE) can be added to the crude extract that can make the solid particles form a loose sponge-like structure to prevent the solid particles from forming dense particles and clogging the filter (Buyel et al., 2015a). However, bag and depth filters not only absorb HCP but may also bind the target PD, resulting in a substantial loss of PD (Yigzaw et al., 2006), which is not the case for sterile filter systems (Rühl et al., 2018).

Finally, in the protein purification process, the target protein is separated from HCP, further improving protein purity. The current protein purification methods can be roughly divided into: 1) Salting-out precipitation: Adding ammonium sulfate to separate the protein from the solution (Wingfield, 2001). 2) Size exclusion chromatography: Separation based on the size and shape of the protein (Burgess, 2018). 3) Ion exchange (IEX) chromatography: Separation based on the difference in protein charge. For example, anion exchange (AEX) or cation exchange (CEX) (Duong-Ly and Gabelli, 2014). 4) Affinity chromatography: Utilizing the specific binding between protein molecules of different structures to separate them (Kimple et al., 2013). For example, Immobilized metal affinity chromatography (IMAC) (Cheung et al., 2012).

The final ultrafiltration/diafiltration (UF/DF) is used for the removal of residual HCP, protein concentration, and buffer exchange (Cromwell et al., 2006; Opdensteinen et al., 2018).

For PD produced in stably or transiently transformed leaves, the DSP process can be omitted in case of stably transformed edible seeds.

I.6. Aim of the thesis

FGF21 is a potential PD drug candidate to treat NAFLD and NASH, but it needs to be exclusively targeted to the liver, which can be achieved by oral administration, since the portal vein goes from the intestine directly to the liver before entering the blood system. The translocation from the intestine to the blood might be achieved by the fusion to transferrin (FGF21-Tf). However, Tf prolongs the half-life of the fusion protein and promotes circulation in the blood, but after translocation, subsequent separation of FGF21 and Tf can be achieved by introducing a furin cleavage site (FGF21-F-Tf). Moreover, for oral administration, FGF21 needs to be protected from the acidic conditions in the stomach and transported from the intestine to the portal vein, and plant matrices can provide protection from acids and enzymes in the stomach by *in planta* bioencapsulation. However, PD needs to be produced in a contained environment such as greenhouse and seed production in greenhouses has to be established.

The aim of the PhD thesis was to establish a seed-based oral delivery system for a FGF21-F-Tf fusion protein.

I.6.1. Optimization tobacco seed yield in contained greenhouses

Since transgenic tobacco needed to be grown in a closed contained environment for commercial PD production, I selected a seed-rich and a leaf-rich *N. tabacum* cultivar as hosts. I used non-transformed plants to investigate different cultivation strategies to maximize seed production and then analyzed the seed yield per area and time.

I.6.2. Stable FGF21-F-Tf expression in seeds of *N. tabacum* SL632

For establishing FGF21-F-Tf production in *N. tabacum* seeds, I generated transgenic seeds as a proof-of-concept for both seed-rich and leaf-rich cultivars. Therefore, I established *in vitro* propagation and transformation of SL632. I also analyzed intact FGF21-F-Tf accumulation in transgenic T0 and T1 seeds and calculated intact FGF21-F-Tf accumulation per area and time in the greenhouse.

I.6.3. Transient FGF21-F-Tf expression in leaves of *N. benthamiana*

For proofing the bioavailability and bioactivity, I also transiently produced FGF21-F-Tf in *N. benthamiana* leaves to increase the stability and accumulation of the FGF21-F-Tf fusion protein.

I.6.4. Purification of nTf338-FGF21-PLUS for proof-of-concept bioavailability and bioactivity studies

To evaluate the oral delivery system, I chose the stabilized FGF21-F-Tf from the transiently transformed *N. benthamiana* and established a purification method so that partially purified protein could be used in *in vitro* and *in vivo* studies with mice by the cooperation partner the German Institute of Human Nutrition Potsdam-Rehbrücke (DIfE).

The main outcome of these experiments was successfully published in “**Hou, H.W., Bishop, C.A., Huckauf, J., Broer, I., Klaus, S., Nausch, H., Buyel, J.F. (2022). Seed- and leaf-based expression of FGF21-transferrin fusion proteins for oral delivery and treatment of non-alcoholic steatohepatitis. Frontiers in Plant Science 13: 998596; 10.3389/fpls.2022.998596**” (doi: 10.3389/fpls.2022.998596), which are described in detail in the following sections.

II. Materials and Methods

II. Materials and Methods

II.1. Preface

The experiments with the MagnICON vectors were conducted at the University of Rostock (UR), while the experiments with the pTRAc vectors were done at the Fraunhofer Institute for Molecular Biology and Applied Ecology IME (IME). The stably transformed tobacco plants were created at the University of Rostock and analyzed at the Fraunhofer Institute for Molecular Biology and Applied Ecology IME. Animal trials were performed at the German Institute of Human Nutrition Potsdam-Rehbrücke (DIfE).

II.2. Materials

The register of equipment and materials is detailed in Table 5, and Table 6 and Table 7 contain lists of chemicals and buffers, respectively.

Table 5. Register of equipment and materials.

Type	Name	Manufacturer
Autoclave	Varioklav	HP Labortechnik GmbH, Germany
Autoclave	CV-EL 12L/18L	CertoClav Sterilizer GmbH, Austria
Autoclave	VX-150	Systec GmbH, Germany
Bead mill	Bead mill 300 MM	Retsch GmbH, Germany
Blender	HR3655/00 Standmixer	Philips B. V., Netherlands
Blotting paper	Whatman paper	Whatman Inc., UK
Blotting membrane	Amersham Protran nitrocellulose membranes	VWR International, USA
Blotting membrane	PVDF membrane	Millipore, USA
Blotting device	Trans Blot Cell	Bio-Rad Inc., USA
Chromatography device	ÄKTA pure	Cytiva, USA
Chromatography column	XK26/20 column	Cytiva, USA
Chromatography resin	Chelating Sepharose Fast Flow resin	Cytiva, USA
Centrifuge	5415R	Eppendorf AG, Germany
Centrifuge	Allegra 25R	Beckman Coulter, USA
Centrifuge	Mikro 200R	Hettich GmbH, Germany
Centrifuge	ROTINA 380 R Robotic	Hettich GmbH, Germany
Centrifugal concentrator	Vivaspin 15R centrifugal concentrator with MWCO of 30 kDa	Sartorius AG, Germany
Clean-bench	B-[MacPro]2-130	Berner International GmbH, Germany
Clean-bench	BioWizard	Kojair Tech Oy, Finland
Conductivity measuring cell	TetraCon 325	WTW GmbH, Germany
Conductometer	Cond 315i	Xylem Analytics Germany Sales GmbH & Co. KG, Germany
Cryotube	Cryo-conservation tube, 2.0 mL	VWR International, USA
Cuvette	Cuvettes ROTILABO®, 1.6 ml	Carl Roth GmbH, Germany
Depth filter	Double-layer PDH4 depth filter, a combination of K700 and KS50	Pall Corporation, USA
Electrophoresis power supply	PowerPac 300	Bio-Rad Inc., USA
Electrophoresis power supply	PowerPac Basic	Bio-Rad Inc., USA
Electrophoresis chamber	XCell SureLock Mini-Cell	Thermo Fischer Scientific Inc., USA
Electrophoresis chamber	XCell SureLock Midi-Cell	Thermo Fischer Scientific Inc., USA

Type	Name	Manufacturer
Filter bag	BP420 bag filter	Fuhr, GmbH, Germany
Filter paper	Filter paper 42 mm Grade 1	Whatman Inc., UK
Filter tissue	MiraCloth 1R	Merck KGaA, Germany
Freezer	GGU 1500, -20°C	Liebherr AG, Switzerland
Freezer	GS58NAW40, -20°C	Siemens AG, Germany
Freezer	HERAfreeze HFU 700 T, -80°C	Thermo Fischer Scientific Inc., USA
Homogenizer	FastPrep-24 5G	MP Biomedicals Inc., USA
Gel electrophoresis chamber	MiniSubCell GT	Bio-Rad Inc., USA
Gel scanning device	Universal Hood II	Bio-Rad Inc., USA
Grinding beads	Chrome-steel beads, 3 mm (CHR-003)	SpheroTech GmbH, Germany
Incubator	ISF1-X (Climo-Shaker)	Kuhner GmbH, Germany
Incubator	Labthem LT-X	Kuhner GmbH, Germany
Incubator	I-30 CLF	Plant Climatics GmbH, Germany
Mini centrifuge	Sprout	Heathrow Scientific LLC., USA
Mini Protein Gels	Invitrogen™ NuPAGE™ 4-12%, Bis-Tris, 1.0–1.5 mm	Thermo Fischer Scientific Inc., USA
Microwave	Micro Chef Fm 3515	Moulinex, France
Magnetic stirrer	KM02	IKA-Werke GmbH, Germany
Magnetic stirrer	RCT basic	IKA-Werke GmbH, Germany
Microplate	96-well CellStar flat clear F-bottom plate	Greiner Bio-One International GmbH, Austria
Microplate	Microplate lids Standard, no cut edges	Nalgene Nunc International Corporation, USA
pH meter	pH3110	Xylem Analytics Germany Sales GmbH & Co. KG, Germany
pH electrode	Minitrode	Xylem Analytics Germany Sales GmbH & Co. KG, Germany
Plate reader	Tecan infinite M200	Tecan Group Ltd., Switzerland
Photometer	Biophotometer 6131	Eppendorf AG, Germany
Peristaltic pump	Masterflex L/S, 1-100 rpm	Cole-Palmer Instrument Company LLC., USA
Pipette	Pipetman P20, 200, 1000 N	Gilson Inc., USA
Pipette	Serological pipette 2 mL, 5 mL, 10 mL, 50 mL	Greiner Bio-One International GmbH, Austria
PCR cyclor	2720 Thermal cyclor	Applied Biosystems, USA
Reaction tubes	Tube 1.5 mL, 2.0 mL	Sarstedt Inc., Germany
Reaction tubes	Tube 15 mL, 50 mL	Greiner Bio-One International GmbH, Austria
Refrigerator	FKUV1610, 4°C	Liebherr AG, Switzerland
Refrigerator	UK 1720, 4°C	Liebherr AG, Switzerland

Type	Name	Manufacturer
Rocker	Mini Gyro-Rocker SSM3	Cole-Palmer Instrument Company LLC., IL, USA
Scale	AZ6101	Sartorius AG, Germany
Scale	BP121S	Sartorius AG, Germany
Scale	BP610	Sartorius AG, Germany
Scale	TE4100	Sartorius AG, Germany
Scale	TE6100	Sartorius AG, Germany
Scanner	CanoScan 5600F	Canon Inc., Japan
Soil	A 400	Stender GmbH, Germany
Sterile filter	Bottle-Top-Filter, 0.2 µm	VWR International, USA
Sterile filter	Midisart 2000 air vent, 0.2 µm	Sartorius AG, Germany
Sterile filter	Sartopore 2 Capsule (pore size of 0.45 and 0.22 µm)	Sartorius AG, Germany
Syringe	Omnifix, 1 mL	Labomedic Medizin- und Labortechnik GmbH, Germany
Syringe	Omnifix, 50 mL	Labomedic Medizin- und Labortechnik GmbH, Germany
Spectrometer	NanoDrop ND-1000	Peqlab Biotechnologie GmbH, Germany
Spectrometer	Synergy HT microplate reader	BioTek Instruments, USA
Software	AIDA Image Analyzer analysis	Elysia-raytest GmbH, Germany
Software	Software Design Expert 11.0	State-Ease, USA
Software	Origin 2020b	OriginLab, USA
Tips	Pipette tips, 10 µL	Sarstedt GmbH, Germany
Tips	Pipette tips, 200 µL	Sarstedt GmbH, Germany
Tips	Pipette tips, 1000 µL	Sarstedt GmbH, Germany
Tips	Sterile filter tips, 10 µL	Sarstedt GmbH, Germany
Tips	Sterile filter tips, 200 µL	Sarstedt GmbH, Germany
Tips	Sterile filter tips, 1000 µL	Sarstedt GmbH, Germany
Turbidimeter	Hach turbidimeter	Hach Lange GmbH, Germany
Temperature-controlled mixer	Thermoshake	Inheco GmbH, Germany
Temperature-controlled mixer	Thermomixer compact	Eppendorf AG, Germany
Temperature-controlled mixer	Thermomixer E-5048	Eppendorf AG, Germany
Ultrapure water device	Arium Pro VF	Sartorius AG, Germany
Vacuum pump	PC 600 series Chemistry pumping unit PC 611NT MD 4C NT CEE	Vacuubrand GmbH & Co KG, Germany
Vortex	Vortex-Genie 2	Scientific Industries, USA

Table 6. List of chemicals.

Type	Name	Manufacturer
Antibiotic	Ampicillin	Duchefa B. V., Netherlands
Antibiotic	Kanamycin	Duchefa B. V., Netherlands
Antibiotic	Carbenicilin	Duchefa B. V., Netherlands
Antibiotic	Cefotaxim	Duchefa B. V., Netherlands
Antibiotic	Rifampicin	Duchefa B. V., Netherlands
Antibody	Goat α -rabbit H+L AP	Jackson ImmunoResearch Laboratories, USA
Antibody	Rabbit anti-DsRed	MBL International Corporation, USA
Antibody	Polyclonal rabbit anti-His	Hölzel Diagnostika Handels GmbH, Germany
Antibody	Polyclonal rabbit anti-human FGF21 (CSB-PA06404A0Rb-100)	Dianova GmbH, Germany
Antibody	goat anti-Rabbit IgG AP-conjugated antibody	Jackson ImmunoResearch Laboratories, USA
Antioxidant	Sodium disulfate ($\text{Na}_2\text{S}_2\text{O}_5$)	Carl Roth GmbH, Germany
Buffer component	Ammonium nitrate (NH_4NO_3)	Carl Roth GmbH, Germany
Buffer component	Calcium hypochlorite ($\text{Ca}(\text{ClO})_2$)	Carl Roth GmbH, Germany
Buffer component	Dimethyl sulfoxide (DMSO)	Carl Roth GmbH, Germany
Buffer component	Disodium hydrogen phosphate dihydrate ($\text{Na}_2\text{HPO}_4 \cdot 2\text{H}_2\text{O}$)	Carl Roth GmbH, Germany
Buffer component	Ethylenediaminetetraacetic acid (EDTA)	Carl Roth GmbH, Germany
Buffer component	Ethanol	Carl Roth GmbH, Germany
Buffer component	Glycine	Carl Roth GmbH, Germany
Buffer component	Glycerol	Duchefa B. V., Netherlands
Buffer component	Imidazole	Carl Roth GmbH, Germany
Buffer component	Methanol	Carl Roth GmbH, Germany
Buffer component	Magnesium sulfate (MgSO_4)	Sigma Aldrich Inc., USA
Buffer component	Magnesium chloride (MgCl_2)	Carl Roth GmbH, Germany
Buffer component	Magnesium sulfate heptahydrate ($\text{MgSO}_4 \cdot 7 \text{H}_2\text{O}$)	Carl Roth GmbH, Germany
Buffer component	2-(N-morpholino)ethanesulfonic acid (MES) monohydrate	Sigma Aldrich Inc., USA
Buffer component	Nickel(II) sulphate hexahydrate ($\text{NiSO}_4 \cdot 6 \text{H}_2\text{O}$)	Carl Roth GmbH, Germany
Buffer component	Potassium chloride (KCl)	Carl Roth GmbH, Germany
Buffer component	Potassium dihydrogen phosphate (KH_2PO_4)	Carl Roth GmbH, Germany
Buffer component	Sodium chloride (NaCl)	Carl Roth GmbH, Germany
Buffer component	Sodium acetate ($\text{C}_2\text{H}_3\text{NaO}_2$)	Carl Roth GmbH, Germany
Buffer component	Tris	Carl Roth GmbH, Germany
Buffer component	Tween-20	Carl Roth GmbH, Germany
Buffer component	Trichloroacetic acid (TCA)	Carl Roth GmbH, Germany

Type	Name	Manufacturer
Fertilizer	Ferty 2 Mega	H. Nitsch & Sohn GmbH, Germany
Fertilizer	Hakaphos Blue	Compo Expert GmbH, Germany
Fertilizer	Hakaphos Red	Compo Expert GmbH, Germany
Fertilizer	Wuxal Super	Hermann Meyer GmbH, Germany
Hormone	2,4-Dichlorophenoxyacetic acid	Duchefa B. V., Netherlands
LDS Gel staining	SimplyBlue SafeStain	Thermo Fischer Scientific Inc., USA
Media component	Agar	Carl Roth GmbH, Germany
Media component	Agarose	Carl Roth GmbH, Germany
Media component	B5-vitamine	Duchefa B. V., Netherlands
Media component	Gamborg B5 Vitamin Mixture	Duchefa B. V., Netherlands
Media component	6-Benzylaminopurine (6-BAP)	Sigma Aldrich Inc., USA
Media component	Fructose	Duchefa B. V., Netherlands
Media component	Plant agar	Duchefa B. V., Netherlands
Media component	Linsmaier and Skoog medium (including vitamins) (L0230)	Duchefa B. V., Netherlands
Media component	Murashige & Skoog Basal Salts Mixture (M0221)	Duchefa B. V., Netherlands
Media component	1-Naphthaleneacetic acid (NAA)	Sigma Aldrich Inc., USA
Media component	Sucrose	Duchefa B. V., Netherlands
Media component	Soy peptone	Carl Roth GmbH, Germany
Media component	Yeast extract	Carl Roth GmbH, Germany
Media component	Tryptone	Carl Roth GmbH, Germany
pH adjustment	Hydrochloride (HCl)	Carl Roth GmbH, Germany
pH adjustment	Sodium hydroxide (NaOH)	Carl Roth GmbH, Germany
Phytohormone	Acetosyringone	Duchefa B. V., Netherlands
Protein standard	Bovine serum albumin (BSA)	Thermo Fischer Scientific Inc., USA
Protein quantification	Pierce™ Bradford Plus Protein Assay Kit	Thermo Fischer Scientific Inc., USA
Protein quantification	Human FGF21 ELISA Kit (ab222506)	Abcam plc, UK
Protein electrophoresis	NuPAGE MES SDS Running Buffer, 20x	Thermo Fischer Scientific Inc., USA
Protein electrophoresis	NuPAGE Sample Reducing Agent, 10x	Thermo Fischer Scientific Inc., USA
Protein electrophoresis	NuPAGE Antioxidant	Thermo Fischer Scientific Inc., USA
Protein electrophoresis	NuPAGE LDS Sample Buffer, 4x	Thermo Fischer Scientific Inc., USA
Western Blotting	N, N-dimethylformamide (DMF)	Carl Roth GmbH, Germany
Western Blotting	5-bromo-4-chloro-3-indolyl-phosphate (BCIP)	Carl Roth GmbH, Germany
Western Blotting	Nitro blue tetrazolium (NBT)	Carl Roth GmbH, Germany
Western Blotting	SignalBoost™ Immunoreaction Enhancer Kit	Merck KGaA, Germany
Technical buffer	pH buffer 4, 7, 10	Xylem Analytics Germany Sales GmbH & Co. KG, Germany

Table 7. List of buffers.

Name	Component	Final concentration [mM] / [g/L]	Comment
Lysogeny broth (LB)	Tryptone	- / 10.0	
	Yeast extract	- / 5.0	Adjust pH to 7.0, then autoclave
	NaCl	- / 10.0	
	Agar	- / 15.0	Optional
Peptone agrobacterium medium (PAM)	Soy Peptone	- / 20.0	
	Yeast extract	- / 0.5	Adjust pH to 7.0, then autoclave
	Fructose	- / 5.0	
	MgSO ₄ •7 H ₂ O	4.0 / 1.0	
	Agar	- / 15.0	Optional
Yeast extract broth (YEB)	Beef extract	- / 5.0	
	Yeast extract	- / 1.0	
	Peptone	- / 5.0	Adjust pH to 7.0, then autoclave
	Sucrose	14.5 / 5.0	
	MgSO ₄ •7 H ₂ O	2.0 / 0.5	
	Agar	- / 15.0	Optional
Linsmaier and Skoog medium for Tobacco (LST)	Linsmaier and Skoog medium (Including vitamins) (L0230)	- / 4.4	
	Sucrose	- / 30.0	Adjust pH to 5.7, then autoclave
	Plant agar	- / 6.5	
B5 infection medium	Gamborg B5 Vitamin Mixture	- / 3.16	
	NH ₄ NO ₃	- / 0.25	Adjust pH to 5.7, then autoclave
	MES Monohydrat	- / 0.50	
	Sucrose	- / 30.0	
ACB agar medium	Murashige & Skoog medium Basal Salts Mixture (M0221)	- / 4.32	
	MES Monohydrat	- / 0.5	
	Sucrose	- / 30.0	Adjust pH to 5.7, then autoclave
	Agarose	- / 6.8	
	B5-vitamine	112 µg mL ⁻¹	
	6-Benzylaminopurine (6-BAP)	1 µg mL ⁻¹	
	1-Naphthaleneacetic acid (NAA)	0.1 µg mL ⁻¹	

Name	Component	Final concentration [mM] / [g/L]	Comment
Infiltration buffer for MagnICON	MES Monohydrat	10 / 2.1	Adjust pH to 5.5
	MgSO ₄	10 / 1.2	
	<i>A. tumefaciens</i> pellet	- / -	Adjust OD _{600nm} to 0.1-0.5
Infiltration buffer for pTRAc	Murashige & Skoog medium Basal Salts Mixture (M0221)	- / 0.5	Adjust pH to 5.6
	Acetosyringone (in DMSO)	0.2 / 0.0392	
	<i>A. tumefaciens</i> pellet	- / -	Adjust OD _{600nm} to 0.1-0.5
Extraction buffer	Na ₂ HPO ₄ •2H ₂ O	25.0 / 4.5	Adjust pH to 8.0
	NaCl	500.0 / 29.2	
	Na ₂ O ₅ S ₂	10.0 / 1.9	Optional
Blotting buffer	Tris	25.0 / 3.0	
	Glycine	192.0 / 14.4	Adjust pH to 8.3
	Methanol	- / 200.0	
phosphate-buffered saline (PBS)	NaCl	137.0 / 8.0	
	KCl	2.7 / 0.2	
	Na ₂ HPO ₄ •2H ₂ O	10.1 / 1.80	Adjust pH to 7.4
	KH ₂ PO ₄	1.7 / 0.24	
PBS (-T)	Tween-20	- / 1.0	Optional
alkaline phosphatase (AP) bufferr	Tris	100.0 / 12.1	
	NaCl	100.0 / 5.8	Adjust pH to 9.6
	MgCl ₂	5.0 / 0.48	
nitro blue tetrazolium/5-bromo-4-chloro-3-indolyl-phosphate (NBT/BCIP) solution	NBT	- / 0.30	
	BCIP	- / 0.15	Dissolve in N, N-dimethylformamide
IMAC equilibration buffer	Na ₂ HPO ₄ •2H ₂ O	20.0 / 3.6	
	NaCl	500.0 / 29.2	Adjust pH to 7.6
IMAC wash buffer	Na ₂ HPO ₄ •2H ₂ O	20.0 / 3.6	
	NaCl	500.0 / 29.2	Adjust pH to 7.6
	imidazole	10.0 / 0.68	
IMAC elution buffer	Na ₂ HPO ₄ •2H ₂ O	20.0 / 3.6	
	NaCl	500.0 / 29.2	Adjust pH to 7.6
	imidazole	150.0 / 20.4	

Name	Component	Final concentration [mM] / [g/L]	Comment
IMAC stripping buffer	Na ₂ HPO ₄ •2H ₂ O	20.0 / 3.6	Adjust pH to 7.5
	NaCl	500.0 / 29.2	
	EDTA	50.0 / 16.4	
IMAC – binding buffer	Na ₂ HPO ₄ •2H ₂ O	20.0 / 3.6	Adjust pH to 7.5
	NaCl	500.0 / 29.2	
	imidazole	30.0 / 2.0	
IMAC – 0.1 M NiSO ₄	NiSO ₄ •6H ₂ O	100.0 / 26.3	
IMAC – 1 M NaCl	NaCl	1000.0 / 58.44	
IMAC – 1 M NaOH	NaOH	1000.0 / 40.0	

II.3. Methods

II.3.1. Plant expression vectors

For all FGF21-Tf fusion constructs, the design elements, amino acid sequences, cloning methods (p9U vector; MagnICON vectors: pICH29921 and pICH31160; pTRAc vector), and the *A. tumefaciens* strains (ICF320 (MagnICON); GV3101::pMP90RK (pTRAc)) are described elsewhere (Hou et al., 2022). The primer amino acid sequences are provided in Table 8, and the constructs for stable and transient expression of FGF21-Transferrin fusion proteins are illustrated in Figure 7.

Table 8. Primers used in this study.

Gene/plasmid type	Primer	AA sequence
pICH29912-FGF21-F-IntN	FGF21_Nt-fw	5'- TGGACTACCACCAGCATTACCAGAAC -3'
	FGF21_Nt-rv	5'- GTGACCTACCTTGGGATGGACCAAC -3'
pICH31160-IntC-Tf	Tf_Nt-fw	5'- CCCCAACTTTGCCAACTCTGTCC -3'
	Tf_Nt-rv	5'- CATTGCGTCAGCCTCCCCATTC-3'
p9U-FGF21-Tf	FGF21-fw_screen	5'- AGCATTACCAGAACCACCCG -3'
	Tf-rv_screen	5'- TGACGACTGCGACAGCATAG -3'
NtWBC1 gene	NtWBC1 F	5'- CAA AGC GAT CAT TCA CTA ACT CGT G -3'
	NtWBC1 R	5'- CGT TTC CCT CAT GAA AAT GTA CC -3'
pEX-K168 containing FGF21-Transferrin	pEX-K168-fw	5'- TGCGGCATCAGAGCAGATT -3'
	pEX-K168-rv	5'- GCTTCCGGCTCGTATGTTGT -3'
pEX-K248 containing FGF21-Transferrin	pEX-K248-fw	5'- GTCGGGGCTGGCTTAACTAT -3'
	pEX-K248-rv	5'- CATTAGGCACCCAGGCTTT -3'
pTRAc containing FGF21-Transferrin	FW(35SS_FI)	5'- TGACGCACAATCCCACTATC -3'
	RV(35SSpA_RI)	5'- CCCTTATCTGGGAAGTACTC -3'

NtWBC1 - Nicotiana tabacum ABC transporter of the White-Brown Complex subfamily

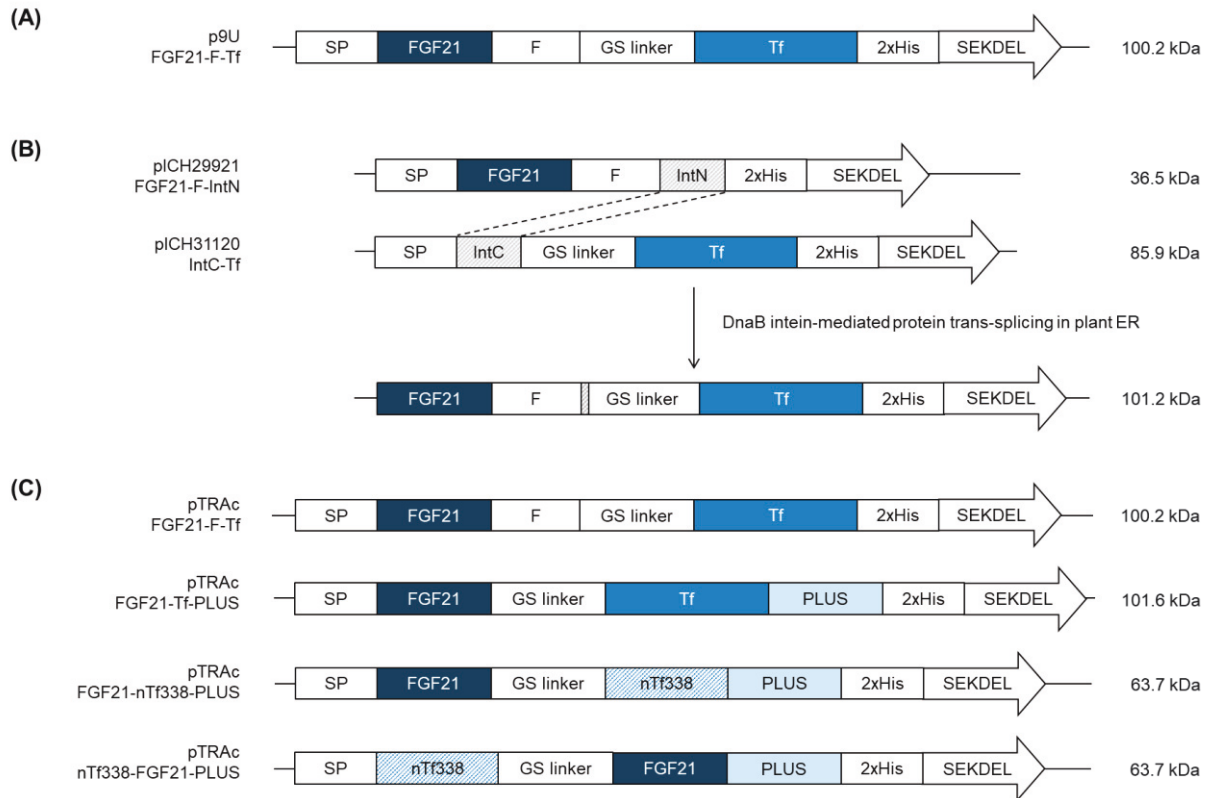


Figure 7. Constructs used for the stable and transient expression of FGF21-Transferrin fusion proteins. (A) p9U stable expression vector containing FGF21-F-Tf in *N. tabacum* SL632 and VG. **(B)** MagnICON transient expression vectors pICH29921 and pICH31120 containing FGF21-F-IntN and IntC-Tf, and **(C)** pTRAc transient expression vectors containing FGF21-F-Tf, FGF21-Tf-PLUS, FGF21-nTf338-PLUS and nTf338-FGF21-PLUS in *N. benthamiana*. SP – ER-targeting signal peptide from Calretikulin of *Nicotiana plumbaginifolia* (Acc. Z71395), MATQRRANPSSLHLITVFSLLVAVVSG; F – furin cleavage site, RRKRSV; GS linker – flexible linker, (GGGS)₃; 2xHis – double-His₆ tag; SEKDEL – ER-retention signal; IntN and IntC – DnaB intein fragments; PLUS – liver-targeting peptide circumsporozoite protein (CSP), position 82-100; nTf338 – N-terminal domain of Tf, position 1-338.

II.3.2. *Agrobacterium tumefaciens* culture

A. tumefaciens strain ICF320 (MagnICON) and *A. tumefaciens* strain GV3101::pMP90RK (pTRAc) were incubated either in LB containing antibiotics (50 $\mu\text{g mL}^{-1}$ rifampicin and 50 $\mu\text{g mL}^{-1}$ kanamycin) (Nausch et al., 2012b) or in PAM containing antibiotics (25 $\mu\text{g mL}^{-1}$ rifampin, 25 $\mu\text{g mL}^{-1}$ kanamycin, and 50 $\mu\text{g mL}^{-1}$ carbenicillin) (Houdelet et al., 2017) for 24-48 h at 28 °C with orbital shaking at 150 rpm as pre- and main cultures with a final OD₆₀₀ of 5.0-10.0 in the main culture.

II.3.3. Plant *in vitro* tissue culture

For *in vitro* tissue culture, tobacco seeds, such as those from *N. tabacum* cultivars Virginia Golta (VG) and SL632 (SL632), were surface sterilized using a saturated calcium hypochlorite solution supplemented with 0.1 % (m v⁻¹) Triton X-100 for 5 min, followed by rinsing with sterile distilled water. The sterilized seeds were germinated on Petri dishes containing LST medium (4.4 g L⁻¹ Linsmaier and Skoog (LS) including vitamins, 30 g L⁻¹ sucrose, 6.5 g L⁻¹ plant agar, pH 5.7) (Duchefa B.V., Netherlands). The shoots were grown at 24 °C/22 °C (day/night) with 16 h photoperiod. Subsequently, 2-week-old shoots were individually transferred to culture containers containing LST medium and continued to grow until intact plants were formed. For propagation, a series of apical bud cuttings were performed on intact plants, transferring the apical buds containing one smaller leaf to new LST medium culture containers until 50 % of the plants had flowered.

II.3.4. Stable transformation

Tobacco sterilized 4-week-old leaves were cut into leaf discs and wounded. Subsequently, the leaf discs were added to B5 infection medium (3.16 g L⁻¹ Gamborg B5 Vitamin Mixture, 0.25 g L⁻¹ Ammonium nitrate, 0.5 g L⁻¹ 2-(N-morpholino)ethanesulfonic acid (MES) monohydrate, 30.0 g of L⁻¹ sucrose, pH 5.7) (Duchefa B.V., Netherlands) containing *Agrobacterium*, co-cultivated at 25 °C for 3 days, and then washed several times with sterile distilled water. Infected leaf discs were inoculated on ACB medium (4.32 g L⁻¹ Murashige & Skoog Basal Salts Mixture, 0.5 g L⁻¹ 2-(N-morpholino)ethanesulfonic acid (MES) monohydrate, 30 g L⁻¹ sucrose, 6.8 g L⁻¹ agarose, 112 µg mL⁻¹ B5-vitamine, 1 µg mL⁻¹ 6-Benzylaminopurine (6-BAP) and 0.1 µg mL⁻¹ 1-Naphthaleneacetic acid (NAA), pH 5.7) containing 100 µg mL⁻¹ kanamycin and 500 µg mL⁻¹ cefotaxim (Duchefa B.V., Netherlands) for 4-6 weeks to select regenerated shoots. Regenerated shoots were transferred to LST medium containing 100 µg mL⁻¹ kanamycin and 500 µg mL⁻¹ cefotaxim (Duchefa B. V., Netherlands). The integration of the transgene was confirmed by PCR, and regenerated transgenic T0 plants were directly transferred into 5-L pots containing peat soil (Stender GmbH, Germany) in the greenhouse for leaf or seed production. Information on *Agrobacterium*-mediated transformation of tobacco leaves is detailed elsewhere (Nausch et al., 2016).

II.3.5. Segregation analysis

Tobacco sterilized seeds were plated simultaneously on LST medium, with or without 100 mg L⁻¹ kanamycin (Duchefa B.V., Netherlands), to evaluate the antibiotic resistance of self-pollinated T1 progenies and the viability of the seeds, respectively. The transgenic rate and seed viability rate were evaluated 6 weeks after germination.

II.3.6. Plant cultivation in the greenhouse

Regenerated shoots (transformants) were transferred to 5-L pots containing peat soil (Stender GmbH, Germany) in the greenhouse. The 3-week-old plants were fertilized with either 0.2 % (m v⁻¹) Hakaphos Blue (Compo Expert GmbH, Germany) or 0.1 % (m v⁻¹) Ferty 2 Mega (H. Nitsch & Sohn GmbH, Germany) until harvest. The entire plant harvest was conducted when flowers had 75 % mature capsules.

II.3.7. Transient transformation

The final OD₆₀₀ of *A. tumefaciens* strain ICF320 (MagnICON) and *A. tumefaciens* strain GV3101::pMP90RK (pTRAc) in the main culture was 5.0-10.0 (Chapter III. 3.2.). The main culture was centrifuged (2,800× g, 10 min, 4 °C), and the *Agrobacterium* pellet was resuspended in 5-6 L of infiltration buffer (MagnICON vectors: 2.1 g L⁻¹ 2-(N-morpholino)ethanesulfonic acid (MES) monohydrate, 1.2 g L⁻¹ Magnesium sulfate, pH 5.5; pTRAc vectors: 0.5 g L⁻¹ Murashige & Skoog Basal Salts Mixture, 0.04 g L⁻¹ Acetosyringone, pH 5.6) to achieve a final OD₆₀₀ of 0.1-0.5. The entire *N. benthamiana* plant was turned upside down and submerged in infiltration buffer, followed by the application of a vacuum of 0.01 MPa (100 mbar) for 2 min. The infiltrated *N. benthamiana* plants were then grown at 24 °C/22 °C (day/night) with 16 h photoperiod and harvested after 10 dpi for MagnICON vectors and 5 dpi for pTRAc vectors.

II.3.8. Protein extraction

Small-scale protein extraction as well as large-scale protein extraction methods are described elsewhere (Hou et al., 2022). In brief, plants were extracted using extraction buffer at a ratio of 10 v m⁻¹ (small-scale extraction) and 3 v m⁻¹ (large-scale extraction). Small-scale extracts, used only for protein analysis, were clarified by centrifugation three times (11,000 rpm, 10 min, 4 °C). On the other hand, large-scale extracts, intended for protein purification, were first clarified using BP-410 bag filters (Fuhr, Germany), then using double-layer PDH4 depth

filters in combination with K700 and KS50 (Pall, Germany), and finally using Sartopore 2 capsules (Sartorius AG, Germany), made from 0.45 μm and 0.20 μm filters. Turbidity, pH and conductivity of extracts and filtrate were measured.

II.3.9. Turbidity measurement

The NTU of the plant extract and clarified filtrate was measured by a Hach turbidimeter (Hach Lange GmbH, Germany) (Knödler et al., 2023; Opdensteinen et al., 2018; Opdensteinen et al., 2021b).

II.3.10. Protein purification using immobilized metal ion affinity chromatography

The His-tagged FGF21-Tf fusion protein was loaded onto an XP26/20 column containing Ni^{2+} Sepharose Fast Flow resin with a column volume of 58 mL, and IMAC purification was carried out using the ÄTKA pure system (Cytiva, USA). Purified His-tagged FGF21-Tf fusion proteins were subjected to PBS buffer exchange using a Vivaspinn 15R centrifugal concentrator (Sartorius AG, Germany) with a 30,000 molecular weight cut-off (MWCO). The IMAC purification method as well as PBS buffer exchange method are described elsewhere (Hou et al., 2022). In brief, the column was equilibrated with 290 mL of IMAC equilibration buffer, followed by the application of 1000-4000 mL of the clarified and sterile filtrated extract, washing with 290 mL of IMAC wash buffer, and elution with 174 mL of IMAC elution buffer.

II.3.11. Protein quantification

The TSP concentration in the extract supernatant was determined using the Pierce Bradford Plus Protein Assay Kit (Thermo Fischer Scientific Inc., USA). Bovine serum albumin (BSA, 2,000 $\mu\text{g mL}^{-1}$) in the kit was diluted with PBS buffer to prepare 6 standards at concentrations of 1,500, 1,000, 750, 500, 250, 125, and 0 $\mu\text{g mL}^{-1}$. In a clear 96-well CellStar F bottom plate (Greiner Bio-One International GmbH, Austria), 5 μL of each sample or BSA standard and 195 μL of Bradford reagent were added per well, thoroughly mixed, and the samples were incubated at 22-24 $^{\circ}\text{C}$ for 10 min. The absorbance was measured at a wavelength of 595 nm using a Tecan Infinity M200 reader (Tecan Group Ltd., Switzerland).

II.3.12. TCA protein precipitation

Each 100 µg or 10 µg TSP per sample was precipitated with 72 % (w v⁻¹) trichloroacetic acid (TCA) to achieve a TCA concentration of 11 %. Samples were incubated on ice for at least 20 min, then centrifuged twice (2,800 × g, 10 min, 4 °C). After centrifugation, the supernatant was removed, and the pellet was air-dried.

II.3.13. LDS-PAGE

Sample pellets were resuspended in NuPAGE LDS Sample Buffer (4x), NuPAGE Sample Reducing Agent (10x), and water, and run on NuPAGE 4-12 % Bis-Tris protein gels in NuPAGE MES SDS Running Buffer (Thermo Fischer Scientific Inc., USA) at 200 V at 22-24 °C for 35 min.

II.3.14. Coomassie-staining

Protein gels (Chapter II.3.13.) were stained with SimplyBlue SafeStain (containing Coomassie G-250) (Thermo Fischer Scientific Inc., USA) at 22-24 °C overnight, then destained with water at 22-24 °C overnight.

II.3.15. Western blot analysis

Proteins separated from NuPAGE 4-12 % Bis-Tris protein gels (Chapter II.3.13.) in Blotting buffer were transferred onto Amersham Protran nitrocellulose membranes (VWR International, USA) using a Trans Blot Cell (Bio-Rad Inc., USA) at 50 V at 22-24 °C for 1 h. The membrane was initially blocking with PBST buffer (PBS buffer containing 0.05 % (w v⁻¹) Tween-20) containing 5 % (w v⁻¹) skimmed milk powder at 22-24 °C for 1 h. After washing three times with PBST buffer for 5 min, the membrane was incubated overnight at 4 °C with a polyclonal rabbit anti-His antibody (1:5,000, Hölzel Diagnostika Handels GmbH, Germany) or a polyclonal rabbit anti-FGF21 antibody (1:5,000, Dianova GmbH, Germany) in Signal Boost ImmunoReaction Enhancer solution I (Merck KGaA, Germany) as the primary antibody. After washing with PBST buffer, for the secondary antibody, the membrane was then incubated at 22-24 °C for 1 h with a goat anti-Rabbit IgG AP-conjugated antibody (1:5,000, Jackson ImmunoResearch Laboratories, USA) in Signal Boost Immune Response Enhancer Solution II (Merck KGaA, Germany).

II.3.16. Densitometric analysis

Western blot membranes (Chapter II.3.15.) were scanned using CanoScan 5600F (Canon Inc., Japan), and Western blot signals were analyzed using the AIDA Image Analyzer analysis software (Elysia-raytest GmbH, Germany).

II.3.17. FGF21 ELISA

FGF21 accumulation in TSP in seed or leaf extracts was determined using the SimpleStep Human FGF21 ELISA kit (Abcam plc., UK). Recombinant FGF21 was quantified according to the manufacturer's instructions.

II.3.18. 3D Structure analysis

Raptor X software was a software to identify dimensional structure analysis (<http://raptorx.uchicago.edu/>).

II.3.19. DoE model building

For the Design of Experiments (DoE) method, the software Design Expert 11.0 (State-Ease, USA) was used.

II.3.20. Statistical analysis

Origin 2020b (OriginLab, USA) was used for statistical analysis and to evaluate all experimental designs. Information on normal distribution, equal variance, and statistical analysis methods is detailed elsewhere (Hou et al., 2022).

III. Results

III. Results

Content of the following sections has been published on the 29.09.2022 as part of “**Hou, H.W., Bishop, C.A., Huckauf, J., Broer, I., Klaus, S., Nausch, H., Buyel, J.F. (2022). Seed- and leaf-based expression of FGF21-transferrin fusion proteins for oral delivery and treatment of non-alcoholic steatohepatitis. *Frontiers in Plant Science* 13: 998596; 10.3389/fpls.2022.998596**” (doi: 10.3389/fpls.2022.998596).



OPEN ACCESS

EDITED BY

Michele Bellucci,
National Research Council (CNR), Italy

REVIEWED BY

Francesca De Marchis,
National Research Council (CNR), Italy
Hugh S. Mason,
Arizona State University, United States

*CORRESPONDENCE

Henrik Nausch
henrik.nausch@ime.fraunhofer.de

SPECIALTY SECTION

This article was submitted to
Plant Biotechnology,
a section of the journal
Frontiers in Plant Science

RECEIVED 20 July 2022

ACCEPTED 29 August 2022

PUBLISHED 29 September 2022

CITATION

Hou H-W, Bishop CA, Huckauf J,
Broer I, Klaus S, Nausch H and Buyel JF
(2022) Seed- and leaf-based
expression of FGF21-transferrin fusion
proteins for oral delivery and treatment
of non-alcoholic steatohepatitis.
Front. Plant Sci. 13:998596.
doi: 10.3389/fpls.2022.998596

COPYRIGHT

© 2022 Hou, Bishop, Huckauf, Broer,
Klaus, Nausch and Buyel. This is an
open-access article distributed under
the terms of the [Creative Commons
Attribution License \(CC BY\)](#). The use,
distribution or reproduction in other
forums is permitted, provided the
original author(s) and the copyright
owner(s) are credited and that the
original publication in this journal is
cited, in accordance with accepted
academic practice. No use, distribution
or reproduction is permitted which
does not comply with these terms.

Seed- and leaf-based expression of FGF21-transferrin fusion proteins for oral delivery and treatment of non-alcoholic steatohepatitis

Hsuan-Wu Hou^{1,2}, Christopher A. Bishop ^{3,4},
Jana Huckauf², Inge Broer ², Susanne Klaus ^{3,4},
Henrik Nausch ^{1*} and Johannes F. Buyel ^{1,5,6}

¹Department Bioprocess Engineering, Fraunhofer Institute for Molecular Biology and Applied Ecology IME, Aachen, Germany, ²Chair for Agrobiotechnology, University of Rostock, Rostock, Germany, ³Department of Physiology of Energy Metabolism, German Institute of Human Nutrition Potsdam-Rehbrücke, Nuthetal, Germany, ⁴Institute of Nutritional Science, University of Potsdam, Nuthetal, Germany, ⁵Institute of Molecular Biotechnology, RWTH Aachen University, Aachen, Germany, ⁶Department of Biotechnology (DBT), Institute of Bioprocess Science and Engineering (IBSE), University of Natural Resources and Life Sciences (BOKU), Vienna, Austria

Non-alcoholic steatohepatitis (NASH) is a global disease with no effective medication. The fibroblast growth factor 21 (FGF21) can reverse this liver dysfunction, but requires targeted delivery to the liver, which can be achieved via oral administration. Therefore, we fused FGF21 to transferrin (Tf) via a furin cleavage site (F), to promote uptake from the intestine into the portal vein, yielding FGF21-F-Tf, and established its production in both seeds and leaves of commercial *Nicotiana tabacum* cultivars, compared their expression profile and tested the bioavailability and bioactivity in feeding studies. Since biopharmaceuticals need to be produced in a contained environment, e.g., greenhouses in case of plants, the seed production was increased in this setting from 239 to 380 g m⁻² a⁻¹ seed mass with costs of 1.64 € g⁻¹ by side branch induction, whereas leaves yielded 8,193 g m⁻² a⁻¹ leave mass at 0.19 € g⁻¹. FGF21-F-Tf expression in transgenic seeds and leaves yielded 6.7 and 5.6 mg kg⁻¹ intact fusion protein, but also 4.5 and 2.3 mg kg⁻¹ additional Tf degradation products. Removing the furin site and introducing the liver-targeting peptide PLUS doubled accumulation of intact FGF21-transferrin fusion protein when transiently expressed in *Nicotiana benthamiana* from 0.8 to 1.6 mg kg⁻¹, whereas truncation of transferrin (nTf338) and reversing the order of FGF21 and nTf338 increased the accumulation to 2.1 mg kg⁻¹ and decreased the degradation products to 7% for nTf338-FGF21-PLUS. Application of partially purified

nTf338-FGF21-PLUS to FGF21^{-/-} mice by oral gavage proved its transfer from the intestine into the blood circulation and acutely affected hepatic mRNA expression. Hence, the medication of NASH *via* oral delivery of nTf338-FGF21-PLUS containing plants seems possible.

KEYWORDS

bioencapsulation, furin cleavage site, liver-targeting PLUS peptide, transferrin-mediated oral delivery, transient and stable transformation

Introduction

To date, non-alcoholic steatohepatitis (NASH) is a widespread disease in developed countries with a total prevalence of 0.4 billion patients (Weiß et al., 2014; Estes et al., 2018; Asrani et al., 2019; Povsic et al., 2019; Younossi et al., 2019; Kasper et al., 2020). NASH is characterized by an excessive accumulation of fat in the liver, which induces inflammation, leading to cirrhosis and liver failure (LaBrecque et al., 2014). Besides liver transplantation, however, there are currently no approved NASH therapeutics available (Moustafa et al., 2016; Mullard, 2020; Albhaisi and Sanyal, 2021), and medication is limited to symptom mitigation (Sharma et al., 2021).

A recently proposed drug candidate for the treatment of NASH is the fibroblast growth factor 21 (FGF21) (Xu et al., 2009; Dushay et al., 2010; Verzijl et al., 2020), an autocrine hormone that induces fat oxidation and inhibits fat synthesis in the liver (Nishimura et al., 2000; Badman et al., 2007; Lundåsen et al., 2007; Feingold et al., 2012; Woo et al., 2013). Though, a limiting factor is the 1–2 h half-life of FGF21 in the blood stream (Kharitonov et al., 2005; Gimeno and Møller, 2014; Zhen et al., 2016; Sonoda et al., 2017), and FGF21 analogs with half-lives of 24 and 98 h were developed by fusing the protein to either IgG (PF-05231023, Pfizer) (Huang et al., 2013; Giragossian et al., 2015; Talukdar et al., 2016) or polyethylene glycol (BMS-986036, Bristol-Myers Squibb) (Sanyal et al., 2018; Charles et al., 2019; Verzijl et al., 2020). These analogs decreased the blood triglycerides up to 20% in clinical trials after subcutaneous or intravenous administration (Talukdar et al., 2016; Charles et al., 2019), but in the case of PF-05231023, led to off-target effects such as altered bone turnover (Talukdar et al., 2016). These off-target effects might be reduced if FGF21 is directed exclusively to the liver *via* oral delivery, rather than administered systemically, as proteins are absorbed in the intestine and directly transported to the liver *via* the portal vein before entering the blood circulation (Schwegler and Lucius, 2022).

In contrast to other recombinant production platforms such as bacteria, yeast, insect or mammalian cell cultures, transgenic plants can be used for oral administration without the need to purify the recombinant protein, since human pathogens do not replicate in plants (Ghag et al., 2021). For example, feeding

tobacco leaves, expressing exendin-4 (Ex-4), to diabetic mice led to a 25% reduction in blood glucose levels (Kwon et al., 2013), whereby the uptake of Ex-4 from the intestine into the blood stream was facilitated through a fusion with cholera toxin B (CTB), mediating the mucosal transfer *via* the ganglioside GM1 receptor. However, CTB is a strong immune trigger, which limits the possibility of long-term application. Therefore, Ex-4 was fused to the non-immunogenic human iron-carrier protein transferrin (Tf), enabling the uptake *via* the enterocyte Tf-receptor. When applied orally, Ex-4-Tf reduced blood glucose levels by 31% compared to the 25 and 20% achieved with Ex-4-CTB and unmodified Ex-4, respectively (Choi et al., 2014). In contrast, when the purified recombinant proteins were administered intraperitoneally, Ex-4-Tf was 12% less effective (44% reduction) than Ex-4 (56% reduction), showing that the Tf domain can affect the bioactivity of the fusion protein.

In this context, plant seeds have been recognized as particularly suitable for oral delivery in the past as they contain 80–350 g kg⁻¹ protein per seed dry mass (SDM), compared to 10–20 g kg⁻¹ protein per leaf fresh mass (LFM) [corresponding to 83–167 g kg⁻¹ leaf dry mass (LDM)] (Buyel, 2016), and display a low protease activity in the development stage, resulting in high recombinant protein yields (Benchabane et al., 2008; Boothe et al., 2010). For example, whereas Tf accumulated to 0.14 g kg⁻¹ LFM in tobacco leaves (Brandsma et al., 2010; Choi et al., 2014; Wang et al., 2014) [corresponding to 1.17 g kg⁻¹ LDM], expression in rice seeds yielded 10.00 g kg⁻¹ SDM (Zhang et al., 2010). Additionally, seeds produce few secondary metabolites that could be regarded as potential impurities and can be stored at ambient conditions after harvest for at least six years (Benchabane et al., 2008; Boothe et al., 2010; Cunha et al., 2011). Accordingly, commercial seed production in greenhouses has already been established for rice (Ventria Bioscience, Junction City, KS, USA¹; Broz et al., 2013) and barley (ORF Genetics, Kópavogur, Island²), and seeds have been used for several oral vaccination trials. In some of the corresponding feeding studies, tobacco seeds were used because the production of recombinant proteins is well established in this system, and

¹ <https://ventria.com/>

² <https://www.orfgenetics.com/>

they are edible due to the absence of alkaloids such as nicotine (Rossi et al., 2013, 2014).

Here, we selected tobacco (*Nicotiana tabacum*) seeds of commercial cultivars Virginia Golta (VG) and SL632 (SL632) as a production platform as these were bred to high leaf and seed biomass (NiCoTa GmbH Rheinstetten, Germany³; Sunchem NL, Amsterdam, Netherlands⁴). We optimized the overall leaf and seed yield per unit area and time in a greenhouse and compared the biomass output of both production systems. For oral delivery, we fused FGF21 to Tf *via* a furin cleavage site and generated stably transformed plants, expressing the fusion protein with the constitutively active 35S promoter/terminator expression cassette from the Cauliflower Mosaic Virus (CaMV) (Odell et al., 1985; Kay et al., 1987). In parallel, we optimized the stability of the fusion protein by domain exchange and shuffling *via* transient expression in *Nicotiana benthamiana* using the same expression cassette. Finally, we analyzed the *in vivo* bioavailability and bioactivity of the optimized FGF21-Tf fusion protein by oral administration to FGF21 knockout (FGF21^{-/-}) mice.

Materials and methods

Cloning of FGF21-transferrin expression constructs

The FGF21-Tf fusion constructs (Figures 1A–D and Supplementary Figure 1) were designed using the following elements: mature human FGF21 without signal peptide (SP) and including the point mutation Ser167Ala to eliminate the O-linked glycosylation site (Kharitonov et al., 2013), a GS flexible linker [(GGGGS)₃] (Choi et al., 2014), a furin cleavage site (RRKRSV) (Duckert et al., 2004; Kwon et al., 2018), mature human Tf or the N-terminal domain of Tf (nTf338) (Mason et al., 1996), the N-terminal and C-terminal parts of the DnaB intein (Evans et al., 2000; Sun et al., 2001; Kempe et al., 2009), and the liver-targeting peptide PLUS of the circumsporozoite protein CSP (Lu et al., 2014; Ma et al., 2014, 2017; Tavernier et al., 2020). The calreticulin SP of *Nicotiana plumbaginifolia* and the ER retention signal (SEKDEL) were used for targeting to the endoplasmic reticulum (ER). All constructs contained a C-terminal double His-tag for Immobilized Metal Ion Affinity Chromatography (IMAC) purification (Khan et al., 2006).

The amino acid sequences for the individual proteins (Figures 1A,B and Supplementary Figure 1) were assembled *in silico* and back-translated into a nucleotide sequence and codon-optimized for *N. tabacum* using the Eurofins gene optimizer software (Eurofins, Ebersberg, Germany). BamHI/NruI, BsaI/BsaI, and NcoI/XbaI restriction sites were

added to the 5' and 3' end of the final nucleotide sequence to allow directional cloning into the p9U (DNA Cloning Service e.K., Hamburg, Germany), the MagnICON vectors pICH29921 and pICH31160 (Gleba et al., 2005; Marillonnet et al., 2005; Giritch et al., 2006) and the pTRAc vector (Maclean et al., 2007), respectively. The final nucleotide sequences were synthesized by Eurofins and delivered in pEX vectors from which they were transferred into the target vectors *via* restriction/ligation. The final vectors were verified by sequencing before introducing them into the *Agrobacterium tumefaciens* strains C58C1 (p9U), ICF320 (MagnICON) and GV3101:pMP90RK (pTRAc).

Stable transformation of *Nicotiana tabacum*

Nicotiana tabacum cultivars VG and SL632 were used in this study. The seeds were surface sterilized in a saturated calcium hypochlorite solution with 0.1% (m v⁻¹) Triton X-100 for 5 min. The seeds were rinsed with sterile distilled water several times and then germinated on Linsmaier and Skoog (LS) medium (Duchefa, Harleem, Netherlands) supplemented with 30 g L⁻¹ sucrose, 6.5 g L⁻¹ plant agar and adjusted to pH 5.7. The plants were maintained at 24/22°C day/night temperature with a 16 h photoperiod. Subsequently, 4-week-old tobacco leaves were used for *Agrobacterium*-mediated transformation (Nausch et al., 2016). Regenerated shoots were selected on LS medium containing 0.1 g L⁻¹ kanamycin and 0.5 g L⁻¹ cefotaxim. Transgene integration was confirmed by PCR using FGF21- and Tf-specific primers (Supplementary Table 1).

Plant cultivation in the greenhouse

Transgenic individuals were transferred from tissue culture 4 weeks after the last subculture directly into 5-L pots containing peat soil (Stender, Schermbeck, Germany). Plants were fertilized twice a week using 0.2% (m v⁻¹) Hakaphos Blue (Compo Expert, Münster, Germany) or 0.1% (m v⁻¹) Ferty 2 Mega (Nitsch & Sohn, Kreuztal, Germany).

Transient transformation of *Nicotiana benthamiana*

The *N. benthamiana* plants were grown in the greenhouse until the age of 6–8 weeks in peat soil (Stender, Schermbeck, Germany) and fertilized with 0.2% (m v⁻¹) Hakaphos Blue or 0.1% (m v⁻¹) Ferty 2 Mega, in both cases with additional illumination (140 μmol s⁻¹ m⁻²) to ensure a 16 h photoperiod. *A. tumefaciens* was cultivated either in lysogeny broth (LB) (Nausch et al., 2012b) or peptone agrobacterium medium (PAM) (Houdelet et al., 2017) containing antibiotics (MagnICON – 50 mg L⁻¹ rifampicin and 50 mg L⁻¹

³ <http://nicota.de/de/index.html>

⁴ <https://sunchem.nl/>

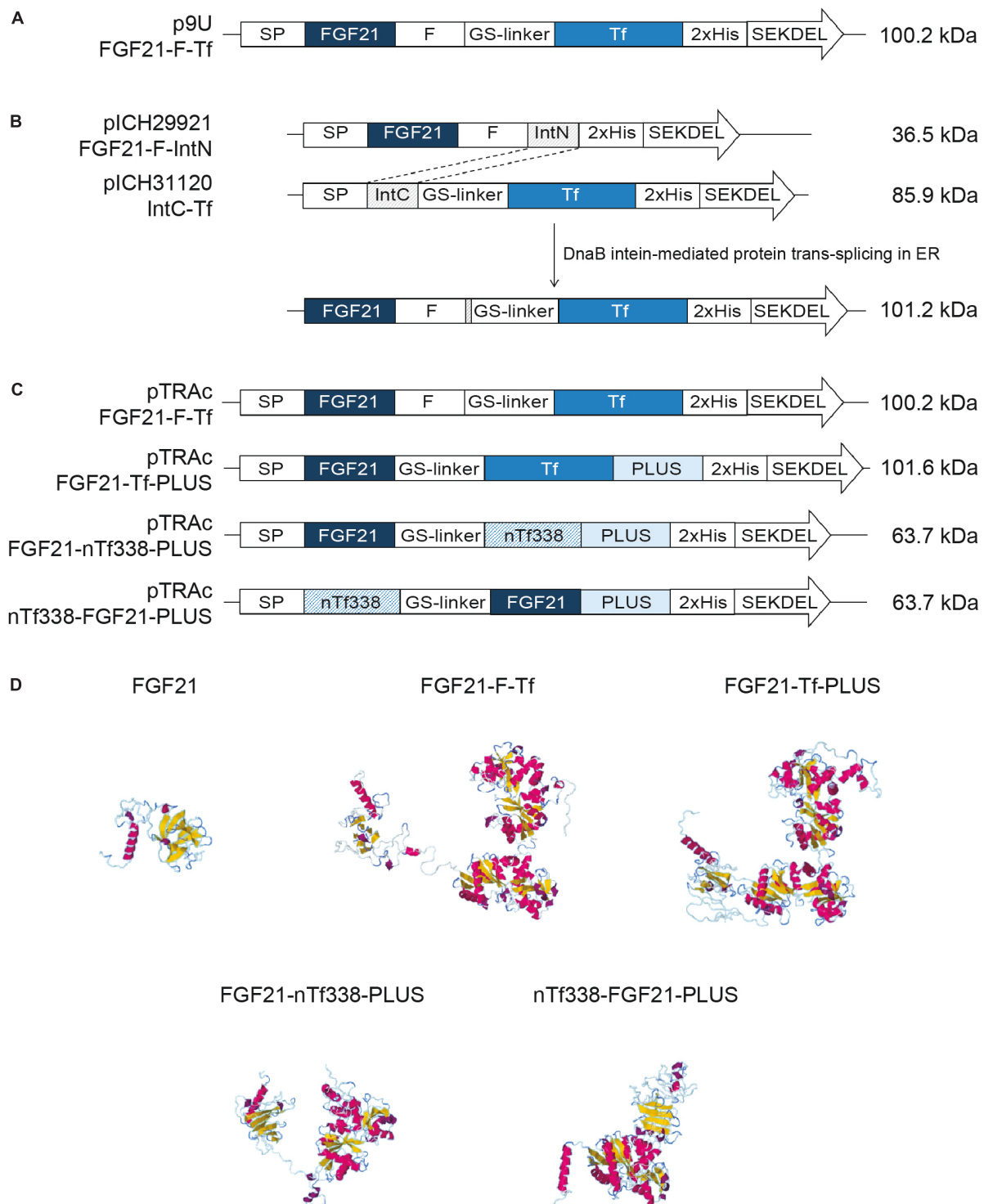


FIGURE 1

Constructs and models used for the stable and transient expression of FGF21-transferrin fusion proteins. **(A)** p9U stable expression vector containing FGF21-F-Tf in *N. tabacum* SL632 and VG. **(B)** MagniCON transient expression vectors pICH29921 and pICH31120 containing FGF21-F-IntN and IntC-Tf and **(C)** pTRAc transient expression vectors containing FGF21-F-Tf, FGF21-Tf-PLUS, FGF21-nTf338-PLUS, and nTf338-FGF21-PLUS in *N. benthamiana*. **(D)** The three-dimensional structures of different FGF21-Tf fusion proteins predicted by submitting the amino acid sequence to the RaptorX software (<http://raptorx.uchicago.edu/>). SP, signal peptide; F, furin cleavage site, RRKRSV; GS linker, flexible linker, (GGGGS)₃; 2xHis, double-His₆ tag; SEKDEL, ER-retention signal; IntN and IntC, DnaB intein fragments; PLUS, liver-targeting peptide circumsporozoite protein (CSP), aa 82–100; nTf338, N-terminal domain of Tf, aa 1–338.

kanamycin; pTRAc – 25 mg L⁻¹ rifampicin, 25 mg L⁻¹ kanamycin and 50 mg L⁻¹ carbenicillin) for 24–48 h at 28°C in an orbital shaker (150 rpm) before dilution 1:100 in the same medium. After another 24–48 h of incubation at 28°C, the bacteria were centrifuged (2,800 × g, 15 min, 22°C) and resuspended in infiltration buffer [MagnICON – 10 mM 2-(N-morpholino)ethanesulfonic acid (MES), 10 mM magnesium sulfate, pH 5.5; pTRAc – 0.5 g L⁻¹ MS basal salts and 0.2 mM acetosyringone, pH 5.6] to a final OD_{600nm} of 0.1–0.5. For vacuum infiltration, *N. benthamiana* plants were submerged upside down into the bacterial suspension, a vacuum of 100 mbar applied for 2 min in a desiccator, and the plants then returned to normal growth conditions. *N. benthamiana* leaf material was harvested 10 days post-infection (dpi) for the MagnICON vectors and 5 dpi for the pTRAc vectors.

Small-scale protein extraction

Each 100 mg seed or leaf material were homogenized in extraction buffer (25 mM sodium phosphate, 500 mM sodium chloride and 10 mM sodium bisulfite, pH 8.0) at a biomass/buffer ratio of 1:10 and 1:3, respectively, using a FastPrep-24 5G (MP Biomedicals, Irvine, CA, USA) and 0.5 g Zirconia/Silica beads for 3× at 8 Hz for 40 s with 30 s breaks on ice in between. The homogenate was clarified by 2 × centrifugation (13,520 × g, 20 min, 4°C) and the supernatant, containing the FGF21-transferrin fusion protein, collected.

Large-scale protein extraction for immobilized metal ion affinity chromatography purification

The extraction and purification for IMAC was carried at 4°C. Each 800 g leaf material was homogenized in extraction buffer (25 mM sodium phosphate, 500 mM sodium chloride and 10 mM sodium bisulfite, pH 8.0) at a ratio of 1:3 biomass using an HR3655/00 Standmixer (Philips, Amsterdam, Netherlands) 3× for 30 s with 30 s breaks. In the standard protocol, the homogenate was initially clarified by a BP420 bag filter (Fuhr, Klein-Winternheim, Germany), then passed through a combination of K700 (6–15 µm nominal retention rating) and KS50 (1 µm nominal retention rating) depth filters (Pall Corporation, New York, NY, USA) or applied to 2 × ultracentrifugation (15,900 × g, 30 min, 4°C) before final sterile filtration using Sartopore 2 Capsule (pore size of 0.45 and 0.22 µm) (Sartorius, Göttingen, Germany). The clarified extract (free of cell debris, which remained in the filter cake), containing the FGF21-transferrin, was used for further purification.

His-tagged FGF21-transferrin was purified on an ÄTKA pure system (GE Healthcare, Chicago, IL, USA) by applying 4 L filtrated extract to a XP26/20 column packed with 58 mL

IMAC Chelating Sepharose Fast Flow resin charged with Ni²⁺ ions. After washing with 5 column volume (CV) extraction buffer, the FGF21-transferrin fusion protein was eluted with 3 CV elution buffer (25 mM sodium phosphate, 500 mM sodium chloride and 150 mM imidazole, pH 7.6). A Vivaspin 15R centrifugal concentrator with a molecular weight cut off (MWCO) of 30 kDa (Sartorius, Göttingen, Germany) was used for buffer exchange into phosphate buffered saline (PBS) (137 mM sodium chloride, 2.7 mM potassium chloride, 12.5 mM disodium hydrogen phosphate, 2.0 mM potassium dihydrogen phosphate, pH 7.4).

Protein quantification, Western blot, densitometric analysis, and ELISA

The total soluble protein (TSP) concentration in extracts and supernatants, including the FGF21-transferrin fusion protein and the host cell proteins (HCPs), was quantified *via* Pierce Coomassie Protein Assay-Kit (Thermo Fisher Scientific, Waltham, MA, USA).

For Western blot analysis, 100 µg or 10 µg TSP per sample were precipitated with trichloroacetic acid (TCA) and resuspended in NuPAGE LDS sample buffer, optionally supplemented with 0.5% (v v⁻¹) β-mercaptoethanol and 100 mM dithiothreitol (DTT). Samples that were extracted with the NuPAGE LDS sample buffer were directly applied to Western blot analysis. The samples were denatured at 70°C for 10 min, separated on Invitrogen Novex NuPAGE 4–12% (m v⁻¹) Bis-Tris protein gels (Thermo Fisher Scientific, Waltham, MA, USA) at 200 V at 22–24°C for 35 min, and transferred to Amersham Protran nitrocellulose membranes (VWR, Radnor, PA, USA) at 50 V at 22–24°C for 1 h using a Trans Blot Cell (Bio-Rad Laboratories, Hercules, CA, USA). The membrane was blocked with PBS containing 0.05% (m v⁻¹) Tween-20 (PBST) and 5% (m v⁻¹) skimmed milk powder for 1 h at 22–24°C. After washing 3× with PBST for 5 min, the membrane was probed at 4°C overnight with a polyclonal rabbit anti-His antibody (Hölzel Diagnostika Handels, Cologne, Germany) diluted 1:5,000 (0.1 mg L⁻¹) or a polyclonal rabbit anti-FGF21 antibody (Dianova, Hamburg, Germany) diluted 1:5,000 (0.2 mg L⁻¹) in Signal Boost ImmunoReaction Enhancer solution I (Merck, Darmstadt, Germany). Following another wash in PBST, the membrane was probed at 22–24°C for 1 h with a horseradish peroxidase (HRP)-conjugated goat anti-rabbit diluted 1:5,000 (0.06 mg L⁻¹) in Signal Boost ImmunoReaction Enhancer solution II. After another wash with PBST, the signal was detected using the NBT/BCIP alkaline phosphatase system (Thermo Fisher Scientific, Waltham, MA, USA). Densitometric analysis of Western blot signals were conducted using the AIDA Image Analyzer analysis software (Elysia-raytest, Straubenhardt, Germany).

TABLE 1 Plant traits of *N. tabacum* SL632 and VG under different cultivation strategies in the greenhouse.

<i>N. tabacum</i> cultivar	Parameter	Description	Unit	Uncut	1 × top	1 × cut
SL632	1	Treatment time	dps	na	62.0 ± 0.9 (a)	57.8 ± 1.0 (b)
	2	Flowering of main stem	dps	61.8 ± 0.8	na	na
	3	Side branches with inflorescence	–	21.5 ± 4.7 (a)	28.4 ± 3.4 (b)	26.7 ± 3.4 (b)
	4	Side branch inflorescence flowering time after seeding	dps	61.8 ± 0.8 (a)	72.3 ± 3.2 (b)	82.0 ± 4.9 (c)
	5	Plant height	cm	219.5 ± 14.1 (a)	206.4 ± 11.5 (a)	206.6 ± 12.6 (a)
	6	Seed harvest	dps	135.6 ± 11.0 (a)	140.8 ± 12.2 (ab)	149.3 ± 6.2 (b)
	7	Total SDM per plant	g	42.7 ± 4.7 (a)	61.4 ± 6.6 (b)	67.9 ± 11.9 (b)
	8	Seed productivity	g d ⁻¹	~0.315	~0.436	~0.455
VG	1	Treatment time	dps	na	66.3 ± 1.6 (a)	62.0 ± 1.5 (b)
	2	Flowering of main stem	dps	65.0 ± 1.0	na	na
	3	Side branches with inflorescence	–	18.9 ± 2.4 (ab)	15.4 ± 3.0 (a)	22.1 ± 5.6 (b)
	4	Side branch inflorescence flowering time after seeding	dps	65.0 ± 1.0 (a)	72.2 ± 6.7 (b)	86.3 ± 5.4 (c)
	5	Plant height	cm	197.8 ± 18.7 (a)	221.3 ± 17.5 (b)	217.6 ± 11.6 (b)
	6	Seed harvest	dps	107.4 ± 0.5 (a)	117.1 ± 4.1 (b)	127.8 ± 3.9 (c)
	7	Total SDM per plant	g	18.0 ± 4.9 (a)	24.4 ± 4.4 (a)	43.1 ± 8.7 (b)
	8	Seed productivity	g d ⁻¹	~0.168	~0.208	~0.337

Numbers represent mean ± SD. Significance was calculated by one-way ANOVA with Bonferroni correction with an alpha threshold of 0.05 and significance groups indicated by letters (a, b, and c). The number of biologic replicates was $n = 12$ (parameter 1–6) and $n = 4–5$ (parameter 7). a, b, c – significance groups ($p < 0.05$). SDM, seed dry mass; dps, days post seeding; na, not applicable.

The FGF21 ELISA was carried out using the SimpleStep human FGF21 ELISA Kit (Abcam, Cambridge, UK) for both *in planta* and *in vivo* quantifications.

Intact FGF21-transferrin fusion protein accumulation was obtained through multiplying the ELISA-derived total product concentration by the fraction of intact FGF21-transferrin determined *via* anti-FGF21 Western blot analysis.

Animals and oral delivery experimental setup

Oral delivery experiments were performed in adult FGF21^{-/-} mice generated previously (Ost et al., 2016) that were group-housed and allowed *ad libitum* access to food and water prior to experiment. Mice were maintained on a 12 h light/dark cycle. Prior to oral gavage, mice were individually housed and fasted for 16 h overnight. Since in previous studies (Camporez et al., 2013; Emanuelli et al., 2014), 1 mg kg⁻¹ d⁻¹ was applied to mice to obtain an FGF21-mediated stimulation.

the FGF21-mice received a 0.5 mL bolus of partially purified nTf338-FGF21-PLUS, i.e., freeze-dried FGF21-transferrin that contained a substantial fraction of HCPs, dissolved in water to a concentration of 50 µg L⁻¹ FGF21 and 44 g L⁻¹ HCP derived from IMAC purification of mock-infiltrated *N. benthamiana* plants. The control mice were gavaged with HCP only. After 4 h, mice were euthanized with an overdose of Ketamine/Xylazine and Isoflurane and subsequent heart puncture. Following blood collection, tissues were isolated and snap frozen in liquid nitrogen. All experiments were approved by the Ethics Committee of the Ministry for Environment, Health and Consumer Protection of Brandenburg, Germany (approval no. 2347-9-2020).

Plasma samples for the FGF21 ELISA were undiluted, and 30 mg ground tissue was homogenized in tissue extraction buffer [10 mM Tris-HCl and 0.02% (m v⁻¹) Triton X-100, pH 7.4] at a ratio of 1:3 tissue mass using a TissueLyser LT (Qiagen GmbH, Germany) for 3 min at 50 Hz, and subsequent freeze-thaw (–20°C overnight) and centrifugation (23,000 × g, 20 min, 4°C).

mRNA analysis was performed as previously described (Weitkunat et al., 2016). Briefly, total RNA was extracted from 30 mg ground tissue using peqGOLD TriFast reagent (VWR, Germany). Following DNase treatment, cDNA synthesis was performed with 1 μ g RNA to a final concentration of 5 mg L⁻¹ according to suppliers' protocol (LunaScript RT SuperMix, NEB, Germany). Gene expression was calculated as ddCT, using *B2m* as the normalizer gene (Supplementary Table 1), where the control group was set to a value of 1.

Three-dimensional structure analysis

The three-dimensional structure analysis of the FGF21-transferrin fusion proteins was conducted by submitting the amino acid sequence to the RaptorX software⁵ (Källberg et al., 2012).

Statistical methods

Statistical analysis was performed in Origin 2020b (OriginLab, Northampton, MA, USA). The Shapiro–Wilk- and *F*-test of OriginPro was used to ensure normal distribution and equal variance of the dataset, followed by a univariate ANOVA (including the *post hoc* Bonferroni test). *p*-Values of 0.05 (* and letters), 0.01 (**) and 0.001 (***) were considered to indicate significant, strongly significant and highly significant differences as indicated in the individual experiments. There were no non-normal distributed data.

Results

Pruning increases tobacco seed yield in the greenhouse

Biopharmaceutical safety is often ensured by the production in contained environments, e.g., greenhouses in case of plants (Holtz et al., 2015). The corresponding cultivation conditions have been well established for the cultivar *N. tabacum* VG (Nausch et al., 2016), which is why we selected this cultivar in this study. The cultivar *N. tabacum* SL632 was also included in this study (Sunchem NL, Amsterdam, Netherlands) because this cultivar is nicotine-free and has been bred to a high seed yield of >9 tons SDM per hectare and year under open field conditions (Sunchem NL, Amsterdam, Netherlands⁴). However, SL632 has not yet been used for seed production in a greenhouse setting and thus required cultivation strategy adaptation to increase seed productivity.

Under standard cultivation conditions (uncut), both tobacco cultivars grew up to a height of 1.98–2.20 m, and

when harvested after 136 and 107 days, SL632 yielded ~43 g SDM per plant compared to 18 g SDM per plant in case of VG (Table 1). Noteworthy, the higher seed biomass of SL632 resulted from both an increased seed number and mass, e.g., a thousand SDM of ~0.107 g (SL632) compared to ~0.082 g (VG) (Supplementary Table 2). We reasoned that seed yields per plant can be increased through additional side branches with inflorescences. The latter are induced if the apical dominance of the main shoot is suppressed, for example by removing the tip of the main shoot either by cutting it at a height of ~1 m (1× cut) or by removing the top ~0.2 m (1× top, Table 1). Both approaches delayed the harvest time by 10–20% but at the same time generated up to 30% more side branches, which increased the seed yield by ~50% in case of SL632 and ~100% in case of VG (Table 1). We assume that the 1× cut effect on VG was more pronounced than for SL632 because VG formed less side branches in the uncut state than SL632 (Table 1). Nevertheless, the absolute seed yield of SL632 was approximately twofold higher than that of VG, and the production costs per seed biomass were lowest for cutting of SL632 with 1.64 € g⁻¹ (Table 2).

In contrast to seeds, the production of leaf biomass is well established for tobacco (Conley et al., 2011; Nausch et al., 2016) and *N. benthamiana* used for transient expression (Holtz et al., 2015; Buyel et al., 2017; Huebbers and Buyel, 2021). In this case, leaves can be harvested after ~6 weeks compared to the ~21 weeks for seeds (without seed drying) required for SL632 after cutting. Typical LFM yields were ~340, ~460, and ~155 g per plant for SL632, VG and *N. benthamiana* with production costs of 0.19 € g⁻¹ (SL632), 0.14 € g⁻¹ (VG) and 0.13 € g⁻¹ (*N. benthamiana*) (Table 2). Moreover, due to the 50% lower staff costs, leaf biomass production averaged only 10% of the total costs of seed production (Table 2). In this context semi-automated cultivation systems might be of interest, which can reduce the cultivation costs by more than 90% (Huebbers and Buyel, 2021).

Accumulation of FGF21-F-Tf in tobacco seeds was limited by *in planta* degradation

For oral delivery of FGF21 *via* tobacco seeds, we used mature human FGF21 without O-glycosylation site to obtain a homogenous product as previously described (Kharitonov et al., 2013) and fused the coding region of mature human FGF21 to Tf, which mediates the transfer from the intestine to the portal vein *via* the Tf-receptor (Figure 1A–D and Supplementary Figure 1; Choi et al., 2014). We included a GS-linker to avoid steric hindrance between FGF21 and Tf, and a furin cleavage site, yielding FGF21-F-Tf (Wilbers et al., 2016). The furin cleavage site does not occur in plants but should facilitate the release of FGF21 from Tf during uptake in the enterocytes of the intestine. Since Tf requires disulfide

⁵ <http://raptorx.uchicago.edu/>

TABLE 2 Operating expenses (OPEX) for tobacco seed and leaf biomass production per plant in the greenhouse via different cultivation strategies.

Tobacco cultivar	Biomass type	Cultivation strategy	Seed and leaf production* (week)	Working hours (h)	Labor costs (€)	Consumable costs (€)	Total costs per plant (€)	SDM/LFM yield per plant (g)	Costs per SDM/LFM (€ g ⁻¹)
SL632	Transgenic seed	Uncut	28	1.0	89.9	1.4	91.3	42.7	2.14
	Transgenic seed	1 × Top	29	1.2	107.7	1.4	109.1	61.4	1.78
	Transgenic seed	1 × Cut	30	1.3	109.9	1.4	111.3	67.9	1.64
	Transgenic leaf	Uncut	6	0.7	62.6	1.4	64.0	340.3	0.19
VG	Transgenic seed	Uncut	24	1.0	89.9	1.4	91.3	18.0	5.07
	Transgenic seed	1 × top	25	1.2	107.7	1.4	109.1	24.4	4.47
	Transgenic seed	1 × cut	27	1.3	109.9	1.4	111.3	43.1	2.58
	Transgenic leaf	Uncut	6	0.7	62.6	1.4	64.0	464.2	0.14
Nb	Transient leaf	Uncut	6	0.2	20.6	0.3	20.8	155.0	0.13

Costs per plant were calculated per batch based on a batch size of 72 plants for *N. tabacum* cv. SL632 (SL632) and VG (VG) and 400 plants for *N. benthamiana* (Nb). Labor costs were those of a technical assistant in Germany (2021; 87 € h⁻¹; full overhead calculation). Consumables covered water, soil, fertilizer, and energy expenses. Nb, *N. benthamiana*; LFM, leaf fresh mass; SDM, seed dry mass; SL632, *N. tabacum* cv. SL632; VG, *N. tabacum* cv. VG. *Seed production includes plant growth until seed harvest (Table 1) and seed drying 8 weeks.

bonds for authentic folding (Mason et al., 1996), the FGF21-F-Tf fusion protein was targeted to the ER. Therefore, we substituted the endogenous N-terminal SP of FGF21 with that of calreticulin of *N. plumbaginifolia*, because the plant SP can improve the accumulation level compared to the native one in plants (Shaalit et al., 2007; De Marchis et al., 2011). We also added the ER retention signal SEKDEL to the C-terminus of Tf because the ER displays a lower proteolytic activity compared to the apoplast (Benchabane et al., 2008), which might favor the accumulation level. Finally, in order to compare accumulation levels in seeds to leaves, and we employed the constitutive 35S CaMV expression cassette (Figure 1A).

We first expressed the fusion protein transiently in *N. benthamiana* using the MagnICON system (Figure 1B) (Marillonnet et al., 2004, 2005; Giritch et al., 2006). FGF21 and Tf were co-expressed as separate proteins that were post-translationally fused via an intein tag (Evans et al., 2000; Sun et al., 2001; Kempe et al., 2009) as the insert size of the viral replicon was limited to 2 kbp. FGF21 levels measured with an ELISA indicated a yield of 2.1 mg kg⁻¹ LFM (Table 3). However, while the anti-FGF21 Western blot showed the expected FGF21-F-Tf full-length size (~100 kDa), the anti-His Western blot revealed the presence of free Tf (~80 kDa) (Supplementary Figure 2A). To identify whether this observation was due to imperfect coupling of Tf to FGF21 via the intein tag or a result of proteolytic degradation, a pTRAc vector was used for expression, since this vector facilitated the expression of FGF21-F-Tf as a single in-frame fusion protein (Figure 1C). This approach yielded 1.2 mg kg⁻¹ LFM according to the anti-FGF21-ELISA (Table 3) and degradation products were detected in addition to the intact fusion protein both in anti-FGF21 (Figure 2A and Supplementary Figure 2A) and anti-His (Figure 2B and Supplementary Figure 2A) Western blots. Based on a densitometric analysis, ~33% of FGF21-F-Tf was degraded in anti-FGF21 Western blot and ~32% in anti-His Western blot, reducing the accumulation level of intact FGF21-F-Tf to 0.8 and 0.9 mg kg⁻¹ LFM (Table 3, Figures 2A,B, and Supplementary Figure 2A). Degraded product was found even when extracting FGF21-F-Tf in denaturing LDS sample buffer, suggesting that degradation occurred *in planta* and not during the extraction process (Supplementary Figure 2B). Nevertheless, we proceeded to the generation of transgenic plants with the FGF21-F-Tf construct (Figure 1A) because others studies indicated that seeds are a suitable platform to produce recombinant proteins that are susceptible to proteolytic degradation (Yao et al., 2015).

When cultivating SL632 in tissue culture before the transformation, the first SL632 plants started to flower after the second or third passage (with 3 weeks per passage), which limited the vegetative propagation to six passages. On the other hand, VG flowered only occasionally, was propagated for at least 19 passages and provided almost twice the number of positive

TABLE 3 FGF21 accumulation level of FGF21-transferrin fusion constructs in crude extract.

Plant	Type ^a	Vector	Fusion protein (mg kg ⁻¹ biomass)	Total FGF21 fusion protein in crude extract (mg kg ⁻¹ TSP)	Intact FGF21 fusion protein in crude extract		Biological replicates	Biomass (kg m ⁻² a ⁻¹)	Intact FGF21 fusion protein yield (mg m ⁻² a ⁻¹)
					Anti-FGF21 WB (mg kg ⁻¹ biomass)	Anti-His WB (mg kg ⁻¹ biomass)			
<i>N. tabacum</i> SL632	Transgenic seed	p9U	FGF21-F-Tf	9.1 ± 0.3	63.6 ± 2.1	6.7 ± 0.2	2.2 ± 0.1	0.38	2.55
<i>N. tabacum</i> SL632	Transgenic leaf	p9U	FGF21-F-Tf	6.1 ± 0.2	68.5 ± 1.8	5.6 ± 0.2	3.3 ± 0.1	8.19	45.86
<i>N. tabacum</i> VG	Transgenic seed	p9U	FGF21-F-Tf	8.7 ± 0.0	84.2 ± 0.3	6.4 ± 0.0	2.1 ± 0.0	0.24	1.54
<i>N. tabacum</i> VG	Transgenic leaf	p9U	FGF21-F-Tf	2.4 ± 0.0	105.5 ± 1.4	2.2 ± 0.0	2.0 ± 0.0	11.17	24.57
<i>N. benthamiana</i>	Transient leaf	MagniCON	FGF21-F-Tf	2.1 ± 0.0	115.7 ± 1.7	2.1 ± 0.0	0.0 ± 0.0	11.94	25.07
		pTRAc	FGF21-F-Tf	1.2 ± 0.3	151.6 ± 51.4	0.8 ± 0.2	0.9 ± 0.1	11.94	9.55
		pTRAc	FGF21-Tf-PLUS	2.1 ± 0.7	446.9 ± 106.6	1.6 ± 0.5	1.3 ± 0.4	11.94	19.10
		pTRAc	FGF21-nTf338-PLUS	2.0 ± 0.6	427.9 ± 132.2	1.6 ± 0.5	1.3 ± 0.4	11.94	19.10
		pTRAc	nTf338-FGF21-PLUS	2.3 ± 0.6	361.1 ± 136.3	2.1 ± 0.5	1.9 ± 0.5	11.94	25.07

Numbers represent mean ± SD. Total FGF21 fusion protein was determined by the FGF21 ELISA and intact FGF21 fusion protein was obtained by correcting ELISA data by anti-FGF21 and anti-His Western blot analysis and estimation of the relative amount of intact fusion protein and cleaved FGF21. Biomass refers to leaf fresh mass (LFM) or seed dry mass (SDM), which were calculated with the help of the data shown in Table 2. ^aNumber for transgenic plants refer to seeds of the T1 generation and leaves of the T2 generation. WB, Western blot.

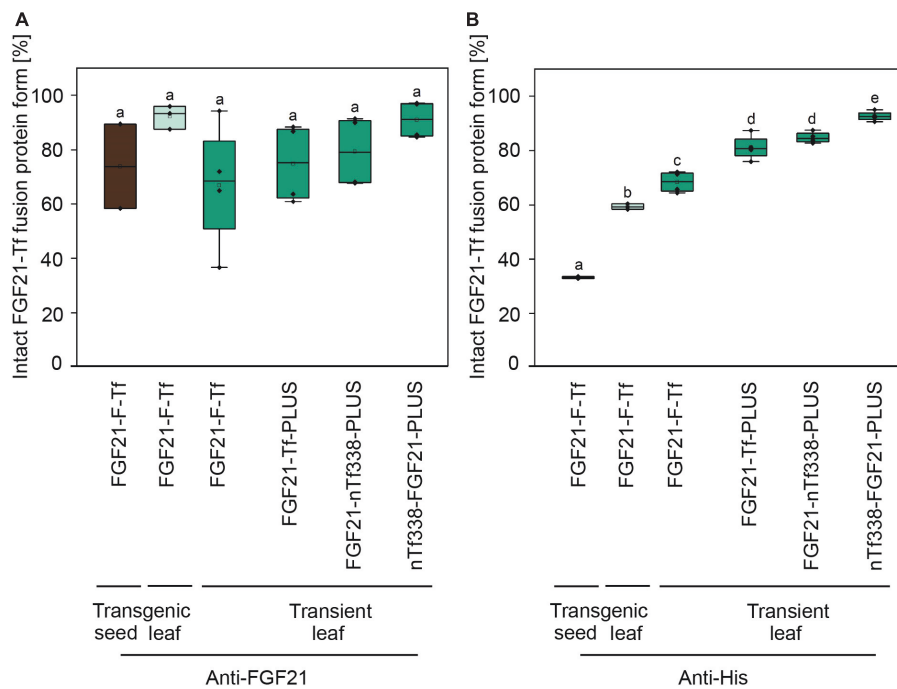


FIGURE 2

Degree of degradation during extraction of optimized FGF21-transferrin fusion proteins in *N. tabacum* SL632 (SL1-1) and in *N. benthamiana*. Relative fraction of the intact FGF21-Tf fusion proteins in plant extracts, detected by (A) anti-FGF21 and (B) anti-His Western blots and band intensities quantified using the AIDA Image Analyzer analysis software. $n = 3$, biological replicates.

transformants (Supplementary Tables 3, 4). Noteworthy, in VG the GFP control yielded twofold more positive transformants compared to the FGF21-F-Tf, indicating a potential negative impact on the cell viability (Supplementary Table 4). However, the T0 seed viability was equal to the control (Supplementary Table 5), which contradicts to that assumption.

While the highest FGF21-F-Tf accumulation in seeds of the T0 transformant of SL632 was 2.2-fold higher compared to VG (Figure 3A), the maximal FGF21-F-Tf yield was similar with $\sim 6.5 \text{ mg kg}^{-1}$ SDM in seeds of the T1 descendants for both cultivars (Figure 3B and Table 3). This complies with previous studies in which the expression of C5a and IL6, produced in seeds and leaves of transgenic tobacco, increased by about an order of magnitude from T0 to T1 (Nausch et al., 2012a,b). However, the increase in the FGF21-F-Tf was only observed in each one T1 individual of SL632 and VG, while in the other T1 plants the yield was similar or lower compared to the T0 transformant.

Unexpectedly, FGF21-F-Tf degradation was even higher in transgenic seeds, reaching $\sim 67\%$ in the anti-His Western blot (Figure 2 and Supplementary Figure 3), and might be the reason for the low yield of intact FGF21-F-Tf of $\sim 6.5 \text{ mg kg}^{-1}$ SDM in both cultivars (Table 3). Noteworthy, FGF21-F-Tf degradation in transgenic leaves of the same plants was substantially lower with 41% (Figure 2 and Supplementary Figure 3), and intact

FGF21-F-Tf accumulated at 5.6 (SL632) and 2.2 (VG) mg kg^{-1} LFM (Table 3).

However, when using a denaturing LDS sample buffer instead of the extraction buffer (Supplementary Figure 3), the ratio of intact to degraded FGF21-F-Tf was similar in leaves but higher in seeds. This suggested that not all recombinant protein was extracted from seeds and that a substantial fraction of intact FGF21-F-Tf might be deposited in insoluble protein bodies or protein storage vacuoles.

Nevertheless, only the soluble FGF21-F-Tf might be relevant for the oral application. Accordingly, when combining the accumulation levels of soluble FGF21-F-Tf with the biomass productivity data (Tables 1, 2), yields of intact FGF21-F-Tf were 18-fold (SL632) and 16-fold (VG) higher in leaves compared to seeds with a productivity of 45.86 (SL632) and 24.57 (VG) $\text{mg m}^{-2} \text{ a}^{-1}$ in leaves compared to 2.55 (SL632) and 1.54 (VG) $\text{mg m}^{-2} \text{ a}^{-1}$ in seeds (Table 3).

Fusion protein degradation was reduced by furin cleavage site removal and truncation of transferrin

We modified the fusion protein to minimize degradation and to increase the FGF21 yield, and tested the new fusion proteins via transient expression in *N. benthamiana*

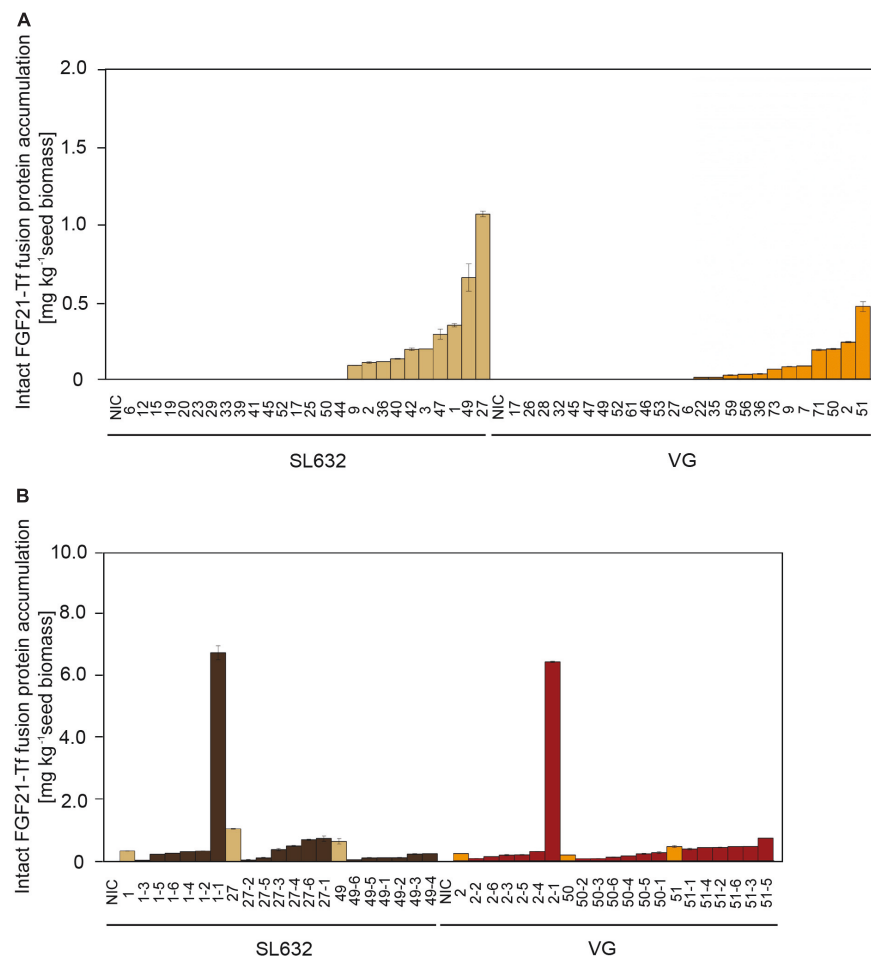


FIGURE 3

Intact FGF21-F-Tf fusion protein yield in seeds of T0 and T1 transformants in *N. tabacum* SL632 and VG. (A) Intact FGF21-F-Tf fusion protein accumulation in seeds of T0 transformants. (B) Intact FGF21-F-Tf fusion protein accumulation in seeds of T1 descendants of selected T0 transformants 1, 27, and 49 of SL632 and 2, 50, and 51 of VG. Intact FGF21-F-Tf fusion protein accumulation was obtained through multiplying the ELISA-derived total product concentration by the fraction of intact FGF21-F-Tf determined via anti-FGF21 Western blot analysis. $n = 2$, biological replicates, i.e., different leaf samples from the same plant. NIC, near-isogenic control plants.

(Figure 1C). We analyzed the structures of all fusion protein variants *in silico*, by submitting the amino acid sequence to the RaptorX software (see text footnote 5), to identify potential steric hindrances prior to cloning, but did not observe any problems (Figure 1D). First, we removed the furin site from the fusion protein to rule out unintended degradation *in planta*. Because this modification may increase serum half-life of FGF21, triggering deleterious side effects (Talukdar et al., 2016), we included the PLUS peptide that mediates exclusive uptake by liver cells (Lu et al., 2014; Ma et al., 2014, 2017; Taverner et al., 2020). The resulting FGF21-Tf-PLUS construct (Figure 1) accumulated to $1.6 \text{ mg kg}^{-1} \text{ LFM}$, which was twice the concentration of FGF21-F-Tf (Table 3), and degradation was reduced from 32 to 19% (Figure 2).

We also reasoned that the large size of the fusion protein of $>100 \text{ kDa}$ may provide unnecessary protease cleavage sites

and could potentially limit accumulation, which has been reported for other fusion proteins produced in transgenic tobacco (Phan et al., 2014). Using only the first 338 n-terminal amino acids (nTf338), which mediate Tf receptor binding (Mason et al., 1996), did not increase the accumulation of the resulting FGF21-nTf338-PLUS fusion protein but reduced degradation to 15% (Figure 2 and Table 3). Changing the domain sequence (nTf338-FGF21-PLUS) lowered degradation to 7%, while the accumulation of intact fusion protein increased to 2.1 or $5.8 \text{ mg kg}^{-1} \text{ LFM}$ when only non-senescent leaves were processed (Tables 3, 4).

However, the higher accumulation level might not only result from an increased stability/reduced degradation of the fusion proteins, but also from an increased expression for which the mRNA level can be an indicator. The analysis of the latter and testing different codon-optimized construct variants

TABLE 4 Comparison of purification process performance for nTf338-FGF21-PLUS extracted from non-senescent, transiently transformed *N. benthamiana* leaves, using filtration or centrifugation as the major clarification step.

Method	Depth filtration ^a				Ultracentrifugation ^b			
	Overall recovery (%)	Step recovery (%)	Yield ($\mu\text{g kg}^{-1}$ biomass)	Purity (%)	Overall recovery (%)	Step recovery (%)	Yield ($\mu\text{g kg}^{-1}$ biomass)	Purity (%)
Homogenate	100.00	–	2,930.1 \pm 628.9	0.05 \pm 0.02	100.00	–	5,779.0 \pm 119.6	0.05 \pm 0.00
Bag filtrate	76.3 \pm 0.9	76.3 \pm 0.9	2,234.5 \pm 460.9	0.06 \pm 0.03	55.5 \pm 2.9	55.5 \pm 2.9	3,206.7 \pm 236.4	0.04 \pm 0.00
Clarification (centrifugation or filtration)	4.2 \pm 2.0	5.5 \pm 2.6	121.3 \pm 52.2	0.01 \pm 0.00	52.5 \pm 2.4	94.7 \pm 0.7	3,035.3 \pm 200.5	0.03 \pm 0.00
Sterile filtrate	3.6 \pm 1.7	85.5 \pm 4.9	104.5 \pm 46.1	0.01 \pm 0.00	36.6 \pm 0.4	69.9 \pm 4.0	2,116.7 \pm 19.5	0.02 \pm 0.00
IMAC flow through	2.8 \pm 1.5	76.8 \pm 11.0	82.4 \pm 43.0	0.04 \pm 0.02	35.2 \pm 0.4	96.1 \pm 0.1	2,033.2 \pm 19.9	0.08 \pm 0.01
IMAC wash	2.7 \pm 1.5	95.8 \pm 2.9	79.7 \pm 42.6	0.06 \pm 0.02	34.9 \pm 0.4	99.1 \pm 0.0	2,014.5 \pm 20.1	0.08 \pm 0.01
IMAC elution	2.3 \pm 1.4	84.4 \pm 11.2	58.7 \pm 39.8	0.14 \pm 0.04	31.7 \pm 0.3	90.9 \pm 0.0	1,324.8 \pm 8.9	0.19 \pm 0.00

Yield and purity were determined by FGF21-ELISA and Bradford assay. ^a*n* = 3; ^b*n* = 2. IMAC, immobilized metal-ion affinity chromatography.

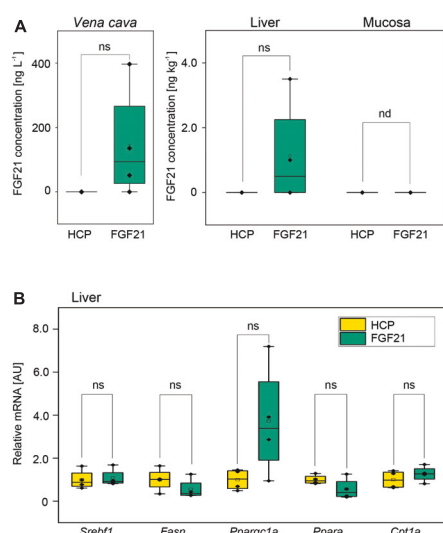


FIGURE 4 The mean bioavailability and bioactivity of the purified fusion protein nTf338-FGF21-PLUS in *in vivo* animal bolus feeding trial. FGF21^{-/-} knockout mice were starved for 16 h and gavaged with a 0.5 mL bolus of partially purified nTf338-FGF21-PLUS dissolved in water to a concentration of 50 $\mu\text{g L}^{-1}$ FGF21 and 44 g L^{-1} HCP (FGF21 group) or HCP only (HCP group). After 4 h, mice were sacrificed. (A) FGF21 concentration in the Vena cava, liver and mucosa of via FGF21-ELISA. (B) mRNA expression levels of the gene *Srebf1*, *Fasn*, *Ppargc1a*, *Ppara*, and *Cpt1a*, determined in liver tissue via qPCR (primer are listed in [Supplementary Table 1](#)). Numbers represent mean \pm SD. Significance was calculated by pair-sample t-test with **p* < 0.05, ***p* < 0.01, and ****p* < 0.001. *n* = 4, biological replicates. ns, not significant; nd, not detectable.

for the same fusion protein might be done in the future to further improve the accumulation level of nTf338-FGF21-PLUS.

In this context might replicating geminiviral vectors such as the BeYDV (Diamos et al., 2020) be used as alternative to the non-replicating pTRAc vector, used in the study, since the geminiviral DNA replicon does not have an insert size limitation as well and might increase the transgene copy number, transcription rate and mRNA level.

Nevertheless, based on the sevenfold increase in the accumulation of FGF21-F-Tf, when switching from transient to transgenic expression in leaves (Table 3), we assume that nTf338-FGF21-PLUS will exhibit a similar increase once stably transformed into tobacco plants.

Depth filtration limited the recovery of nTf338-FGF21-PLUS

The accumulation levels obtained in transiently and stably transformed plants was not sufficient for animal feeding studies for which the concentration needed to be > 50 mg kg^{-1} biomass in order to be able to apply 1 $\text{mg kg}^{-1} \text{d}^{-1}$ of nTf338-FGF21-PLUS per mice like in previous studies (Camporez et al., 2013; Emanuelli et al., 2014). Hence, we purified transiently expressed nTf338-FGF21-PLUS from *N. benthamiana* leaves, using a previously reported protocol (Menzel et al., 2018; Opdensteinen et al., 2021a,b). Whereas the step recovery average > 75% for most process steps, it was limited to ~5% for the depth filtration (Table 4). Using flocculants in combination with wide-pore filters or filters that are free of diatomaceous earth can help to resolve this bottleneck in the future (Buyel and Fischer, 2014; Buyel et al., 2015). However, even though knowing that this operation can be difficult to scale up and may need replacement in a large-scale process, in this proof-of-concept study, we replaced depth filtration by ultracentrifugation, yielding a step

recovery of ~95%. This indicated that some nTf338-FGF21-PLUS may be attached to particulate matter, which is retained by the filters. Adding low concentrations of detergents, such as Triton X-100, may help to increase the recovery in the future. Nevertheless, the overall recovery of the centrifugation-based process was ~32% corresponding to ~1.3 mg kg⁻¹ LFM (Table 4).

Irrespective of the method, the purity remained below 0.2% FGF21 relative to the TSP after IMAC (Table 4 and Supplementary Figure 4). This was an unusual result and the low initial nTf338-FGF21-PLUS concentration was a likely reason for unspecific HCP binding to the resin, reducing the product purity due to co-elution. In the future, the purification might be simplified and/or improved by incorporating alternative HCP precipitation strategies such as heat or pH (Buyel et al., 2016; Opdensteinen et al., 2021a).

Because previous animal feeding trials have successfully used freeze-dried, re-suspended leaf material, crude extracts or partially purified recombinant protein, e.g., CTB-Ex-4 or Ex-4-Tf, without any obvious negative impact of the impurities (Kwon et al., 2013; Choi et al., 2014; Phan et al., 2020), we proceeded with the partially purified nTf338-FGF21-PLUS

nTf338-FGF21-PLUS was bioactive and enabled selective FGF21 uptake into the liver without impacting bioactivity

The bioavailability and bioactivity of partially purified nTf338-FGF21-PLUS was tested *in vivo* using FGF21^{-/-} knockout mice. When nTf338-FGF21-PLUS was dissolved in water and orally gavaged (25 µg in 0.5 ml per mouse), FGF21 could be detected by ELISA in plasma obtained from the *Vena cava* in three and in liver homogenates in two out of four treated mice after 4 h (Figure 4A and Supplementary Figure 5A). In none of the supplemented mice could FGF21 be detected in the intestinal mucosa suggestive of an efficient transfer from the intestine to the liver.

Gene expression analysis of the liver revealed that the expression of the master regulator of fatty acid synthesis, the sterol regulatory element binding transcription factor 1 (*Srebf1*), was unaffected by FGF21, while its downstream target, the fatty acid synthase (*Fasn*) (Horton et al., 2002), seemed to be downregulated (Figure 4B and Supplementary Figure 5B). Unexpectedly, the expression of the regulator of fatty acid oxidation *Ppara* (peroxisome proliferator-activated receptor alpha) seemed also to be downregulated, while the expression of one of the targets of *Ppara*, *Cpt1a* (carnitine palmitoyltransferase 1a), a key enzyme in β -oxidation, (Ventura-Clapier et al., 2008) was unchanged (Figure 4B and Supplementary Figure 5B). However, the expression of a master regulator of mitochondrial biogenesis *Ppargc1a*, the gene encoding peroxisome proliferator-activated receptor gamma coactivator 1-alpha (PGC-1 α) (Jornayvaz and Shulman, 2010).

even though not significant, seemed to be upregulated as expected. These data indicated that orally delivered nTf338-FGF21-PLUS can affect hepatic lipid metabolism.

Discussion

We showed that a plant-derived FGF21-transferrin fusion protein can be used for oral delivery of FGF21 as a potential therapeutic of NASH and provide an initial comparison of different production options and associated costs in transgenic seeds and leaves which both might be used for oral delivery.

We demonstrated for SL632 that the tobacco seed yield can be improved by pruning to 380 g m⁻² a⁻¹ in a greenhouse with manufacturing costs of 1.64 € g⁻¹ SDM compared to 8,193 g m⁻² a⁻¹ and costs of 0.19 € g⁻¹ LFM for leaves.

When comparing SL632 seeds and VG leaves as production platforms, the biomass productivity per unit area and time was up to 30-fold higher (Table 3) and the production costs up to 15-fold lower for leaves (Table 2). However, ~98% of the costs were labor costs and assuming that these can be reduced by 90% when using semi-automated greenhouse facility (Huebbers and Buyel, 2021), the overall seed and leave production costs might be below 0.05 and 0.01 € g⁻¹ (Nandi et al., 2005). Based on a recent clinical study with rice seeds, 6 g can be sufficient for oral vaccination (Yuki et al., 2021) and costs of <0.50 € per dose would also be affordable for developing countries and thus drastically lower compared to therapeutics, containing purified recombinant protein from transiently transformed leaves of up to 500 € per dosage (Tusé et al., 2014).

Independent from that, we produced an intact, bioactive FGF21-F-Tf fusion protein, accumulating to 6.7 and 5.6 mg kg⁻¹ in transgenic tobacco seeds and leaves respectively, whereas transient expression in *N. benthamiana* leaves generated up to 2.1 mg kg⁻¹. The yield of FGF21-F-Tf in seeds was 22-fold higher compared to recombinant IL6 for which the constitutive 35S CaMV expression cassette has been used as well but substantially lower compared to other proteins that were expressed with a seed-specific promoter/terminator in tobacco seeds at accumulation levels of 190–6,500 mg kg⁻¹ SDM (Supplementary Table 6; Fiedler and Conrad, 1995; Kusnadi et al., 1998; De Jaeger et al., 2002; Cheung et al., 2009; Zimmermann et al., 2009; Zhang et al., 2010; Nausch et al., 2012b; Hensel et al., 2015; Hernandez-Velazquez et al., 2015; Weichert et al., 2016; Ceballo et al., 2017; Queiroz et al., 2019). Therefore, using a seed-specific expression cassette might increase FGF21-Tf fusion protein yields in the future.

However, the accumulation of FGF21-F-Tf was limited by proteolytic degradation (Figure 2 and Supplementary Figures 2, 3) and the removal of the furin cleavage site reduced the amount of degradation products. On the one hand, this indicated that even though the mammalian protease furin does not occur in plants (Wilbers et al., 2016), furin-like plant proteases such as Kex2p may cleave furin sites (Kinal

et al., 1995). This observation contradicts previous reports in which recombinant proteins, containing a furin cleavage site, did not exhibit degradation in plants (Verma et al., 2010; Boyhan and Daniell, 2011; Kang et al., 2018; Kwon et al., 2018; Mamedov et al., 2019; Margolin et al., 2020). On the other hand, degradation may not be linked to the furin cleavage site itself but to the GS-linker region surrounding the furin site as observed for other fusion proteins (Benchabane et al., 2008) and as reported for the GS-linker (Chen et al., 2012). Such a non-exclusive cleavage is in agreement with our finding that removing the furin cleavage site reduced but did not completely prevent FGF21-transferrin degradation (Figure 2 and Supplementary Figure 2). In this respect, other linkers could be tested in the future to increase FGF21-transferrin fusion protein stability, e.g., a rigid EA-linker (Supplementary Table 7; Amet et al., 2009; Kim et al., 2010; Fu et al., 2011; Wang et al., 2011, 2014; Chen et al., 2012, 2018; Choi et al., 2014; Liu et al., 2020). However, a linker may not be necessary at all as we showed by using the liver-targeting PLUS peptide (Lu et al., 2014; Ma et al., 2014, 2017; Taverner et al., 2020). In a next step, the accumulation of this optimized construct in combination with a seed-specific expression cassette should be tested in transgenic seeds to obtain accumulation levels sufficient for oral delivery.

Alternatively to tobacco, other crops such as rice, barley, maize or pea and soybean can be used for the production of FGF21-transferrin fusion proteins as well (Supplementary Table 6), since these crops yield similar quantities of recombinant protein. For example, Tf yielded 10.00 g kg⁻¹ in rice seeds (Supplementary Table 6). In addition, commercial, semi-automated greenhouse facilities have been established for rice (Ventria Bioscience, Junction City, KS, USA) (see text footnote 1) and barley (ORF Genetics, Kópavogur, Island) (see text footnote 2).

Importantly, more FGF21-F-Tf degradation was observed in transgenic seeds (67%) than in transgenic leaves (41%) (Figure 2), indicating that, opposed to the common notion (Benchabane et al., 2008), protein expression in seeds may not always be advantageous in terms of product stability and accumulation. The reduced degradation of FGF21-F-Tf in leaves might also explain why the yield in transgenic leaves was only slightly lower compared to seeds with 5.6 mg kg⁻¹ LFM and 6.7 mg kg⁻¹ SDM for SL632 (Table 3), even though the 8- to 30-fold lower protein content in leaves, i.e., 1–2% protein per LFM in leaves compared to 25–30% protein per SDM, would suggest a drastically higher difference, assuming that the activity of the CaMV expression cassette is similar in both tissues. Therefore, transgenic leaves may be a more suitable platform for the production of FGF21-transferrin fusion proteins than seeds. Noteworthy, due to the higher accumulation, transgenic leaves even outcompeted the transient transformation by up to fivefold (Table 3).

Bioavailability and hepatic bioactivity of nTf3338-FGF21-PLUS after oral delivery was evidenced by a first *in vivo*

trial using FGF21^{-/-} mice (Figure 4). This is in agreement with previous studies in which partially purified recombinant protein has been used for oral delivery in mice without any obvious negative impact of the plant-related impurities (Choi et al., 2014). Our study also confirmed that Tf can be used to mediate an uptake from the intestine to blood as shown for Ex-4 (Choi et al., 2014), while the PLUS peptide enabled exclusive delivery to the liver as demonstrated for endostatin (Lu et al., 2014; Ma et al., 2014, 2017; Taverner et al., 2020). The observed effects on liver gene expression are in line with the known beneficial hepatic effects of FGF21 such as a reduction of lipid accumulation and improvement of mitochondrial function (Tillman and Rolph, 2020).

Data availability statement

The original contributions presented in this study are included in the article/Supplementary material, further inquiries can be directed to the corresponding author.

Ethics statement

The animal study was reviewed and approved by the Ethics Committee of the Ministry for Environment, Health and Consumer Protection of Brandenburg, Germany (approval no. 2347-9-2020).

Author contributions

H-WH, HN, CB, SK, IB, and JB conceived the experiments. H-WH and CB conducted the experiments and analyzed the data. H-WH and HN wrote the manuscript. All authors contributed to manuscript revision, read, and approved the submitted version.

Funding

This work was funded by the Deutsche Forschungsgemeinschaft (DFG) under the grant agreement no. NA 1216/3-1 and KL613/25-1 “Oral FGF21 delivery to limit its action to the liver,” and conducted as collaboration between the Fraunhofer Institute for Molecular Biology and Applied Ecology IME, the University of Rostock, and the German Institute of Human Nutrition Potsdam-Rehbrücke.

Acknowledgments

We credit the support of Sonja Konopka, Kerstin Thoss, Dirk Scheffler, Jörg Schuphan as well as of Lina Hollmann and

Paul Reunious, and technical assistance by Carolin Borchert. The experiments with the MagnICON vectors were conducted at the University of Rostock, while the experiments with the pTRAc vectors were done at the Fraunhofer Institute for Molecular Biology and Applied Ecology IME. The stably transformed tobacco plants were created at the University of Rostock and analyzed at the Fraunhofer Institute for Molecular Biology and Applied Ecology IME. Animal trials were performed at the German Institute of Human Nutrition Potsdam-Rehbrücke.

Conflict of interest

The authors declare that the research was conducted in the absence of any commercial or financial relationships that could be construed as a potential conflict of interest.

References

- Albhaisi, S. A. M., and Sanyal, A. J. (2021). New drugs for NASH. *Liver Int.* 41, 112–118.
- Amet, N., Lee, H. F., and Shen, W. C. (2009). Insertion of the designed helical linker led to increased expression of TF-based fusion proteins. *Pharm. Res.* 26, 523–528. doi: 10.1007/s11095-008-9767-0
- Asrani, S. K., Devarbhavi, H., Eaton, J., and Kamath, P. S. (2019). Burden of liver diseases in the world. *J. Hepatol.* 70, 151–171.
- Badman, M. K., Pissios, P., Kennedy, A. R., Koukos, G., Flier, J. S., and Maratos-Flier, E. (2007). Hepatic Fibroblast Growth Factor 21 Is Regulated by PPAR α and Is a Key Mediator of Hepatic Lipid Metabolism in Ketotic States. *Cell Metab.* 5, 426–437. doi: 10.1016/j.cmet.2007.05.002
- Benchabane, M., Goulet, C., Rivard, D., Faye, L., Gomord, V., and Michaud, D. (2008). Preventing unintended proteolysis in plant protein biofactories. *Plant Biotechnol. J.* 6, 633–648. doi: 10.1111/j.1467-7652.2008.00344.x
- Boothe, J., Nykiforuk, C., Shen, Y., Zaplachinski, S., Szarka, S., Kuhlman, P., et al. (2010). Seed-based expression systems for plant molecular farming. *Plant Biotechnol. J.* 8, 588–606.
- Boyhan, D., and Daniell, H. (2011). Low-cost production of proinsulin in tobacco and lettuce chloroplasts for injectable or oral delivery of functional insulin and C-peptide. *Plant Biotechnol. J.* 9, 585–598. doi: 10.1111/j.1467-7652.2010.00582.x
- Brandsma, M. E., Diao, H., Wang, X., Kohalmi, S. E., Jevnikar, A. M., and Ma, S. (2010). Plant-derived recombinant human serum transferrin demonstrates multiple functions. *Plant Biotechnol. J.* 8, 489–505. doi: 10.1111/j.1467-7652.2010.00499.x
- Broz, A., Huang, N., and Unruh, G. (2013). Plant-Based Protein Biomanufacturing. *GEN Genet. Eng. Biotechnol. News* 33, 32–33.
- Buyel, J. F. (2016). Numeric simulation can be used to predict heat transfer during the blanching of leaves and intact plants. *Biochem. Eng. J.* 109, 118–126.
- Buyel, J. F., and Fischer, R. (2014). Flocculation increases the efficacy of depth filtration during the downstream processing of recombinant pharmaceutical proteins produced in tobacco. *Plant Biotechnol. J.* 12, 240–252. doi: 10.1111/pbi.12132
- Buyel, J. F., Gruchow, H. M., and Fischer, R. (2015). Depth Filters Containing Diatomite Achieve More Efficient Particle Retention than Filters Solely Containing Cellulose Fibers. *Front. Plant Sci.* 6:1134. doi: 10.3389/fpls.2015.01134
- Buyel, J. F., Hubbuch, J., and Fischer, R. (2016). Comparison of Tobacco Host Cell Protein Removal Methods by Blanching Intact Plants or by Heat Treatment of Extracts. *J. Vis. Exp.* 114:e54343.
- Buyel, J. F., Twyman, R. M., and Fischer, R. (2017). Very-large-scale production of antibodies in plants: The biologization of manufacturing. *Biotechnol. Adv.* 35, 458–465. doi: 10.1016/j.biotechadv.2017.03.011
- Camporez, J. P., Jornayvaz, F. R., Petersen, M. C., Pesta, D., Guigni, B. A., Serr, J., et al. (2013). Cellular mechanisms by which FGF21 improves insulin sensitivity in male mice. *Endocrinology* 154, 3099–3109.
- Ceballo, Y., Tiel, K., Lopez, A., Cabrera, G., Perez, M., Ramos, O., et al. (2017). High accumulation in tobacco seeds of hemagglutinin antigen from avian (H5N1) influenza. *Transgenic Res.* 26, 775–789. doi: 10.1007/s11248-017-0047-9
- Charles, E. D., Neuschwander-Tetri, B. A., Pablo Frias, J., Kundu, S., Luo, Y., Tiruchurai, G. S., et al. (2019). Pegbelfermin (BMS-986036), PEGylated FGF21, in Patients with Obesity and Type 2 Diabetes: Results from a Randomized Phase 2 Study. *Obesity* 27, 41–49. doi: 10.1002/oby.22344
- Chen, X., Zaro, J. L., and Shen, W. C. (2012). Fusion Protein Linkers: Property, Design and Functionality. *Adv. Drug Deliv. Rev.* 65, 1357–1369.
- Chen, Y. S., Zaro, J. L., Zhang, D., Huang, N., Simon, A., and Shen, W. C. (2018). Characterization and Oral Delivery of Proinsulin-Transferrin Fusion Protein Expressed Using ExpressTec. *Int. J. Mol. Sci.* 19, 378–390. doi: 10.3390/ijms19020378
- Cheung, S. C., Sun, S. S., Chan, J. C., and Tong, P. C. (2009). Expression and subcellular targeting of human insulin-like growth factor binding protein-3 in transgenic tobacco plants. *Transgenic Res.* 18, 943–951. doi: 10.1007/s11248-009-9286-8
- Choi, J., Diao, H., Feng, Z. C., Lau, A., Wang, R., Jevnikar, A. M., et al. (2014). A fusion protein derived from plants holds promising potential as a new oral therapy for type 2 diabetes. *Plant Biotechnol. J.* 12, 425–435. doi: 10.1111/pbi.12149
- Conley, A. J., Zhu, H., Le, L. C., Jevnikar, A. M., Lee, B. H., Brandle, J. E., et al. (2011). Recombinant protein production in a variety of *Nicotiana* hosts: A comparative analysis. *Plant Biotechnol. J.* 9, 434–444. doi: 10.1111/j.1467-7652.2010.00563.x
- Cunha, N. B., Murad, A. M., Cipriano, T. M., Araújo, A. C., Aragão, F. J., Leite, A., et al. (2011). Expression of functional recombinant human growth hormone in transgenic soybean seeds. *Transgenic Res.* 20, 811–826. doi: 10.1007/s11248-010-9460-z
- De Jaeger, G., Scheffer, S., Jacobs, A., Zambre, M., Zobel, O., Goossens, A., et al. (2002). Boosting heterologous protein production in transgenic dicotyledonous seeds using *Phaseolus vulgaris* regulatory sequences. *Nat. Biotechnol.* 20, 1265–1268. doi: 10.1038/nbt755
- De Marchis, F., Balducci, C., Pompa, A., Riise Stensland, H. M., Guaragno, M., Paggiotti, R., et al. (2011). Human α -mannosidase produced in transgenic tobacco plants is processed in human α -mannosidosis cell lines. *Plant Biotechnol. J.* 9, 1061–1073. doi: 10.1111/j.1467-7652.2011.00630.x

Publisher's note

All claims expressed in this article are solely those of the authors and do not necessarily represent those of their affiliated organizations, or those of the publisher, the editors and the reviewers. Any product that may be evaluated in this article, or claim that may be made by its manufacturer, is not guaranteed or endorsed by the publisher.

Supplementary material

The Supplementary Material for this article can be found online at: <https://www.frontiersin.org/articles/10.3389/fpls.2022.998596/full#supplementary-material>

- Diamos, A. G., Hunter, J. G. L., Pardhe, M. D., Rosenthal, S. H., Sun, H., Foster, B. C., et al. (2020). High Level Production of Monoclonal Antibodies Using an Optimized Plant Expression System. *Front. Bioeng. Biotechnol.* 7:472. doi: 10.3389/fbioe.2019.00472
- Duckert, P., Brunak, S., and Blom, N. (2004). Prediction of proprotein convertase cleavage sites. *Protein Eng. Des. Sel.* 17, 107–112.
- Dushay, J., Chui, P. C., Gopalakrishnan, G. S., Varela-Rey, M., Crawley, M., Fisher, F. M., et al. (2010). Increased Fibroblast Growth Factor 21 in Obesity and Nonalcoholic Fatty Liver Disease. *Gastroenterology* 139, 456–463.
- Emanuelli, B., Vienberg, S. G., Smyth, G., Cheng, C., Stanford, K. I., Arumugam, M., et al. (2014). Interplay between FGF21 and insulin action in the liver regulates metabolism. *J. Clin. Invest.* 124, 515–527.
- Estes, C., Razavi, H., Loomba, R., Younossi, Z., and Sanyal, A. J. (2018). Modeling the epidemic of nonalcoholic fatty liver disease demonstrates an exponential increase in burden of disease. *Hepatology* 67, 123–133. doi: 10.1002/hep.29466
- Evans, T. C., Martin, D., Kolly, R., Panne, D., Sun, L., Ghosh, I., et al. (2000). Protein trans-splicing and cyclization by a naturally split intein from the *dnaE* gene of *Synechocystis* species PCC6803. *J. Biol. Chem.* 275, 9091–9094. doi: 10.1074/jbc.275.13.9091
- Feingold, K. R., Grunfeld, C., Heuer, J. G., Gupta, A., Cramer, M., Zhang, T., et al. (2012). FGF21 is increased by inflammatory stimuli and protects leptin-deficient ob/ob mice from the toxicity of sepsis. *Endocrinology* 153, 2689–2700. doi: 10.1210/en.2011-1496
- Fiedler, U., and Conrad, U. (1995). High-level production and long-term storage of engineered antibodies in transgenic tobacco seeds. *Biotechnology* 13, 1090–1093. doi: 10.1038/nbt1095-1090
- Fu, H., Pang, S., Xue, P., Yang, J., Liu, X., Wang, Y., et al. (2011). High levels of expression of fibroblast growth factor 21 in transgenic tobacco (*Nicotiana benthamiana*). *Appl. Biochem. Biotechnol.* 165, 465–475. doi: 10.1007/s12010-011-9265-4
- Ghag, S. B., Adki, V. S., Ganapathi, T. R., and Bapat, V. A. (2021). Plant Platforms for Efficient Heterologous Protein Production. *Biotechnol. Bioprocess. Eng.* 26, 546–567.
- Jimeno, R. E., and Moller, D. E. (2014). FGF21-based pharmacotherapy—potential utility for metabolic disorders. *Trends Endocrinol. Metab.* 25, 303–311. doi: 10.1016/j.tem.2014.03.001
- Giragossian, C., Vage, C., Li, J., Pelletier, K., Piché-Nicholas, N., Rajadhyaksha, M., et al. (2015). Mechanistic investigation of the preclinical pharmacokinetics and interspecies scaling of PF-05231023, a fibroblast growth factor 21-antibody protein conjugate. *Drug Metab. Dispos.* 43, 803–811. doi: 10.1124/dmd.114.061713
- Giritch, A., Marillonnet, S., Engler, C., van Eldik, G., Botterman, J., Klimyuk, V., et al. (2006). Rapid high-yield expression of full-size IgG antibodies in plants coinfecting with noncompeting viral vectors. *Proc. Natl. Acad. Sci. U. S. A.* 103, 14701–14706.
- Gleba, Y., Klimyuk, V., and Marillonnet, S. (2005). Magnification—a new platform for expressing recombinant vaccines in plants. *Vaccine* 23, 2042–2048. doi: 10.1016/j.vaccine.2005.01.006
- Hensel, G., Floss, D. M., Arcalis, E., Sack, M., Melnik, S., Altmann, F., et al. (2015). Transgenic Production of an Anti HIV Antibody in the Barley Endosperm. *PLoS One* 10:e0140476. doi: 10.1371/journal.pone.0140476
- Hernandez-Velazquez, A., Lopez-Quesada, A., Ceballo-Camara, Y., Cabrera-Herrera, G., Tiel-Gonzalez, K., Mirabal-Ortega, L., et al. (2015). Tobacco seeds as efficient production platform for a biologically active anti-HBsAg monoclonal antibody. *Transgenic Res.* 24, 897–909. doi: 10.1007/s11248-015-9890-8
- Holtz, B. R., Berquist, B. R., Bennett, L. D., Kommineni, V. J., Munigunt, R. K., White, E. L., et al. (2015). Commercial-scale biotherapeutics manufacturing facility for plant-made pharmaceuticals. *Plant Biotechnol. J.* 13, 1180–1190. doi: 10.1111/pbi.12469
- Horton, J. D., Goldstein, J. L., and Brown, M. S. (2002). SREBPs: Activators of the complete program of cholesterol and fatty acid synthesis in the liver. *J. Clin. Invest.* 109, 1125–1131.
- Houdelet, M., Galinski, A., Holland, T., Wenzel, K., Schillberg, S., and Buyel, J. F. (2017). Animal component-free *Agrobacterium tumefaciens* cultivation media for better GMP-compliance increases biomass yield and pharmaceutical protein expression in *Nicotiana benthamiana*. *Biotechnol. J.* 12:1600721. doi: 10.1002/biot.201600721
- Huang, J., Ishino, T., Chen, G., Rolzin, P., Osothprarop, T. F., Retting, K., et al. (2013). Development of a novel long-acting antidiabetic FGF21 mimetic by targeted conjugation to a scaffold antibody. *J. Pharmacol. Exp. Ther.* 346, 270–280. doi: 10.1124/jpet.113.204420
- Huebbers, J. W., and Buyel, J. F. (2021). On the verge of the market – Plant factories for the automated and standardized production of biopharmaceuticals. *Biotechnol. Adv.* 46:e107681. doi: 10.1016/j.biotechadv.2020.107681
- Jornayvaz, F. R., and Shulman, G. I. (2010). Regulation of mitochondrial biogenesis. *Essays Biochem.* 47, 69–84.
- Källberg, M., Wang, H., Wang, S., Peng, J., Wang, Z., Lu, H., et al. (2012). Template-based protein structure modeling using the RaptorX web server. *Nat. Protoc.* 7, 1511–1522.
- Kang, H., Park, Y., Lee, Y., Yoo, Y. J., and Hwang, I. (2018). Fusion of a highly N-glycosylated polypeptide increases the expression of ER-localized proteins in plants. *Sci. Rep.* 8, 4612–4621. doi: 10.1038/s41598-018-22860-2
- Kasper, P., Martin, A., Lang, S., Kütting, F., Goers, T., Demir, M., et al. (2020). NAFLD and cardiovascular diseases: A clinical review. *Clin. Res. Cardiol.* 110, 921–937.
- Kay, R., Chan, A., Daly, M., and McPherson, J. (1987). Duplication of CaMV 35S Promoter Sequences Creates a Strong Enhancer for Plant Genes. *Science* 236, 1299–1302. doi: 10.1126/science.236.4806.1299
- Kempe, K., Rubtsova, M., and Gils, M. (2009). Intein-mediated protein assembly in transgenic wheat: Production of active barnase and acetolactate synthase from split genes. *Plant Biotechnol. J.* 7, 283–297. doi: 10.1111/j.1467-7652.2008.00399.x
- Khan, F., He, M., and Taussig, M. J. (2006). Double-Hexahistidine Tag with High-Affinity Binding for Protein Immobilization, Purification, and Detection on Ni-Nitrilotriacetic Acid Surfaces. *Anal. Chem.* 78, 3072–3079. doi: 10.1021/ac060184l
- Kharitononkov, A., Beals, J. M., Micanovic, R., Striffler, B. A., Rathnachalam, R., and Wroblewski, V. J. (2013). Rational design of a fibroblast growth factor 21-based clinical candidate, LY2405319. *PLoS One* 8:e58575. doi: 10.1371/journal.pone.0058575
- Kharitononkov, A., Shiyanova, T. L., Koester, A., Ford, A. M., Micanovic, R., Galbreath, E. J., et al. (2005). FGF-21 as a novel metabolic regulator. *J. Clin. Invest.* 115, 1627–1635.
- Kim, B. J., Zhou, J., Martin, B., Carlson, O. D., Maudsley, S., Greig, N. H., et al. (2010). Transferrin fusion technology: A novel approach to prolonging biological half-life of insulinotropic peptides. *J. Pharmacol. Exp. Ther.* 334, 682–692. doi: 10.1124/jpet.110.166470
- Kinal, H., Park, C. M., Berry, J. O., Koltin, Y., and Bruenn, J. A. (1995). Processing and secretion of a virally encoded antifungal toxin in transgenic tobacco plants: Evidence for a Kex2p pathway in plants. *Plant Cell* 7, 677–688. doi: 10.1105/tpc.7.6.677
- Kusnadi, A. R., Hood, E. E., Witcher, D. R., Howard, J. A., and Nikolov, Z. L. (1998). Production and purification of two recombinant proteins from transgenic corn. *Biotechnol. Prog.* 14, 149–155.
- Kwon, K. C., Nityanandam, R., New, J. S., and Daniell, H. (2013). Oral delivery of bioencapsulated exendin-4 expressed in chloroplasts lowers blood glucose level in mice and stimulates insulin secretion in beta-TC6 cells. *Plant Biotechnol. J.* 11, 77–86. doi: 10.1111/pbi.12008
- Kwon, K. C., Sherman, A., Chang, W. J., Kamesh, A., Biswas, M., Herzog, R. W., et al. (2018). Expression and assembly of largest foreign protein in chloroplasts: Oral delivery of human FVIII made in lettuce chloroplasts robustly suppresses inhibitor formation in haemophilia A mice. *Plant Biotechnol. J.* 16, 1148–1160. doi: 10.1111/pbi.12859
- LaBrecque, D. R., Abbas, Z., Anania, F., Ferenci, P., Khan, A. G., Goh, K. L., et al. (2014). World Gastroenterology Organisation global guidelines: Nonalcoholic fatty liver disease and nonalcoholic steatohepatitis. *J. Clin. Gastroenterol.* 48, 467–473. doi: 10.1097/MCG.0000000000000116
- Liu, Y., Wang, H. Y., Shao, J., Zaro, J. L., and Shen, W. C. (2020). Enhanced insulin receptor interaction by a bifunctional insulin-transferrin fusion protein: An approach to overcome insulin resistance. *Sci. Rep.* 10:e7724. doi: 10.1038/s41598-020-64731-9
- Lu, X., Jin, X., Huang, Y., Wang, J., Shen, J., Chu, F., et al. (2014). Construction of a novel liver-targeting fusion interferon by incorporation of a *Plasmodium* region I-plus peptide. *Biomed. Res. Int.* 2014:e261631. doi: 10.1155/2014/261631
- Lundäsen, T., Hunt, M. C., Nilsson, L. M., Sanyal, S., Angelin, B., Alexson, S. E., et al. (2007). PPAR α is a key regulator of hepatic FGF21. *Biochem. Biophys. Res. Commun.* 360, 437–440.
- Ma, Y., Bao, D. M., Zhang, J. J., Jin, X. B., Wang, J., Yan, W., et al. (2017). Antitumor activities of Liver-targeting peptide modified Recombinant human Endostatin in BALB/c-nu mice with Hepatocellular carcinoma. *Sci. Rep.* 7:e14074. doi: 10.1038/s41598-017-14320-0
- Ma, Y., Jin, X. B., Chu, F. J., Bao, D. M., and Zhu, J. Y. (2014). Expression of liver-targeting peptide modified recombinant human endostatin and preliminary

- study of its biological activities. *Appl. Microbiol. Biotechnol.* 98, 7923–7933. doi: 10.1007/s00253-014-5818-0
- Maclean, J., Koekemoer, M., Olivier, A. J., Stewart, D., Hitzeroth, I. I., Rademacher, T., et al. (2007). Optimization of human papillomavirus type 16 (HPV-16) L1 expression in plants: Comparison of the suitability of different HPV-16 L1 gene variants and different cell-compartment localization. *J. Gen. Virol.* 88, 1460–1469. doi: 10.1099/vir.0.82718-0
- Mamedov, T., Musayeva, I., Acsora, R., Gun, N., Gulec, B., Mammadova, G., et al. (2019). Engineering, and production of functionally active human Furin in *N. benthamiana* plant: In vivo post-translational processing of target proteins by Furin in plants. *PLoS One* 14:e0213438. doi: 10.1371/journal.pone.0213438
- Margolin, E., Oh, Y. J., Verbeek, M., Naude, J., Ponndorf, D., Meshcheriakova, Y. A., et al. (2020). Co-expression of human calreticulin significantly improves the production of HIV gp140 and other viral glycoproteins in plants. *Plant Biotechnol. J.* 18, 2109–2117. doi: 10.1111/pbi.13369
- Marillonnet, S., Giritch, A., Gils, M., Kandzia, R., Klimyuk, V., and Gleba, Y. (2004). In planta engineering of viral RNA replicons: Efficient assembly by recombination of DNA modules delivered by *Agrobacterium*. *Proc. Natl. Acad. Sci. U. S. A.* 101, 6852–6857. doi: 10.1073/pnas.0400149101
- Marillonnet, S., Thoeringer, C., Kandzia, R., Klimyuk, V., and Gleba, Y. (2005). Systemic *Agrobacterium tumefaciens*-mediated transfection of viral replicons for efficient transient expression in plants. *Nat. Biotechnol.* 23, 718–723. doi: 10.1038/nbt1094
- Mason, A. B., Woodworth, R. C., Oliver, R. W., Green, B. N., Lin, L. N., Brandts, J. F., et al. (1996). Production and isolation of the recombinant N-lobe of human serum transferrin from the methylotrophic yeast *Pichia pastoris*. *Protein Expr. Purif.* 8, 119–125. doi: 10.1006/prep.1996.0081
- Menzel, S., Holland, T., Boes, A., Spiegel, H., Fischer, R., and Buyel, J. F. (2018). Downstream processing of a plant-derived malaria transmission-blocking vaccine candidate. *Protein Expr. Purif.* 152, 122–130.
- Moustafa, K., Makhzoum, A., and Tremouillaux-Guiller, J. (2016). Molecular farming on rescue of pharma industry for next generations. *Crit. Rev. Biotechnol.* 36, 840–850. doi: 10.3109/07388551.2015.1049934
- Mullard, A. (2020). FDA rejects NASH drug. *Nat. Rev. Drug Discov.* 19:501.
- Nandi, S., Yalda, D., Lu, S., Nikolov, Z., Misaki, R., Fujiyama, K., et al. (2005). Process development and economic evaluation of recombinant human lactoferrin expressed in rice grain. *Transgenic Res.* 14, 237–249. doi: 10.1007/s11248-004-8120-6
- Nausch, H., Hausmann, T., Ponndorf, D., Hühns, M., Hoedtker, S., Wolf, P., et al. (2016). Tobacco as platform for a commercial production of cyanophycin. *N. Biotechnol.* 33, 842–851. doi: 10.1016/j.nbt.2016.08.001
- Nausch, H., Mikschofsky, H., Koslowski, R., Meyer, U., Broer, I., and Huckauf, J. (2012a). Expression and Subcellular Targeting of Human Complement Factor C5a in *Nicotiana* species. *PLoS One* 7:e53023. doi: 10.1371/journal.pone.0053023
- Nausch, H., Mikschofsky, H., Koslowski, R., Meyer, U., Broer, I., and Huckauf, J. (2012b). High-level transient expression of ER-targeted human interleukin 6 in *Nicotiana benthamiana*. *PLoS One* 7:e48938. doi: 10.1371/journal.pone.0048938
- Nishimura, T., Nakatake, Y., Konishi, M., and Itoh, N. (2000). Identification of a novel FGF, FGF-21, preferentially expressed in the liver. *Biochim. Biophys. Acta* 1492, 203–206. doi: 10.1016/s0167-4781(00)00067-1
- Odell, J. T., Nagy, F., and Chua, N. H. (1985). Identification of DNA sequences required for activity of the cauliflower mosaic virus 35S promoter. *Nature* 313, 810–812.
- Opdensteinen, P., Lobanov, A., and Buyel, J. F. (2021a). A combined pH and temperature precipitation step facilitates the purification of tobacco-derived recombinant proteins that are sensitive to extremes of either parameter. *Biotechnol. J.* 16:e2000340. doi: 10.1002/biot.202000340
- Opdensteinen, P., Meyer, S., and Buyel, J. F. (2021b). *Nicotiana* spp. for the Expression and Purification of Functional IgG3 Antibodies Directed Against the *Staphylococcus aureus* Alpha Toxin. *Front. Chem. Eng.* 3:737010. doi: 10.3389/fceng.2021.737010
- Ost, M., Coleman, V., Voigt, A., van Schothorst, E. M., Keipert, S., van der Stelt, I., et al. (2016). Muscle mitochondrial stress adaptation operates independently of endogenous FGF21 action. *Mol. Metab.* 5, 79–90. doi: 10.1016/j.molmet.2015.11.002
- Phan, H. T., Hause, B., Hause, G., Arcalis, E., Stoger, E., Maresch, D., et al. (2014). Influence of elastin-like polypeptide and hydrophobin on recombinant hemagglutinin accumulations in transgenic tobacco plants. *PLoS One* 9:e99347. doi: 10.1371/journal.pone.0099347
- Phan, H. T., van Pham, T., Ho, T. T., Pham, N. B., Chu, H. H., Vu, T. H., et al. (2020). Immunization with Plant-Derived Multimeric H5 Hemagglutinins Protect Chicken against Highly Pathogenic Avian Influenza Virus H5N1. *Vaccines* 8, 593–610. doi: 10.3390/vaccines8040593
- Povsic, M., Wong, O. Y., Perry, R., and Bottomley, J. (2019). A Structured Literature Review of the Epidemiology and Disease Burden of Non-Alcoholic Steatohepatitis (NASH). *Adv. Ther.* 36, 1574–1594.
- Queiroz, L. N., Maldaner, F. R., Mendes, E. A., Sousa, A. R., D'Alastta, R. C., Mendonça, G., et al. (2019). Evaluation of lettuce chloroplast and soybean cotyledon as platforms for production of functional bone morphogenetic protein 2. *Transgenic Res.* 28, 213–224. doi: 10.1007/s11248-019-00116-7
- Rossi, L., Dell'Orto, V., Vagni, S., Sala, V., Reggi, S., and Baldi, A. (2014). Protective effect of oral administration of transgenic tobacco seeds against verocytotoxic *Escherichia coli* strain in piglets. *Vet. Res. Commun.* 38, 39–49. doi: 10.1007/s11259-013-9583-9
- Rossi, L., Di Giancamillo, A., Reggi, S., Domeneghini, C., Baldi, A., Sala, V., et al. (2013). Expression of verocytotoxic *Escherichia coli* antigens in tobacco seeds and evaluation of gut immunity after oral administration in mouse model. *J. Vet. Sci.* 14, 263–270. doi: 10.4142/jvs.2013.14.3.263
- Sanyal, A., Charles, E. D., Neuschwander-Tetri, B. A., Loomba, R., Harrison, S. A., Abdelmalek, M. F., et al. (2018). Pegbelfermin (BMS-986036), a PEGylated fibroblast growth factor 21 analogue, in patients with non-alcoholic steatohepatitis: A randomised, double-blind, placebo-controlled, phase 2a trial. *Lancet* 392, 2705–2717. doi: 10.1016/S0140-6736(18)31785-9
- Schwegler, J. S., and Lucius, R. (2022). *Der Mensch - Anatomie und Physiologie, 7., überarbeitete Auflage.* CNE Bibliothek. Stuttgart, NY: Thieme.
- Shaalit, Y., Bartfeld, D., Hashmueli, S., Baum, G., Brill-Almon, E., Galili, G., et al. (2007). Production of glucocerebrosidase with terminal mannose glycans for enzyme replacement therapy of Gaucher's disease using a plant cell system. *Plant Biotechnol. J.* 5, 579–590. doi: 10.1111/j.1467-7652.2007.00263.x
- Sharma, M., Premkumar, M., Kulkarni, A. V., Kumar, P., Reddy, D. N., and Rao, N. P. (2021). Drugs for Non-alcoholic Steatohepatitis (NASH): Quest for the Holy Grail. *J. Clin. Transl. Hepatol.* 9, 40–50. doi: 10.14218/JCTH.2020.0055
- Sonoda, J., Chen, M. Z., and Baruch, A. (2017). FGF21-receptor agonists: An emerging therapeutic class for obesity-related diseases. *Horm. Mol. Biol. Clin. Investig.* 30, 1–13. doi: 10.1515/hmbci-2017-0002
- Sun, L., Ghosh, I., Paulus, H., and Xu, M. Q. (2001). Protein trans-splicing to produce herbicide-resistant acetolactate synthase. *Appl. Environ. Microbiol.* 67, 1025–1029.
- Talukdar, S., Zhou, Y., Li, D., Rossulek, M., Dong, J., Somayaji, V., et al. (2016). A Long-Acting FGF21 Molecule, PF-05231023, Decreases Body Weight and Improves Lipid Profile in Non-human Primates and Type 2 Diabetic Subjects. *Cell Metab.* 23, 427–440. doi: 10.1016/j.cmet.2016.02.001
- Taverner, A., MacKay, J., Laurent, F., Hunter, T., Liu, K., Mangat, K., et al. (2020). Cholix protein domain I functions as a carrier element for efficient apical to basal epithelial transcytosis. *Tissue Barriers* 8:e1710429. doi: 10.1080/21688370.2019.1710429
- Tillman, E. J., and Rolph, T. (2020). FGF21: An Emerging Therapeutic Target for Non-Alcoholic Steatohepatitis and Related Metabolic Diseases. *Front. Endocrinol.* 11:601290. doi: 10.3389/fendo.2020.601290
- Tusé, D., Tu, T., and McDonald, K. A. (2014). Manufacturing economics of plant-made biologics: Case studies in therapeutic and industrial enzymes. *Biomed. Res. Int.* 2014:e256135. doi: 10.1155/2014/256135
- Ventura-Clapier, R., Garnier, A., and Veksler, V. (2008). Transcriptional control of mitochondrial biogenesis: The central role of PGC-1 α . *Cardiovasc. Res.* 79, 208–217.
- Verma, D., Moghimi, B., LoDuca, P. A., Singh, H. D., Hoffman, B. E., Herzog, R. W., et al. (2010). Oral delivery of bioencapsulated coagulation factor IX prevents inhibitor formation and fatal anaphylaxis in hemophilia B mice. *Proc. Natl. Acad. Sci. U. S. A.* 107, 7101–7106. doi: 10.1073/pnas.0912181107
- Verzijl, C. R. C., Van De Peppel Ivo, P., Struik, D., and Jonker, J. W. (2020). Pegbelfermin (BMS-986036): An investigational PEGylated fibroblast growth factor 21 analogue for the treatment of nonalcoholic steatohepatitis. *Expert Opin. Investig. Drugs* 29, 125–133. doi: 10.1080/13543784.2020.1708898
- Wang, Y., Chen, Y. S., Zaro, J. L., and Shen, W. C. (2011). Receptor-Mediated Activation of a Proinsulin-Transferrin Fusion Protein in Hepatoma Cells. *J. Control. Release* 155, 386–392.
- Wang, Y., Shao, J., Zaro, J. L., and Shen, W. C. (2014). Proinsulin-Transferrin Fusion Protein as a Novel Long-Acting Insulin Analog for the Inhibition of Hepatic Glucose Production. *Diabetes* 63, 1779–1788. doi: 10.2337/db13-0973

- Weichert, N., Hauptmann, V., Helmold, C., and Conrad, U. (2016). Seed-Specific Expression of Spider Silk Protein Multimers Causes Long-Term Stability. *Front. Plant Sci.* 7:6. doi: 10.3389/fpls.2016.00006
- Weitkunat, K., Schumann, S., Nickel, D., Kappo, K. A., Petzke, K. J., Kipp, A. P., et al. (2016). Importance of propionate for the repression of hepatic lipogenesis and improvement of insulin sensitivity in high-fat diet-induced obesity. *Mol. Nutr. Food Res.* 60, 2611–2621. doi: 10.1002/mnfr.201600305
- Weiß, J., Rau, M., and Geier, A. (2014). Non-alcoholic fatty liver disease: Epidemiology, clinical course, investigation, and treatment. *Dtsch. Arztebl. Int.* 111, 447–452.
- Wilbers, R. H., Westerhof, L. B., van Raaij, D. R., van Adrichem, M., Prakasa, A. D., Lozano-Torres, J. L., et al. (2016). Co-expression of the protease furin in *Nicotiana benthamiana* leads to efficient processing of latent transforming growth factor- β 1 into a biologically active protein. *Plant Biotechnol. J.* 14, 1695–1704. doi: 10.1111/pbi.12530
- Woo, Y. C., Xu, A., Wang, Y., and Lam, K. S. L. (2013). Fibroblast Growth Factor 21 as an emerging metabolic regulator: Clinical perspectives. *Clin. Endocrinol.* 78, 489–496. doi: 10.1111/cen.12095
- Xu, J., Stanislaus, S., Chinookoswong, N., Lau, Y. Y., Hager, T., Patel, J., et al. (2009). Acute glucose-lowering and insulin-sensitizing action of FGF21 in insulin-resistant mouse models—association with liver and adipose tissue effects. *Am. J. Physiol. Endocrinol. Metab.* 297, 1105–1114. doi: 10.1152/ajpendo.00348.2009
- Yao, J., Weng, Y., Dickey, A., and Wang, K. Y. (2015). Plants as Factories for Human Pharmaceuticals: Applications and Challenges. *Int. J. Mol. Sci.* 16, 28549–28565.
- Younossi, Z., Tacke, F., Arrese, M., Chander Sharma, B., Mostafa, I., Bugianesi, E., et al. (2019). Global Perspectives on Nonalcoholic Fatty Liver Disease and Nonalcoholic Steatohepatitis. *Hepatology* 69, 2672–2682.
- Yuki, Y., Nojima, M., Hosono, O., Tanaka, H., Kimura, Y., Satoh, T., et al. (2021). Oral Mucorice-CTB vaccine for safety and microbiota-dependent immunogenicity in humans: A phase 1 randomised trial. *Lancet Microbe* 2, 429–440. doi: 10.1016/S2666-5247(20)30196-8
- Zhang, D., Nandi, S., Bryan, P., Pettit, S., Nguyen, D., Santos, M. A., et al. (2010). Expression, purification, and characterization of recombinant human transferrin from rice (*Oryza sativa* L.). *Protein Expr. Purif.* 74, 69–79. doi: 10.1016/j.pep.2010.04.019
- Zhen, E. Y., Jin, Z., Ackermann, B. L., Thomas, M. K., and Gutierrez, J. A. (2016). Circulating FGF21 proteolytic processing mediated by fibroblast activation protein. *Biochem. J.* 473, 605–614. doi: 10.1042/BJ20151085
- Zimmermann, J., Saalbach, I., Jahn, D., Giersberg, M., Haehnel, S., Wedel, J., et al. (2009). Antibody expressing pea seeds as fodder for prevention of gastrointestinal parasitic infections in chickens. *BMC Biotechnol.* 9:79. doi: 10.1186/1472-6750-9-79

Supplementary Material

Supplementary Tables

Table S1. Primers used in this study.

Primer	Sequence
FGF21_Nt-fw	5'-TGGACTACCACCAGCATTACCAGAAC-3'
FGF21_Nt-rv	5'-GTGACCTACCTTGGGATGGACCAAC-3'
Tf_Nt-fw	5'-CCCCAACTTTGCCAACTCTGTCC-3'
Tf_Nt-rv	5'-CATTGCGTCAGCCTCCCCATTC-3'
B2m-fw	5'-CCTTCAGCAAGGACTGGTCT-3'
B2m-rv	5'-TGTCTCGATCCCAGTAGACG-3'
Srebf1-fw	5'-GAGGATAGCCAGGTCAAAGC-3'
Srebf1-rv	5'-AGGATTGCAGGTCAGACACA-3'
Fasn-fw	5'-TTGATGATTCAAGGAGTGGA-3'
Fasn-rv	5'-TTACACCTTGCTCCTTGCTG-3'
Ppargc1a-fw	5'-AGCCGTGACCACTGACAACGAG-3'
Ppargc1a-rv	5'-GCTGCATGGTTCTGAGTGCTAAG-3'
Ppara-fw	5'-TGGCAAAGTCTTAGTGCCAGA-3'
Ppara-rv	5'-TCACTAGGTCACACAGCCTCT-3'
Cpt1a-fw	5'-CCAAACCCACCAGGCTACA-3'
Cpt1a-rv	5'-GCACTGCTTAGGGATGTCTCTATG-3'

Table S2. Seed traits SL632 and VG. Numbers represent mean \pm standard deviation. Significance was calculated by one-way ANOVA (Bonferroni) with * $p < 0.05$, ** $p < 0.01$ and *** $p < 0.001$. n=21-25, technical replicates.

Parameter	Unit	<i>N. tabacum</i> cultivar		Significance
		SL632	VG	
Seed length	$\mu\text{m seed}^{-1}$	799.2 ± 48.8	672.9 ± 43.6	***
Seed width	$\mu\text{m seed}^{-1}$	535.8 ± 49.4	501.4 ± 35.4	*
Thousand SDM	mg cultivar^{-1}	106.6 ± 4.6	82.2 ± 3.8	***

SDM – seed dry mass.

Table S3. Propagation of *N. tabacum* SL632 and VG. Numbers represent mean \pm standard deviation. n=21, biological replicates.

Propagation	Unit	<i>N. tabacum</i> cultivar	
		SL632	VG
Average length of passage in tissue culture	day	21.0 ± 0.0	23.1 ± 2.7
Maximum number of passages until 50% of the plants flowered	number	6th	>19th

Table S4. Transgenic T0 events in *N. tabacum* SL632 and VG. Numbers represent mean \pm standard deviation. n=2-3, biological replicates.

Stable transformation	Unit	<i>N. tabacum</i> cultivar			
		SL632		VG	
		GFP	FGF21-F-Tf	GFP	FGF21-F-Tf
Shoot/Explant	-	0.8 ± 0.1	1.1 ± 0.3	0.3 ± 0.1	0.6 ± 0.1
Positive rooted shoots	%	59%	62%	74%	37%
Number of T0 events	number	23	26	33	26

Table S5. T1 segregation analysis of FGF21-F-Tf in *N. tabacum* SL632 and VG. Numbers represent mean \pm standard deviation. n=3, biological replicates.

<i>N. tabacum</i> cultivar	T1 event	Germinating seeds	Km-resistant descendants
SL632	NIC	$87 \pm 4\%$	0%
	1	$87 \pm 6\%$	$86 \pm 8\%$
	27	$96 \pm 4\%$	$95 \pm 5\%$
	49	$92 \pm 4\%$	$93 \pm 7\%$
VG	NIC	$85 \pm 8\%$	0%
	2	$97 \pm 2\%$	$92 \pm 4\%$
	50	$96 \pm 2\%$	$97 \pm 3\%$
	51	$87 \pm 6\%$	$94 \pm 4\%$

NIC – near-isogenic control plants. Km – kanamycin.

Table S6. Yield of recombinant proteins in seeds of different crops. Numbers represent mean \pm standard deviation.

Plant	Recombinant protein	Promoter/Terminator	Protein accumulation in seed [mg kg ⁻¹ SDM]	Reference
Tobacco	FGF21-F-Tf	p35s/t35s	6.7 \pm 0.2	This study
	Interleukin 6	p35s/t35s	303	(Nausch et al., 2012b)
	scFv antibody	pLeb4/t35s	230	(Fiedler and Conrad, 1995)
	Insulin-like growth factor binding protein-3	pPhas/tPhas	800	(Cheung et al., 2009)
	Hemagglutinin	pPhas/tArc	3,000	(Ceballo et al., 2017)
	Anti-hepatitis B surface antigen antibody	pPhas/tArc	6,500	(Hernandez-Velazquez et al., 2015)
	FLAG multimeric protein	pUSP/t35s	190	(Weichert et al., 2016)
Rice	Transferrin	pGt1/tNos	10,000	(Zhang et al., 2010)
Barley	Anti-HIV antibody	pGlo1/tNos	1,200	(Hensel et al., 2015)
Maize	β -glucuronidase	pUbi/tPinII	1,300	(Kusnadi et al., 1998)
Pea	Anti-Eimeria antibody	pUSP/t35s	1,800	(Zimmermann et al., 2009)
Soybean	Bone morphogenetic proteins 2	pCon/tCon	9,300	(Queiroz et al., 2019)
Arabidopsis	murine single chain variable fragment G4	pPhas/tArc	10,000-15,000	(de Jaeger et al., 2002)

SDM – seed dry mass; p35 – CaMV promoter; pCon – β -conglycinin α -subunit promoter; pGlo1 – *Avena sativa* Globulin 1 promoter; pGt1 – *Oryza sativa* seed storage protein glutenin 1 promoter; pLeb4 *Vicia faba* Legumin B4 promoter of the 11S globulin; pPhas - *Phaseolus vulgaris* promoter of the 7S globulin; pUbi – *Zea mays* upquitin 1 promoter; pUSP – *Vicia faba* unknown seed protein promoter; t35s – CaMV terminator; tArc – *Phaseolus vulgaris* terminator of the arcelin 5-I seed storage protein; tCon – β -conglycinin α -subunit terminator; tNos – *Agrobacterium tumefaciens* nopal synthase terminator; tPhas - *Phaseolus vulgaris* terminator of the 7S globulin; tPinII - *Solanum tuberosum* potato proteinase inhibitor II terminator.

- Ceballo, Y., Tiel, K., Lopez, A., Cabrera, G., Perez, M., Ramos, O., Rosabal, Y., Montero, C., Menassa, R., Depicker, A. and Hernandez, A. (2017). High accumulation in tobacco seeds of hemagglutinin antigen from avian (H5N1) influenza. *Transgenic Res.* **26**, 775-789.
- Cheung, S. C., Sun, S. S., Chan, J. C. and Tong, P. C. (2009). Expression and subcellular targeting of human insulin-like growth factor binding protein-3 in transgenic tobacco plants. *Transgenic Res.* **18**, 943-951.
- De Jaeger, G., Scheffer, S., Jacobs, A., Zambre, M., Zobell, O., Goossens, A., Depicker, A. and Angenon, G. (2002). Boosting heterologous protein production in transgenic dicotyledonous seeds using *Phaseolus vulgaris* regulatory sequences. *Nat Biotechnol.* **20**, 1265-1268.
- Fiedler, U. and Conrad, U. (1995). High-level production and long-term storage of engineered antibodies in transgenic tobacco seeds. *Biotechnology.* **13**, 1090-1093
- Hensel, G., Floss, D. M., Arcalis, E., Sack, M., Melnik, S., Altmann, F., Rutten, T., Kumlehn, J., Stoger, E. and Conrad, U. (2015). Transgenic Production of an Anti HIV Antibody in the Barley Endosperm. *PLoS One.* **10**, e0140476.
- Hernandez-Velazquez, A., Lopez-Quesada, A., Ceballo-Camara, Y., Cabrera-Herrera, G., Tiel-Gonzalez, K., Mirabal-Ortega, L., Perez-Martinez, M., Perez-Castillo, R., Rosabal-Ayan, Y., Ramos-Gonzalez, O.,

- Enriquez-Obregon, G., Depicker, A. and Pujol-Ferrer, M. (2015). Tobacco seeds as efficient production platform for a biologically active anti-HBsAg monoclonal antibody. *Transgenic Res.* **24**, 897-909.
- Kusnadi, A. R., Hood, E. E., Witcher, D. R., Howard, J. A. and Nikolov, Z. L. (1998). Production and purification of two recombinant proteins from transgenic corn. *Biotechnol Prog.* **14**, 149-155.
- Nausch, H., Mikschofsky, H., Koslowski, R., Meyer, U., Broer, I. and Huckauf, J. (2012b). High-level transient expression of ER-targeted human interleukin 6 in *Nicotiana benthamiana*. *PLoS One.* **7**, e48938.
- Queiroz, L. N., Maldaner, F. R., Mendes, É. A., Sousa, A. R., D'Allatta, R. C., Mendonça, G., Mendonça, D. B. S. and Aragão, F. J. L. (2019). Evaluation of lettuce chloroplast and soybean cotyledon as platforms for production of functional bone morphogenetic protein 2. *Transgenic Res.* **28**, 213-224.
- Weichert, N., Hauptmann, V., Helmold, C. and Conrad, U. (2016). Seed-Specific Expression of Spider Silk Protein Multimers Causes Long-Term Stability. *Front Plant Sci.* **7**, e6.
- Zhang, D., Nandi, S., Bryan, P., Pettit, S., Nguyen, D., Santos, M. A. and Huang, N. (2010). Expression, purification, and characterization of recombinant human transferrin from rice (*Oryza sativa* L.). *Protein Expr Purif.* **74**, 69-79.
- Zimmermann, J., Saalbach, I., Jahn, D., Giersberg, M., Haehnel, S., Wedel, J., Macek, J., Zoufal, K., Glünder, G., Falkenburg, D. and Kipriyanov, S. M. (2009). Antibody expressing pea seeds as fodder for prevention of gastrointestinal parasitic infections in chickens. *BMC Biotechnol.* **9**, 79-100.

Table S7. Linkers described for FGF21-transferrin fusion proteins.

Linker	Fusion protein	Heterologous host	Compartment	Reference
DDDDK*	GFP-FGF21	<i>Nicotiana benthamiana</i>	Cytosol	(Fu et al., 2011)
LE**	ProINS-Tf	HEK293	Extracellular space	(Wang et al., 2011; Wang et al., 2014; Chen et al., 2018; Liu et al., 2020)
		<i>Oryza sativa</i> seeds	Apoplasm	(Chen et al., 2018)
(PEAPTD) ₂	GLP1-Tf	<i>Saccharomyces cerevisiae</i>	Extracellular space	(Kim et al., 2010)
	Ex4-Tf	<i>Saccharomyces cerevisiae</i>	Extracellular space	(Kim et al., 2010)
(LEA(EAAAK) ₄ ALEA (EAAAK) ₄ ALE)	G-CSF-Tf	HEK293	Extracellular space	(Amet et al., 2009; Chen et al., 2012)
	FIX-Tf	HEK293	Extracellular space	(Amet et al., 2009; Chen et al., 2012)
(GGGGS) ₃	G-CSF-Tf	HEK293	Extracellular space	(Amet et al., 2009; Chen et al., 2012)
	FIX-Tf	HEK293	Extracellular space	(Amet et al., 2009; Chen et al., 2012)
	Ex4-Tf	<i>Nicotiana benthamiana</i>	ER	(Choi et al., 2014)

*enterokinase cleavage site. **XhoI – restriction site.

- Amet, N., Lee, H.F. and Shen, W.C. (2009). Insertion of the designed helical linker led to increased expression of Tf-based fusion proteins. *Pharm Res.* **26**, 523-528.
- Chen, X., Zaro, J. L. and Shen, W. C. (2012). Fusion Protein Linkers: Property, Design and Functionality. *Adv Drug Deliv Rev.* **65**, 1357-1369.
- Chen, Y. S., Zaro, J. L., Zhang, D., Huang, N., Simon, A. and Shen, W. C. (2018). Characterization and Oral Delivery of Proinsulin-Transferrin Fusion Protein Expressed Using ExpressTec. *Int J Mol Sci.* **19**, 378-390.
- Choi, J., Diao, H., Feng, Z.-C., Lau, A., Wang, R., Jevnikar, A. M. and Ma, S. (2014) A fusion protein derived from plants holds promising potential as a new oral therapy for type 2 diabetes. *Plant Biotechnol J.* **12**, 425-435.
- Fu, H., Pang, S., Xue, P., Yang, J., Liu, X., Wang, Y., Li, T., Li, H. and Li, X. (2011). High levels of expression of fibroblast growth factor 21 in transgenic tobacco (*Nicotiana benthamiana*). *Appl Biochem Biotechnol.* **165**, 465-475.
- Kim, B. J., Zhou, J., Martin, B., Carlson, O. D., Maudsley, S., Greig, N. H., Mattson, M. P., Ladenheim, E. E., Wustner, J., Turner, A., Sadeghi, H. and Egan, J. M. (2010). Transferrin fusion technology: a novel approach to prolonging biological half-life of insulinotropic peptides. *J Pharmacol Exp Ther.* **334**, 682-692.
- Liu, Y., Wang, H. Y., Shao, J., Zaro, J. L. and Shen, W. C. (2020). Enhanced insulin receptor interaction by a bifunctional insulin-transferrin fusion protein: an approach to overcome insulin resistance. *Sci Rep.* **10**, e7724.
- Wang, Y., Chen, Y. S., Zaro, J. L. and Shen, W. C. (2011). Receptor-Mediated Activation of a Proinsulin-Transferrin Fusion Protein in Hepatoma Cells. *J Control Release.* **155**, 386-392.
- Wang, Y., Shao, J., Zaro, J. L. and Shen, W. C. (2014). Proinsulin-Transferrin Fusion Protein as a Novel Long-Acting Insulin Analog for the Inhibition of Hepatic Glucose Production. *Diabetes.* **63**, 1779-1788.

Supplementary Figures

>p9U-FGF21-F-Tf

MATQRRANPSSLHLITVFSLLVAVVSGHPIPDSSPLLQFGGQVRQRYLYTDDAQQTEAHLEIREDGTVGGAADQS
PESLLQLKALKPGVIQILGVKTSRFLCQRPDGALYGLHFDPEACSFRELLLEDGYNVYQSEAHGLPLHLPGNKS
PHRDPAPRGPAPFLPLPGLPPALPEPPGILAPQPPDVGSSDPLAMVGPSQGRSPSYASRRKRSVGGGSGGGGSG
GGGSVPDKTVRWCAVSEHEATKQSFDRHMKSVIPSDGPSVACVKKASYLDCIRAIANEADAVTL DAGLVYDAY
LAPNNLKPVVAEFYGSKEDEPQTFYYAVAVVKKDSGFQMNQLRGKKSCHTGLGRSAGWNIPIGLLYCDLPEPRKPL
EKAVANFFSGSCAPCADGTDFPQLCQLCPGCGCSTLNQYFGYSGAFKCLKDGAGDVAFVKHSTIFENLANKADR
QYELLCLDNTRKPVDEYKDCHLAQVPSHTTVVARSMGGKEDLIWELLNQAQEHFGKDKSKEFQLFSSPHGKDLLFK
DSAHGFLKVPPRMDAKMYLGYEYVTAIRNLREGTCPEAPTDECKPVKWCALSHHERLKCDEWSVNSVGKIECVSA
ETTEDCIAKIMNGEADAMSLDGGFVYIAGKCGLPVLAENYNKSDNCEDTPEAGYFAIAVVKKASASDLTWDNLKG
KKSCHTAVGRTAGWNI PMGLLYNKINHCRFDEFFSEGCAPGSKKDSLCKLCMGSGNLNCEPNNKEGYGYTGAF
RCLVEKGDVAFVKHQVTPQNTGGKNPDPWAKNLNEKDYELLCLDGTRKPVVEYANCHLARAPNHAVVTRKDKEAC
VHKILRQQQHLFGSNVTDSCGNFCLFRSETKDLLFRDDTVCLAKLHNRNTYEKYLGEYVAVGNLRKCSTSSLL
EACTFRRPLEHHHHHHSRAWRHPQFGGHHHHHSEKDEL*

>pICH29912-FGF21-F-IntN

MATQRRANPSSLHLITVFSLLVAVVSGHPIPDSSPLLQFGGQVRQRYLYTDDAQQTEAHLEIREDGTVGGAADQS
PESLLQLKALKPGVIQILGVKTSRFLCQRPDGALYGLHFDPEACSFRELLLEDGYNVYQSEAHGLPLHLPGNKS
PHRDPAPRGPAPFLPLPGLPPALPEPPGILAPQPPDVGSSDPLAMVGPSQGRSPSYASRRKRSVRESGCISGDSL
ISLASTGKRVS IKDLLDEKDFEIWAIN EQTMKLESAKVS RVFCTGKKLVYILKTRLGRTIKATANHRFLTIDGWK
RLDELSLKEHIALPRKLESSSLQLGLEHHHHHHSRAWRHPQFGGHHHHHSEKDEL*

>pICH31120-IntC-Tf

MATQRRANPSSLHLITVFSLLVAVVSGSPEIEKLSQSDIYWDSIVSITETGVVEVFDLTVPGPHNFVANDIIVHN
SIEQDGGGGSGGGGSGGGGSVPDKTVRWCAVSEHEATKQSFDRHMKSVIPSDGPSVACVKKASYLDCIRAIAN
EADAVTL DAGLVYDAYLAPNNLKPVVAEFYGSKEDEPQTFYYAVAVVKKDSGFQMNQLRGKKSCHTGLGRSAGWNI
PIGLLYCDLPEPRKPLEKAVANFFSGSCAPCADGTDFPQLCQLCPGCGCSTLNQYFGYSGAFKCLKDGAGDVAFV
KHSTIFENLANKADRQYELLCLDNTRKPVDEYKDCHLAQVPSHTTVVARSMGGKEDLIWELLNQAQEHFGKDKSK
EFQLFSSPHGKDLLFKDSAHGFLKVPPRMDAKMYLGYEYVTAIRNLREGTCPEAPTDECKPVKWCALSHHERLKC
DEWSVNSVGKIECVSAETTEDCIAKIMNGEADAMSLDGGFVYIAGKCGLPVLAENYNKSDNCEDTPEAGYFAIA
VVKKASASDLTWDNLKGKKSCHTAVGRTAGWNI PMGLLYNKINHCRFDEFFSEGCAPGSKKDSLCKLCMGSGNLN
CEPNNKEGYGYTGAFRCLVEKGDVAFVKHQVTPQNTGGKNPDPWAKNLNEKDYELLCLDGTRKPVVEYANCHLA
RAPNHAVVTRKDKEACVHKILRQQQHLFGSNVTDSCGNFCLFRSETKDLLFRDDTVCLAKLHNRNTYEKYLGEY
VAVGNLRKCSTSSLLEACTFRRPLEHHHHHHSRAWRHPQFGGHHHHHSEKDEL*

>pTRAc-FGF21-F-Tf

MATQRRANPSSLHLITVFSLLVAVVSGHPIPDSSPLLQFGGQVRQRYLYTDDAQQTEAHLEIREDGTVGGAADQS
PESLLQLKALKPGVIQILGVKTSRFLCQRPDGALYGLHFDPEACSFRELLLEDGYNVYQSEAHGLPLHLPGNKS
PHRDPAPRGPAPFLPLPGLPPALPEPPGILAPQPPDVGSSDPLAMVGPSQGRSPSYASRRKRSVGGGSGGGGSG
GGGSVPDKTVRWCAVSEHEATKQSFDRHMKSVIPSDGPSVACVKKASYLDCIRAIANEADAVTL DAGLVYDAY
LAPNNLKPVVAEFYGSKEDEPQTFYYAVAVVKKDSGFQMNQLRGKKSCHTGLGRSAGWNIPIGLLYCDLPEPRKPL
EKAVANFFSGSCAPCADGTDFPQLCQLCPGCGCSTLNQYFGYSGAFKCLKDGAGDVAFVKHSTIFENLANKADR
QYELLCLDNTRKPVDEYKDCHLAQVPSHTTVVARSMGGKEDLIWELLNQAQEHFGKDKSKEFQLFSSPHGKDLLFK
DSAHGFLKVPPRMDAKMYLGYEYVTAIRNLREGTCPEAPTDECKPVKWCALSHHERLKCDEWSVNSVGKIECVSA
ETTEDCIAKIMNGEADAMSLDGGFVYIAGKCGLPVLAENYNKSDNCEDTPEAGYFAIAVVKKASASDLTWDNLKG
KKSCHTAVGRTAGWNI PMGLLYNKINHCRFDEFFSEGCAPGSKKDSLCKLCMGSGNLNCEPNNKEGYGYTGAF
RCLVEKGDVAFVKHQVTPQNTGGKNPDPWAKNLNEKDYELLCLDGTRKPVVEYANCHLARAPNHAVVTRKDKEAC

VHKILRQQQHFLFGSNVTDSCGNFCLFRSETKDLLFRDDTVCLAKLHNRNTYEKYLGEYVAVGNLRKCSTSSLL
EACTFRRPLEHHHHHHSRAWRHPQFGGHHHHHSEKDEL*

>pTRAc-FGF21-Tf-PLUS

MATQRRANPSSLHLITVFSLLVAVVSGHPIPDSSPLLQFGGQVRQRYLYTDDAQQTEAHLEIREDGTVGGAADQSPESLLQLK
ALKPGVIQILGVKTSRFLCQRPDGLYGLSLHFDPEACSFRELLLEDGYNVYQSEAHGLPLHLPGNKSPHRDPAPRGPARFLPL
PGLPPALPEPPGILAPQPPDVGSSDPLAMVGPSQGRSPSYASGGGSGGGSGGGGSPDKTVRWCADVSEHEATKCQSFDRHM
KSVIPSDGPSVACVKKASYLDCIRAIANEADAVTLDAGLVYDAYLAPNNLKPVVAEFYGSKEDPQTFYYAVAVVKKDSGFQM
NQLRGKKSCHTGLGRSAGWNIPIGLLYCDLPEPRKPLEKAVANFFSGSCAPCADGTDFFQLCQLCPGCGCSTLNQYFGYSGAF
KCLKDGAGDVAFVKHSTIFENLANKADRDOYELLCLDNTRKPVDEYKDCHLAQVPSHTTVVARSMGGKEDIWELLNQAQEHFGK
DKSKEFQLFSSPHGKDLLFKDSAHGFLKVPPRMDAKMYLGYYVTAIRNLREGTCPEAPTDECKPVKWCALSHHERLKCDWS
VNSVGKIECVSAETTEDCIAKIMNGEADAMSLDGGFVYIAGKCLVPVLAENYNKSDNCEDTPEAGYFAIAVVKKSASDLTWD
NLKGKKSCHTAVGRTAGWNI PMGLLYNKINHCRFDEFFSEGCAPGSKKDSSLCKLCMGSGNLNCEPNNKEGYGYTGAFRCLV
EKGDVAFVKHQVTPQNTGGKNPDPWAKNLNEKYELLCLDGTRKPVVEYANCHLARAPNHAVVTRKDKEACVHKILRQQQHFL
GSNVTDSCGNFCLFRSETKDLLFRDDTVCLAKLHNRNTYEKYLGEYVAVGNLRKCSTSSLLEACTFRRPDNEKLKPKHKK
LKQPADGLEHHHHHHSRAWRHPQFGGHHHHHSEKDEL*

>pTRAc-FGF21-nTf338-PLUS

MATQRRANPSSLHLITVFSLLVAVVSGHPIPDSSPLLQFGGQVRQRYLYTDDAQQTEAHLEIREDGTVGGAADQSPESLLQLK
ALKPGVIQILGVKTSRFLCQRPDGLYGLSLHFDPEACSFRELLLEDGYNVYQSEAHGLPLHLPGNKSPHRDPAPRGPARFLPL
PGLPPALPEPPGILAPQPPDVGSSDPLAMVGPSQGRSPSYASGGGSGGGSGGGGSPDKTVRWCADVSEHEATKCQSFDRHM
KSVIPSDGPSVACVKKASYLDCIRAIANEADAVTLDAGLVYDAYLAPNNLKPVVAEFYGSKEDPQTFYYAVAVVKKDSGFQM
NQLRGKKSCHTGLGRSAGWNIPIGLLYCDLPEPRKPLEKAVANFFSGSCAPCADGTDFFQLCQLCPGCGCSTLNQYFGYSGAF
KCLKDGAGDVAFVKHSTIFENLANKADRDOYELLCLDNTRKPVDEYKDCHLAQVPSHTTVVARSMGGKEDIWELLNQAQEHFGK
DKSKEFQLFSSPHGKDLLFKDSAHGFLKVPPRMDAKMYDNEKLKPKHKKLKQPADGLEHHHHHHSRAWRHPQFGGHHHHHS
EKDEL*

>pTRAc-nTf338-FGF21-PLUS

MATQRRANPSSLHLITVFSLLVAVVSGVPDKTVRWCADVSEHEATKCQSFDRHMKSVIPSDGPSVACVKKASYLDCIRAIANE
ADAVTLDAGLVYDAYLAPNNLKPVVAEFYGSKEDPQTFYYAVAVVKKDSGFQMNQLRGKKSCHTGLGRSAGWNIPIGLLYCDL
PEPRKPLEKAVANFFSGSCAPCADGTDFFQLCQLCPGCGCSTLNQYFGYSGAFKCLKDGAGDVAFVKHSTIFENLANKADRDOY
ELLCLDNTRKPVDEYKDCHLAQVPSHTTVVARSMGGKEDIWELLNQAQEHFGKDKSKEFQLFSSPHGKDLLFKDSAHGFLKVP
PRMDAKMYGGGSGGGSGGGSGHPIPDSSPLLQFGGQVRQRYLYTDDAQQTEAHLEIREDGTVGGAADQSPESLLQLKALKP
GVIQILGVKTSRFLCQRPDGLYGLSLHFDPEACSFRELLLEDGYNVYQSEAHGLPLHLPGNKSPHRDPAPRGPARFLPLPGLP
PALPEPPGILAPQPPDVGSSDPLAMVGPSQGRSPSYASDNEKLKPKHKKLKQPADGLEHHHHHHSRAWRHPQFGGHHHHHS
EKDEL*

Figure S1. Amino acids sequences of FGF21-transferrin fusion proteins used for the stable and transient expression. *Light blue:* ER-targeting signal peptide from Calreticulin of *Nicotiana plumbaginifolia* (Acc. Z71395); *Orange:* FGF21 mature protein with Ser167Ala mutation (underlined) to eliminate the O-glycosylation site; *Green:* Furin cleavage site to separate FGF21 from transferrin in the enterocytes to release FGF21 into the blood serum; *Light red:* GS-Linker to separate FGF21 and Tf; *Black:* Transferrin mature protein (n-terminal domain nTf338 double underlined); *Dark purple:* double His6-Tag; *Dark blue:* ER retention signal; *Dark Red:* Extensin from DnaB for transplicing; *Light purple:* PLUS liver targeting peptide of the CSP protein.

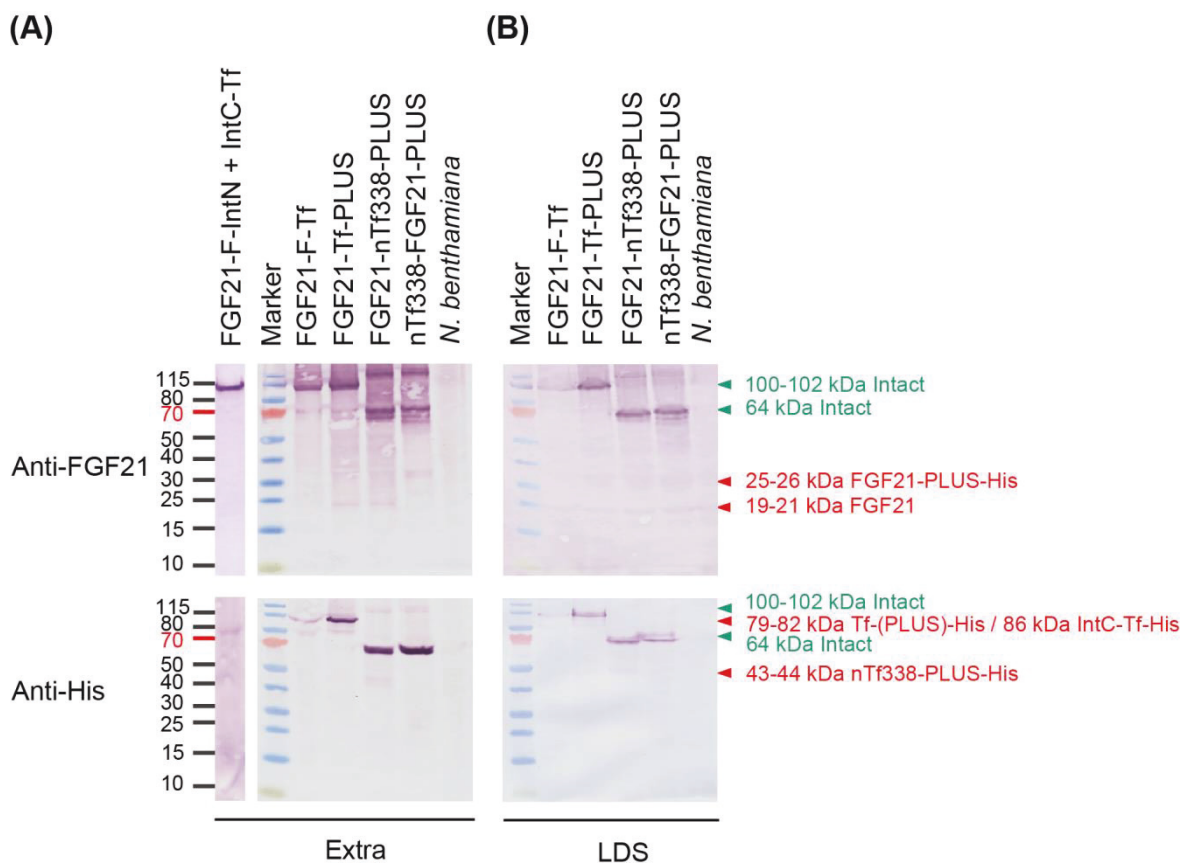


Figure S2. Western blot analysis of modified FGF21-transferrin fusion proteins produced in *N. benthamiana* using magnICON and pTRAc systems. MagnICON transient expression: co-expression of FGF21-F-IntN plus IntC-Tf. and pTRAc transient system: single expression of FGF21-F-Tf, FGF21-Tf-PLUS, FGF21-nTf338-PLUS and nTf338-FGF21-PLUS. Each 100 mg leaf materials were extracted in (A) extraction buffer (Extra) or (B) LDS buffer (LDS). Leaf crude extracts under extraction and LDS buffer containing 100 μ g of total soluble protein and 20 μ L of total volume were subjected to NuPAGE 4–12% Bis-Tris protein gels, respectively. The electroblotted proteins were probed with primary anti-FGF21/-His6 rabbit polyclonal antibody (1:5,000) and then secondary goat anti-Rabbit IgG alkaline phosphate (AP)-conjugated antibody (1:5,000). *Green arrows*: intact fusion protein, *red arrows*: degraded fusion protein.

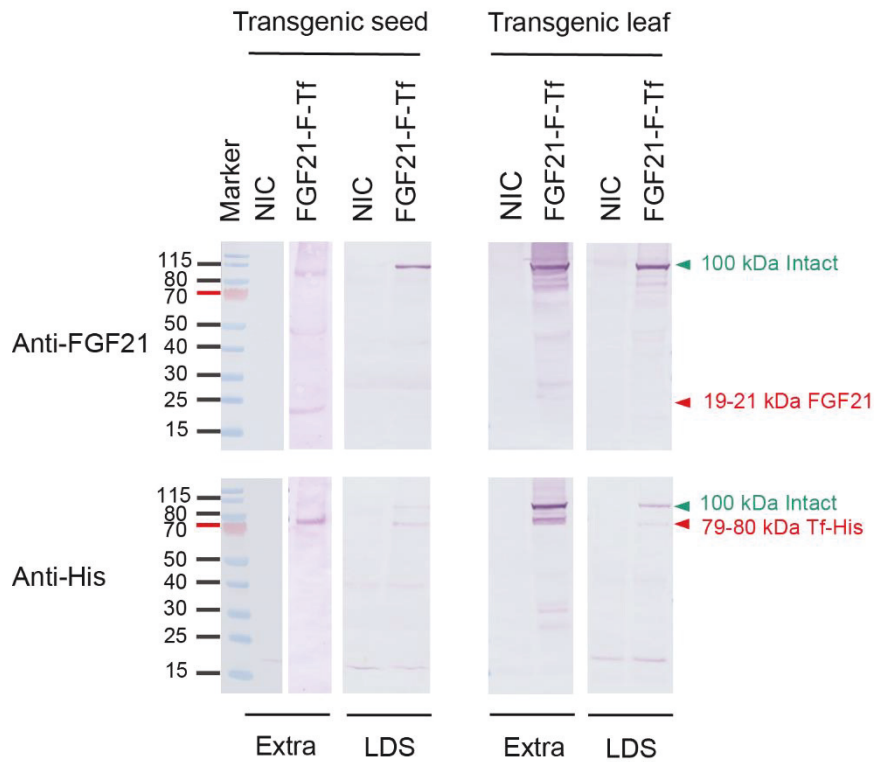
(A)**(B)**

Figure S3. Western blot analysis of FGF21-transferrin fusion proteins in *N. tabacum* SL632. Transgenic seed (A) and transgenic leaf (B). Each 100 mg plant material was extracted in extraction buffer (Extra) or LDS buffer (LDS). Seed and leaf crude extracts under extraction and LDS buffer containing 100 μ g of total soluble protein and 20 μ L of total volume were subjected to NuPAGE 4–12% Bis-Tris protein gels, respectively. The electroblotted proteins were probe with primary anti-FGF21/-His6 rabbit polyclonal antibody (1:5,000) and then secondary goat anti-Rabbit IgG alkaline phosphate (AP)-conjugated antibody (1:5,000). *Green arrows*: intact fusion protein, *red arrows*: degraded fusion protein.

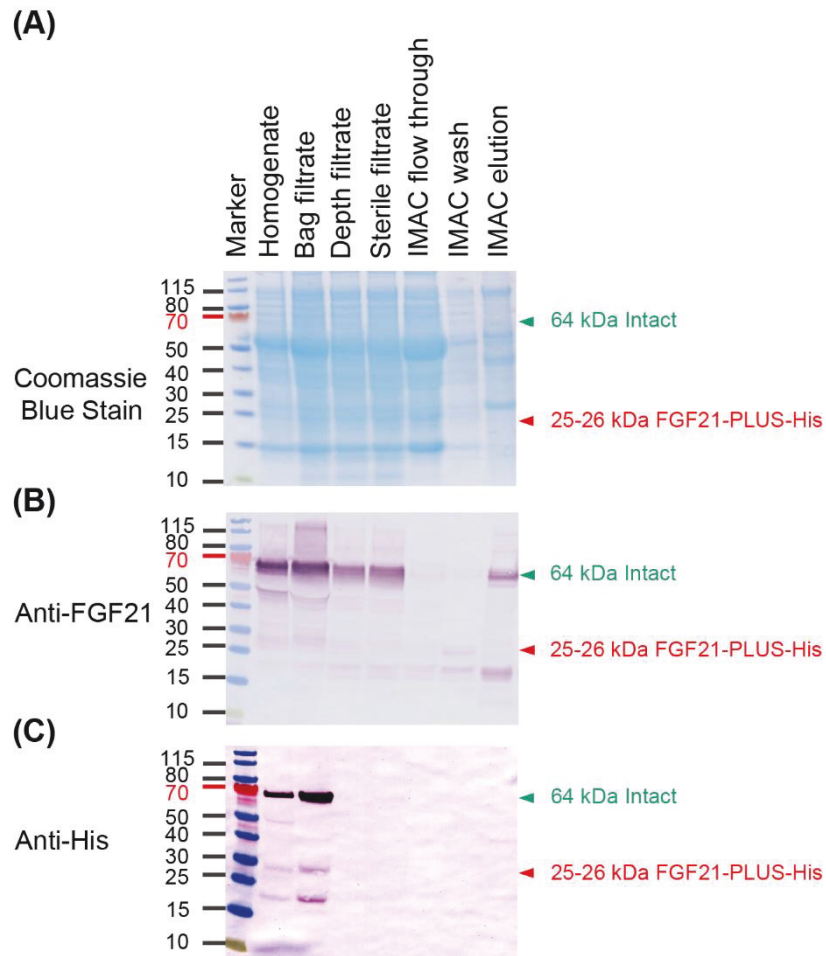


Figure S4. Coomassie-stained NuPAGE LDS gel and Western blot analysis of purification process fractions for nTF338-FGF21-PLUS extracted from non-senescent, transiently transformed *N. benthamiana* leaves, using depth filtration for clarification. Each 800 g leaf material was homogenized in extraction buffer and purified by Immobilized Metal Ion Affinity Chromatography (IMAC). Leaf samples containing 100 µg of total soluble protein (TSP) were subjected to NuPAGE 4–12% Bis-Tris protein gels. (A) Coomassie stained gel, (B) FGF21-Western blot and (C) His-Western blot. The electroblotted proteins were probed with primary anti-FGF21/-His6 rabbit polyclonal antibody (1:5,000) and then secondary goat anti-Rabbit IgG alkaline phosphate (AP)-conjugated antibody (1:5,000). *Green arrows*: intact fusion protein, *red arrows*: degraded fusion protein.

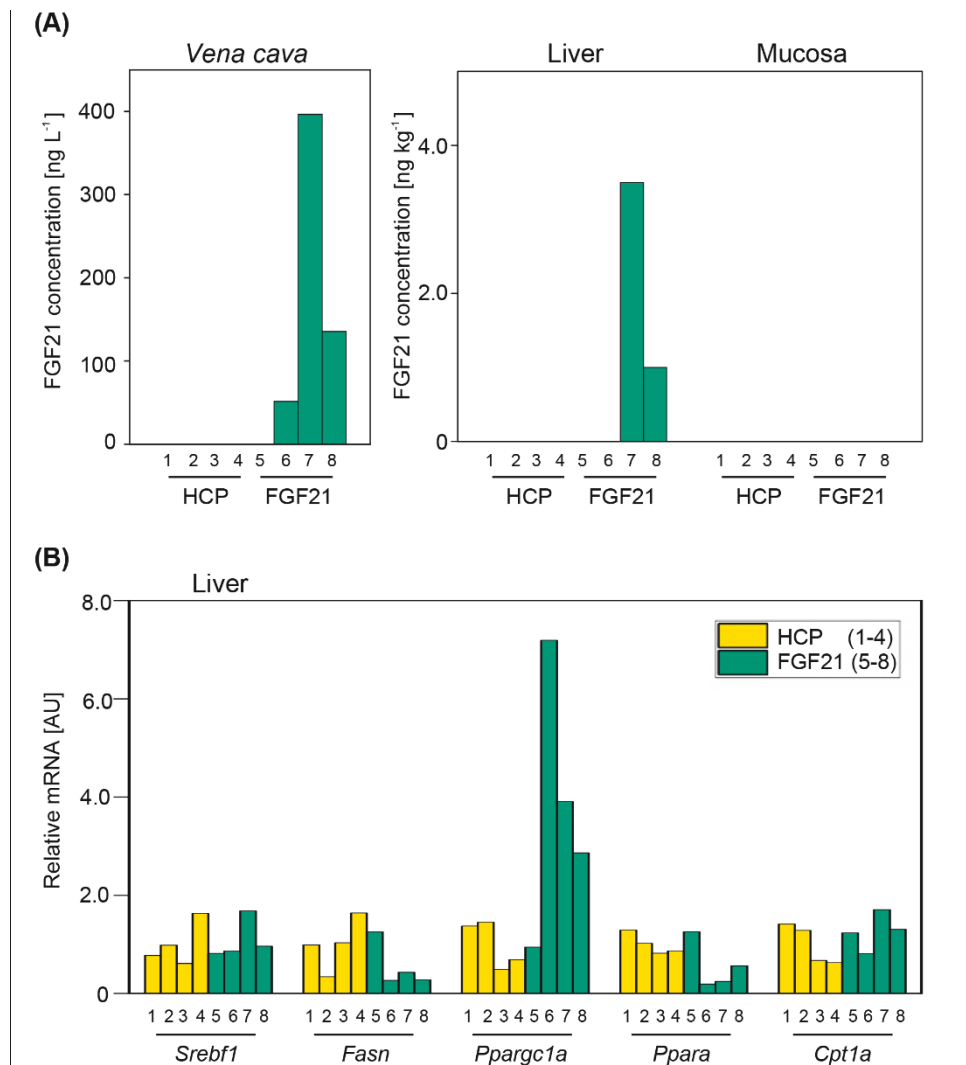


Figure S5. The bioavailability and bioactivity of the purified fusion protein nTf338-FGF21-PLUS of individual mice in an *in vivo* animal bolus feeding trial after 4 h. FGF21^{-/-} knockout mice were starved for 16 h and gavaged with a 0.5 mL bolus of partially purified nTf338-FGF21-PLUS dissolved in water to a concentration of 50 µg L⁻¹ FGF21 and 44 g L⁻¹ HCP (FGF21 group) or HCP only (HCP group). After 4 h, mice were killed. (A) FGF21 concentration in the *Vena cava*, liver and mucosa of via FGF21-ELISA. (B) mRNA expression levels of the gene *Srebf1*, *Fasn*, *Pparg1a*, *Ppara* and *Cpt1a* were determined in liver tissue via qPCR (primer are listed in Table S7). Mice 1-4: feeded with HCP (IMAC-purified plant host cell proteins from *N. benthamiana* leaves), mice 5-8: gavaged with FGF21 (IMAC-purified nTf338-FGF21-PLUS from *N. benthamiana* leaves).

III.1. Optimization tobacco seed yield in contained greenhouses

The production of PD (biopharmaceutical) needs to be carried out in a controlled environment, such as a plant greenhouse (Holtz et al., 2015). Tobacco has not yet been used for greenhouse seed production and appropriate cultivation strategies need to be developed to maximize seed yield.

III.1.1. Seed-rich cultivar SL632 was selected for seed production in the greenhouse

For seed production, I chose the *N. tabacum* cultivar SL632 (Sunchem N.L., Netherlands) due to its nicotine-free nature and specifically bred high seed yield in field conditions (Chapter I.4.3.). Additionally, I included the *N. tabacum* cultivar VG, predominantly used in greenhouses for leaf production (Conley et al., 2011; Nausch et al., 2016). VG, however, is cultivated for high leaf yield rather than high seed yield, serving as a comparative reference (NiCoTa GmbH, Germany).

Regarding seed traits, SL632 displayed dimensions of 799.2 μm in length, 535.8 μm in width, and a thousand seed dry mass (SDM) of 106.6 mg, surpassing VG, which measured 672.9 μm in length, 501.4 μm in width, and had an SDM of 82.2 mg (Table 9).

Table 9. Seed traits SL632 and VG. Numbers represent mean \pm standard deviation. Significance was calculated by one-way ANOVA (Bonferroni) with * $p < 0.05$, ** $p < 0.01$ and *** $p < 0.001$. $n=21-25$, technical replicates.

Parameter	Unit	<i>N. tabacum</i> cultivar		Significance
		SL632	VG	
Seed length	$\mu\text{m seed}^{-1}$	799.2 \pm 48.8	672.9 \pm 43.6	***
Seed width	$\mu\text{m seed}^{-1}$	535.8 \pm 49.4	501.4 \pm 35.4	*
Thousand SDM	mg cultivar $^{-1}$	106.6 \pm 4.6	82.2 \pm 3.8	***

SDM – seed dry mass.

Since the focus in the past was on producing tobacco leaves, tobacco seeds were collected for the next germination by covering only one inflorescence with a bag and removing the others. However, the aim of study was to maximize the harvest of tobacco inflorescences, and standard bags might not have been the most suitable choice for this purpose. Hence, I compared 2 types of tobacco bags, the Vlies bag (size: 40 x 60 mm, Baumann Saatzuchtbedarf GmbH, Germany) (Figure 8A) and the Crispac-Beutel bag (Super-Micro-

Lochung 0.5mm, size: 330 x 500 mm, Baumann Saatzuchtbedarf GmbH, Germany) (Figure 8B). The Vlies bag, heavier and opaque, increased inflorescence mass, caused breakage, and demanded frequent openings during cultivation for seed development checks. Due to these drawbacks, I opted for the Crispac-Beutel bag in subsequent fertilization and cultivation trials when the inflorescence bloomed.

In summary: 1) SL632 exhibits advantageous large and heavy seed properties, rendering it an ideal protein expression platform for producing FGF21. 2) The Crispac-Beutel bag's effectiveness in reducing humidity and fouling inside the bag, consequently preventing mold in the seed capsules.

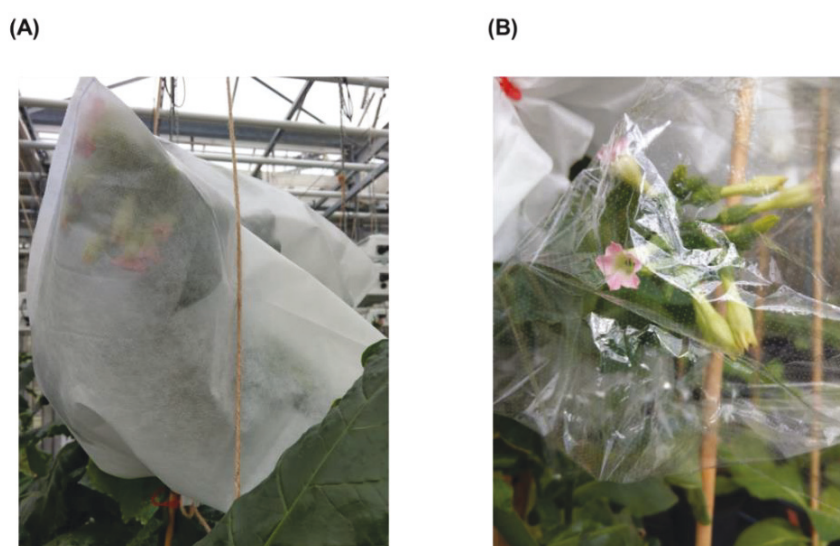


Figure 8. Different types of bags used in the greenhouse for tobacco cultivation. Photos illustrating (A) Vlies bag and (B) Crispac-Beutel bag.

III.1.2. Greenhouse cultivation strategies for tobacco focus on leaf production

Since greenhouse tobacco was grown only for leaf production and not seed production, greenhouse tobacco cultivation strategies were tailored for maximum leaf yield rather than seed yield. The aim of the study was to achieve high tobacco seed yields in the greenhouse. I analyzed the seed yield and time per unit area of untransformed SL632 and VG under standard cultivation (uncut), and studied different cultivation strategies (1× top, 1× cut, 6× cut) to maximize seed production.

In order to determine a suitable greenhouse setting for tobacco cultivation, I analyzed two typical greenhouse setting systems for tobacco leaf production at the University of Rostock (UR) in Rostock and Fraunhofer IME (IME) in Aachen (Table 10). Additionally, I documented the UR and IME greenhouse maps (Figure 9) and their timelines detailing their cultivation processes, including seeding, shoot transfer, topping/cutting, flowering, and harvest times (Figure 10).

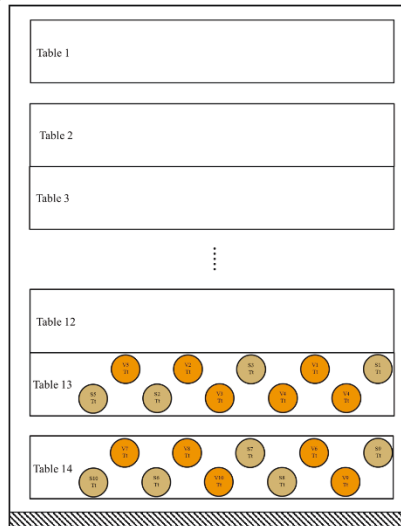
The typical greenhouse cultivation practices for tobacco focus on leaf production rather than seed production. Specifically, tobacco is commonly cultivated in the greenhouse under standard cultivation (uncut) to yield leaves. Seeds are initially sown in smaller pots, and after germination, each shoot is transplanted into larger pots. These pots are then placed onto tables with a watering system, and the plants are provided with additional illumination. The cultivation process involves no cutting, with leaf harvesting from the main stem and/or one inflorescence (uncut), etc.

With respect to the fertilizers, the NPK ratio represents the volume percent of nitrogen (chemical symbol N), phosphorus (P) and potassium (K) in the product, and it affects leaf and seed yield. In general, tobacco leaf production requires high N content, and fertilizers like Hakaphos Blue (NPK 15+10+15) or Ferty 2 Mega (NPK ratio, 16+06+26) for high biomass-forming crops and Wuxal Super (NPK 8+8+6) for low biomass-forming crops are used. On the other hand, tobacco seed production requires high K content, such as Hakaphos Red (NPK 8+12+24).

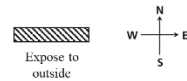
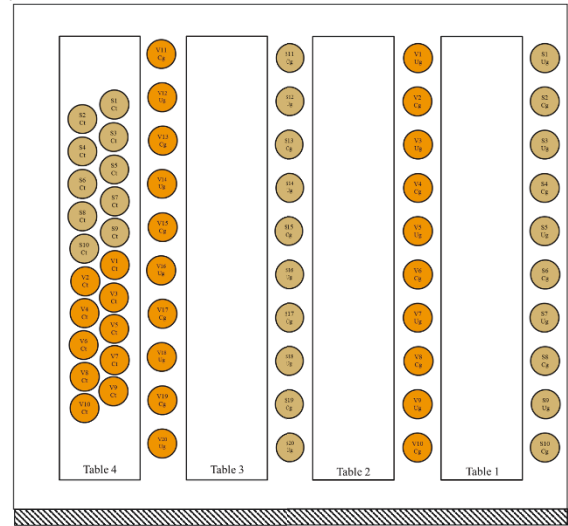
Table 10. Greenhouse tobacco parameter settings.

Trial	1 st Fertilization	1 st Cultivation	2 nd Cultivation	3 rd Cultivation	4 th Cultivation
Cultivation location	UR, Rostock	UR, Rostock	IME, Aachen	IME, Aachen	IME, Aachen
Geographic position (Latitude/Longitude)	54°05'19"N/ 12°08'25"E	54°05'19"N/ 12°08'25"E	50°46'35"N/ 6°05'00"E	50°46'35"N/ 6°05'00"E	50°46'35"N/ 6°05'00"E
Harvest product	Leaf	Seed	Seed	Seed	Seed
Cultivation strategy	uncut	1× top	1× cut, uncut	1× cut, 6× cut	1× cut, 1× top uncut
Seed age	7 months	7 months	3 months	3 months	3 months
Plant pot for seeding	2.2-L pot	2.2-L pot	1.7-L pot	Tissue culture MS plate and 8.7-L plant growing tray	1.7-L pot
Plant pot for cultivation	5.0-L pot	5.0-L pot	5.0-L pot	5.0-L pot	5.0-L pot
Plant distance	15-60 cm	15-60 cm	60 cm	60 cm	60 cm
Table size (L/W/H)	450/162/44 cm	450/162/44 cm	600/152/94 cm	600/152/94 cm	600/152/94 cm
Lamp and table distance	160 cm	160 cm	260 cm	260 cm	260 cm
Lamp light source	Metal halide lamp, Philips MASTER HPI-T E40 400W - 645 coldwhite	Metal halide lamp, Philips MASTER HPI-T E40 400W - 645 coldwhite	Sodium vapour lamp, MASTER SON-T PIA Plus 400W	Sodium vapour lamp, MASTER SON-T PIA Plus 400W	Sodium vapour lamp, MASTER SON-T PIA Plus 400W
Soil composition	A 400, NPK mineral trace elements, pH ~5.5- 6.0, Salinity ~0.9 g L ⁻¹	A 400, NPK mineral trace elements, pH ~5.5- 6.0, Salinity ~0.9 g L ⁻¹	A 400, NPK mineral trace elements, pH ~5.5- 6.0, Salinity ~0.9 g L ⁻¹	A 400, NPK mineral trace elements, pH ~5.5- 6.0, Salinity ~0.9 g L ⁻¹	A 400, NPK mineral trace elements, pH ~5.5- 6.0, Salinity ~0.9 g L ⁻¹
Fertilizer composition and concentration	Wuxal Super, NPK 8+8+6, 0.5 % (m v ⁻¹) Hakaphos Red, NPK 8+12+24, 0.2 % (m v ⁻¹)	Hakaphos Blue, NPK 15+10+15, 0.2 % (m v ⁻¹)	Ferty 2 Mega, NPK 16+06+26, 0.1 % (m v ⁻¹)	Ferty 2 Mega, NPK 16+06+26, 0.1 % (m v ⁻¹)	Ferty 2 Mega, NPK 16+06+26, 0.1 % (m v ⁻¹)
Fertilization system	Hand irrigation	Hand irrigation	Flood irrigation Drip irrigation	Drip irrigation	Drip irrigation
Fertilization position	Table	Table	Table Ground	Table	Table
Fertilization frequency	Once a week, manually	Twice a week, manually	Daily, automatically	Daily, automatically	Daily, automatically

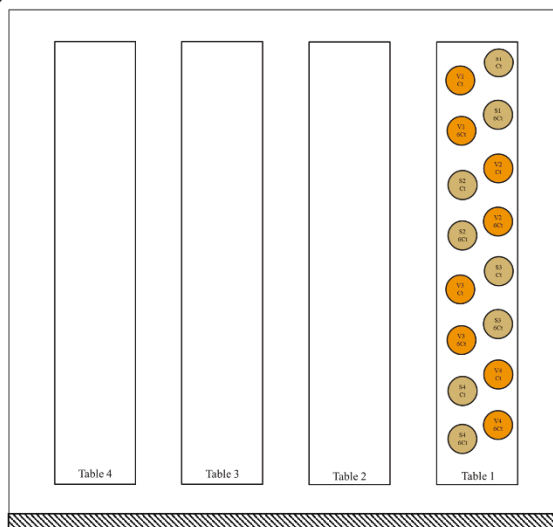
UR – University of Rostock; IME – Fraunhofer IME. 1× top and 1× cut – removing the tip of the main shoot either by removing the top ~0.2 m or cutting it at a height of ~1 m; 6× cut – after 1× cut, subsequent removing new growth side branches; NPK – nitrogen, phosphorus and potassium.

(A) 1st cultivation

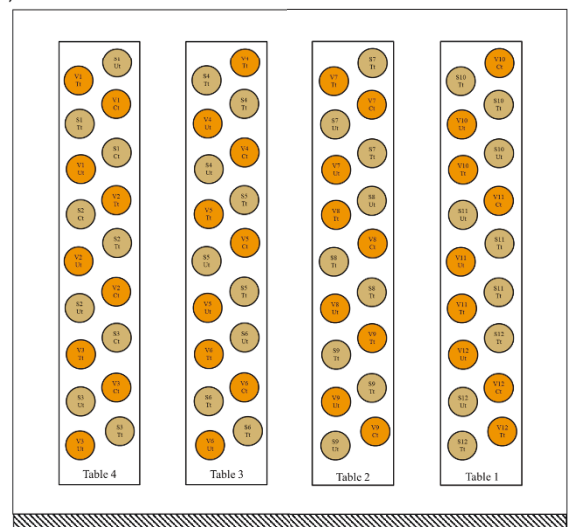
Position	Cultivar	Cultivation	No. of plants	Color
Table	SL632	1× top	10	Tt
Table	VG	1× top	10	Tt

(B) 2nd cultivation

Position	Cultivar	Cultivation	No. of plants	Color
Table	SL632	1× cut	10	Ct
Table	VG	1× cut	10	Ct
Ground	SL632	1× cut	10	Cg
Ground	VG	1× cut	10	Cg
Ground	SL632	uncut	10	Ug
Ground	VG	uncut	10	Ug

(C) 3rd cultivation

Position	Cultivar	Cultivation	No. of plants	Color
Table	SL632	1× cut	4	Ct
Table	VG	1× cut	4	Ct
Table	SL632	6× cut	4	6Ct
Table	VG	6× cut	4	6Ct

(D) 4th cultivation

Position	Cultivar	Cultivation	No. of plants	Color
Table	SL632	1× top	12	Tt
Table	VG	1× top	12	Tt
Table	SL632	1× cut	12	Ct
Table	VG	1× cut	12	Ct
Table	SL632	uncut	12	Ut
Table	VG	uncut	12	Ut

Figure 9. Map design for four cultivation trials in the greenhouse. The 1st cultivation trial was conducted at the University of Rostock in Rostock, and the subsequent 2nd-4th cultivation trials were conducted at Fraunhofer IME in Aachen. (A) The 1st cultivation trial (1× top, on the table, n=10), (B) the 2nd cultivation trial (uncut and 1× cut, on the table and on the ground, n=10), (C) the 3rd cultivation trial (1× cut and 6× cut, on the table, n=4), and (D) the 4th cultivation trial (uncut, 1× cut and 1× top, on the table, n=4). The wide downward diagonal pattern depicted in the figures symbolizes the direction of sunlight entering the greenhouse. Tt – 1× top on the table; Ct – 1× cut on the table; Cg – 1× cut on the ground; Ug – uncut on the ground; 6Ct – 6× cut on the table; Ut – uncut on the table.

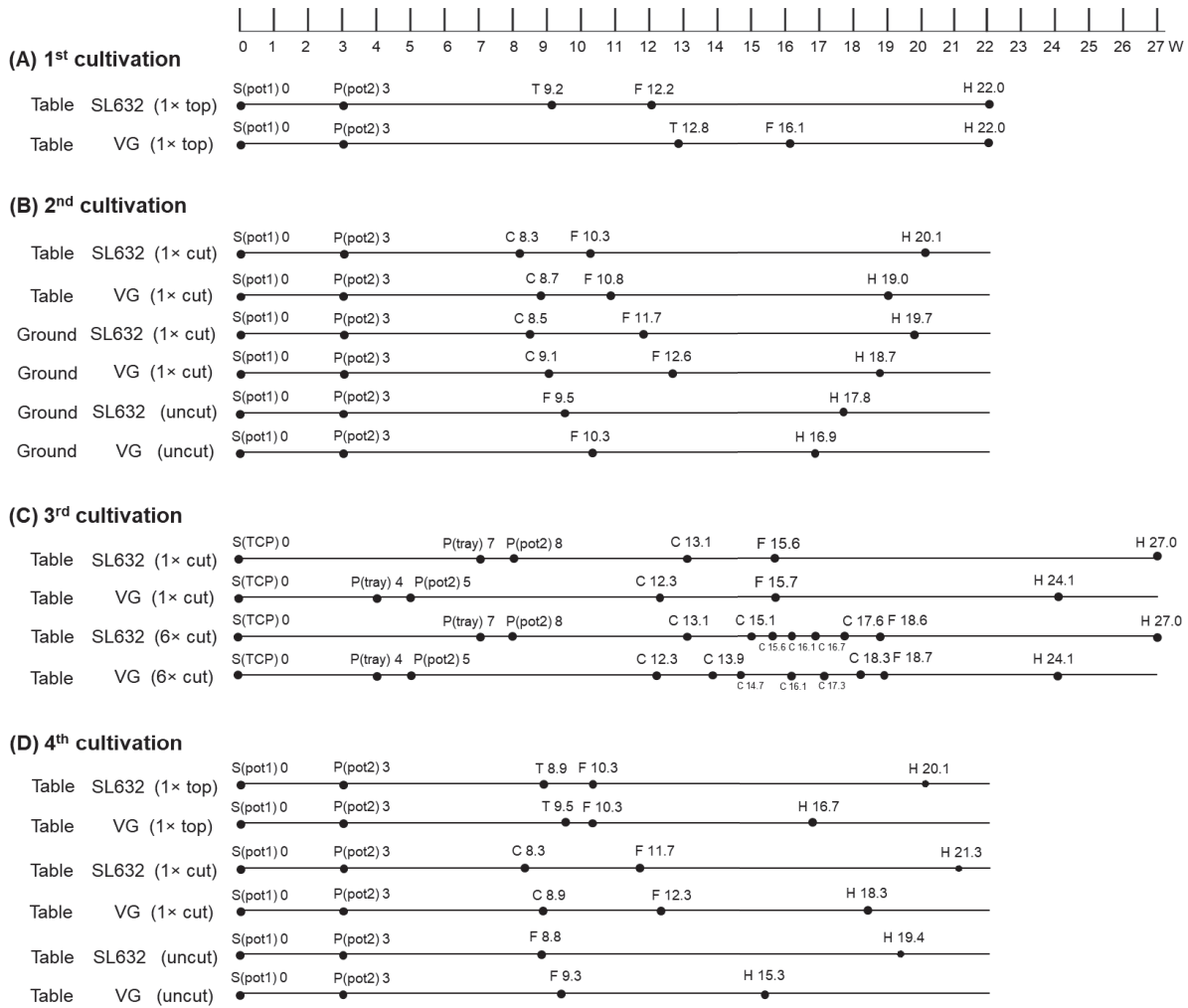


Figure 10. Timetable for four cultivation trials in the greenhouse. The timeline includes: 1) Seeding: Designated as S(pot1) for seeding in specific pot sizes, like 2.2-L or 1.7-L pots, or S(TCP) for seeding in tissue culture MS plates. 2) Shoot Transfer: Indicated as P(pot2) for transferring shoots to larger pot sizes, such as 5-L pots, or P(tray) for transferring them to 8.7-L plant growing trays. 3) Topping/Cutting: Denoted as T for topping and C for cutting. 4) Flowering: Represented by F, marking the stage when plant starts to produce flowers. 5) Harvest: Marked as H, indicating the time when plant is harvested. (H). **(A, B, and D)** In the 1st, 2nd, and 4th cultivation trials, each shoot initially grown in a 2.2-L or 1.7-L pot was transferred individually to a 5-L pot after 3 weeks. **(C)** In the 3rd cultivation trial, all shoots from tissue culture MS plates were first transferred collectively to 8.7-L plant growth trays. After a week of shoot growth, each individual shoot was then transferred to a 5-L pot. Following the transfer to the 5-L pot, each shoot was fertilized after 2 weeks.

III.1.3. For tobacco seed production, a nitrogen-rich fertilizer is optimal

Since fertilizer composition affected tobacco leaf and seed yield, I studied which fertilizer (NPK ratio) (Chapter III.1.2.) was suitable for tobacco seed production (Table 6, 1st Fertilization in UR). First, according to Nausch et al (2016), I chose Hakaphos Blue fertilizer with an NPK ratio of 15+10+15. Under SL632 and VG standard cultivation conditions (uncut), it took ~9 wps and 12 wps until mature seed could be harvested from the inflorescence of the main stem (data not shown). Most notably, after the uncut tobacco plants on the table at 12 wps had grown to a height of 2 m (both SL632 and VG), the upper part of the inflorescence was burnt by the light (data not shown), so I did not determine the seed yield. Nevertheless, seed capsules from unburned inflorescences showed that when Hakaphos Blue was used, SL632 produced 0 % shrunken seed capsules, 29 % undeveloped seed capsules, and 71 % fully developed seed capsules, while VG produced 0 % shrunken seed capsules, 5 % undeveloped seed capsules, and 95 % fully developed seed capsules (Figure 11).

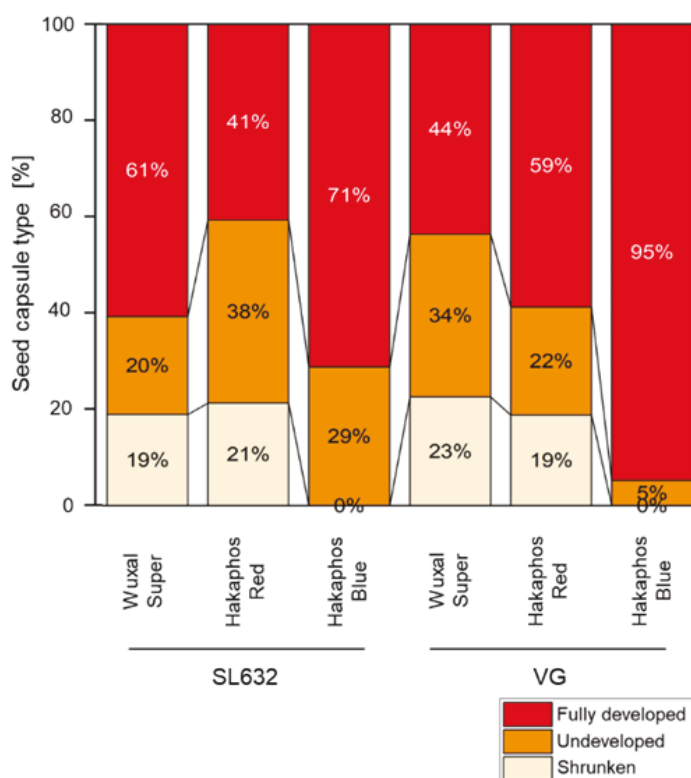


Figure 11. Seed capsule type in *N. tabacum* SL632 and VG under different fertilizer conditions. Under the fertilizers with NPK ratios of 8+8+6 (Wuxal Super), 8+12+14 (Hakaphos Red), and 15+10+15 (Hakaphos Blue), plants were harvested at ~10 wps for SL632 with Wuxal Super, ~12 wps for VG with Wuxal Super, ~10 wps for SL632 with Hakaphos Red, ~15 wps for VG with Hakaphos Red, and at 12 wps for both SL632 and VG with Hakaphos Blue. n=1-3 biological replicates. Fully developed – full developed seed capsule; Undeveloped – undeveloped seed capsule; Shrink – shrink seed capsule (without seeds); wps – weeks post seeding.

As an alternative to Hakaphos Blue, I then used a common tobacco fertilizer with an NPK ratio of 8+8+6 (Wuxal Super). With Wuxal Super, the main stem harvest time for mature seeds was ~10 wps for SL632 and ~12 wps for VG (data not shown). Notably, using this fertilizer resulted in a reduction in plant height by ~0.4 m for SL632 and VG (data not shown), possibly due to the lower overall NPK content. When the leaves and seeds were harvested together at 12 wps, I observed that the leaves were senescent (data not shown), so I harvested seeds instead of leaves. In terms of seed capsule types, SL632 under Wuxal showed 19 % shrunk seed capsules, 20 % undeveloped seed capsules, and 61 % fully developed seed capsules, while SL632 under Hakaphos Blue showed 0 % shrunk seed capsules, 29 % undeveloped seed capsules, and 71 % fully developed seed capsule (Figure 11). VG under Wuxal showed 23 % shrunk seed capsules, 34 % undeveloped seed capsules, and 44 % fully developed seed capsules, while VG under Hakaphos Blue showed 0 % shrunk seed capsules, 5 % undeveloped seed capsules, and 95 % fully developed seed capsules (Figure 11).

As another alternative fertilizer, I also used a fertilizer with increased K content, i.e., an NPK ratio of 8+12+14 (Hakaphos Red). In this case, the main stem harvest time for mature seeds was ~10 wps for SL632 and ~ 15 wps for VG (data not shown). Similar to Wuxal Super, seeds were harvested at 12 wps when leaves became senescent. SL632 under Hakaphos Red had 21 % shrunk seed capsules, 38 % undeveloped seed capsules, and 41 % fully developed seed capsules, while SL632 under Hakaphos Blue had 0 % shrunk seed capsules, 29 % undeveloped seed capsules and 71 % fully developed seed capsules (Figure 11). On the other hand, VG under Hakaphos Red had 19 % shrunk seed capsules, 22 % undeveloped seed capsules, and 59 % fully developed seed capsules, while VG under Hakaphos Blue had 0 % shrunk seed capsules, 5 % undeveloped seed capsules, and 95 % fully developed seed capsule (Figure 11).

In summary, 1) when tobacco SL632 and VG were grown under standard cultivation (uncut) in the greenhouse using high N fertilizers and harvested until the seeds mature, it was not possible to harvest leaves and seeds at the same time. 2) Wuxal and Hakaphos Red as fertilizers yielded shrunk seeds, which was not the case for Hakaphos Blue with high N and high K. Consequently, Hakaphos Blue should be preferred for seed production. 3) Without cutting, tobacco plants grew so high that the inflorescences were burnt by the lights in the greenhouse, reducing the overall seed yield, and alternative cutting strategies were required. Hence, different cultivation strategies such as topping and cutting might offer the opportunity to harvest both leaves and seeds in parallel and increase the seed yield.

Notably, when grown with Hakaphos Blue, SL632 had more shrunken seeds than VG, possibly because SL632 continuously produced new flowers, whereas VG did not exhibit the same continuous flowering.

III.1.4. Seed production can be increased in principle via topping and cutting

To improve seed yield in the greenhouse and prevent the burning of the inflorescences (Chapter III 1.3.), I conducted four cultivation strategies: 1× top (1st cultivation), 1× cut (2nd cultivation), 6× cut (3rd cultivation), and a side-by-side comparison (4th cultivation, uncut, 1× cut, and 1× top) (Figure 12). The purpose was to break apical dominance and induce multiple side branches to obtain multiple inflorescences per plant instead of just one inflorescence per plant.

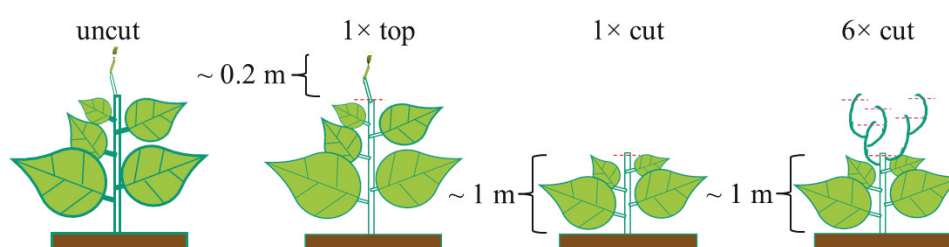


Figure 12. The definition of cultivation strategy in the greenhouse. Illustrations of the uncut, 1× top, 1× cut, and 6× cut cultivation treatments.

III.1.4.1. Seed yield of 1× top SL632 was ~4-fold higher compared to 1× top VG but inflorescences grew into the lights and leaves could not be harvested in parallel

Since Hakaphos Blue fertilizer with an NPK ratio of 15+10+15 had proven suitable for seed production in SL632 and VG cultivation (Chapter III 1.3.), I used this fertilizer in the 1st cultivation trial in the UR greenhouse (Figure 9A, Figure 10A). The aim of this 1st cultivation trial was to understand 2 questions: 1) Whether green leaves and seeds could be harvested in parallel to produce recombinant protein in leaves and seeds via topping (unlike the uncut plants, Chapter III.1.3.). 2) Whether SL632 produced more seeds than the conventional cultivar VG.

To enhance both LFM and SDM productivities, the 1st cultivation strategy (1× top) was to break apical dominance of the main stem during the vegetative stage and induce multiple side

branches not only to obtain more leaves but also to yield more inflorescences per plant that could be harvested in parallel instead of the conventional strategy of one inflorescence per plant. At the time point when the first inflorescence appeared, I had cut off the first ~0.2 m of the inflorescence at the top (1× top, Figure 13A) to have a main stem as high as possible, so that as many side branches as possible could be formed.

In terms of plant traits, 1× top VG with height of ~2 m per plant was 0.7 m taller than 1× top SL632 with a height of 1.3 m per plant, and VG was still burnt by the lights. Independent of that, 1× top SL632 was 3.7 wps faster than 1× top VG in terms of topping treatment and side branches starting flowering, but both had similar numbers of side branches with inflorescence per plant. The harvest time was when SL632 finished seed production, I harvested both SL632 and VG cultivars together at 22 wps, however, at that time, VG had not finished seed production (Table 11).

Regarding LFM productivity, 1× top VG yielded as high as 872.6 g LFM per plant and was 1.6-fold higher than 1× top SL632 with 541.3 g LFM per plant. However, the leaves were yellow, not green, at the 22 wps harvest (data not shown). In contrast, concerning SDM productivity, 1× top SL632 yielded as high as 10.0 g SDM per plant and was ~4-fold higher than 1× top VG with 2.3 g SDM per plant, indicating that 1× top SL632 seemed to have produced more seeds than 1× top VG (Table 11).

In summary, there were three problems in 1st cultivation trial (1× top): 1) It was not possible to harvest green leaves and seeds together since when seeds matured, the leaves became senescent, indicating protein degradation. Hence, focus should be solely on seed production. 2) Both 1× top SL632 and VG were still so tall on the table that the upper part of the inflorescence was burned by the lamp lights, resulting in reduced seed production. 3) 1× top delayed seed production. Most importantly, 1× top did not seem to increase the seed yield since it broke the apical dominance in the late vegetative stage, hindering the formation of multiple side-branches. Considering an alternative to topping, cutting might be suitable for increasing seed production.

III.1.4.2. Cutting can be used to limit the plant height

Considering the three problems related to height, growth stage, and the fact that both seeds and leaves could not be harvest in parallel in the 1st cultivation trial (1× top) in the UR greenhouse (Chapter III 1.4.1.), I designed the 2nd cultivation trial (1× cut, Figure 9B, Figure 10B), the 3rd cultivation trial (6× cut, Figure 9C, Figure 10C), and a side-by-side comparison of the different strategies (4th cultivation trial, uncut, 1× cut, and 1× top, Figure 9D, Figure 10D, Figure 12) in the IME greenhouse.

Notably, in the 2nd-4th cultivation trials in the IME greenhouse, in terms of fertilizers, I used Ferty 2 Mega (NPK ratio, 16+06+26), similar to Hakaphos Blue (NPK ratio, 15+10+15), for SL632 and VG cultivation. The harvest time was defined as when flowers had 75 % mature capsules, and the entire tobacco plant was then harvested.

III.1.4.2.1. 1× cut increased the seed yield of SL632 and VG by 1.5-fold

The 2nd cultivation strategy (1× cut) in the IME greenhouse aimed to cut tobacco plants when they reached a height of 1 m (1× cut, Figure 13B). This strategy might also prevent the problem of tobacco plants reaching a height of 2 m. While topping broke the apical dominance at the late vegetative stage, focusing only on seed production might be worthwhile to break the apical dominance directly at the beginning of the vegetative growth phase, allowing more time for side branch production. Cutting at a 1 m height could achieve this. Moreover, since the leaves on the side branches were newly formed, they might not have been senescing at the time of harvest.

In SL632 and VG cultivation, to solve the problem that the plants on the table grew too high on the table, reaching the lamps and resulting in burned flowers and reduced SDM productivity, I developed a solution by designing plants both on the ground (uncut and 1× cut) and on the table (1× cut) (Figure 9B, Figure 10B). To grow the plants on the ground, I used drip irrigation as a fertilization system instead of flood irrigation for table plants. By employing these three settings, the SDM per plant of the table plants (uncut) could be calculated, providing further insight into how high SDM per plant could be achieved in SL632 (Table 11).

For the plants on the ground (uncut and 1× cut), in terms of plant height, uncut SL632 and 1× cut SL632 had similar heights, while uncut VG with a height of ~2.3 m per plant was 1.1-fold lower than the 1× cut VG with a height of ~2.4 m per plant. Moreover, in the case of SL632,

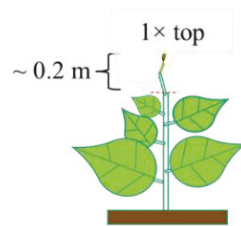
the 1× cut plants were a week earlier than the uncut plants in the timing of the cutting treatment, while the 1× cut plants were 2 weeks later than the uncut plants in side branches starting flowering and seed harvest, similar to VG. Nevertheless, both cultivars had similar numbers of side branches with inflorescence per plant. Regarding SDM productivity, 1× cut SL632 and 1× cut VG yielded up to 65.3 g and 46.1 g SDM per plant, while uncut SL632 and uncut VG produced 42.7 g and 31.7 g SDM per plant. Both cultivars showed a 1.5-fold increase in SDM per plant after the cutting process (Table 11).

For the plants on the table and ground (1× cut), regarding plant height, both SL632 and VG plants on the table (1× cut) and on ground (1× cut) were ~2.2 m and ~2.4 m, respectively, but the 9-week treatment time was the same. In terms of side branch inflorescence flowering time after seeding, plants on the table (1× cut) were ~1 week earlier than plants on ground (1× cut). Additionally, plant on the table (1× cut) had relatively 60 % and 77 % more side branches with inflorescences compared to plants on the ground (1× cut), corresponding to 34.9 (SL632, 1× cut, table) and 20.9 (SL632, 1× cut, ground), as well as 29.9 (VG, 1× cut, table) and 23.0 (VG, 1× cut, ground). However, their harvest times were similar, ~20 wps (SL632) and ~19 wps (VG). In terms of SDM productivity, 1× cut SL632 on the table and 1× cut VG on the table yielded up to 46.1 g and 49.9 g SDM per plant (Table 11).

Using these three SDM per plant data from these conditions (e.g., uncut plants on the ground, 1× cut on the ground, and 1× cut on the table), uncut SL632 and VG on the table were 30.2 g SDM per plant and 34.3 g SDM per plant.

In summary, the 2nd cultivation trial (1× cut) showed that 1× cut increased the seed yield of both SL632 and VG compared with uncut condition. Based on this, cutting not just once but multiple times might solve the problem of the height and further increase seed yield.

(A)



(B)

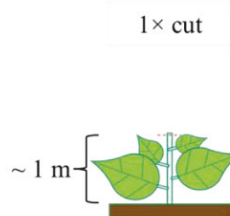


Figure 13. 1× top and 1× cut strategies in the greenhouse. (A) Illustration and photos of the 1× top treatment. The 1× top strategy was to cut off the first ~ 0.2 m inflorescence at the top (as shown in the right photo, 1× top inflorescence image). (B) Illustration and photos of the 1× cut treatment. The 1× cut strategy was to cut when the tobacco plants reached a height of 1 m (as shown in the right photo, 1× cut inflorescence image).

Table 11. Plant traits in *N. tabacum* SL632 and VG under 3 cultivation strategies in the greenhouse. Numbers represent mean \pm standard deviation. Significance was calculated by one-way ANOVA (Bonferroni) with letter < 0.05 and significance groups indicated in letters (a, b, c). The number of biologic replicates was n=8-9 (1st-2nd trials) and n=3 (3rd trial).

<i>N. tabacum</i> cultivar	Parameter	Description	Unit	1st table + 1x top n=10	2nd ground + uncut n=9	2nd ground + 1x cut n=8	2nd table + 1x cut n=9	3rd table + 1x cut n=3	3rd table + 6x cut n=3
SL632	1	Treatment time	dps	64.2 \pm 1.3	na	59.5 \pm 1.7 (a)	58.1 \pm 1.1 (a)	92.0 \pm 0.0 (a)	92.0 \pm 0.0 (a)
	2	1st cutting side branch	dps	na	na	na	na	na	106.0 \pm 0.0
		5th cutting side branch	dps	na	na	na	na	na	123.0 \pm 0.0
	3	Flowering of main stem	dps	na	66.4 \pm 1.7	na	na	na	na
	4	Side branches with inflorescence	-	5.4 \pm 2.1	17.9 \pm 2.3 (b)	20.9 \pm 3.5 (b)	34.9 \pm 4.5 (a)	53.3 \pm 3.5 (a)	39.0 \pm 4.6 (b)
	5	Side branch inflorescence flowering time after seeding	dps	85.6 \pm 3.0	66.4 \pm 1.7 (c)	82.1 \pm 1.1 (b)	72.3 \pm 5.9 (a)	109.0 \pm 0.0 (a)	130.0 \pm 0.0 (b)
	6	Plant height	cm	132.7 \pm 10.3	232.0 \pm 9.4 (a)	243.8 \pm 14.4 (a)	226.1 \pm 20.8 (a)	264.0 \pm 5.3 (a)	247.7 \pm 17.8 (a)
	7	Seed harvest	dps	154.0 \pm 0.0	124.3 \pm 0.7 (c)	138.0 \pm 0.0 (b)	141.0 \pm 1.6 (a)	189.0 \pm 0.0 (a)	189.0 \pm 0.0 (a)
	8	Total SDM per plant	g	10.0 \pm 4.0	42.7 \pm 10.1 (a)	65.3 \pm 12.2 (b)	46.1 \pm 10.7 (a)	51.8 \pm 6.1 (a)	39.0 \pm 17.5 (a)
<i>N. tabacum</i> cultivar	Parameter	Description	Unit	1st table + 1x top n=10	2nd ground + uncut n=10	2nd ground + 1x cut n=8	2nd table + 1x cut n=9	3rd table + 1x cut n=3	3rd table + 6x cut n=3
VG	1	Treatment time	dps	89.9 \pm 2.0	na	63.4 \pm 1.2 (b)	61.1 \pm 1.8 (a)	86.0 \pm 0.0 (a)	86.0 \pm 0.0 (a)
	2	1st cutting side branch	dps	na	na	na	na	na	97.0 \pm 0.0
		5th cutting side branch	dps	na	na	na	na	na	128.0 \pm 0.0
	3	Flowering of main stem	dps	na	72.2 \pm 0.6	na	na	na	na
	4	Side branches with inflorescence	-	4.9 \pm 1.0	18.5 \pm 2.5 (c)	23.0 \pm 3.0 (b)	29.9 \pm 5.3 (a)	44.3 \pm 2.5 (a)	17.7 \pm 3.2 (b)
	5	Side branch inflorescence flowering time after seeding	dps	112.7 \pm 5.5	72.2 \pm 0.6 (a)	88.5 \pm 2.4 (b)	75.4 \pm 7.4 (a)	110.0 \pm 0.0 (a)	131.0 \pm 0.0 (b)
	6	Plant height	cm	200.3 \pm 26.8	228.2 \pm 13.2 (ab)	243.1 \pm 4.5 (b)	213.0 \pm 20.9 (a)	265.3 \pm 8.5 (a)	268.3 \pm 62.5 (a)
	7	Seed harvest	dps	154.0 \pm 0.0	118.6 \pm 0.5 (c)	131.0 \pm 0.0 (b)	133.0 \pm 0.0 (a)	169.0 \pm 0.0 (a)	169.0 \pm 0.0 (a)
	8	Total SDM per plant	g	2.3 \pm 1.2	31.7 \pm 4.9 (b)	46.1 \pm 14.5 (a)	49.9 \pm 11.6 (a)	48.0 \pm 2.1 (a)	6.8 \pm 2.5 (b)

a, b, c – significance groups ($p < 0.05$); SDM – seed dry mass; dps – days post seeding; na – not applicable.

III.1.4.2.2. 6× cut had no benefit on the seed yield compared to 1× cut

The 3rd cultivation strategy (6× cut) in the IME greenhouse was to make multiple cuts on the plants on the table to test whether 1) plant height could be reduced and 2) the seed production could be increased (6× cut, Figure 9C, Figure 10C). Multiple cutting was to cut continuously all side branches that grew to the light to direct resources to the lower side branches. The definition of 6× cut consisted of 1× cutting of the main stem (1× cut) followed by 5× cutting of the secondary main stems (5× cut). The 1× cut aimed to remove the tip of the main shoot by cutting it at a height of ~1 m to break apical dominance during the vegetative stage, whereas the 6× cut was to prevent the formation of secondary main stems (Figure 12).

In this trial, SL632 or VG plants were treated at the same time, such as treatment time and harvest time, so the 3rd cultivation trial was used as a pre-test. Even with 1× cut and 6× cut treatments, the height of SL632 and VG was still more than 2.2 m. Overall, SL632 grew slower, resulting in the seed harvest being delayed by 2.9 weeks compared to VG. Notably, under the 6× cut treatment, SL632 and VG showed a significant reduction, with 73 % and 40 % fewer side branches with inflorescences, compared to the 1× cut. In terms of SDM productivity for SL632, 6× cut yielded up to 39.0 g SDM per plant, which was 1.3-fold lower than 1× cut with 51.8 g SDM per plant. The impact was even more pronounced for VG, as the 6× cut drastically reduced the SDM from 48.0 g SDM per plant (1× cut) to 6.8 g SDM per plant (6× cut) (Table 11).

In summary, there were two problems in the 3rd cultivation trial (6× cut): 1) Despite the 6× cut treatment, both SL632 and VG plants on the table remained tall (more than 2 m). 2) The 6× cut significantly decreased SDM productivity in comparison to the 1× cut, indicating a substantial reduction in seed yield potential. Consequently, the 6× cut did not increase seed yield, because 6× cut might inhibit the formation of side branch with inflorescence, resulting in lower seed yield, whereas 1× cut should be used to increase seed yield.

III.1.4.3. Side-by-side comparison of different strategies showed that 1× cut yielded the highest seed biomass with SL632 producing more 1.6-fold more seeds than VG

Since multiple greenhouse parameters such as different locations (UR/Rostock and IME/Aachen) and cultivation conditions (including soil type, fertilizer type, fertilizer frequency, and fertilizer system) affected the comparability of the different trials, I conducted a side-by-side experiment (4th cultivation trial, all plants on the table) in the IME greenhouse.

This trial aimed to directly compare different cultivation strategies, such as uncut, 1× cut and 1× top (Figure 9D, Figure 10D, Figure 12).

Under uncut cultivation conditions, both SL632 and VG cultivars grew up to a height of ~2 m and had similar times of flowering of main stem and numbers of side branches with inflorescence. However, they showed different seed harvest times and seed yields at 19 wps with 42.7 g SDM per plant (SL632, uncut) and 15 wps with 18.0 g SDM per plant (VG, uncut) (Table 12).

In the case of SL632, 1× cut and 1× top plants failed to reduce plant height below 2 m. Compared to uncut, side branches starting flowering delayed by 2-3 weeks but induced 1.2-fold and 1.3-fold more side branches. They also delayed the harvest time from 19 wps to 21 wps (SL632, 1× cut) and 20 wps (SL632, 1× top), yielded 1.6-fold and 1.5-fold more seeds with 67.9 g and 61.4 g SDM per plant (Table 12).

Similar to SL632, VG plants under 1× cut and 1× top conditions were more than 2 m tall, but both strategies delayed the side branches starting flowering time and increased the number of side branches. They also delayed harvest time from 15 wps to 18 wps (VG, 1× cut) and 17 wps (VG, 1× top). VG also increased relative seed yield by 2.4-fold and 1.4-fold, yielding up to 43.1 g and 24.4 g SDM per plant, but still lower absolute yield than SL632 (Table 12). The more pronounced effect in VG in case of 1× cut might be explained by the fact that uncut SL632 formed 2.4-fold more side branches than uncut VG. This indicated that the apical dominance seemed to be reduced in SL632 and thus cutting and topping were less effective.

Additionally, combining data from SDM per plant and seed harvest time, SL632 had higher seed productivity than VG regardless of cultivation strategy. For example, SL632 was ~0.315 g per day (uncut), ~0.436 g per day (1× top) and ~0.455 g per day (1× cut), while VG was ~0.168 g per day (uncut), ~0.208 g per day (1× top) and ~0.337 g per day (1× cut). In terms of the seed yield per unit area and time of untransformed tobacco under different greenhouse cultivation conditions, the SDM productivity for SL632 was 0.24 kg m⁻² a⁻¹ (uncut), 0.34 kg m⁻² a⁻¹ (1× top), and 0.38 kg m⁻² a⁻¹ (1× cut). Whereas VG was 0.10 kg m⁻² a⁻¹ (uncut), 0.14 kg m⁻² a⁻¹ (1× top), and 0.24 kg m⁻² a⁻¹ (1× cut) (Table 12).

In summary, in side-by-side experiment, 1× top seemed to be less effective than 1× cut in SDM productivity, and 1× cut had the highest seed yield in SL632 and VG. For example, 1× cut SL632 had a seed yield of 67.9 g SDM per plant, which was 1.6-fold higher than 1× cut VG with 43.1 g SDM per plant. This demonstrated that SL632 is suitable to produce PD in seeds in a greenhouse setting.

Table 12. Plant traits of *N. tabacum* SL632 and VG under different cultivation strategies in the greenhouse. The area of each plant in the greenhouse is 0.36 m². Numbers represent mean \pm standard deviation. Significance was calculated by one-way ANOVA with Bonferroni correction with an alpha threshold of 0.05 and significance groups indicated by letters (a, b, c). The number of biologic replicates was n=12 (parameter 1-6) and n=4-5 (parameter 7).

<i>N. tabacum</i> cultivar	Parameter	Description	Unit	uncut	1x top	1x cut
SL632	1	Treatment time	dps	na	62.0 \pm 0.9 (a)	57.8 \pm 1.0 (b)
	2	Flowering of main stem	dps	61.8 \pm 0.8	na	na
	3	Side branches with inflorescence	-	21.5 \pm 4.7 (a)	28.4 \pm 3.4 (b)	26.7 \pm 3.4 (b)
	4	Side branch inflorescence flowering time after seeding	dps	61.8 \pm 0.8 (a)	72.3 \pm 3.2 (b)	82.0 \pm 4.9 (c)
	5	Plant height	cm	219.5 \pm 14.1 (a)	206.4 \pm 11.5 (a)	206.6 \pm 12.6 (a)
	6	Seed harvest	dps	135.6 \pm 11.0 (a)	140.8 \pm 12.2 (ab)	149.3 \pm 6.2 (b)
	7	Total SDM per plant	g	42.7 \pm 4.7 (a)	61.4 \pm 6.6 (b)	67.9 \pm 11.9 (b)
	8	Seed productivity	g d ⁻¹	~0.315	~0.436	~0.455
	9	Seed yield per unit area and time	kg m ⁻² a ⁻¹	0.24	0.34	0.38
VG	1	Treatment time	dps	na	66.3 \pm 1.6 (a)	62.0 \pm 1.5 (b)
	2	Flowering of main stem	dps	65.0 \pm 1.0	na	na
	3	Side branches with inflorescence	-	18.9 \pm 2.4 (ab)	15.4 \pm 3.0 (a)	22.1 \pm 5.6 (b)
	4	Side branch inflorescence flowering time after seeding	dps	65.0 \pm 1.0 (a)	72.2 \pm 6.7 (b)	86.3 \pm 5.4 (c)
	5	Plant height	cm	197.8 \pm 18.7 (a)	221.3 \pm 17.5 (b)	217.6 \pm 11.6 (b)
	6	Seed harvest	dps	107.4 \pm 0.5 (a)	117.1 \pm 4.1 (b)	127.8 \pm 3.9 (c)
	7	Total SDM per plant	g	18.0 \pm 4.9 (a)	24.4 \pm 4.4 (a)	43.1 \pm 8.7 (b)
	8	Seed productivity	g d ⁻¹	~0.168	~0.208	~0.337
	9	Seed yield per unit area and time	kg m ⁻² a ⁻¹	0.10	0.14	0.24

a, b, c – significance groups ($p < 0.05$); SDM – seed dry mass; dps – days post seeding; na – not applicable.

III.1.5. The cost for seed production were 11- to 36-fold higher compared to the leaf production, but this might be compensated by the fact that no processing of seeds is required for oral delivery

Generally, tobacco is used for greenhouse tobacco leaf production, and tobacco leaf biomass has been established (Conley et al., 2011; Nausch et al., 2016). To calculate production costs for PD production in stably transformed *N. tabacum* plants under different strategies in the greenhouse, I considered both seed and leaf productivity. As reference I further included data for transiently transformed *N. benthamiana*. In terms of production costs per SDM, SL632 and VG and *N. benthamiana* were economically compared under different cultivation strategies (uncut, 1× top, and 1× cut, Table 13), while in terms of production costs per LFM only the uncut cultivation was considered. The production costs included costs for capital investment (CAPEX) and operating expenses (OPEX). However, in this study, I excluded the CAPEX costs because I considered the greenhouse as a given.

OPEX could be separated into costs for consumables and labor costs. First, consumable costs included water, soil (0.10 € L⁻¹, Stender GmbH, Germany), fertilizer (2.10 € kg⁻¹, H. Nitsch & Sohn GmbH, Germany), water (2.12 € m⁻³, STAWAG Energie GmbH, Germany), and energy costs (0.23 € kWh⁻¹, STATISTA GmbH, Germany), totaling ~100 € per batch. The costs per plant were calculated per batch based on a batch size of 72 plants for SL632 and VG and 400 plants for *N. benthamiana*. Accordingly, consumable costs per plant were 1.40 € per SL632 or VG plant and 0.30 € per *N. benthamiana* plant. The SDM production time included the time from sowing to harvest and seed drying, totaling 28-30 wps for SL632 and 24-27 wps for VG. However, the LFM production time for SL632, VG and *N. benthamiana* was 6 wps (Table 13).

Next, in labor costs, I referred to the costs of technical assistants in Germany, which was 87 € h⁻¹ (costs in 2022). The weekly labor working hour included time for sowing, separation from the plant tray to the pot, fixing plants with ropes and bamboo sticks, performing cutting treatments, inspecting plants, and harvesting. The weekly labor working hours for SDM and LFM for SL632 and VG were 1.0-1.3 h (transgenic seed, uncut, 1× top, and 1× cut) and 0.7 h (transgenic leaf, uncut), respectively, while LFM of *N. benthamiana* was 0.2 h (uncut), corresponding to labor costs per plant were 90-110 €, 63 € and 21 €, respectively (Table 13).

By combining total costs per plants and SDM/LFM yield per plants, I calculated costs per SDM and costs per LFM (Table 13).

In terms of SDM production, 1× cut had the highest seed yield in SL632 and VG, with SL632 having ~2-fold higher seed yield (69.7 g per plant, 1.3 h) than VG (43.1 g per plant, 1.3 h). Accordingly, 1× cut SL632 had the lowest production cost per SDM at 1.64 € g⁻¹ compared to 2.58 € g⁻¹ for VG (Table 13).

For SL632, the ~1.6-fold higher SDM per plant compensated for the 1.3-fold higher staff effort associated with 1× cut (67.9 g per plant, 1.3 h) compared to uncut (42.7 g per plant, 1.0 h), and the SDM production costs were reduced from 2.14 € g⁻¹ (uncut) to 1.64 € g⁻¹ (1× cut), respectively. For VG, the ~2.4-fold higher SDM per plant compensated the 1.3-fold higher staff effort that was associated with the 1× cut (43.1 g per plant, 1.3 h) compared to uncut (18.0 g per plant, 1.0 h) and the SDM production costs were reduced from 5.07 € g⁻¹ (uncut) to 2.58 € g⁻¹ (1× cut), respectively (Table 13).

In addition, the SDM yield per unit area and time of 1× cut plants was ~1.6-2.4 times higher than that of uncut plants, ranging from 0.38 kg m⁻² a⁻¹ (1× cut SL632) to 0.24 kg m⁻² a⁻¹ (uncut SL632) and 0.24 kg m⁻² a⁻¹ (1× cut VG) to 0.10 kg m⁻² a⁻¹ (uncut VG) (Table 13). In contrast to SDM, the LFM yields of uncut plants at 6 wps were 340.3 g (SL632), 464.2 g (VG) and 155.0 per plant (*N. benthamiana*), respectively, with LFM production costs of 0.19 € g⁻¹ (SL632), 0.14 € g⁻¹ (VG) and 0.13 € g⁻¹ (*N. benthamiana*). Additionally, the LFM yield per unit area and time of uncut plants were 8.19 kg m⁻² a⁻¹ (SL632), 11.17 kg m⁻² a⁻¹ (VG) and 11.94 kg m⁻² a⁻¹ (*N. benthamiana*) (Table 13).

In summary, 1) the LFM production costs were almost the same for uncut VG (0.13 € g⁻¹) and uncut *N. benthamiana* (0.14 € g⁻¹) compared to uncut SL632 (0.19 € g⁻¹). 2) Compared with the LFM production costs, the SDM production costs of VG (1× cut) and SL632 (1× cut) were 11.3-fold and 36.2-fold higher, corresponding to 2.58 € g⁻¹ and 1.64 € g⁻¹. However, these higher production costs might be compensated by the fact that seeds do not need to be processed for application, which makes up to 80 % of the overall production costs.

Table 13. Operating expenses (OPEX) for tobacco seed and leaf biomass production per plant in the greenhouse via different cultivation strategies. Costs per plant were calculated per batch based on a batch size of 72 plants for *N. tabacum* cv. SL632 (SL632) and VG (VG) and 400 plants for *N. benthamiana*. Labor costs were those of a technical assistant in Germany (2021; 87 € h⁻¹; full overhead calculation). Consumables covered water, soil, fertilizer and energy expenses.

Tobacco cultivar	Biomass type	Cultivation strategy	Seed and leaf production*	Working hours	Labor costs	Consumable costs	Total costs per plant	SDM/LFM Yield per plant	Costs per SDM/LFM	Biomass per unit area and time
			[week]	[h]	[€]	[€]	[€]	[g]	[€ g ⁻¹]	[kg m ⁻² a ⁻¹]
SL632	Transgenic seed	Uncut	28	1.0	89.9	1.4	91.3	42.7	2.14	0.24
	Transgenic seed	1× Top	29	1.2	107.7	1.4	109.1	61.4	1.78	0.34
	Transgenic seed	1× Cut	30	1.3	109.9	1.4	111.3	67.9	1.64	0.38
	Transgenic leaf	Uncut	6	0.7	62.6	1.4	64.0	340.3	0.19	8.19
VG	Transgenic seed	Uncut	24	1.0	89.9	1.4	91.3	18.0	5.07	0.10
	Transgenic seed	1× Top	25	1.2	107.7	1.4	109.1	24.4	4.47	0.14
	Transgenic seed	1× Cut	27	1.3	109.9	1.4	111.3	43.1	2.58	0.24
	Transgenic leaf	Uncut	6	0.7	62.6	1.4	64.0	464.2	0.14	11.17
<i>N. benthamiana</i>	Transient leaf	Uncut	6	0.2	20.6	0.3	20.8	155.0	0.13	11.94

LFM – leaf fresh mass; SDM – seed dry mass; SL632 – *N. tabacum* cv. SL632; VG – *N. tabacum* cv. VG. *Seed production includes plant growth until seed harvest (Table 8) and seed drying 8 weeks.

III.2. Stable FGF21-Transferrin expression in seeds of *N. tabacum* SL632

For establishing oral delivery of FGF21, I aimed to specifically target FGF21 to the liver. To achieve this goal, FGF21 needs to be protected from the acidic conditions in the stomach and transported through the enterocytes from the intestine to the portal vein. Therefore, I established a seed-based oral delivery system for FGF21.

III.2.1. An FGF21-F-Tf fusion protein with a molecular mass of 100 kDa was designed with no steric hindrance between the fusion partners

FGF21 is a protein with several PTMs such as disulfide bridges and O-glycosylation (Chapter I.2.1.). Since O-glycosylation was not necessary for its biological activity and O-glycosylation is completely different between plants and mammals, a point mutation Ser167Ala was introduced (Chapter I.2.4.). To facilitate FGF21 uptake into the bloodstream, it was fused with Tf, inducing transcytosis from the intestine to the portal vein via the Tf receptor (Chapter I.3.1.), resulting in the construct named FGF21-Transferrin (FGF21-Tf).

However, Tf also prolongs the serum half-life of the fusion protein and promotes blood circulation (Chapter I.3.2.). To separate it after translocation, Furin protease was used. Furin, expressed in mammalian enterocytes but absent in plants, facilitates the release of FGF21 from Tf in intestinal enterocytes. Furin, expressed in mammalian enterocytes but absent in plants, facilitates the release of FGF21 from Tf in intestinal enterocytes.

To achieve this, a furin cleavage site (F) that is absent in plants (Chapter I.3.3.) was inserted between FGF21 and Tf, resulting in the construct named FGF21-F-Tf (Figure 14A). Additionally, an additional GS-linker, composed of 3 repeats of GGGGS (Choi et al., 2014), was included to prevent steric hindrance between FGF21 and Tf and ensure the accessibility of the Furin cleavage site.

The idea was that the FGF21-F-Tf fusion protein is cut into free FGF21 and F-Tf after uptake into the small intestine. FGF21 not taken up by the liver is rapidly degraded due to its short half-life. Since Tf requires disulfide bridges to fold into its native conformation, the FGF21-F-Tf fusion protein was targeted to the ER (Mason et al., 1996) using the N-terminal signal peptide from the Calreticulin of *N. plumbaginifolia* (Acc. Z71395)

(MATQRRANPSSLHLITVFSLLVAVVSG) and C-terminal retention signal (SEKDEL) (Chapter I.3.1.).

For Western blot detection and IMAC purification, a double His₆ tag was added to the C-terminal Tf (Figure 14A). Before cloning, I submitted the amino acid sequence to Raptor X software to assess potential steric hindrance by analyzing the *in silico* structure of FGF21-F-Tf. When compared with native FGF21, no steric hindrance was observed in the alpha helix and beta-sheet regions (Figure 14B).

The final FGF21-F-Tf fusion protein had a molecular mass of 100 kDa, corresponding to a coding region of 2.0 kb.

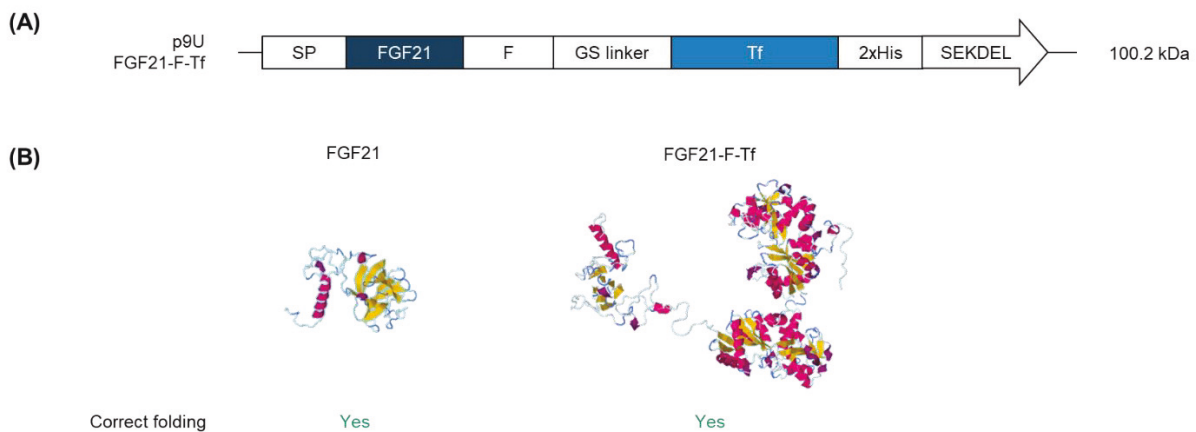


Figure 14. Construct and model used for the stable expression of FGF21-Transferrin fusion protein. (A) p9U stable expression vector containing FGF21-F-Tf in *N. tabacum* SL632 and VG. **(B)** The 3D structures of FGF21 and FGF21-Tf fusion protein predicted by submitting the amino acid sequence to the RaptorX software (<http://raptorx.uchicago.edu/>). SP – ER-targeting signal peptide from Calreticulin of *Nicotiana plumbaginifolia* (Acc. Z71395), MATQRRANPSSLHLITVFSLLVAVVSG; F – furin cleavage site, RRKRSV; GS linker – flexible linker, (GGGGS)₃; 2xHis – double-His₆ tag; SEKDEL – ER-retention signal.

III.2.2. *In vitro* plant tissue culture of SL632 is limited by rapid flowering

For stable transformation, the plants needed to be grown *in vitro* under sterile conditions. Since SL632 was bred to have a short vegetative period and rapid seed production, I analyzed the duration and propagation frequency of one passage/transformant in both SL632 and VG.

The strategy during tissue culture propagation was to cut off one leaf containing the stem from SL632 or VG when their leaves reached the top lid of the LST media container and transferred it to the new LST medium. This cutting process continued until the plants flowered, with the maximum number of passages defined as when 50 % of the plants flowered.

The average passage time of tissue culture for SL632 was 21 days, ~2 days faster than the 23 days of VG. SL632 showed an early flowering phenomenon, allowing up to 6 passages. The seed-rich SL632 started flowering after two passages, and flowering plants did not produce new leaves. Therefore, further passage was not possible. In contrast, the leaf-rich VG could grow in tissue cultured with continuous passaging every 23 days and could be cultivated for at least 19 passages with only occasional flowering (Table 14).

In summary, SL632 propagation was impacted by early flowering for only 6 generations. This indicates that SL632 was difficult to maintain in tissue culture for transformation usage.

Table 14. Propagation of *N. tabacum* SL632 and VG. Numbers represent mean \pm standard deviation. Significance was calculated by one-way ANOVA (Bonferroni) with * $p < 0.05$, ** $p < 0.01$ and *** $p < 0.001$. n=21, technical replicates.

Propagation	Unit	<i>N. tabacum</i> cultivar		Significance
		SL632	VG	
Average length of passage in tissue culture	day	21.0 \pm 0.0	23.1 \pm 2.7	***
Maximum number of passages until 50 % of the plants flowered	number	6th	>19th	***

III.2.3. Stable transformation efficacy of FGF21-F-Tf in SL632 was similar to VG

In tobacco stable transformation, the non-toxic green fluorescent protein (GFP) as a control and the target FGF21-F-Tf were transformed into SL632 and VG using the *A. tumefaciens* strain C58C1. To express FGF21-F-Tf in the whole plants, I used the constitutive cauliflower mosaic virus (CaMV) 35S promoter. Therefore, FGF21-F-Tf and GFP were cloned into the stable transformation T-DNA vector pLH9000 (Acc. AF458478) with the CaMV double enhancer, the 35S core promoter, and 35S terminator, called p9U-FGF21-F-Tf (Figure 14A), and p9U-GFP vectors (data not shown).

The T0 transgenic GFP and FGF21-F-Tf plants were selected on kanamycin-containing medium, as the T-DNA vector contained the Neomycin Phosphotransferase II selectable marker gene (*nptII*), conferring kanamycin resistance. Total genomic DNA was isolated from crude leaf extracts of T0 transgenic plants and control non-transgenic plants. Subsequently, polymerase chain reaction (PCR) screening was performed to confirm the presence of the

GFP or FGF21-F-Tf gene, along with the control endogenous tobacco gene NtWBC1 (*N. tabacum* ABC transporter of the White-Brown Complex subfamily) (data not shown).

In terms of GFP transformation efficiency, SL632 yielded lower numbers of regenerated shoots (2.2) and percentage of positive rooted shoots (59%) compared to VG (2.9 and 74%, respectively). Notably, VG showed a higher number of positive shoots per explant (2.2) compared to SL632 (1.3). For GFP transformation, SL632 produced 23 T0 transformants while VG generated 33 T0 transformants (Table 15).

In terms of FGF21-F-Tf transformation efficiency, both SL632 and VG exhibited lower numbers of regenerated shoots, with 0.6 and 1.1, respectively. However, SL632 showed a higher percentage of positive rooted shoots at 62 % compared to VG's 37 %. Remarkably, when considering the number of positive shoots per explant, both SL632 and VG showed similar transformation efficiencies of 0.4. Both SL632 and VG yielded an equal count of 26 transformants each for FGF21-F-Tf (Table 15).

In summary, both SL632 and VG yielded 26 transformants for FGF21-F-Tf.

Table 15. Transgenic T0 events in *N. tabacum* SL632 and VG. Numbers represent mean \pm standard deviation. n=2-3, biological replicates.

Stable transformation	Unit	<i>N. tabacum</i> cultivar			
		SL632		VG	
		GFP	FGF21-F-Tf	GFP	FGF21-F-Tf
Shoot/Explant	-	2.2 \pm 1.7	0.6 \pm 0.1	2.9 \pm 1.8	1.1 \pm 0.3
Positive rooted shoots	%	59 %	62 %	74 %	37 %
Positive shoots/Explant	-	1.3	0.4	2.2	0.4
Number of T0 events	number	23	26	33	26

III.2.4. FGF21-F-Tf accumulation in stably transformed SL632 and VG

For animal feeding studies, previous studies demonstrated the application of 1 mg kg⁻¹ d⁻¹ of FGF21 per mouse (Camporez et al., 2013; Emanuelli et al., 2014). Therefore, FGF21-F-Tf concentrations required >50 mg kg⁻¹ biomass. Hence, I aimed to search for T0 transformants that achieved this accumulation level or, if suitable T0 plants were not available, to increase the accumulation level via breeding.

III.2.4.1. Intact FGF21-F-Tf accumulation in seeds achieved to 6.7 mg kg⁻¹ SDM

III.2.4.1.1. T0 seeds yielded 1.44 mg kg⁻¹ SDM

The 26 FGF21-F-Tf transgenic events from SL632 and VG were individually cultivated in the greenhouse to produce T0 seeds (Figure 15A, Table 15). To quantify total FGF21-F-Tf fusion protein accumulation in T0 seeds, seed material was homogenized in extraction buffer at a ratio of 1:10 and quantified via FGF21-ELISA. In the T0 seed events in SL632 and VG, total FGF21-F-Tf fusion protein yielded in the three elite events: 0.47 mg kg⁻¹ SDM (SL632, event 1), 0.89 mg kg⁻¹ SDM (SL632, event 49) and 1.44 mg kg⁻¹ SDM (SL632, event 27), as well as 0.26 mg kg⁻¹ SDM (VG, event 50), 0.32 mg kg⁻¹ SDM (VG, event 2) and 0.63 mg kg⁻¹ SDM (VG, event 51). Among them, SL632 event 27 (1.44 mg kg⁻¹ SDM) and VG event 51 (0.63 mg kg⁻¹ SDM) had the highest total accumulation levels (Figure 15A).

To determine the protein integrity of the FGF21-F-Tf fusion protein, 100 µg of the TSP of the seed extract was applied to Western blots with anti-FGF21 and anti-His antibodies. Considering the detection limit of the anti-His antibody and anti-FGF21 antibody, the total FGF21-F-Tf fusion protein should have been higher than 90 ng in 100 µg TSP. This means that FGF21-F-Tf should have had an accumulation level of at least 9.0 mg kg⁻¹ SDM. However, I did not perform anti-His and anti-FGF21 Western blots as the total FGF21-F-Tf fusion protein with 1.44 mg kg⁻¹ SDM in T0 seeds was below that limit (Figure 15A).

III.2.4.1.2. T1 seeds yielded 6.7 mg kg⁻¹ SDM

To increase FGF21-F-Tf accumulation for animal feeding studies, I selected 3 best-performing T0 events in SL632 (event 1, 27, and 49) and VG (event 2, 50, and 51) for T1 seed production (Figure 15A). After T1 breeding, the highest accumulation of total FGF21-F-Tf fusion protein in T1 seeds reached 9.1 mg kg⁻¹ SDM (SL632, event 1-1) and 8.7 mg kg⁻¹ SDM (VG, event 2-1) (Figure 15B). Compared to T0 seeds containing 0.47 mg kg⁻¹ SDM (SL632, event 1) and 0.32 mg kg⁻¹ SDM (VG, event 2), there was a 19-fold increase for SL632 event 1-1 (reaching 9.1 mg kg⁻¹ SDM) and a 27-fold increase for VG event 2-1 (reaching 8.7 mg kg⁻¹ SDM).

To assess the protein integrity of FGF21-F-Tf, I conducted Western blots on transgenic SL632 T1 seeds (SL632, event 1-1) (Extra, Figure 16A). The FGF21-ELISA results indicated that this event yielded 9.1 mg kg⁻¹ SDM (Figure 15B). However, while the anti-FGF21 Western blot revealed intact FGF21-F-Tf fusion protein with 100 kDa and free FGF21-(F)-

(GS) with 19-21 kDa, the anti-His Western blot only showed a band corresponding to the size of FGF21-F-Tf degradation products (F-GS-Tf, GS-Tf, or Tf) with 79-80 kDa (Extra, Figure 16A).

Since the FGF21-ELISA measures total FGF21-F-Tf fusion proteins, including both intact and degraded forms, the amount determined by the ELISA must be corrected with the help of the Western blot data. For example, 9.1 mg kg⁻¹ SDM were detected by the FGF21-ELISA in the SL632 elite event (SL632, event 1-1).

Based on densitometry analysis of the anti-FGF21 Western blots, the intact FGF21-F-Tf form made up 74 %, while the FGF21 degradation product accounted for 26 %, corresponding to 6.7 mg kg⁻¹ SDM and 2.4 mg kg⁻¹ SDM for SL632, respectively (Extra, Figure 17A, Table 16). In the anti-His Western Blot, the intact FGF21-F-Tf form made up 33 %, while the Tf degradation product accounted for 67 %. Based on the 6.7 mg kg⁻¹ SDM calculated in the anti-FGF21 Western blot for the intact form and the Tf degradation product, these percentages corresponded to 2.2 mg kg⁻¹ SDM and 4.5 mg kg⁻¹ SDM (Extra, Figure 17B, Table 16). Based on this calculation definition, VG T1 seeds (VG, event 2-1) with 8.7 mg kg⁻¹ SDM yielded the intact form at 6.4 mg kg⁻¹ SDM, the FGF21 degradation product at 2.3 mg kg⁻¹ SDM, and the Tf degradation product at 4.3 mg kg⁻¹ SDM (Table 16).

In summary, the highest accumulation of intact FGF21-F-Tf fusion protein in T1 seeds reached 6.7 mg kg⁻¹ SDM (SL632, event 1-1) and 6.4 mg kg⁻¹ SDM (VG, event 2-1). These findings are consistent with previous studies, demonstrating that plant breeding increases leaf protein accumulation (Nausch et al., 2012a, 2012b). However, they were ~10-fold lower compared to the necessary accumulation level of >50 mg kg⁻¹ biomass for animal trials (Chapter III.2.4.). Despite this, given the observed increase between T0 and T1 plants, achieving this level might be possible through selective breeding in the T2 or T3 generation. Nevertheless, as the instability of FGF21-F-Tf compromised accumulation in tobacco seeds, it might be more meaningful to design a more stable fusion protein for expression in seeds.

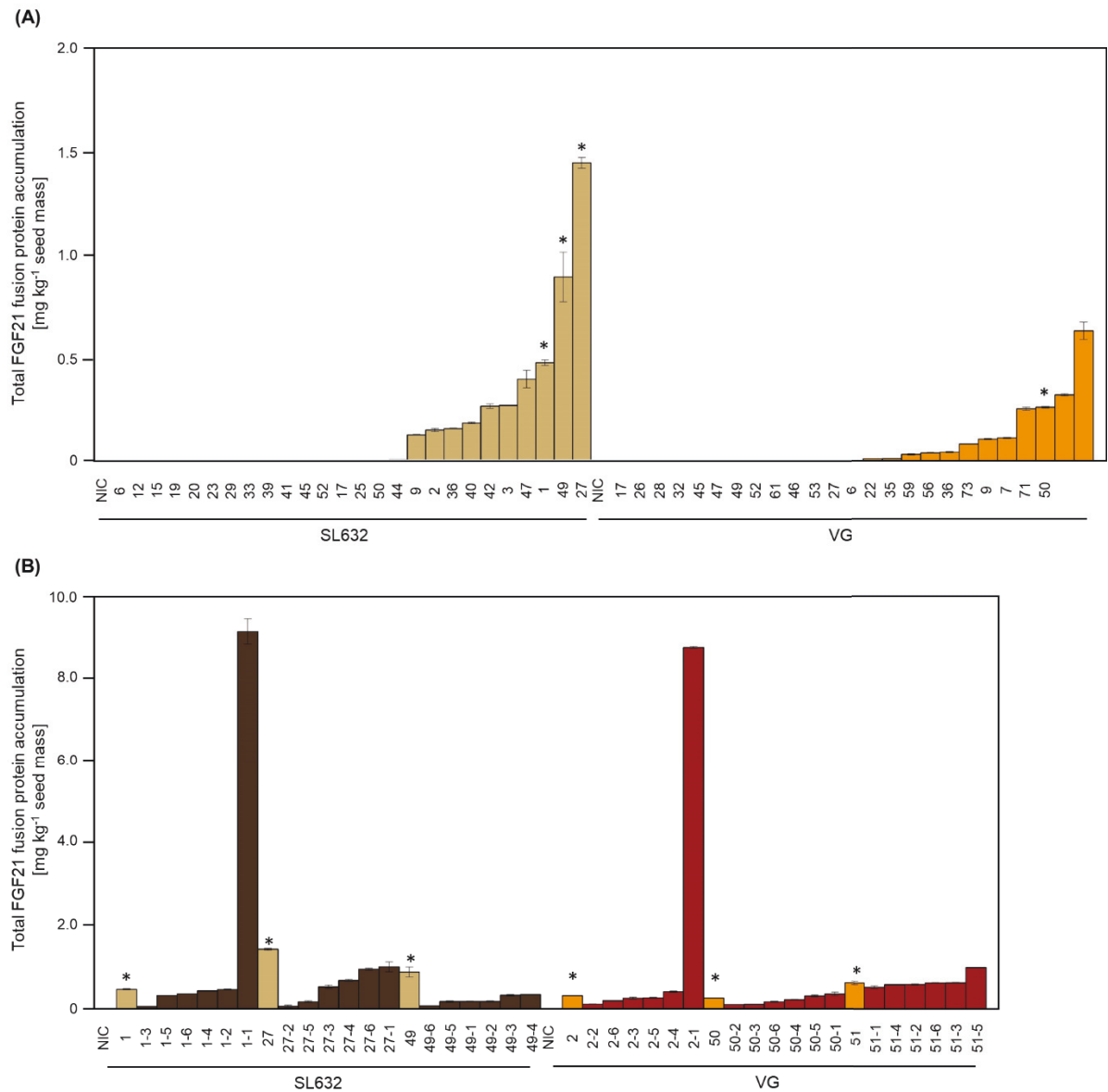


Figure 15. Total FGF21-Transferrin fusion protein yield in seeds of *N. tabacum* SL632 and VG. (A) Total FGF21 fusion protein accumulation in seeds of T0 transformants. **(B)** Total FGF21 fusion protein accumulation in seeds of T1 descendants of 3 selected T0 transformants. Total FGF21 fusion protein accumulation was obtained by FGF21-ELISA data. n=2, biological replicates. NIC – near-isogenic control plants.

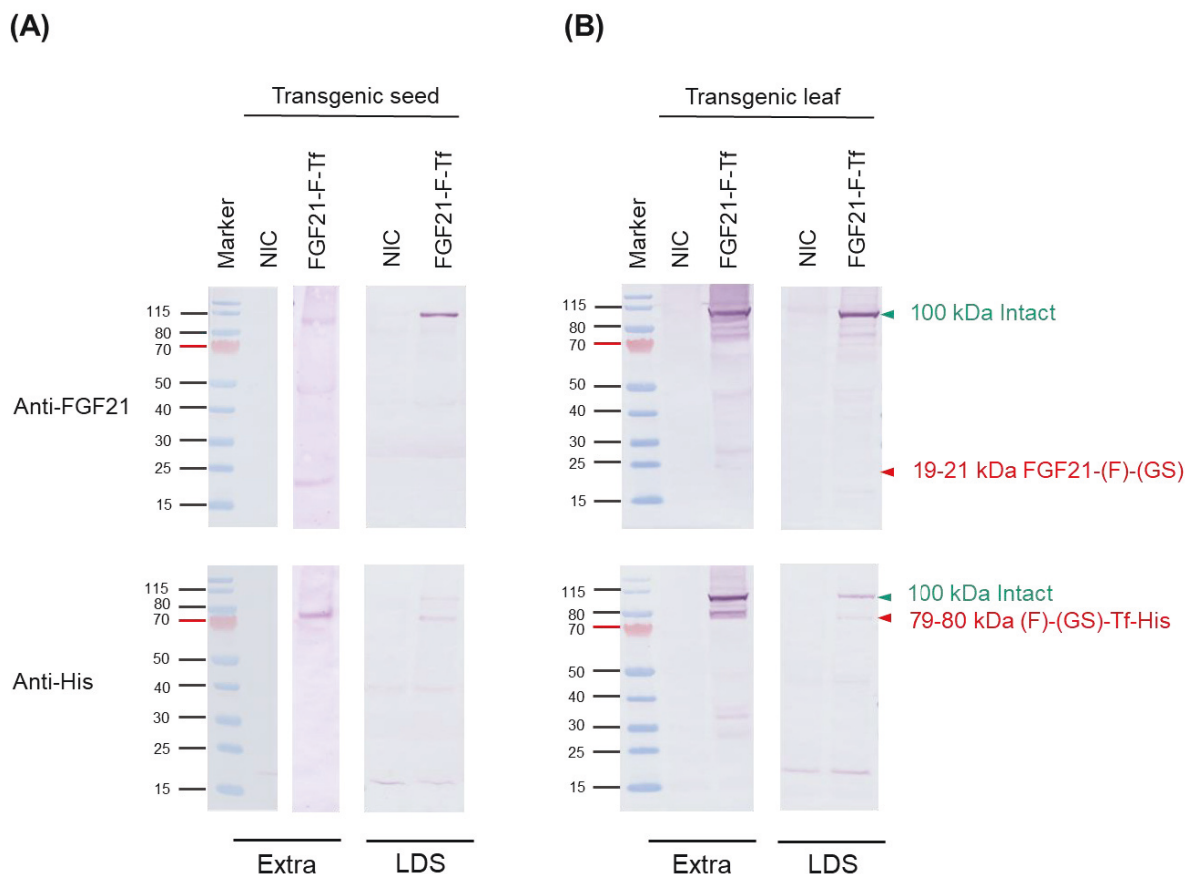


Figure 16. Western blot analysis of FGF21-Transferrin fusion proteins in *N. tabacum* SL632 (event 1-1). Each 100 mg transgenic seed **(A)** and transgenic leaf **(B)** expressing FGF21-F-Tf were extracted in extraction buffer or LDS buffer. Seed and leaf crude extracts containing 100 µg of total soluble protein and 20 µL of total volume were subjected to NuPAGE 4-12 % Bis-Tris protein gels. The electroblotted proteins were probe with primary anti-FGF21/-His₆ rabbit polyclonal antibody (1:5,000) and then secondary goat anti-Rabbit IgG alkaline phosphate (AP)-conjugated antibody (1:5,000). Extra – extraction buffer; LDS – LDS buffer.

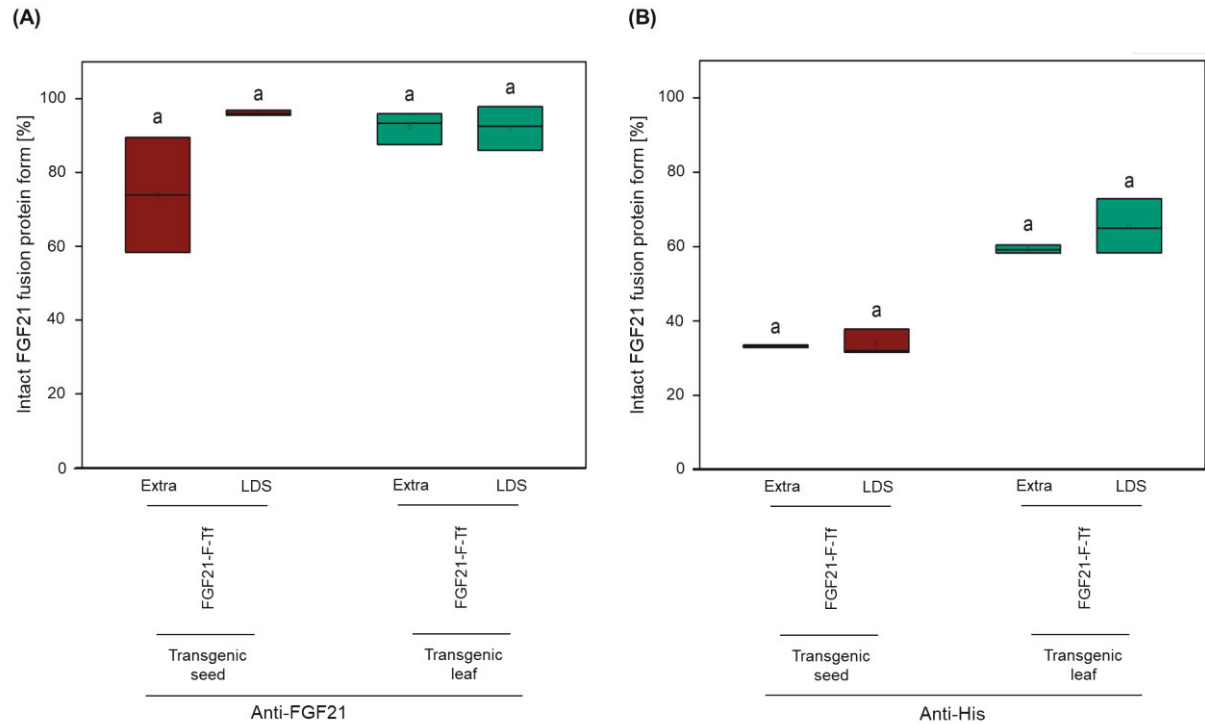


Figure 17. Degree of degradation during extraction of FGF21-Transferrin fusion proteins in *N. tabacum* SL632 (event 1-1). Relative fraction of the FGF21-Tf fusion proteins in plant extracts, detected by **(A)** anti-FGF21 and **(B)** anti-His Western blots. Each 100 mg transgenic seeds and leaves expressing FGF21-F-Tf were extracted in extraction buffer or LDS buffer. Extract samples containing 100 µg of total soluble protein and 20 µL of total volume were subjected to NuPAGE 4-12 % Bis-Tris protein gels, respectively. The electroblotted proteins were probe with primary anti-FGF21/-His₆ rabbit polyclonal antibody (1:5,000) and then secondary goat anti-Rabbit IgG alkaline phosphate (AP)-conjugated antibody (1:5,000). Western blots band intensities were quantified using the AIDA Image Analyzer analysis software. n=2, biological replicates. Extra – extraction buffer; LDS – LDS buffer.

Table 16. FGF21 accumulation level of FGF21-Transferrin fusion constructs in crude extract. Numbers represent mean \pm standard deviation. Total FGF21 fusion protein was determined by the FGF21 ELISA and intact FGF21 fusion protein was obtained by correcting ELISA data by anti-FGF21 and anti-His Western blot analysis and estimation of the relative amount of intact fusion protein and cleaved FGF21.

Plant	Type ^a	Vector	Total FGF21 fusion protein per TSP [mg kg ⁻¹ TSP]	FGF21-ELISA Total FGF21 fusion protein in crude extract [mg kg ⁻¹ biomass]	Anti-FGF21 WB			Anti-His WB			Biological replicates	Biomass [kg m ⁻² a ⁻¹]	Intact FGF21 yield [mg m ⁻² a ⁻¹]		
					Intact FGF21 fusion protein in crude extract [mg kg ⁻¹ biomass]	%	Degraded FGF21 fusion protein in crude extract [mg kg ⁻¹ biomass]	%	Intact FGF21 fusion protein in crude extract [mg kg ⁻¹ biomass]	%	Tf degradation product in crude extract [mg kg ⁻¹ biomass]	%			
<i>N. tabacum</i> SL632	Transgenic seed	p9U	63.6 ± 2.1	9.1 ± 0.3	6.7 ± 0.2	74	2.4 ± 0.1	26	2.2 ± 0.1	33	4.5 ± 0.1	67	2	0.38	2.55
<i>N. tabacum</i> SL632	Transgenic leaf	p9U	68.5 ± 1.8	6.1 ± 0.2	5.6 ± 0.2	92	0.5 ± 0.0	8	3.3 ± 0.1	59	2.3 ± 0.1	41	2	8.19	45.86
<i>N. tabacum</i> VG	Transgenic seed	p9U	84.2 ± 0.3	8.7 ± 0.0	6.4 ± 0.0	74	2.3 ± 0.0	26	2.1 ± 0.0	33	4.3 ± 0.0	67	2	0.24	1.54
<i>N. tabacum</i> VG	Transgenic leaf	p9U	105.5 ± 1.4	2.4 ± 0.0	2.2 ± 0.0	92	0.2 ± 0.0	8	2.0 ± 0.0	92	0.2 ± 0.0	8	2	11.17	24.57

^a number for transgenic plants refers to seeds of the T1 generation and leaves of the T2 generation. WB – Western blot.

III.2.4.2. Transgenic FGF21-F-Tf transformants were events with multiple integrations but showed normal seed viability (multi-copy-events)

The aim in plant breeding and animal studies was to select transgene single integration events. In the case of multi-copy events, the copy number of the progeny might change due to segregation, thereby affecting the expression of the target protein in the progeny. To address this, I conducted T1 segregation analysis on 6 T0 transgenic tobacco progenies, e.g., SL632 (events 1, 27, and 49) and VG (events 2, 50, and 51) (Table 17).

Table 17. T1 segregation analysis of FGF21-F-Tf in *N. tabacum* SL632 and VG. Numbers represent mean \pm standard deviation. n=3, biological replicates.

<i>N. tabacum</i> cultivar	T1 event	Germinating seeds	Km-resistant descendants
SL632	NIC	87 \pm 4 %	0 %
	1	87 \pm 6 %	86 \pm 8 %
	27	96 \pm 4 %	95 \pm 5 %
	49	92 \pm 4 %	93 \pm 7 %
VG	NIC	85 \pm 8 %	0 %
	2	97 \pm 2 %	92 \pm 4 %
	50	96 \pm 2 %	97 \pm 3 %
	51	87 \pm 6 %	94 \pm 4 %

NIC – near-isogenic control plants; Km – kanamycin.

During the T1 segregation analysis, T0 seeds were cultivated for 6 weeks in kanamycin-containing LST medium, utilizing the *nptII* selectable marker gene within the T-DNA for kanamycin resistance. This property was utilized to estimate the number of functional insertions integrated into the genome. After 6 weeks of T1 segregation, null-segregants died in the kanamycin medium. A transgenic rate (kanamycin-resistant descendants) equal to 75 % indicates a single integration event, while a rate exceeding 75 % suggests a multiple integration event.

In the T1 segregation of transgenic FGF21-F-Tf plants, both SL632 events or VG events showed transgenic rates exceeding 75 %, ranging from 86 % to 95 % (SL632, event 1, 27,

and 49) and 92 % to 97 % (VG, event 2, 50 and 51). Additionally, beyond the T1 segregation analysis, I assessed the impact of FGF21-F-Tf on seed viability by examining the germination rate (germinating seeds) of the 6 transgenic tobacco events. These seeds were cultivated for 6 weeks in a kanamycin-free medium (Table 17).

The 6 FGF21-F-Tf T1 events demonstrated higher survival rates compared to the 2 near-isogenic control (NIC) controls with an empty vector. The survival rates ranged from 87 % to 96 % (SL632, event 1, 27, and 49) and 87 % (SL632, event NIC), as well as 87% to 97 % (VG, event 2, 50, and 51) and 85 % (VG, event NIC) (Table 17).

In summary, the analysis revealed that all 6 transgenic tobacco events were multiple integration events, and it was observed that the FGF21-F-Tf protein had no effect on seed viability.

III.2.4.3. FGF21-F-Tf degradation was less in leaves than in seeds and degradation occurred during plant production

Similar to the analysis conducted on seeds (Chapter III.2.4.1.), I also investigated the accumulation of total and intact FGF21-F-Tf in leaves. The use of a constitutive CaMV 35S expression cassette for stable transformation of FGF21-F-Tf suggested its presence not only in seeds but also in leaves. Considering that proteases tend to increase with leaf age, and to understand the impact of leaf age on FGF21-F-Tf fusion protein accumulation, I chose T1 transformants SL632 (event 1-1) and VG (event 2-1) to generate T2 leaves.

I harvested T2 leaves at different ages, including 4 wps (whole leaves), 6 wps (top, middle, and bottom leaves), and 8 wps (top, middle, and bottom leaves). The terms "top", "middle" and "bottom" leaves were defined respectively as developing, fully-developed mature, and senescing leaves (Figure 18).

In SL632 T2 leaves (event 1-1), total FGF21-F-Tf fusion protein accumulation, as measured by FGF21-ELISA, reached up to 0.5 mg kg⁻¹ LFM in whole leaves at 4 wps. This compared to 1.7 mg kg⁻¹ LFM in top leaves, 1.0 mg kg⁻¹ LFM in middle leaves, and 0.3 mg kg⁻¹ LFM in bottom leaves at 6 wps. Furthermore, at 8 wps, the accumulation was 6.1 mg kg⁻¹ LFM in top leaves, 1.3 mg kg⁻¹ LFM in middle leaves, and 0.4 mg kg⁻¹ LFM in bottom leaves (Figure 18).

In VG T2 leaves (event 2-2), similar total FGF21-F-Tf fusion protein accumulation was observed. For instance, at 4 wps, the accumulation was 0.4 mg kg⁻¹ LFM in whole leaves at 4

wps, contrasting with 1.8 mg kg⁻¹ LFM in top leaves, 0.8 mg kg⁻¹ LFM in middle leaves, and 0.2 mg kg⁻¹ LFM in bottom leaves at 6 wps. Furthermore, at 8 wps, the accumulation was 2.4 mg kg⁻¹ LFM in top leaves, 1.1 mg kg⁻¹ LFM in middle leaves, and 0.2 mg kg⁻¹ LFM in bottom leaves (Figure 18).

In the end, the total FGF21-F-Tf fusion protein in 8 wps top leaves accumulated up to 6.1 mg kg⁻¹ LFM (SL632, event 1-1) and 2.4 mg kg⁻¹ LFM (VG, event 2-2) (Figure 18). This indicates a potential reduction in protein expression, an increase in protease activity, or a combination of both during leaf aging, transitioning from young, developing (top) to old, mature/senescing (bottom) leaves.

Next, I determined the protein integrity of the FGF21-F-Tf fusion protein via Western blot analysis. In SL632 T2 leaves (event 1-1, 8 wps top) (Extra, Figure 16FigureB), based on densitometry analysis of the anti-FGF21 Western blots, the intact FGF21-F-Tf form made up 92 % and the FGF21 degradation product made up 8 %, which corresponded to 5.6 mg kg⁻¹ LFM and 0.5 mg kg⁻¹ LFM, respectively (Extra, Figure 17A, Table 16). In contrast, in densitometric analysis of the anti-His Western blots, the intact FGF21-F-Tf form yielded 59 %, and the Tf degradation product accounted for 41 %, with 3.3 mg kg⁻¹ LFM and 2.3 mg kg⁻¹ LFM (Extra, Figure 17B, Table 16). In VG T2 leaves (event 2-1, 8 wps top), the intact form yielded 2.2 mg kg⁻¹ LFM, the FGF21 degradation product amounted to 0.2 mg kg⁻¹ LFM, and the Tf degradation product also measured 0.2 mg kg⁻¹ LFM (Table 16).

III.2.4.4. FGF21-F-Tf degradation occurs *in planta* and not during extraction

Since FGF21-F-Tf degradation occurred in seeds and leaves, I further determined when the FGF21-F-Tf fusion protein was degraded. Protein degradation may occur during plant production or extraction, and to exclude protein degradation during extraction, SL632 (event 1-1) seeds and leaves were extracted directly in LDS buffer instead of extraction buffer (LDS, Figure 17).

The LDS buffer increased the intact FGF21-F-Tf form from 74 % to 96 % in transgenic seeds but not in transgenic leaves, as the intact FGF21-F-Tf form remained at the same level, 92 % (Extra and LDS, Figure 17A). However, in the His-Western blots, LDS buffer and extraction buffer showed similar intact FGF21-F-Tf forms in transgenic seeds and leaves, with 33 % and 34 % (seeds) and 59 % and 65 % (leaves) (Extra and LDS, Figure 17B).

In summary, FGF21-F-Tf degradation occurred *in planta* and was even less in transgenic leaves, according to the anti-FGF21 Western blot with 8 % (leaves) and 26 % (seeds), as well as the anti-His Western blot with 41 % (leaves) and 67 % (seeds). This indicates that protein expression in seeds might not have always been advantageous in terms of product stability and accumulation. Nevertheless, protein degradation of FGF21-F-Tf predominantly occurred during plant production, not the extraction process.

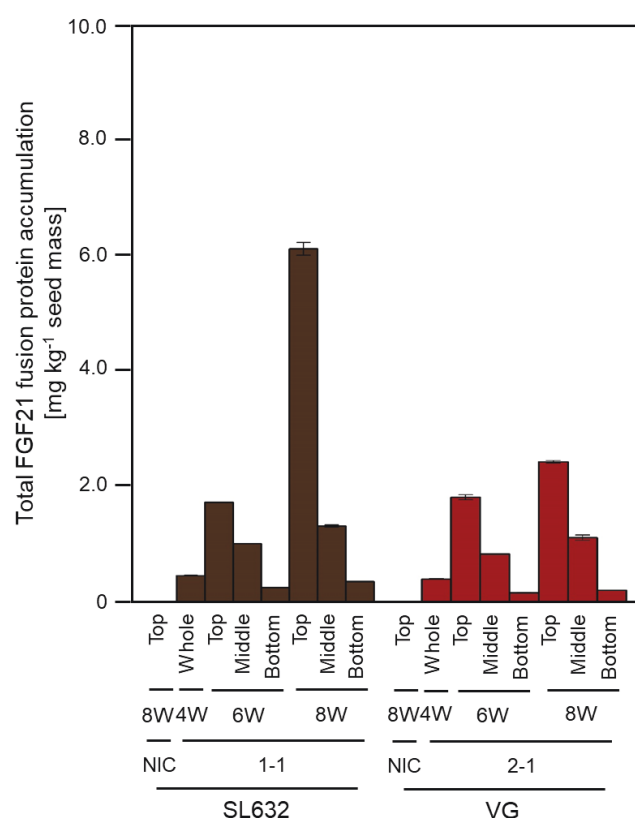


Figure 18. Total FGF21-Transferrin fusion protein yield in leaves of *N. tabacum* SL632 and VG. Total FGF21 fusion protein accumulation in leaves of T2 descendants of one selected T1 transformants. Total FGF21 fusion protein accumulation was obtained by FGF21-ELISA data. n=2, biological replicates. NIC – near-isogenic control plants.

III.3. Transient FGF21-F-Tf expression in leaves of *N. benthamiana*

An unexpectedly high degree of degradation of FGF21-F-Tf was observed in seeds and leaves (Chapter III.2.4.4.). The latter demonstrated that the stability of FGF21-F-Tf in seeds could be optimized in leaves. In this context, leaf constructs could be rapidly tested by transient expression in *N. benthamiana*.

III.3.1. Transient expression of FGF21-F-Tf using magnICON vector system

For high-yield transient expression, I expressed FGF21-F-Tf fusion protein using the replicating viral magnICON vector system (Table 18). For example, the pICH29912, based on crucifer-infecting tobamovirus/turnip vein-clearing virus (cr-TMV/TVCCV) RdRP, and the pICH31160, based on PVX RdRP, with subgenomic promoter and terminator, achieved accumulation levels of up to 6 g kg⁻¹ LFM (Castilho et al., 2014). However, it can only accommodate coding regions of up to 2.0 kb (Chapter I.5.1.2.) (Gleba et al., 2005; Marillonnet et al., 2005), whereas the *fgf21-f-tf* coding region is ~2.8 kb in length. Therefore, I split *fgf21-f-tf* into two fragments (e.g., *fgf21-f* and *tf*) and fused them to the N- and C-terminal parts of the *DnaB intein* coding sequence. Both had an ER retention signal at the C-terminus, resulting in FGF21-F-IntN (pICH29912-FGF21-F-IntN) (Figure 19A) and IntC-Tf (pICH31160-IntC-Tf) constructs (Figure 19B).

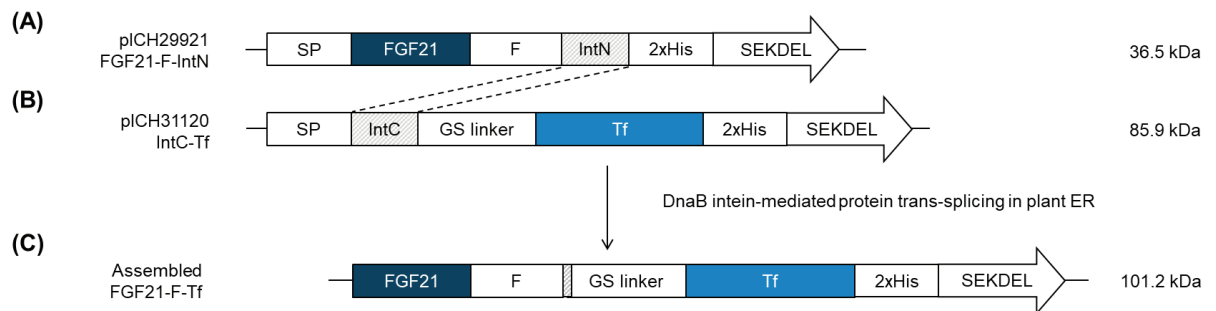


Figure 19. Constructs used for the transient expression of FGF21-Transferrin fusion protein. MagnICON transient expression vectors pICH29921 and pICH31120 containing (A) FGF21-F-IntN and (B) IntC-Tf. (C) Co-expression of FGF21-IntN and IntC-Tf in a cell of *N. benthamiana*. SP – ER-targeting signal peptide from Calretikulin of *Nicotiana plumbaginifolia* (Acc. Z71395), MATQRRANPSSLHLITVFSLLVAVVSG; F – furin cleavage site, RRKRSV; GS linker – flexible linker, (GGGGS)₃; 2xHis – double-His₆ tag; SEKDEL – ER-retention signal; IntN and IntC – DnaB intein fragments.

After transient expression of co-expressed FGF21-IntN and IntC-Tf in a cell of *N. benthamiana*, the two ER-retained FGF21-F-IntN and IntC-Tf proteins underwent post-translational fusion through the intein tag in the plant ER, using intein-mediated trans-splicing mechanisms (Figure 19C) (Evans, JR et al., 2000; Kempe et al., 2009; Sun et al., 2001).

This strategy yielded 2.1 mg FGF21 kg⁻¹ FLM, as measured by FGF21-ELISA (magnICON, FGF21-F-Tf, Table 18). In the Western blot, after co-expression of FGF21-F-IntN and IntC-Tf at 10 dpi, two different fragments were detected: the FGF21-antibody detected a 101 kDa fragment corresponding to the anticipated size of the intact FGF21-F-Tf fusion protein, whereas the His-antibody detected an 86 kDa fragment, corresponding to the size of IntC-Tf or its degradation product (Figure 20).

Based on this, there were two possible explanations: 1) The first possibility is that FGF21-F-IntN accumulated at lower levels than IntC-Tf, so that not all IntC-Tf fused with FGF21-F-IntN, resulting in only excess IntC-Tf being detected. 2) The second possibility is that FGF21-F-IntN and IntC-Tf accumulated at similar levels, fused but then split again into FGF21(-F) and Tf, whereby the FGF21 fragment is rapidly degraded. This might result either from an intrinsic instability of the linker or by cleavage of the linker region by endogenous plant proteases. However, I also expressed the fusion partners FGF21-IntN and IntC-Tf alone and could not detect both of them in the Western blot (Figure 20).

This implies that the fusion partners alone accumulated at substantially lower levels than the fusion proteins, which in turn implies that both fragments were unstable. This assumption makes the second possibility more likely. Hence, FGF21-F-Tf expression as a single fusion protein needs to be achieved.

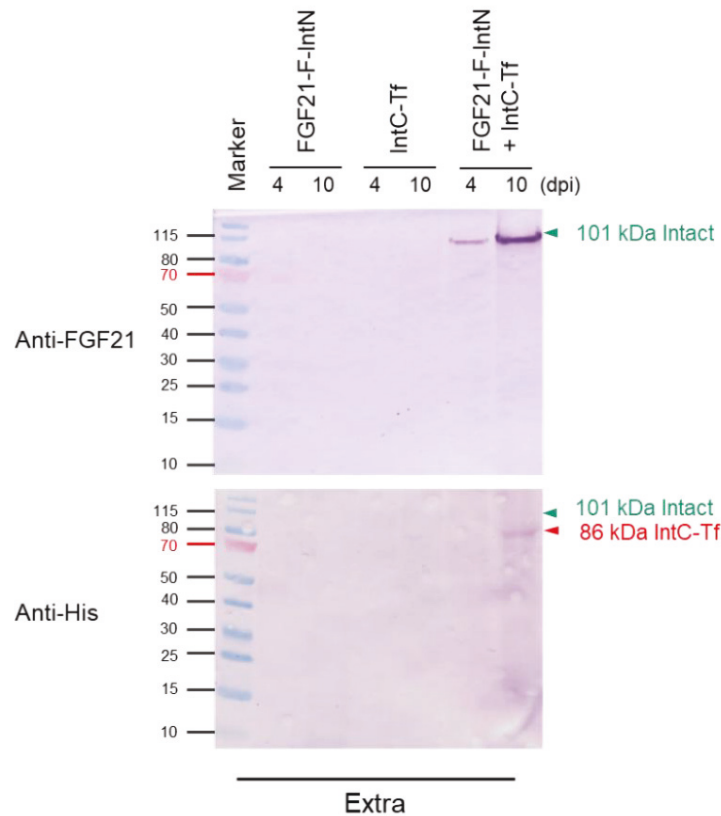


Figure 20. Western blot analysis of modified FGF21-Transferrin fusion proteins produced in *N.benthamiana* using magnICON. MagnICON transient expression: single expression FGF21-F-IntN and IntC-Tf and co-expression of FGF21-F-IntN plus IntC-Tf. Leaf samples were harvest at 4-14 dpi. Each 100 mg leaf materials were extracted in extraction buffer. Leaf samples under extraction buffer containing 100 μ g of total soluble protein and 20 μ L of total volume were subjected to NuPAGE 4-12 % Bis-Tris protein gels, respectively. The electroblotted proteins were probe with primary anti-FGF21/-His₆ rabbit polyclonal antibody (1:5,000) and then secondary goat anti-Rabbit IgG alkaline phosphate (AP)-conjugated antibody (1:5,000). dpi – days post infiltration; Extra – extraction buffer.

III.3.2. Transient expression of FGF21-F-Tf using pTRAc vector system

To obtain the intact fusion protein, FGF21-F-Tf as a single in-frame fusion protein was cloned into a non-viral pTRAc vector, which can contain >8 kbp inserts. Additionally, the pTRAc vector contained a double enhanced CaMV 35S promoter and a polyadenylation signal/terminator from CaMV provided by pPAM (GenBank AY027531) derivative, similar to the expression cassette of p9U vector. To construct the pTRAc vector, I used the sequence from the stable transformation vector p9U-FGF21-F-Tf (Chapter III.2.3.) (Figure 21A).

This approach yielded 1.2 mg kg⁻¹ LFM in the FGF21-ELISA (pTRAc, FGF21-F-Tf, Table 18). However, intact FGF21-F-Tf form with 100 kDa and its degradation product (F-GS-Tf, GS-Tf or Tf) with 79-81 kDa were detected in the anti-FGF21 and the anti-His Western blot (Extra, Figure 22A). Based on densitometry analysis of the anti-FGF21-Western blots, the intact form made up 67 % and the FGF21 degradation product 33 %, which corresponded to 0.8 mg kg⁻¹ leaf LFM and 0.4 mg kg⁻¹ leaf LFM, respectively (Extra, Figure 23A, Table 18). In the anti-His Western blot, the intact form and the Tf degradation product were 68 % and 32 %, and since the 68 % were equal to 0.5 mg kg⁻¹ LFM, the 32 % for Tf degradation product corresponded to 0.3 mg kg⁻¹ LFM (Extra, Figure 23B, Table 18).

To determine protein degradation during extraction similar to that of stable seeds (Chapter III.2.4.1.) and stable leaves (Chapter III.2.4.3.), transiently transformed *N. benthamiana* leaves were directly extracted in LDS buffer, whereas FGF21-F-Tf degradation products with 19-20 kDa (FGF21-F-GS, FGF21-F, or FGF21) and 79-81 kDa (F-GS-Tf, GS-Tf, or Tf) were still present in the anti-FGF21- and anti-His-Western blots (LDS, Figure 22B). Based on densitometric analysis of the FGF21-Western blot, LDS buffer increased the the intact FGF21-F-Tf form from 67 % to 92 % (Extra and LDS, Figure 23A), while in the His-Western blot, LDS buffer and extraction buffer yielded similar amounts of the intact FGF21-F-Tf form with 66 % and 68 % (Extra and LDS, Figure 23B).

Noteworthy, the degree of degradation of transiently transformed leaves with 33 % (Extra, anti-FGF21-Western blot) and 32 % (Extra, anti-His Western blot) degradation products seemed to be higher than that of stable transformed leaves with 8 % (Extra, anti-FGF21-Western blot) and 41 % (Extra, anti-His Western blot) degradation products (Chapter III.2.4.3.).

In summary, the transient expression of FGF21-F-Tf as one protein with the pTRAc vector system confirmed that degradation occurred *in planta* and not during the extraction process. Nevertheless, using the pTRAc vector system made it possible to produce intact FGF21-F-Tf.

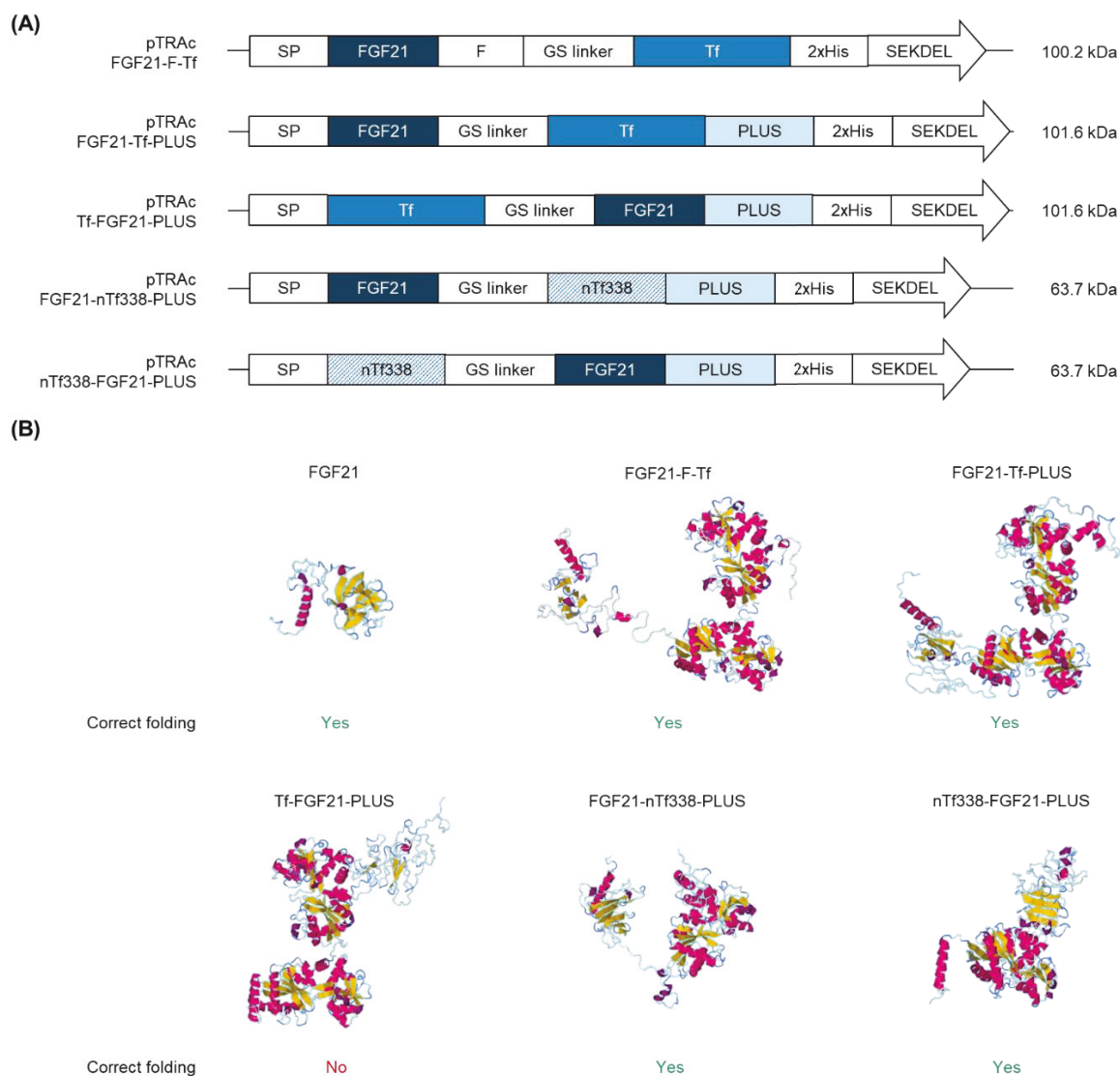


Figure 21. Constructs and models used for the transient expression of FGF21-Transferrin fusion proteins. **(A)** pTRAc transient expression vectors containing FGF21-F-Tf, FGF21-Tf-PLUS, Tf-FGF21-PLUS, FGF21-nTf338-PLUS, and nTf338-FGF21-PLUS in *N. benthamiana*. **(B)** The 3D structures of different FGF21-Tf fusion proteins predicted by submitting the amino acid sequence to the RaptorX software (<http://raptorx.uchicago.edu/>). SP – ER-targeting signal peptide from Calretikulin of *Nicotiana plumbaginifolia* (Acc. Z71395), MATQRRANPSSLHLITVFSLLVAVVSG; F – furin cleavage site, RRKRSV; GS linker – flexible linker, (GGGGS)₃; 2xHis – double-His₆ tag; SEKDEL – ER-retention signal; IntN and IntC – DnaB intein fragments; PLUS – liver-targeting peptide circumsporozoite protein (CSP), position 82-100; nTf338 – N-terminal domain of Tf, position 1-338.

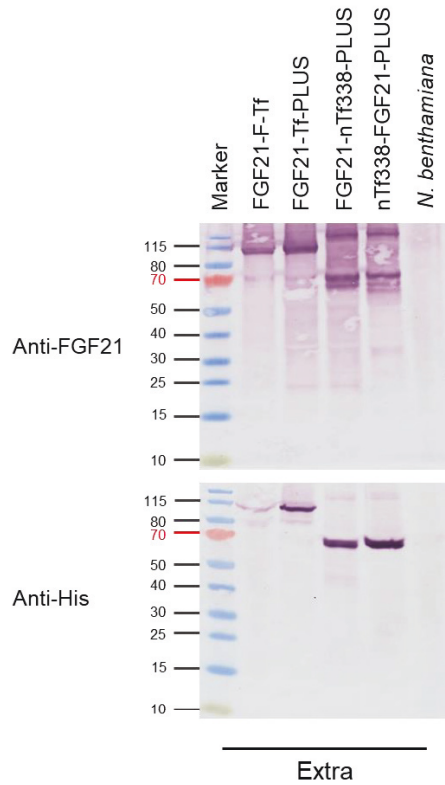
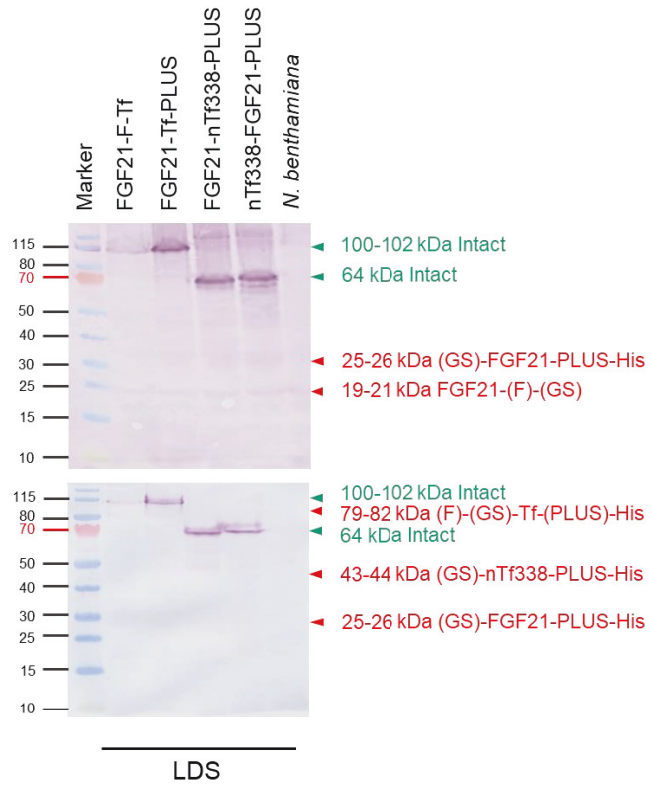
(A)**(B)**

Figure 22. Western blot analysis of modified FGF21-Transferrin fusion proteins produced in *N. benthamiana* using pTRAc systems. pTRAc transient system: single expression of FGF21-F-Tf, FGF21-Tf-PLUS, FGF21-nTf338-PLUS, and nTf338-FGF21-PLUS. Leaf samples were harvest at 5 dpi. Each 100 mg leaf materials were extracted in (A) extraction buffer or (B) LDS buffer. Leaf samples under extraction buffer and LDS buffer containing 100 μ g of total soluble protein and 20 μ L of total volume were subjected to NuPAGE 4-12 % Bis-Tris protein gels, respectively. The electroblotted proteins were probe with primary anti-FGF21/-His₆ rabbit polyclonal antibody (1:5,000) and then secondary goat anti-Rabbit IgG alkaline phosphate (AP)-conjugated antibody (1:5,000). dpi – days post infiltration; Extra – extraction buffer; LDS – LDS buffer.

III.3.3. Optimization of FGF21-F-Tf to improve accumulation and stability

Although previous studies have shown that the furin cleavage site was not recognized in plants, the FGF21-F-Tf fusion protein was degraded in stably and transiently transformed plants (Chapters III 2.4. and III 3.2.), which suggests that there are also furin-like proteases in plants that may cleave the furin cleavage site.

III.3.3.1. FGF21 fused to full-length Tf without furin cleavage site reduced the amount of degradation products

To test this hypothesis, I first investigated whether the degraded fragments were caused by accidental cleavage of the furin site (F) *in planta* and removed the sequence from the fusion protein, named as FGF21-Tf. However, since removing the furin cleavage site might increase the serum half-life of FGF21 when it enters the bloodstream via Tf fusion partner, thus promoting systemic distribution and unintended side effects (Chapter I 2.4.), I added the PLUS peptide to the C-terminus of FGF21-Tf, which mediated exclusive uptake by the liver, resulting in the FGF21-Tf-PLUS construct (Figure 21A) (Chapter III 2.1.).

The PLUS peptide (19 AA, DNEKLRKPKHKKLKQPADG, 2.09 kDa) was derived from the N-end of the circumsporozoite protein (CSP) that coated the malarial sporozoite (*Plasmodium falsiparum*) and targeted the liver for infection by binding to the highly sulfated heparan sulfate proteoglycans found on liver cells (Lu et al., 2014; Ma et al., 2014; Taverner et al., 2020; Yan et al., 2017). Previous studies have also shown that the PLUS fusion proteins had no apparent toxicological effects (Zeng et al., 2017) compared to full-length CSP (Iyori et al., 2013). For FGF21-Tf-PLUS, I identified potential steric hindrance prior to cloning and analyzed its structure *in silico* by submitting the amino acid sequence to Raptor X software. After comparing with native FGF21, I did not observe any problems based on alpha helix and beta-sheet (Figure 21B).

The resulting FGF21-Tf-PLUS construct accumulated at 1.6 mg kg⁻¹ LFM (intact form) in transiently transformed *N. benthamiana* compared to 0.8 mg kg⁻¹ LFM (intact form) for FGF21-F-Tf construct (Table 18). The level of FGF21 degradation products was reduced from 33 % to 25 % (anti-FGF21 Western blot), whereas the level of Tf degradation products was reduced 32 % to 19 % (anti-His Western blot) (Extra, Figure 22A, Extra, Figure 23).

Next, to determine an optimal fusion orientation for the maximal activity of FGF21, I also considered changing the order of FGF21 and full-length Tf (named as Tf-FGF21-PLUS construct) (Figure 21A). However, Raptor X software analysis showed that Tf-FGF21-PLUS lost the alpha helix and beta-sheet structure of FGF21, so I did not clone this construct (Figure 21B).

In summary, the removal of the furin cleavage site increased accumulation levels and improved the degradation of the FGF21-Tf fusion protein.

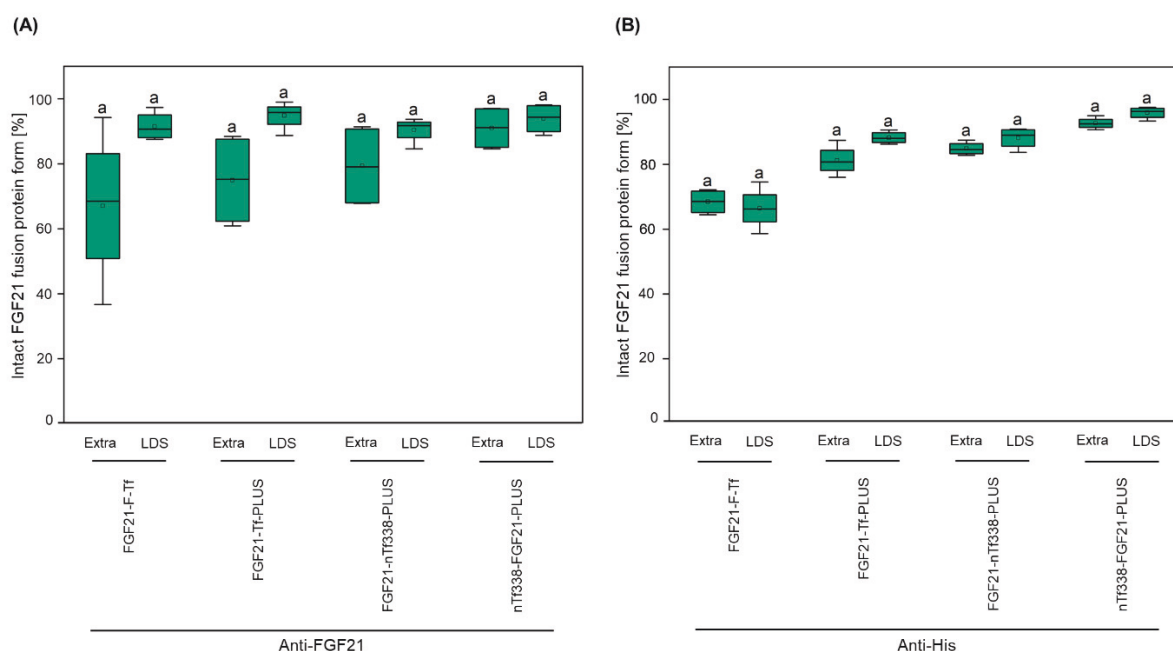


Figure 23. Degree of degradation during extraction of optimized FGF21-Transferrin fusion proteins in *N. benthamiana*. Relative fraction of the FGF21-Tf fusion proteins in leaf crude extracts, detected by (A) anti-FGF21 and (B) anti-His Western blots in leaf crude extract. Transient leaves expressing FGF21-F-Tf, FGF21-Tf-PLUS, FGF21-nTf338-PLUS, and nTf338-FGF21-PLUS were extracted in extraction buffer or LDS buffer. Extract samples containing 100 µg of total soluble protein and 20 µL of total volume were subjected to NuPAGE 4-12 % Bis-Tris protein gels, respectively. The electroblotted proteins were probe with primary anti-FGF21/-His₆ rabbit polyclonal antibody (1:5,000) and then secondary goat anti-Rabbit IgG alkaline phosphate (AP)-conjugated antibody (1:5,000). n=3, biological replicates. Extra – extraction buffer; LDS – LDS buffer.

III.3.3.2. FGF21 fused to the C-terminal domain of nTf338 without furin cleavage site had substantial impact

I also reasoned that the large size of the fusion protein of >100 kDa might limit the accumulation, since in previous studies recombinant proteins with a size of 20-50 kDa consistently showed higher accumulation levels than targets with a size of 50-100 kDa (University of Rostock, unpublished data). In addition, other studies have shown that fusion proteins produced in transgenic tobacco provide unnecessary protease cleavage sites, which may limit the accumulation (Phan et al., 2014).

In this context, a previous study showed that the N-terminal half molecule of Tf (nTf, position 1-338 from 679 AA of the mature protein), when expressed in *P. pastoris*, was correctly folded and retained the ability to bind iron (Mason et al., 1996). Further studies showed that the decisive TfR binding motif was located in this N-terminal part of Tf (Eckenroth et al., 2011; Steere et al., 2012), demonstrating that the truncated nTf fusion proteins were efficiently taken up by cells through TfR-mediated endocytosis (Qi et al., 2018).

Since nTf338 also mediated TfR binding (Mason et al., 1996) (Chapter I.3.), I truncated the full-length Tf (679 AA) to the N-terminal 338 AA (nTf338, position 1-338 from 679 AA), resulting in FGF21-nTf3338-PLUS (Figure 21A). Replacing full-length Tf (669 AA) with the truncated nTf (338 AA) reduced the size of the fusion protein by 38 kDa, from 103 kDa to 65 kDa for the unprocessed protein, and from 100 kDa to 62 kDa for the ER retrieved variant.

Moreover, since another study, in which FGF21 has been fused to the Fc domain of an IgG1 antibody either at the N- or C-terminus, yielding Fc-FGF21 and FGF21-Fc, and FGF21 was only active when Fc was fused to the N-terminus of FGF21 (Fc-FGF21) (Hecht et al., 2012) (Chapter I.2.1.), I therefore investigated the fusion orientation of nTf338 and changed the order of FGF21 and nTf338, resulting in the nTf3338-FGF21-PLUS construct (Figure 21A).

Additionally, I analyzed the alpha helix and beta-sheet structures of two truncated FGF21-Tf fusion proteins (FGF21-nTf3338-PLUS and nTf3338-FGF21-PLUS) *in silico* by the Raptor X software. After comparing with native FGF21, I observed that their alpha helix and beta-sheet structures were no problem (Figure 21B).

Unlike expected, FGF21-nTf338-PLUS did not affect the accumulation of the intact fusion protein, but reduced the degradation products to 21 % (anti-FGF21 Western blot) and 15 %

(anti-His Western blot). In contrast, nTf338-FGF21-PLUS reduced degradation to 9 % (anti-FGF21 Western blot) and 7 % (anti-His Western blot) and increased intact nTf338-FGF21 accumulation level up to 2.1 mg kg⁻¹ LFM (Extra, Figure 22A, Extra, Figure 23, Table 18). In transiently transformed *N. benthamiana* leaves of nTf338-FGF21-PLUS, even up to 5.8 mg kg⁻¹ LFM was obtained when older leaves with symptoms of senescence were excluded, and only green leaves were used for processing (Table 21).

In summary, FGF21 fused to the C-terminus of nTf338 (nTf338-FGF21-PLUS) could improve the accumulation of the intact fusion protein and reduce degradation product.

Table 18. FGF21 accumulation level of FGF21-Transferrin fusion constructs in crude extract. Numbers represent mean \pm standard deviation. Total FGF21 fusion protein was determined by the FGF21 ELISA and intact FGF21 fusion protein was obtained by correcting ELISA data by anti-FGF21 and anti-His Western blot analysis and estimation of the relative amount of intact fusion protein and cleaved FGF21.

Plant	Type ^a	Vector	Total FGF21 fusion protein per TSP [mg kg ⁻¹ TSP]	FGF21-ELISA Total FGF21 fusion protein in crude extract [mg kg ⁻¹ biomass]	Anti-FGF21 WB				Anti-His WB				Biological replicates	Biomass [kg m ⁻² a ⁻¹]	Intact FGF21 yield [mg m ⁻² a ⁻¹]
					Intact FGF21 fusion protein in crude extract [mg kg ⁻¹ biomass]	%	Degraded FGF21 fusion protein in crude extract [mg kg ⁻¹ biomass]	%	Intact FGF21 fusion protein in crude extract [mg kg ⁻¹ biomass]	%	Tf degradation product in crude extract [mg kg ⁻¹ biomass]	%			
<i>N. tabacum</i> SL632	Transgenic seed	p9U FGF21-F-Tf	63.6 \pm 2.1	9.1 \pm 0.3	6.7 \pm 0.2	74	2.4 \pm 0.1	26	2.2 \pm 0.1	33	4.5 \pm 0.1	67	2	0.38	2.55
<i>N. tabacum</i> SL632	Transgenic leaf	p9U FGF21-F-Tf	68.5 \pm 1.8	6.1 \pm 0.2	5.6 \pm 0.2	92	0.5 \pm 0.0	8	3.3 \pm 0.1	59	2.3 \pm 0.1	41	2	8.19	45.86
<i>N. tabacum</i> VG	Transgenic seed	p9U FGF21-F-Tf	84.2 \pm 0.3	8.7 \pm 0.0	6.4 \pm 0.0	74	2.3 \pm 0.0	26	2.1 \pm 0.0	33	4.3 \pm 0.0	67	2	0.24	1.54
<i>N. tabacum</i> VG	Transgenic leaf	p9U FGF21-F-Tf	105.5 \pm 1.4	2.4 \pm 0.0	2.2 \pm 0.0	92	0.2 \pm 0.0	8	2.0 \pm 0.0	92	0.2 \pm 0.0	8	2	11.17	24.57
<i>N. benthamiana</i>	Transient leaf	MagnICON	115.7 \pm 1.7	2.1 \pm 0.0	2.1 \pm 0.0	100	0.0 \pm 0.0	0	0.0 \pm 0.0	0	2.1 \pm 0.0	100	2	11.94	25.07
		pTRAc	151.6 \pm 51.4	1.2 \pm 0.3	0.8 \pm 0.2	67	0.4 \pm 0.1	33	0.5 \pm 0.1	68	0.3 \pm 0.1	32	3	11.94	9.55
		pTRAc	446.9 \pm 106.6	2.1 \pm 0.7	1.6 \pm 0.5	75	0.5 \pm 0.2	25	1.3 \pm 0.4	81	0.3 \pm 0.1	19	3	11.94	19.10
		pTRAc	427.9 \pm 132.2	2.0 \pm 0.6	1.6 \pm 0.5	79	0.4 \pm 0.1	21	1.3 \pm 0.4	85	0.2 \pm 0.1	15	3	11.94	19.10
		pTRAc	361.1 \pm 136.3	2.3 \pm 0.6	2.1 \pm 0.5	91	0.2 \pm 0.1	9	1.9 \pm 0.5	93	0.1 \pm 0.0	7	3	11.94	25.07

III.4. Purification of nTf338-FGF21-PLUS for proof-of-concept bioavailability and bioactivity studies

Recombinant proteins, such as PD, partially purified from tobacco leaves via His-tag/IMAC, have been successfully used in oral administration trials with animals like mice, demonstrating that the impurities caused no significant side effects (Choi et al., 2014). Since the accumulation levels of the modified FGF21-Tf fusion protein obtained in transiently and stably transformed plants were insufficient for animal feeding studies, I partially purified modified FGF21-Tf fusion proteins from transient leaves for use in animal feeding studies.

III.4.1. nTf338-FGF21-PLUS was stable in crude extract for 6 h at 20 °C

In terms of FGF21 bioactivity, it is crucial for the modified FGF21-Tf fusion proteins to remain intact during extraction. Since the four FGF21-Tf fusion proteins (FGF21-F-Tf, FGF21-Tf-PLUS, FGF21-nTf338-PLUS, and nTf338-FGF21-PLUS) seemed to be instable in leaf crude extracts (Chapter III.3.), I determined whether they could be purified at large-scale without substantial degradation via DoE in a D-optimal response surface design with 36 runs and a fraction of design space (FDS) of 1.0, if the effect-to-noise ratio is >1.7 , i.e., an effect can be detected with a 95 % likelihood, if the effect size is >1.7 -fold compared to the standard deviation (Table 19).

Leaf crude extracts of four FGF21-Tf fusion proteins were incubated at different temperatures (4 °C and 20 °C) and times (0 h, 24 h, 48 h, and 72 h) and the accumulation levels of the four FGF21-Tf fusion proteins were analyzed by the FGF21-ELISA.

For the accumulation of the four FGF21-Tf fusion proteins, a significant reduced cubic model with a non-significant Lack of Fit and a $R^2 = 0.86$, an adjusted $R^2 = 0.85$, and a predicted $R^2 = 0.82$ (Table 19), indicating that the model could fit the measured accumulation data and predict the impact of the different factors on it. In this model, the temperature (factor A), time (factor B), their interaction (AB), and B^2 were found to be significant.

Table 19. Characterization of the D-optimal design model for relative stability in crude leaf extracts of four FGF21-Tf fusion proteins incubated at different temperatures and times. Factors with F-value and p-value. Significance was calculated by one-way ANOVA (Bonferroni) with $p < 0.05$.

Design Summary

File Version	11.0.0.3			
Study Type	Response Surface		Subtype	Randomized
Design Type	D-optimal	Point Exchange	Runs	36
Design Model	Reduced Cubic		Block	No Blocks

Relative stability [%]

Source	df	F-value	p-value	
Model	4	48.66	<0.0001	significant
A-Temperature	1	76.02	<0.0001	
B-Time	1	94.78	<0.0001	
AB	1	15.68	0.0004	
B²	1	6.22	0.0181	
Lack of Fit	24			not significant
R²	0.8626			
Adjusted R²	0.8449			
Predicted R²	0.8186			

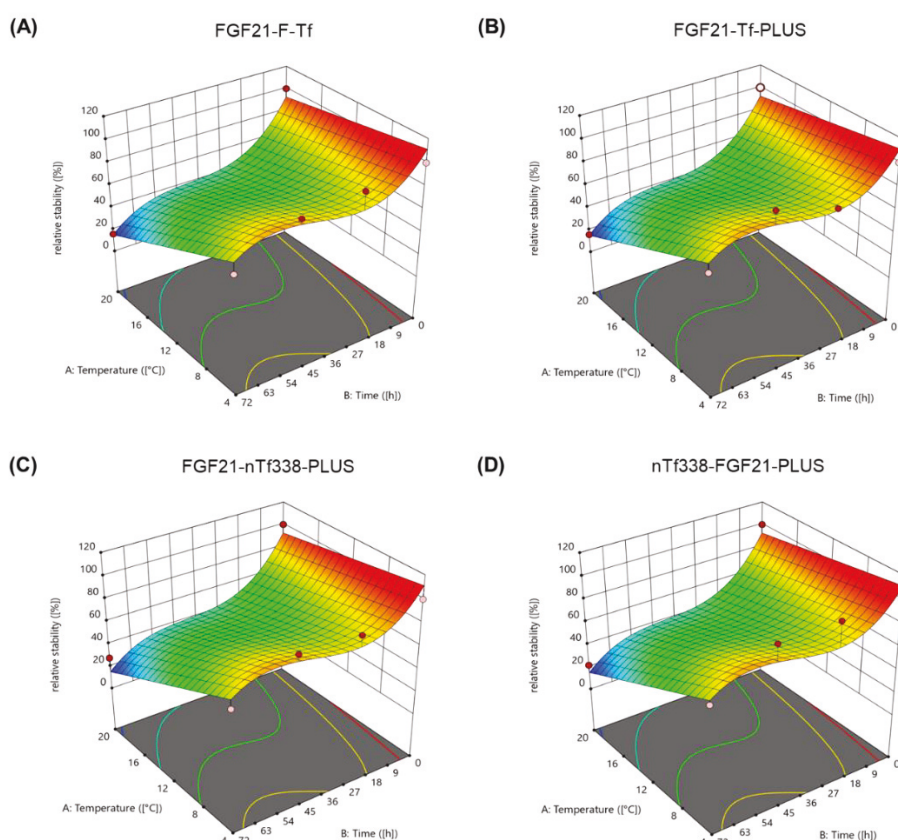


Figure 24. Stability testing by the D-optimal design of four FGF21-Transferrin fusion proteins. Four fusion proteins (A) FGF21-F-Tf, (B) FGF21-Tf-PLUS, (C) FGF21-nTf338-PLUS, and (D) nTf338-FGF21-PLUS. Leaf samples were harvested at 5 dpi. Each 10 g leaf materials were extracted in 30 mL of extraction buffer at a ratio of 1:3. Leaf crude extracts were under incubation temperature at 4 °C and 20 °C and time at 0 h, 24 h, 48 h, and 72 h. The accumulation levels of the four FGF21-Transferrin fusion proteins were analyzed by FGF21-ELISA. The stability of all fusion proteins was analyzed in a D-optimal design by submitting relative stability, incubation temperature, and incubation time to the DoE software. dpi – days post infiltration; DoE – design of experiments.

At 4 °C, only ~0-20 % of the four FGF21-Tf fusion proteins degraded within 24 h, which increased to ~30-35 % degradation products within 72 h. In contrast, at 20 °C, the four FGF21-Tf fusion proteins degraded more rapidly with ~30-75 % degradation products within 24 h and ~70-85 % degradation products within 72 h. However, FGF21-F-Tf and FGF21-Tf-PLUS degraded more rapidly within 24 h at 20 °C with ~65-75 % degradation products compared to ~30-70 % for FGF21-nTf338-PLUS and nTf338-FGF21-PLUS (Figure 24).

Due to the higher stability of two truncated FGF21-Tf fusion proteins FGF21-nTf338-PLUS and nTf338-FGF21-PLUS in leaf crude extracts, I focused on them and performed further stability testing at higher temporal resolution by anti-FGF21 and anti-His Western blots, e.g., at 0 h, 1 h, 3 h, 6 h, 24 h, 48 h, and 72 h at 4 °C and 20 °C, respectively, and also determined the fraction of intact fusion protein and FGF21/Tf degradation products.

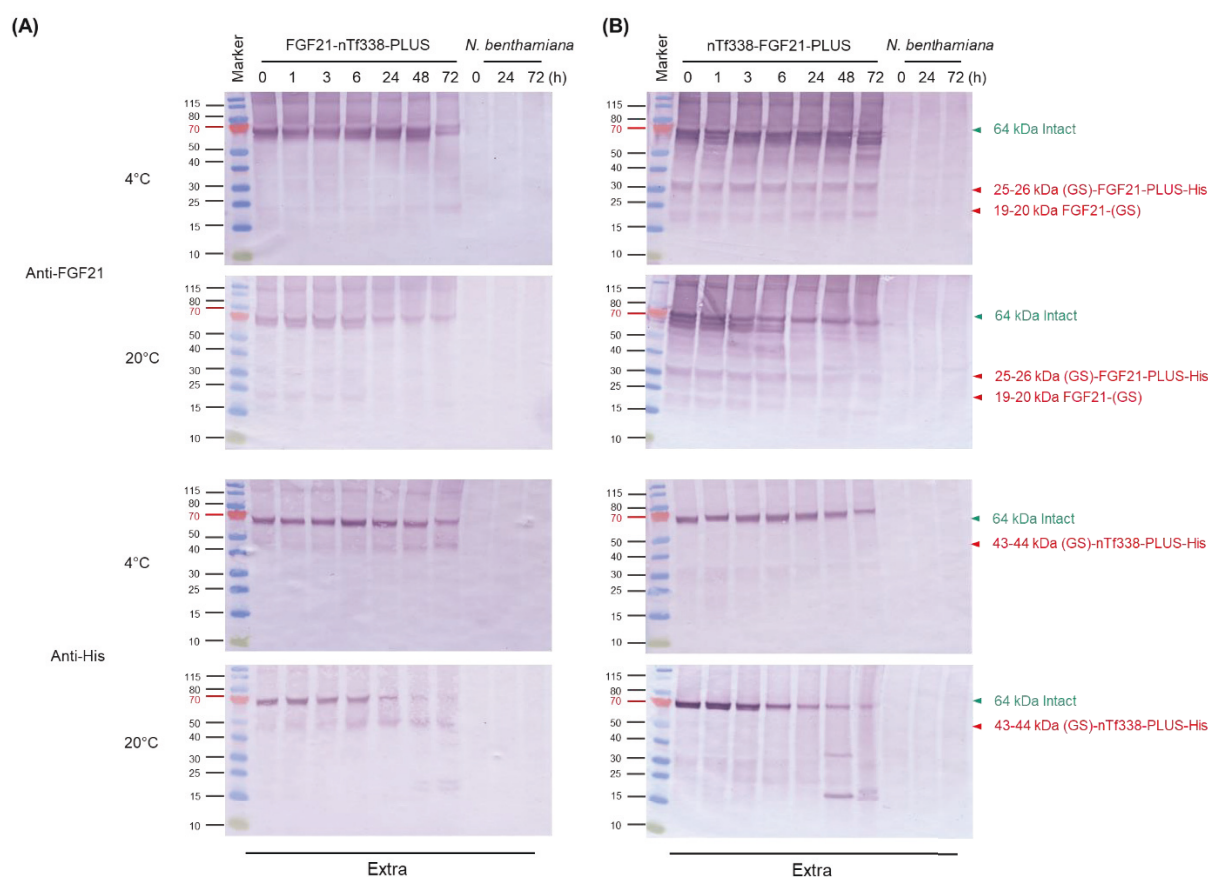


Figure 25. Stability testing by Western blot analysis of two truncated FGF21-Tf fusion proteins. (A) FGF21-nTf338-PLUS and (B) nTf338-FGF21-PLUS were conducted the stability test. Leaf samples were harvested at 5 dpi. Each 10 g leaf materials were extracted in 30 mL of extraction buffer at a ratio of 1:3. Leaf crude extracts were under incubation temperature at 4 °C and 20 °C and time at 0 h, 1 h, 3 h, 6 h, 24 h, 48 h, and 72 h. Leaf crude extracts containing 100 µg of total soluble protein and 20 µL of total volume were subjected to NuPAGE 4-12 % Bis-Tris protein gels, respectively. The electroblotted proteins were probe with primary anti-FGF21/-His₆ rabbit polyclonal antibody (1:5,000) and then secondary goat anti-Rabbit IgG alkaline phosphate (AP)-conjugated antibody (1:5,000). dpi – days post infiltration; Extra – extraction buffer.

At 0 h, both for FGF21-nTf338-PLUS and nTf338-FGF21-PLUS degradation products were not detected in the anti-FGF21 and ant-His-Western blot with a size of 19-20 kDa for FGF21-(GS), 25-26 kDa for (GS)-FGF21-PLUS-His, and 43-44 kDa for (GS)-nTf338-PLUS-His (Figure 25).

In the anti-FGF21 Western blots, at 4 °C, the intact forms of both FGF21-nTf338-PLUS and nTf338-FGF21-PLUS remained constant within 48 h at 100 %, but within 72 h, the degradation products of FGF21-nTf338-PLUS (e.g., 19-20 kDa for FGF21-(GS)) increased to ~40 %, whereas the amount of degradation products of nTf338-FGF21-PLUS (e.g., 25-26 kDa for (GS)-FGF21-PLUS-His) remained at 0 %. At 20 °C, FGF21-nTf338-PLUS remained constant at 100 % within 6 h, but degradation products increased to ~20 % at 24 h, ~25 % at

48 h, and ~40 % at 72 h. However, nTf338-FGF21-PLUS degradation products increased to ~5 % at 1 h, ~20 % at 3 h, ~30 % at 6 h, ~50 % at 24 h, ~40 % at 48 h and ~50 % at 72 h (Figure 26A).

In the anti-His Western blots, at 4 °C, FGF21-nTf338-PLUS was degraded by ~10 % within 48 h (e.g., 43-44 kDa (GS)-nTf338-PLUS-His degradation product), while nTf338-FGF21-PLUS was not degraded (e.g., 25-26 kDa (GS)-FGF21-PLUS-His degradation product), but both were degraded by ~20 % within 72 h. At 20 °C, FGF21-nTf338-PLUS was not degraded at 6 h, but degraded by ~30 % within 24 h, ~50 % within 48 h, and ~50 % within 72 h. However, nTf338-FGF21-PLUS was degraded by ~30 % within 6 h, ~50 % within 24 h, ~50% within 48 h and ~60 % within 72 h (Figure 26B).

In summary, nTf338-FGF21-PLUS was less stable in the crude leaf extract compared to FGF21-nTf338-PLUS. Hence, for large-scale purification without substantial degradation, leaf crude extracts of FGF21-nTf338-PLUS and nTf338-FGF21-PLUS need to be performed either within 48 h at 4 °C or within 6 h at 20 °C.

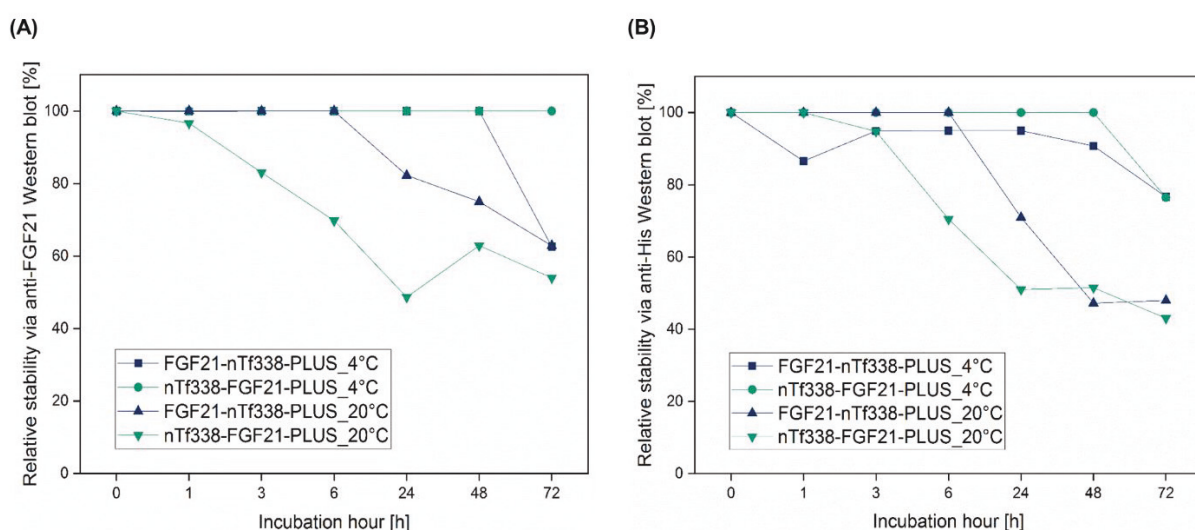


Figure 26. Degree of relative stability during stability testing of two truncated FGF21-Tf fusion proteins. Relative fraction of the two truncated FGF21-Tf fusion proteins in plant extracts, detected by (A) anti-FGF21 and (B) anti-His Western blots. Leaf crude extract samples containing 100 µg of total soluble protein were subjected to NuPAGE 4-12 % Bis-Tris protein gels. The electroblotted proteins were probe with primary anti-FGF21/-His₆ rabbit polyclonal antibody (1:5,000) and then secondary goat anti-Rabbit IgG alkaline phosphatase (AP)-conjugated antibody (1:5,000). Western blots band intensities were quantified using the AIDA Image Analyzer analysis software. n=1, biological replicate.

III.4.2. Large-scale purification of nTf338-FGF21-PLUS was impacted by substantial loss during depth filtrations

Taking into account the previous study, which demonstrated that the C-terminal of FGF21 is crucial for receptor binding to FGF21 and should not be blocked by a fusion partner (Hecht et al., 2012) (Chapter I.2.1.). In this study, I selected nTf338-FGF21-PLUS for large-scale purification.

III.4.2.1 Intracellular expression of nTf338-F-PLUS required tissue homogenization and clarification to remove solid particles that result from the cell lysis

I purified transiently expressed nTf338-FGF21-PLUS from leaves of *N. benthamiana*. Due to the instability of nTf338-FGF21-PLUS in the crude leaf extract (Chapter III.4.1.), the extract was kept at 4 °C during extraction and purification.

Since nTf338-FGF21-PLUS accumulated in the ER of the plant cells, the plant tissue needed to be homogenized for cell lysis, using a blade-based homogenizer. However, tissue homogenization and cell lysis also generated large amounts of insoluble, dispersed particles in the crude extract, which are measured as turbidimetric turbidity units (NTU). These particles are incompatible with chromatography-based purification methods like IMAC for His-tagged proteins, and typical concentrations of 10,000-40,000 NTU in the crude extracts need to be reduced down to 10 NTU (Carvalho et al., 2019) (Chapter I.5.2.). Therefore, I used a previously reported protocol based on lab-scale equipment (Menzel et al., 2016; Opdensteinen et al., 2021b; Opdensteinen et al., 2021a).

However, for large-scale removal of the insoluble particles from the nTf338-FGF21-PLUS containing leaf extracts, I compared lab-scale with large-scale clarification and filtration equipment: 1) Pre-filtration via miracloth filter (22-25 µm) (lab-scale) and bag filter (1-800 µm) (large-scale), 2) Centrifugation via ultracentrifugation (16.000 × g, for 20 min at 4 °C) (lab-scale) and depth filtration via depth filter (6-15 µm) (large-scale), and 3) Microfiltration via sterile filter (0.45 µm and 0.22 µm) (lab-scale) and bottle-top filter (0.22 µm) (large-scale). In terms of particle removal efficiency using crude extracts from WT *N. benthamiana* plants, which had NTU values in the crude extract range from 10,120 to 14,240 NTU (average $11,840.0 \pm 1,684.0$ NTU) (Table 20).

Table 20. Removal of insoluble particles with different filtration methods. The contamination with solid particles was measured via nephelometric turbidity units (NTU) and the relative particle removal calculated as %. Numbers represent mean \pm standard deviation. n=1-3, biological replicates.

Process step 1	Particle loss [%]	Process step 2	Particle loss [%]	Process step 3	Particle loss [%]
Bag filter	33.2 \pm 3.0	Depth filter	99.6 \pm 0.4	Bottle-top filter	24.0 \pm 1.4
Miracloth filter	33.3 \pm 2.3	Ultracentrifugation	100.0 \pm 0.0	Sterile capsule	33.0 \pm 16.3

For the pre-filtration, the particle removal efficiency of the miracloth filter and bag filter was similar moderate with \sim 33 %. When comparing centrifugation and depth filtration, both methods removed almost all solid particles with an efficiency of \sim 100 %. For the microfiltration, the sterile filter outperformed the bottle-top filter, with particle removal of 33 % compared to 24 % (Table 20). This indicates that centrifugation and depth filtration are key to removing most dispersed particles, and sterile filtration might be superior to filtration via bottle-top filter.

Based on this, the preferred set-up for large-scale purification of nTf338-FGF21-PLUS is as follows: Bag filter, depth filter and sterile filter. In a validation experiment with WT *N. benthamiana* plants, this set-up reduced the initial turbidity in the crude extract by from 10,986.7 NTU to 2.3 NTU (bag filter, depth filter, and sterile filter), which is sufficient for chromatography-based IMAC purification.

III.4.2.2. nTf3338-F-PLUS recovery seemed to be limited by binding to filters

For nTf338-FGF21-PLUS purification, I used IMAC because the C-terminal nTf338-FGF21-PLUS contained a double His₆ tag (Figure 21A). During filtration and purification, nTf338-FGF21-PLUS yield, recovery, and purity were calculated by measuring TSP and FGF21 concentrations in the individual filtration and purification fractions using Bradford and FGF21-ELISA (Table 21).

Although most process steps had step recoveries $>$ 75 % for nTf338-FGF21-PLUS, depth filtration yielded only a recovery \sim 5 %. This indicated that nTf338-FGF21-PLUS may bind to filters containing diatomaceous earth (DE). Therefore, the ultracentrifugation was tested as well and yielded a recovery \sim 95 %, which increased the overall recovery of nTf338-FGF21-PLUS from 2 % to 32 % and might therefore be preferred, even though the scalability is not as high as for depth filtration (Buyel et al., 2015a; Roush and Lu, 2008).

Table 21. Comparison of purification process performance for nTF338-FGF21-PLUS extracted from non-senescent, transiently transformed *N. benthamiana* leaves, using filtration or centrifugation as the major clarification step. Yield and purity were determined by FGF21-ELISA and Bradford assay.

Method	Depth filtration ^a					Ultracentrifugation ^b				
	Overall recovery	Step recovery	Loss per step	Yield	Purity	Overall recovery	Step recovery	Loss per step	Yield	Purity
	[%]	[%]	[%]	$\mu\text{g kg}^{-1}$ [biomass]	[%]	[%]	[%]	[%]	$\mu\text{g kg}^{-1}$ [biomass]	[%]
Homogenate	100.00	-	-	2,930.1 \pm 628.9	0.05 \pm 0.02	100.00	-	-	5,779.0 \pm 119.6	0.05 \pm 0.00
Bag filtrate	76.3 \pm 0.9	76.3 \pm 0.9	23.7 \pm 7.4	2,234.5 \pm 460.9	0.06 \pm 0.03	55.5 \pm 2.9	55.5 \pm 2.9	44.5 \pm 2.9	3,206.7 \pm 236.4	0.04 \pm 0.00
Clarification (centrifugation or filtration)	4.2 \pm 2.0	5.5 \pm 2.6	94.5 \pm 2.6	121.3 \pm 52.2	0.01 \pm 0.00	52.5 \pm 2.4	94.7 \pm 0.7	5.3 \pm 0.7	3,035.3 \pm 200.5	0.03 \pm 0.00
Sterile filtrate	3.6 \pm 1.7	85.5 \pm 4.9	14.5 \pm 4.9	104.5 \pm 46.1	0.01 \pm 0.00	36.6 \pm 0.4	69.9 \pm 4.0	30.1 \pm 4.0	2,116.7 \pm 19.5	0.02 \pm 0.00
IMAC flow through	2.8 \pm 1.5	76.8 \pm 11.0	24.2 \pm 11.0	82.4 \pm 43.0	0.04 \pm 0.02	35.2 \pm 0.4	96.1 \pm 0.1	3.9 \pm 0.1	2,033.2 \pm 19.9	0.08 \pm 0.01
IMAC wash	2.7 \pm 1.5	95.8 \pm 2.9	4.2 \pm 2.9	79.7 \pm 42.6	0.06 \pm 0.02	34.9 \pm 0.4	99.1 \pm 0.0	0.9 \pm 0.0	2,014.5 \pm 20.1	0.08 \pm 0.01
IMAC elution	2.3 \pm 1.4	84.4 \pm 11.2	15.6 \pm 11.2	58.7 \pm 39.8	0.14 \pm 0.04	31.7 \pm 0.3	90.9 \pm 0.0	9.1 \pm 0.0	1,324.8 \pm 8.9	0.19 \pm 0.00

^a n=3; ^b n=2. IMAC – immobilized metal-ion affinity chromatography.

Regardless of the depth filtration or ultracentrifugation method used, the purity only increased from 0.05 % (homogenate) to 0.2 % (IMAC elution) based on the TSP, measured by Bradford (Table 21). This was confirmed by the Coomassie-stained NuPAGE LDS gel, in which a substantial amounts of host cell protein (HCP) were detected in the IMAC fractions, including the IMAC eluate (Figure 27A). However, the reason for that might be the low concentration of nTf338-FGF21-PLUS in the crude extracts of 2.9-5.8 mg kg⁻¹ biomass and might be higher if the concentration can be increased >100 mg kg⁻¹ biomass.

Both in the anti-FGF21 and anti-His Western blot, a 64 kDa fragment corresponding to the expected size of the intact nTF338-FGF21-PLUS fusion protein was detected in the crude extract, but in the IMAC eluate, the protein could only be detected in the anti-FGF21 Western blot (Figure 27B). The reasons for this could not be identified. However, in the anti-FGF21 Western blot, nTf338-FGF21-PLUS seemed to be stable as the relative amount of intact nTf338-FGF21-PLUS and degradation products was similar in the crude extracts and the

different filtration and purification fractions, including the IMAC eluate, with 55 % (intact form) and 45% degradation products (Figure 27B).

For the animal feeding studies, the IMAC eluates were pooled, the elution buffer exchanged with PBS, and subsequently concentrated, resulting in an nTF338-FGF21-PLUS concentration of 1.7-7.3 $\mu\text{g mL}^{-1}$ and TSP / HCP impurities of 6.0 mg mL^{-1} , respectively (data not shown).

In summary, the overall recoveries for the depth filtration-based and centrifugation-based processes in purification were ~2 % and ~32 %, corresponding to ~0.06 mg kg^{-1} LFM and ~1.3 mg kg^{-1} LFM, respectively. Even though depth filtration is easier to scale-up, ultracentrifugation might be preferred for the purification of nTf338-FGF21-PLUS.

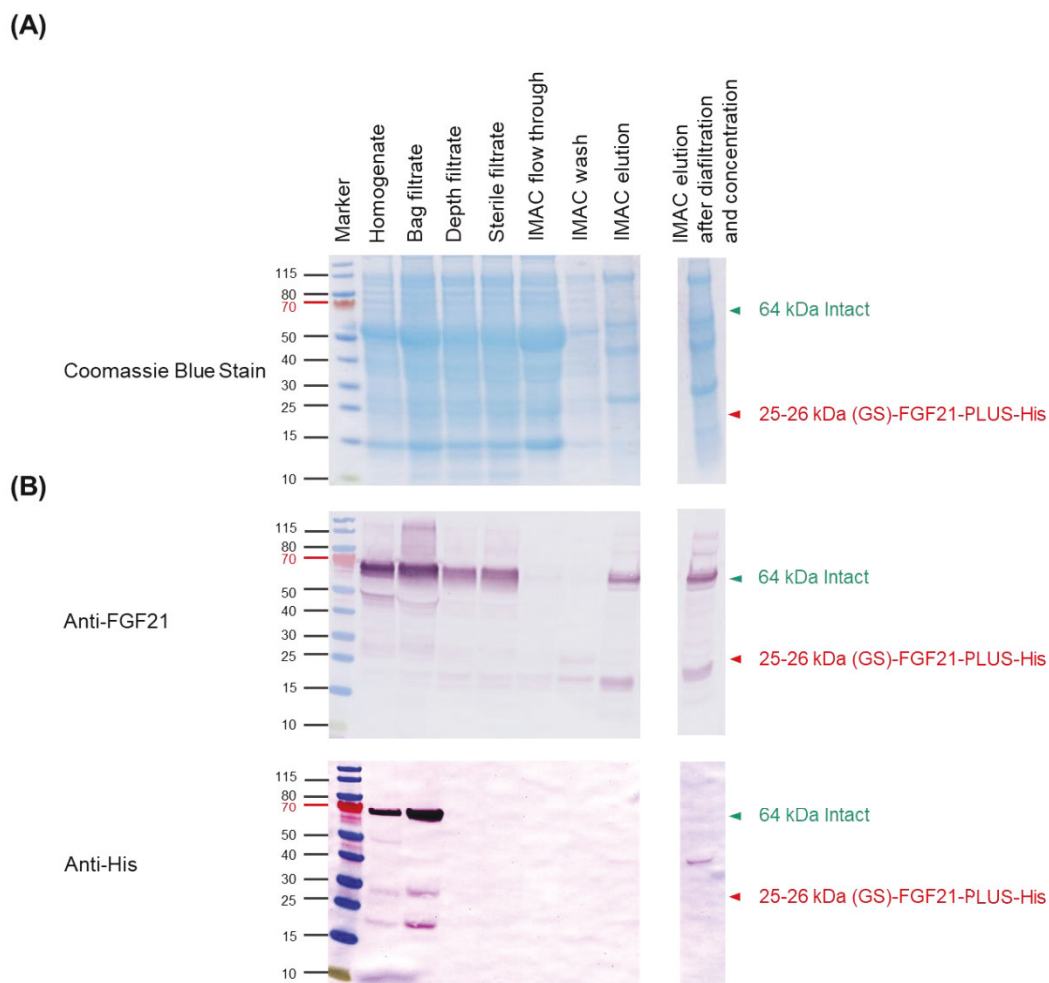


Figure 27. Coomassie-stained NuPAGE LDS gel and Western blot analysis of purification process fractions for nTF338-FGF21-PLUS extracted from non-senescent, transiently transformed *N. benthamiana* leaves, using depth filtration for clarification. Each 800 g leaf material was homogenized in extraction buffer and purified by IMAC and applied PBS buffer diafiltration and concentration using 30 kDa centrifugal filter. Leaf samples containing 100 μ g of total soluble protein were subjected to NuPAGE 4-12 % Bis-Tris protein gels. **(A)** Coomassie stained gel, **(B)** FGF21-Western blot and His-Western blot. The electroblotted proteins were probed with primary anti-FGF21/-His₆ rabbit polyclonal antibody (1:5,000) and then secondary goat anti-Rabbit IgG alkaline phosphate (AP)-conjugated antibody (1:5,000). IMAC – immobilized metal-ion affinity chromatography; PBS – phosphate-buffered saline.

IV. Discussion

IV. Discussion

IV.1. Optimization tobacco seed yield in contained greenhouses yielded a competitive production platform

For the oral delivery of FGF21 through tobacco seeds, I chose seed-rich SL632 as a host for its recombinant expression in stably transformed plants, established the seed production in a greenhouse setting, and compared it to leaf-rich VG tobacco and leaf production as a reference.

Compared to the normal tobacco cultivation in the greenhouse without cutting, the seed yield increased by 1.6-fold (SL632) and 2.4-fold (VG) via 1× cut, which broke the apical dominance of the main stem and induced the formation of side branches (Table 13).

For tobacco SL632 and VG, their seed yields were $0.38 \text{ kg m}^{-2} \text{ a}^{-1}$ and $0.24 \text{ kg m}^{-2} \text{ a}^{-1}$, and their seed production costs were $1.64 \text{ € g}^{-1} \text{ SDM}$ and $2.58 \text{ € g}^{-1} \text{ SDM}$, respectively. However, their leaf yields were $8.19 \text{ kg m}^{-2} \text{ a}^{-1}$ and $11.17 \text{ kg m}^{-2} \text{ a}^{-1}$, and their leaf production costs were $0.19 \text{ € g}^{-1} \text{ LFM}$ and $0.14 \text{ € g}^{-1} \text{ LFM}$, respectively. The latter was similar to the leaf yield and production costs for *N. benthamiana*, with $11.94 \text{ kg m}^{-2} \text{ a}^{-1}$ and $0.13 \text{ € g}^{-1} \text{ LFM}$, typically used for production of PD via transient transformation as an alternative to stable transformation (Table 13). Thus, when comparing SL632 seeds and VG leaves as production platforms, the biomass production rate per unit area and time was 30-fold lower (Table 16), and the production costs were 12-fold higher (Table 13) for seeds compared to leaves.

However, labor costs account for 98 % of the overall production cost of seeds and leaves (Table 13), and these could potentially be reduced by approximately 90 % by using semi-automated greenhouse facilities (Huebbers and Buyel, 2021; Nandi et al., 2016), as has already been established for barley (ORF Genetics, Island) and rice seeds (Ventria Bioscience, USA) in greenhouses. For example, in a clinical study using transgenic rice seeds as an oral vaccine, the vaccine cost was $0.08 \text{ € g}^{-1} \text{ seed}$ (Chapters I.5.1.1. and I.5.1.2.) (Yuki et al., 2021).

In addition, the higher cultivation costs for seeds compared to leaves in the greenhouse might be compensated by the fact that seeds do not need to be processed after harvest, and PD does not require purification from seeds for oral delivery, as is necessary for leaves, which is a substantial cost factor. For example, in a clinical study using rice seeds as an oral vaccine, the costs of $0.08 \text{ € g}^{-1} \text{ seed}$ corresponded to $28 \text{ € g}^{-1} \text{ PD}$ without purification (for a PD

accumulation of 3 g kg⁻¹ SDM) (Yuki et al., 2021) compared to 500-1,000 € g⁻¹ PD and 100-500 € g⁻¹ PD for PD purified either from stably or transiently transformed tobacco (Chapters I.5.1.1. and I.5.1.2.) (Knödler et al., 2023; Ridgley et al., 2023; Tusé et al., 2014), which is 4-36-fold higher compared to PD costs for transgenic rice seeds (Yuki et al., 2021).

Hence, the production of PD for oral delivery is possible in a greenhouse setting and, in principle, substantially more cost-effective compared to the production in leaves.

IV.2. Stable FGF21-Transferrin expression in seeds of *N. tabacum* SL632 was impacted by the instability of the fusion protein

To enable oral delivery via transfer from the small intestine into the portal vein of the bloodstream, I designed the FGF21-F-Tf fusion protein. FGF21 was coupled to Tf for translocation through the enterocytes of the intestine, and a furin cleavage site was introduced for the separation of FGF21 from Tf during/after translocation. For oral delivery, I established the *in vitro* stable transformation protocol for SL632 to introduce the FGF21-F-Tf expression cassette.

However, SL632 exhibited early flowering in *in vitro* tissue culture compared to VG, the reference cultivar, affecting the transformability of SL632 (Table 14). Similarly, the transformation efficiency in terms of positive shoots per explant was lower for SL632 compared to VG for both FGF21-F-Tf and GFP, used as a non-toxic control (Table 15). Although transgenic FGF21-F-Tf transformants showed normal seed vigor (Table 16), the lower transformability did not seem to be related to the transgene but rather to the cultivar SL632. Nevertheless, I successfully obtained stably transformed SL632 producing FGF21-F-Tf.

However, FGF21-F-Tf was instable, with 41-67 % degradation products relative to the total amount of FGF-F-Tf protein observed *in planta* in both seeds and leaves (Figure 17, Table 16). This instability seemed to be related to the furin cleavage site in FGF-F-Tf. This finding is in opposite to previous studies that produced recombinant fusion proteins with furin cleavage sites in plants and did not observe any cleavage (Boyhan and Daniell, 2011; Kang et al., 2018; Kwon et al., 2018; Margolin et al., 2020; Verma et al., 2010). Although the mammalian furin protease does not occur in plants (Wilbers et al., 2016), a previous study demonstrated the presence of a furin-like Kex2p-like endoprotease in tobacco (Kinal et al., 1995), which might have recognized the furin site in the FGF21-F-Tf protein.

Alternatively, the degradation of FGF21-F-Tf might not be related to the furin site but to the flexible GS-linker next to the furin cleavage site (Benchabane et al., 2008; Chen et al., 2013). If so, substituting the flexible GS-linker with a more stable linker could be considered to enhance the stability and integrity of the future FGF21-Tf fusion protein. For example, the DK linker (enterokinase cleavable linker, DDDDK), the LE linker (dipeptide linker, LE), the PD linker (non-helical polypeptide linker, (PEAPTD)₂), and the EA linker (rigid linker, (LEA(EAAAK)₄ALEA(EAAAK)₄ALE)) (Table 22).

Table 22. Linkers described for FGF21-Transferrin fusion proteins.

Linker type	Linker AA sequence	Fusion protein	Heterologous host	Compartment	Reference
EK cleavable	DDDDK*	GFP-FGF21	<i>Nicotiana benthamiana</i>	Cytosol	(Fu et al., 2011)
Dipeptide	LE**	ProINS-Tf	HEK293	Extracellular space	(Chen et al., 2018; Liu et al., 2020; Wang et al., 2011b; Wang et al., 2014b)
			<i>Oryza sativa</i> seeds	Apoplasm	(Chen et al., 2018)
Non-helical polypeptide	(PEAPTD) ₂	GLP1-Tf	<i>Saccharomyces cerevisiae</i>	Extracellular space	(Kim et al., 2010)
		Ex4-Tf	<i>Saccharomyces cerevisiae</i>	Extracellular space	(Kim et al., 2010)
Rigid	(LEA(EAAAK) ₄ ALEA (EAAAK) ₄ ALE)	G-CSF-Tf	HEK293	Extracellular space	(Amet et al., 2009; Chen et al., 2013)
		FIX-Tf	HEK293	Extracellular space	(Amet et al., 2009; Chen et al., 2013)
Flexible	(GGGGS) ₃	G-CSF-Tf	HEK293	Extracellular space	(Amet et al., 2009; Chen et al., 2013)
		FIX-Tf	HEK293	Extracellular space	(Amet et al., 2009; Chen et al., 2013)
		Ex4-Tf	<i>Nicotiana benthamiana</i>	ER	(Choi et al., 2014)

*EK – enterokinase cleavage site, **XhoI – restriction site, AA – amino acid.

Nevertheless, the instability of FGF21-F-Tf might have limited the accumulation of intact FGF21-F-Tf, resulting in 6.7 mg kg⁻¹ SDM in T1 seeds and 5.6 mg kg⁻¹ LFM in T2 leaves (Table 16), which is below the 50 mg kg⁻¹ SDM/LFM required for oral delivery (Chapter III.2.4.). Notably, my case study showed similar accumulation levels of intact FGF21-F-Tf in T1 seeds (6.7 mg kg⁻¹ SDM) and T2 leaves (5.6 mg kg⁻¹ LDM) with less degradation of FGF21-F-Tf in leaves (41 %) compared to seeds (67 %) (Figure 17, Table 16).

This contradicts the general view that the recombinant protein production of transgenic seeds is higher than that of transgenic leaves, which is explained by 1) the higher protein content in seeds with 80 - 350 g kg⁻¹ protein per SDM, compared to leaves with 10 - 20 g kg⁻¹ protein per LFM respectively (equivalent to 85 - 170 g kg⁻¹ leaf dry mass (LDM)) (Benchabane et al., 2008; Boothe et al., 2010; Frega et al., 1991), and 2) the view that seeds exhibit a low protease activity, resulting in high recombinant protein yields (Benchabane et al., 2008; Boothe et al., 2010). Previous publications, for instance, reported yields of recombinant proteins from 30.4 mg to 6.5 g kg⁻¹ SDM and 3.0 mg to 1.0 g kg⁻¹ LFM for stable transformed

plants (Table 2, Table 3). Transgenic Tf, as an example, yielded in rice seeds and tobacco leaves 10 g kg^{-1} SDM and 0.14 g kg^{-1} LFM (equivalent to 1.2 g kg^{-1} LDM) respectively (Table 3, Table 23). However, the findings of this study differ from previous reports and the prevailing opinion, indicating that protein expression in seeds may not always be beneficial to product stability and accumulation and mainly depends on the recombinant protein to be produced.

Nevertheless, even though the 6.7 mg kg^{-1} SDM in T1 seeds was below the 50 mg kg^{-1} SDM/LFM required for oral delivery in animal feeding studies, previous studies have shown that recombinant protein production can reach this accumulation level in transgenic tobacco seeds (Table 2, Table 3). Therefore, the use of tobacco to express FGF21-F-Tf is, in principle, possible, provided a FGF21-F-Tf fusion protein with higher stability is designed.

In addition, to further improve the protein accumulation of FGF21-F-Tf in seeds, a seed-specific promoter can be used to replace the constitutive CaMV 35S promoter, such as the pLeb4, pPhas, pUSP, pGt1, pGlo1, pUbi, and pCon promoter, which showed higher expression levels in seeds (Table 3). Alternatively, other crops as protein expression platforms might be selected to increase protein accumulation in seeds, with protein yields ranging up to $160 \text{ mg} - 15 \text{ g kg}^{-1}$ SDM, such as rice in which Tf rice already yielded 10 g kg^{-1} SDM (Table 3).

This demonstrates that producing PD like FGF21-F-Tf in seeds at the required accumulation level of 50 mg kg^{-1} SDM is achievable with optimized constructs and expression cassettes.

Table 23. Yield of FGF21 and Tf recombinant proteins in plants. Numbers represent mean \pm standard deviation.

Transformation	Plant	Recombinant protein	Promoter/Terminator	Protein accumulation in transient leaves [mg kg ⁻¹ Biomass]	Reference
Transient	<i>N. bent</i> leaves	FGF21-F-Tf	TMV-SgPr/ TMV-Sgt	2.1 \pm 0.0	This study
		FGF21	PVX-SgPr/PVX-Sgt	5	(Fu et al., 2011)
		Ex-4-Tf	p35S/tNos	137	(Choi et al., 2014)
		smGFP-hFGF21	PVX-SgPr/PVX-Sgt	450	(Fu et al., 2011)
		FGF21-F-Tf	p35S/t35S	0.8 \pm 0.2	This study
		FGF21-Tf-PLUS	p35S/t35S	1.6 \pm 0.5	This study
		FGF21-nTf338-PLUS	p35S/t35S	1.6 \pm 0.5	This study
		nTf338-FGF21-PLUS	p35S/t35S	2.1 \pm 0.5	This study
Transgenic	Tobacco leaves	FGF21-F-Tf (SL632)	p35S/t35S	5.6 \pm 0.2	This study
		FGF21-F-Tf (VG)	p35S/t35S	2.4 \pm 0.0	This study
		Ex-F-Tf	p35S/tNos	37	(Choi et al., 2014)
	Tobacco seeds	FGF21-F-Tf (SL632)	p35S/t35S	6.7 \pm 0.2	This study
		FGF21-F-Tf (VG)	p35S/t35S	6.4 \pm 0.0	This study
	Rice seeds	Tf	pGt1/tNos	10,000	(Zhang et al., 2010)

TMV-SgPr – TMV subgenomic promoter; PVX-SgPr – PVX subgenomic promoter; p35S – CaMV 35S promoter with duplicated transcriptional enhancer; pGt1 – *Oryza sativa* seed storage protein glutelin 1 promoter; TMV-Sgt – TMV subgenomic terminator; PVX-Sgt – PVX subgenomic terminator; t35S – CaMV 35S terminator; tNos – *Agrobacterium tumefaciens* nopal synthase terminator; TMV – tobacco mosaic virus; PVX – potato virus X; SgPr – subgenomic promoter; Sgt – subgenomic terminator; CaMV – cauliflower mosaic virus.

IV.3. Protein engineering of FGF21-Transferrin via transient expression in leaves of *N. benthamiana* produced a stabilized FGF21-Transferrin variant nTf338-FGF21-PLUS that can be used for stable expression in seeds

To optimize the stability of the FGF21-F-Tf fusion protein, I used the transient transformation system in *N. benthamiana*. First, I employed the replicating virus magnICON vector system, but due to the insert size limitation, FGF21 and Tf were co-expressed and subsequently fused by inteins. However, the co-expression failed, resulting in the detection of only Tf, not FGF21-F-Tf or FGF21 alone. It might be assumed that either 1) different stability of the two protein fragments when expressed separately, leading to the degradation of FGF21 before fusion, or 2) the assembled fusion protein being cleaved into the two fragments after assembly, with FGF21 being completely degraded. In this case, the degradation rate was higher than the production and fusion rate.

For this reason, I then employed the non-viral pTRAc vector system, which has no size limit and can express FGF21-F-Tf directly as a fusion protein, similar to the approach used in stably transformed tobacco plants. Using this system, the protein yielded 0.8 mg kg⁻¹ LFM of intact fusion protein with 33 % additional degradation products compared to 6.7 and 5.6 mg kg⁻¹ SDM/LFM of intact fusion protein and 26 % and 8 % additional degradation products in T1 seeds and T2 leaves of stably transformed tobacco plants (Table 18).

Based on this, the stability and accumulation of the fusion protein was optimized. I removed the furin site and inserted the liver-targeting PLUS peptide instead, resulting in the protein FGF21-Tf-PLUS. This increased the accumulation from 0.8 to 1.6 mg kg⁻¹ LFM of intact fusion protein while decreasing the degradation from 33-32 % to 25-19 % (Table 18). Hence, removal of the furin mitigated the degradation but did not completely prevent it, suggesting that unintended cleavage of the furin site might not be the only reason. The region between FGF21 and Tf seemed to be instable to a certain degree, possibly due to the flexible GS-linker.

Next, I truncated Tf to the relevant N-terminus nTf338, resulting in FGF21-nTf338-PLUS, which accumulated at 1.6 mg kg⁻¹ LFM with 21-15 % degradation products. Changing the orientation of FGF21 and nTf338 to nTf338-FGF21-PLUS resulted in 2.1 mg kg⁻¹ LFM with 9-7 % degradation products (Figure 22, Figure 23, Table 18). Reducing the size of the fusion

protein and changing the orientation improved the stability and accumulation level. These aspects should be considered during recombinant protein design.

Nevertheless, the 2.1 mg kg⁻¹ LFM for nTf338-FGF21-Tf was lower compared to other studies that transiently expressed FGF21 and Tf either alone or as fusion protein. For example, 5 mg kg⁻¹ LFM for FGF21 (Fu et al., 2011), 450 mg kg⁻¹ LFM for GFP-FGF21 (Fu et al., 2011), and 137 mg kg⁻¹ LFM for Ex4-Tf (Choi et al., 2014), being 2.4 -fold, 214-fold, and 65-fold higher (Table 23).

To further improve accumulation and stability of nTf338-Tf-PLUS, the flexible GS-linker might be replaced by other more stable linkers, such as the DK linker (linker AA sequence: DDDDK), the LE linker (linker AA sequence: LE), the PD linker (linker AA sequence: (PEAPTD)₂), and the EA linker (linker AA sequence: (LEA(EAAAK)₄ALEA(EAAAK)₄ALE)) (Table 22). In this context, the 3D structure results by the Raptor X software showed that the FGF21-transferrin fusion proteins with different linkers had no steric hindrance compared to native FGF21, which might impact the stability and activity of these fusion proteins (Figure 28). Therefore, the production of nT338-FGF21-PLUS might be improved in the future by using different linkers.

Nevertheless, it can be assumed that via further optimization of the FGF21-transferrin fusion and its combination with other approaches, such as employing seed-specific promoters, the required 50 mg kg⁻¹ SDM for oral delivery can be obtained in tobacco seeds.

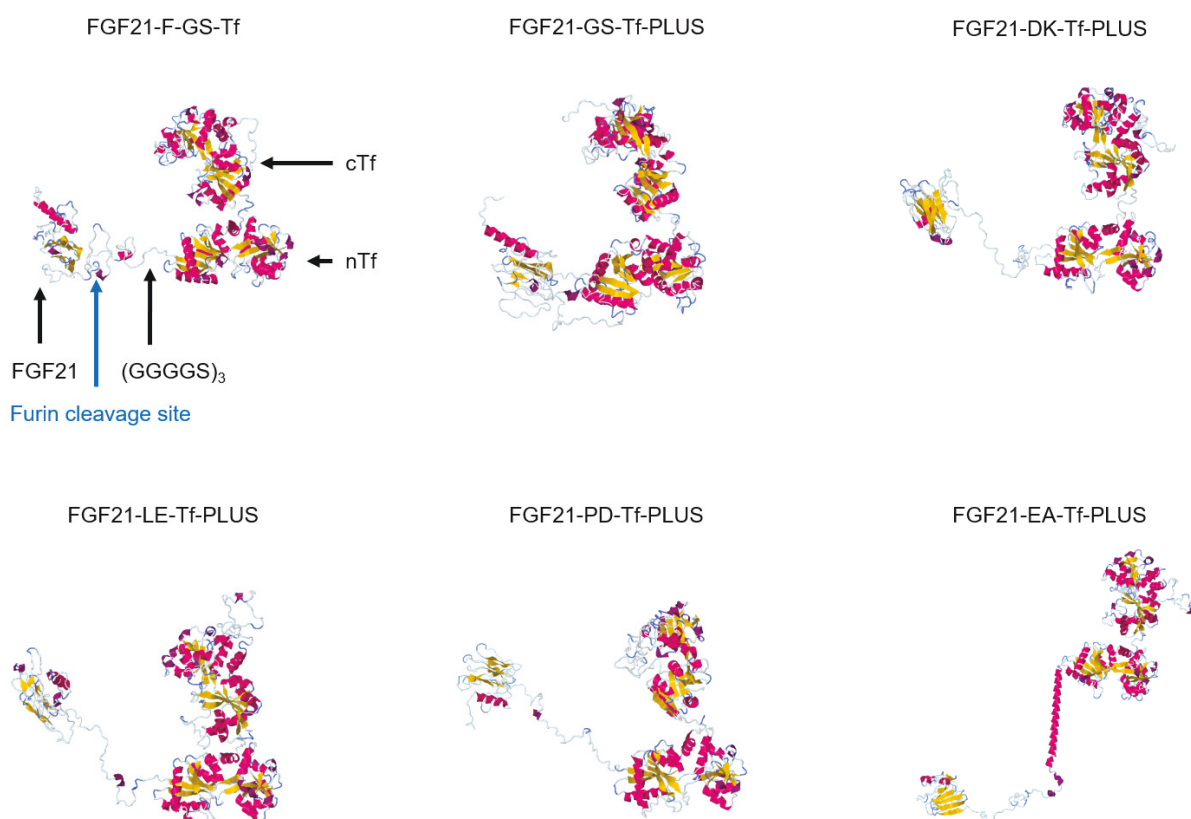


Figure 28. FGF21-Transferrin fusion protein with different linker models. The 3D structures of FGF21-Tf fusion proteins with different linkers predicted by submitting the amino acid sequence to the Raptor X software (<http://raptorx.uchicago.edu/>). PLUS: liver-targeting peptide circumsporozoite protein (CSP), position 82-100; GS linker: flexible linker, (GGGGS)₃; DK linker: enterokinase cleavable linker, DDDDK; LE linker: dipeptide linker, LE; PD linker: non-helical polypeptide linker, (PEAPTD)₂; EA linker: rigid linker, (LEA(EAAAK)₄ALEA(EAAAK)₄ALE).

IV.4. A purification method for nTf338-FGF21-PLUS was established that enabled pre-clinical proof-of-concept bioavailability and bioactivity studies

For the bioavailability and bioactivity studies in mice, the transiently produced nTf338-FGF21-PLUS needed to be purified. For large-scale purification, filtration was suitable to remove solid particles, with depth filtration being the most effective (Table 20). However, depth filtration also resulted in a ~5 % step recovery of nTf338-FGF21-PLUS and a low overall recovery of 2 % (Table 21). Therefore, the yield might be alleviated by improving the filter systems, such as using depth filters in combination with flocculants, DE free filters, or adding low concentrations of detergents like Triton X-100 to the extract (Chapter I.5.2.) (Buyel et al., 2015a; Buyel and Fischer, 2014b).

However, I replaced depth filtration by ultracentrifugation, even though limited in its scalability, which yielded the same particle removal efficiency but a step recovery of ~95 % (Table 21). The final clarification and purification setup resulted in a recovery of 32 % for nTf338-FGF21-PLUS, corresponding to about 1.3 mg kg⁻¹ LFM, respectively (Table 21). The significant loss of 68 % of nTf338-FGF21-PLUS might be contributed to the low overall accumulation in crude extracts with 2.9 - 5.8 mg kg⁻¹ LFM (Table 21), potentially causing unspecific binding of nTf338-FGF21-PLUS to have a relatively high impact. Hence, increasing the accumulation level of nTf338-FGF21-PLUS to >100 mg kg⁻¹ or even >1 g kg⁻¹ LFM might increase the overall recovery up to 80 %, as reported for His-tagged DsRed, purified with a similar procedure.

Similarly, the low purity of nTf338-FGF21-PLUS at 0.2 % (compared to typical purities of 80 % after IMAC purification) might be explained by the low accumulation level of 2.9 - 5.8 mg kg⁻¹ LFM (compared to 100 mg - 6 g kg⁻¹ LFM for other transiently produced recombinant proteins) (Table 21). The low initial product concentration in the extract loaded onto the IMAC might have favored non-specific HCP binding to the IMAC resin, resulting in co-purification, and, thus, low purity (Figure 27). Increasing the accumulation *in planta* might enhance the purity as well.

Nevertheless, nTf338-FGF21-PLUS in this study was only a partially purified protein. However, previous animal feeding trials have successfully used lyophilized, resuspended leaf material, crude extracts, or partially purified recombinant proteins without any apparent adverse effects of impurities, such as CTB-Ex-4 and Ex-4-Tf (Choi et al., 2014; Kwon et al.,

2013; Phan et al., 2020). Based on this, partially purified nTF338-FGF21-PLUS with co-purified HCP might be suitable for testing bioavailability and bioactivity in animal feeding trials with mice, and the partially purified nTF338-FGF21-PLUS was thus delivered to our partner DIfE, as described in "**Hou, H.W., Bishop, C.A., Huckauf, J., Broer, I., Klaus, S., Nausch, H., Buyel, J.F. (2022). Seed and leaf based FGF21- Transferrin fusion protein expression for oral delivery and treatment of non-alcoholic steatohepatitis. *Frontiers in Plant Science* 13:998596; 10.3389/fpls.2022.998596**", which demonstrated that nTF338-FGF21-PLUS is both bioavailable and bioactive.

Hence, the production of FGF21 in plants and plant seeds is a meaningful approach for oral delivery to medicate NASH.

V. Conclusion

V. Conclusion

Finally, I would like to summarize the main findings of my PhD thesis "Establishing the greenhouse-production of FGF21-Transferrin in tobacco seeds and leaves for oral treatment of non-alcoholic steatohepatitis NASH".

FGF21 exhibits the potential to reverse liver dysfunction in pre-clinical trials. However, the systemic long-acting FGF21 analogues developed so far were all injected directly into the blood and had negative effects on other organs due to their long half-life and systemic distribution. I therefore established an oral administration system for FGF21, utilizing transferrin as a carrier and tobacco seeds or leaves as a matrix. This approach offers two major advantages: Firstly, the plant matrix protects FGF21 from stomach acidity and enzymes, releasing it enzymatically in the intestinal lumen. Secondly, fusion with transferrin (FGF21-transferrin) enables direct targeting of FGF21 to the liver, facilitated by transferrin's ability to mediate cellular uptake through enterocytes, allowing transport from the intestine to the portal vein and liver.

In this context, I demonstrated that maximizing SL632 seed yield in the greenhouse involves cutting induced side shoots, resulting in a yield of $380 \text{ g m}^{-2} \text{ a}^{-1}$ with a manufacturing cost of 1.64 € g^{-1} compared to $11.17 \text{ kg m}^{-2} \text{ a}^{-1}$ and 0.14 € g^{-1} for leaves. Importantly, seeds can be directly used for oral delivery without the need for purification, a requirement in leaf production, leading to 4-36-fold lower overall production costs of seed-based PD compared to leaf-based PD. Therefore, seeds are a suitable production platform for the oral delivery of PD.

However, in stably transformed, transgenic SL632 plants producing FGF21-F-Tfs, the unintended cleavage of the furin site and the intrinsic instability of the flexible GS-linker resulted in the degradation of the FGF21-F-T fusion protein in both seeds and leaves, yielding 41-67 % degradation products. This limited the accumulation of intact FGF21-F-T fusion protein to $6.7 \text{ mg kg}^{-1} \text{ SDM}$ and $5.6 \text{ mg kg}^{-1} \text{ LFM}$. To improve the protein integrity and accumulation, I optimized the FGF21-F-Tf fusion protein via transient transformation. This involved removing the furin cleavage site, introducing the liver-targeting peptide PLUS, truncating Tf (nTf338), and changing the order of the fusion partners. The final fusion protein, nTf338-FGF21-PLUS, exhibited significantly reduced degradation with only 9-7 % degradation products and a 3-fold higher accumulation level. Thus, in combination with other approaches such as seed-specific promoters, the optimized nTf338-FGF21-PLUS can be used to achieve higher accumulation levels in future transgenic SL632 seeds.

For the large-scale production in leaves as an alternative to seeds, I established the extraction and purification of nTf338-FGF21-PLUS from transiently transformed plants. Solid particles resulting from tissue homogenization needed removal prior to chromatography-based IMAC purification. Depth filtration effectively reduced dispersed particles but was associated with a ~95 % loss of nTf338-FGF21-PLUS, possibly due to unspecific binding to the filter, resulting in an overall recovery of only 2 %. Therefore, I adapted an ultracentrifugation-based method, similarly effective in removing solid particles, reducing the loss to ~5 %, and increasing the overall recovery to 32 %. However, during nTf338-FGF21-PLUS IMAC purification, the low concentration of nTf338-FGF21-PLUS of 2.9 - 5.8 mg kg⁻¹ LFM in the crude extract seemed to promote non-specific binding of HCP to the chromatography resin, causing extensive co-purification of HCP and resulting in a final purity of less than 1 %. The huge co-purification might be reduced, if accumulation levels of nTf338-FGF21-PLUS can be increased to 100 mg - 6 g kg⁻¹ LFM as for other transiently produced recombinant proteins.

Nevertheless, the partially purified nTf338-FGF21-PLUS demonstrated both bioavailable and bioactive, as shown by the cooperation partner DIfE, e.g., it has been shown to induce mRNA expression of liver target genes in HepG2 cells, and it was transferred from the intestine to the blood circulation by oral gavage in mice.

Concluding, I demonstrated that oral delivery of nTf338-FGF21-PLUS containing seeds might be an alternative to leaf production and, in principle, be used for the treatment of NASH via oral delivery.

VI. Reference

VI. References

- Adams, A. C., Yang, C., Coskun, T., Cheng, C. C., Gimeno, R. E., Luo, Y. and Kharitononkov, A. (2012) The breadth of FGF21's metabolic actions are governed by FGFR1 in adipose tissue. *Molecular metabolism* **2**, 31–37.
- Adem, M., Beyene, D. and Feyissa, T. (2017) Recent achievements obtained by chloroplast transformation. *Plant methods* **13**, 30.
- Ahmad, I., Iwata, T. and Leung, H. Y. (2012) Mechanisms of FGFR-mediated carcinogenesis. *Biochimica et biophysica acta* **1823**, 850–860.
- Albhaisi, S. A. M. and Sanyal, A. J. (2021) New drugs for NASH. *Liver international official journal of the International Association for the Study of the Liver* **41 Suppl 1**, 112–118.
- Amet, N., Lee, H.-F. and Shen, W.-C. (2009) Insertion of the designed helical linker led to increased expression of tf-based fusion proteins. *Pharmaceutical research* **26**, 523–528.
- Anuwatmatee, S., Tang, S., Wu, B. J., Rye, K.-A. and Ong, K. L. (2019) Fibroblast growth factor 21 in chronic kidney disease. *Clinica chimica acta; international journal of clinical chemistry* **489**, 196–202.
- Arntzen, C. (2015) Plant-made pharmaceuticals: from 'Edible Vaccines' to Ebola therapeutics. *Plant biotechnology journal* **13**, 1013–1016.
- Asrani, S. K., Devarbhavi, H., Eaton, J. and Kamath, P. S. (2019) Burden of liver diseases in the world. *Journal of hepatology* **70**, 151–171.
- Badman, M. K., Koester, A., Flier, J. S., Kharitononkov, A. and Maratos-Flier, E. (2009) Fibroblast growth factor 21-deficient mice demonstrate impaired adaptation to ketosis. *Endocrinology* **150**, 4931–4940.
- Badman, M. K., Pissios, P., Kennedy, A. R., Koukos, G., Flier, J. S. and Maratos-Flier, E. (2007) Hepatic fibroblast growth factor 21 is regulated by PPARalpha and is a key mediator of hepatic lipid metabolism in ketotic states. *Cell metabolism* **5**, 426–437.
- Bai, Y., Ann, D. K. and Shen, W.-C. (2005) Recombinant granulocyte colony-stimulating factor-transferrin fusion protein as an oral myelopoietic agent. *Proceedings of the National Academy of Sciences of the United States of America* **102**, 7292–7296.
- Banerjee, D., Flanagan, P. R., Cluett, J. and Valberg, L. S. (1986) Transferrin receptors in the human gastrointestinal tract. Relationship to body iron stores. *Gastroenterology* **91**, 861–869.
- Barany, S. and Szepesszentgyörgyi, A. (2004) Flocculation of cellular suspensions by polyelectrolytes. *Advances in colloid and interface science* **111**, 117–129.

- Basaran, P. and Rodríguez-Cerezo, E. (2008) Plant molecular farming: opportunities and challenges. *Critical reviews in biotechnology* **28**, 153–172.
- Beenken, A. and Mohammadi, M. (2009) The FGF family: biology, pathophysiology and therapy. *Nature Reviews Drug Discovery* **8**, 235–253.
- Benchabane, M., Goulet, C., Rivard, D., Faye, L., Gomord, V. and Michaud, D. (2008) Preventing unintended proteolysis in plant protein biofactories. *Plant biotechnology journal* **6**, 633–648.
- Berglund, E. D., Li, C. Y., Bina, H. A., Lynes, S. E., Michael, M. D., Shanafelt, A. B., Kharitononkov, A. and Wasserman, D. H. (2009) Fibroblast growth factor 21 controls glycemia via regulation of hepatic glucose flux and insulin sensitivity. *Endocrinology* **150**, 4084–4093.
- Boothe, J., Nykiforuk, C., Shen, Y., Zaplachinski, S., Szarka, S., Kuhlman, P., Murray, E., Morck, D. and Moloney, M. M. (2010) Seed-based expression systems for plant molecular farming. *Plant biotechnology journal* **8**, 588–606.
- Boyhan, D. and Daniell, H. (2011) Low-cost production of proinsulin in tobacco and lettuce chloroplasts for injectable or oral delivery of functional insulin and C-peptide. *Plant biotechnology journal* **9**, 585–598.
- Braun, E. and Sauter, D. (2019) Furin-mediated protein processing in infectious diseases and cancer. *Clinical & translational immunology* **8**, e1073.
- Brown, K. J., Vanderver, A., Hoffman, E. P., Schiffmann, R. and Hathout, Y. (2012) Characterization of Transferrin Glycopeptide Structures in Human Cerebrospinal Fluid. *International journal of mass spectrometry* **312**, 97–106.
- Burgess, R. R. (2018) A brief practical review of size exclusion chromatography: Rules of thumb, limitations, and troubleshooting. *Protein expression and purification* **150**, 81–85.
- Buyel, J. F. and Fischer, R. (2014a) Downstream processing of biopharmaceutical proteins produced in plants: the pros and cons of flocculants. *Bioengineered* **5**, 138–142.
- Buyel, J. F. and Fischer, R. (2014b) Scale-down models to optimize a filter train for the downstream purification of recombinant pharmaceutical proteins produced in tobacco leaves. *Biotechnology journal* **9**, 415–425.
- Buyel, J. F., Gruchow, H. M. and Fischer, R. (2015a) Depth Filters Containing Diatomite Achieve More Efficient Particle Retention than Filters Solely Containing Cellulose Fibers. *Frontiers in plant science* **6**, 1134.

- Buyel, J. F., Opdensteinen, P. and Fischer, R. (2015b) Cellulose-based filter aids increase the capacity of depth filters during the downstream processing of plant-derived biopharmaceutical proteins. *Biotechnology journal* **10**, 584–591.
- Buyel, J. F., Twyman, R. M. and Fischer, R. (2015c) Extraction and downstream processing of plant-derived recombinant proteins. *Biotechnology advances* **33**, 902–913.
- Camporez, J. P. G., Jornayvaz, F. R., Petersen, M. C., Pesta, D., Guigni, B. A., Serr, J., Zhang, D., Kahn, M., Samuel, V. T., Jurczak, M. J. and Shulman, G. I. (2013) Cellular mechanisms by which FGF21 improves insulin sensitivity in male mice. *Endocrinology* **154**, 3099–3109.
- Carvalho, S. B., Silva, R. J., Moreira, A. S., Cunha, B., Clemente, J. J., Alves, P. M., Carrondo, M. J., Xenopoulos, A. and Peixoto, C. (2019) Efficient filtration strategies for the clarification of influenza virus-like particles derived from insect cells. *Separation and Purification Technology* **218**, 81–88.
- Castilho, A., Windwarder, M., Gattinger, P., Mach, L., Strasser, R., Altmann, F. and Steinkellner, H. (2014) Proteolytic and N-glycan processing of human α 1-antitrypsin expressed in *Nicotiana benthamiana*. *Plant physiology* **166**, 1839–1851.
- Ceballo, Y., Tiel, K., López, A., Cabrera, G., Pérez, M., Ramos, O., Rosabal, Y., Montero, C., Menassa, R., Depicker, A. and Hernández, A. (2017) High accumulation in tobacco seeds of hemagglutinin antigen from avian (H5N1) influenza. *Transgenic research* **26**, 775–789.
- Charles, E. D., Neuschwander-Tetri, B. A., Pablo Frias, J., Kundu, S., Luo, Y., Tiruchurai, G. S. and Christian, R. (2019) Pegbelfermin (BMS-986036), PEGylated FGF21, in Patients with Obesity and Type 2 Diabetes: Results from a Randomized Phase 2 Study. *Obesity (Silver Spring, Md.)* **27**, 41–49.
- Chen, L., Fu, L., Sun, J., Huang, Z., Fang, M., Zinkle, A., Liu, X., Lu, J., Pan, Z., Wang, Y., Liang, G., Li, X., Chen, G. and Mohammadi, M. (2023) Structural basis for FGF hormone signalling. *Nature* **618**, 862–870.
- Chen, Q. and Davis, K. R. (2016) The potential of plants as a system for the development and production of human biologics. *F1000Research* **5**.
- Chen, X., Zaro, J. L. and Shen, W.-C. (2013) Fusion protein linkers: property, design and functionality. *Advanced drug delivery reviews* **65**, 1357–1369.
- Chen, Y.-S., Zaro, J. L., Zhang, D., Huang, N., Simon, A. and Shen, W.-C. (2018) Characterization and Oral Delivery of Proinsulin-Transferrin Fusion Protein Expressed Using ExpressTec. *International journal of molecular sciences* **19**.

- Cheng, X., Zhu, B., Jiang, F. and Fan, H. (2011) Serum FGF-21 levels in type 2 diabetic patients. *Endocrine research* **36**, 142–148.
- Cheung, R. C. F., Wong, J. H. and Ng, T. B. (2012) Immobilized metal ion affinity chromatography: a review on its applications. *Applied microbiology and biotechnology* **96**, 1411–1420.
- Cheung, S. C. K., Sun, S. S. M., Chan, J. C. N. and Tong, P. C. Y. (2009) Expression and subcellular targeting of human insulin-like growth factor binding protein-3 in transgenic tobacco plants. *Transgenic research* **18**, 943–951.
- Chilton, M. D., Drummond, M. H., Merio, D. J., Sciaky, D., Montoya, A. L., Gordon, M. P. and Nester, E. W. (1977) Stable incorporation of plasmid DNA into higher plant cells: the molecular basis of crown gall tumorigenesis. *Cell* **11**, 263–271.
- Choi, J., Diao, H., Feng, Z.-C., Lau, A., Wang, R., Jevnikar, A. M. and Ma, S. (2014) A fusion protein derived from plants holds promising potential as a new oral therapy for type 2 diabetes. *Plant biotechnology journal* **12**, 425–435.
- Commandeur, U. and Twyman, R. M. (2004) Biosafety Aspects of Molecular Farming in Plants. In: *Molecular Farming*, pp. 251–266.
- Conley, A. J., Zhu, H., Le, L. C., Jevnikar, A. M., Lee, B. H., Brandle, J. E. and Menassa, R. (2011) Recombinant protein production in a variety of *Nicotiana* hosts: a comparative analysis. *Plant biotechnology journal* **9**, 434–444.
- Coppage, A. L., Heard, K. R., DiMare, M. T., Liu, Y., Wu, W., Lai, J. H. and Bachovchin, W. W. (2016) Human FGF-21 Is a Substrate of Fibroblast Activation Protein. *PloS one* **11**, e0151269.
- Coskun, T., Bina, H. A., Schneider, M. A., Dunbar, J. D., Hu, C. C., Chen, Y., Moller, D. E. and Kharitonov, A. (2008) Fibroblast growth factor 21 corrects obesity in mice. *Endocrinology* **149**, 6018–6027.
- Cromwell, M. E. M., Hilario, E. and Jacobson, F. (2006) Protein aggregation and bioprocessing. *The AAPS journal* **8**, E572-579.
- Cunha, N. B., Murad, A. M., Cipriano, T. M., Araújo, A. C. G., Aragão, F. J. L., Leite, A., Vianna, G. R., McPhee, T. R., Souza, Gustavo H M F, Waters, M. J. and Rech, E. L. (2011) Expression of functional recombinant human growth hormone in transgenic soybean seeds. *Transgenic research* **20**, 811–826.
- Dai, Z., Hooker, B. S., Anderson, D. B. and Thomas, S. R. (2000) Expression of *Acidothermus cellulolyticus* endoglucanase E1 in transgenic tobacco: biochemical characteristics and physiological effects. *Transgenic research* **9**, 43–54.

Denkovskienė, E., Paškevičius, Š., Misiūnas, A., Stočkūnaitė, B., Starkevič, U., Vitkauskienė, A., Hahn-Löbmann, S., Schulz, S., Giritch, A., Gleba, Y. and Ražanskienė, A. (2019) Broad and Efficient Control of *Klebsiella* Pathogens by Peptidoglycan-Degrading and Pore-Forming Bacteriocins Klebicins. *Scientific reports* **9**, 15422.

Ding, X., Boney-Montoya, J., Owen, B. M., Bookout, A. L., Coate, K. C., Mangelsdorf, D. J. and Kliewer, S. A. (2012) β Klotho is required for fibroblast growth factor 21 effects on growth and metabolism. *Cell metabolism* **16**, 387–393.

Dolegowska, K., Marchelek-Mysliwiec, M., Nowosiad-Magda, M., Slawinski, M. and Dolegowska, B. (2019) FGF19 subfamily members: FGF19 and FGF21. *Journal of physiology and biochemistry* **75**, 229–240.

Douris, N., Stevanovic, D. M., Fisher, F. M., Cisu, T. I., Chee, M. J., Nguyen, N. L., Zarebidaki, E., Adams, A. C., Kharitononkov, A., Flier, J. S., Bartness, T. J. and Maratos-Flier, E. (2015) Central Fibroblast Growth Factor 21 Browns White Fat via Sympathetic Action in Male Mice. *Endocrinology* **156**, 2470–2481.

Duckert, P., Brunak, S. and Blom, N. (2004) Prediction of proprotein convertase cleavage sites. *Protein engineering, design & selection PEDS* **17**, 107–112.

Duong-Ly, K. C. and Gabelli, S. B. (2014) Using ion exchange chromatography to purify a recombinantly expressed protein. *Methods in enzymology* **541**, 95–103.

Dushay, J., Chui, P. C., Gopalakrishnan, G. S., Varela-Rey, M., Crawley, M., Fisher, F. M., Badman, M. K., Martinez-Chantar, M. L. and Maratos-Flier, E. (2010) Increased fibroblast growth factor 21 in obesity and nonalcoholic fatty liver disease. *Gastroenterology* **139**, 456–463.

Eckenroth, B. E., Steere, A. N., Chasteen, N. D., Everse, S. J. and Mason, A. B. (2011) How the binding of human transferrin primes the transferrin receptor potentiating iron release at endosomal pH. *Proceedings of the National Academy of Sciences of the United States of America* **108**, 13089–13094.

Emanuelli, B., Vienberg, S. G., Smyth, G., Cheng, C., Stanford, K. I., Arumugam, M., Michael, M. D., Adams, A. C., Kharitononkov, A. and Kahn, C. R. (2014) Interplay between FGF21 and insulin action in the liver regulates metabolism. *The Journal of clinical investigation* **124**, 515–527.

Estes, C., Razavi, H., Loomba, R., Younossi, Z. and Sanyal, A. J. (2018) Modeling the epidemic of nonalcoholic fatty liver disease demonstrates an exponential increase in burden of disease. *Hepatology* **67**, 123–133.

- Evans, T. C., JR, Martin, D., Kolly, R., Panne, D., Sun, L., Ghosh, I., Chen, L., Benner, J., Liu, X. Q. and Xu, M. Q. (2000) Protein trans-splicing and cyclization by a naturally split intein from the dnaE gene of *Synechocystis species* PCC6803. *The Journal of biological chemistry* **275**, 9091–9094.
- Fatica, A., Di Lucia, F., Marino, S., Alvino, A., Zuin, M., Feijter, H. de, Brandt, B., Tommasini, S., Fantuz, F. and Salimei, E. (2019) Study on analytical characteristics of *Nicotiana tabacum* L., cv. *Solaris* biomass for potential uses in nutrition and biomethane production. *Scientific reports* **9**, 16828.
- Fazeli, P. K., Lun, M., Kim, S. M., Bredella, M. A., Wright, S., Zhang, Y., Lee, H., Catana, C., Klibanski, A., Patwari, P. and Steinhauser, M. L. (2015) FGF21 and the late adaptive response to starvation in humans. *The Journal of clinical investigation* **125**, 4601–4611.
- Feingold, K. R., Grunfeld, C., Heuer, J. G., Gupta, A., Cramer, M., Zhang, T., Shigenaga, J. K., Patzek, S. M., Chan, Z. W., Moser, A., Bina, H. and Kharitonov, A. (2012) FGF21 is increased by inflammatory stimuli and protects leptin-deficient ob/ob mice from the toxicity of sepsis. *Endocrinology* **153**, 2689–2700.
- Feng, H., Li, X., Song, W., Duan, M., Chen, H., Wang, T. and Dong, J. (2017) Oral Administration of a Seed-based Bivalent Rotavirus Vaccine Containing VP6 and NSP4 Induces Specific Immune Responses in Mice. *Frontiers in plant science* **8**, 910.
- Fiedler, U. and Conrad, U. (1995) High-level production and long-term storage of engineered antibodies in transgenic tobacco seeds. *Bio/technology (Nature Publishing Company)* **13**, 1090–1093.
- Fischer, R., Stoger, E., Schillberg, S., Christou, P. and Twyman, R. M. (2004) Plant-based production of biopharmaceuticals. *Current opinion in plant biology* **7**, 152–158.
- Fisher, F. M., Chui, P. C., Antonellis, P. J., Bina, H. A., Kharitonov, A., Flier, J. S. and Maratos-Flier, E. (2010) Obesity is a fibroblast growth factor 21 (FGF21)-resistant state. *Diabetes* **59**, 2781–2789.
- Fisher, F. M. and Maratos-Flier, E. (2016) Understanding the Physiology of FGF21. *Annual review of physiology* **78**, 223–241.
- Frega, N., Bocci, F., Conte, L. S. and Testa, F. (1991) Chemical composition of tobacco seeds (*Nicotiana tabacum* L.). *Journal of the American Oil Chemists Society* **68**, 29–33.
- Fu, H., Pang, S., Xue, P., Yang, J., Liu, X., Wang, Y., Li, T., Li, H. and Li, X. (2011) High levels of expression of fibroblast growth factor 21 in transgenic tobacco (*Nicotiana benthamiana*). *Applied biochemistry and biotechnology* **165**, 465–475.

- Fukuda, K., Ishida, W., Harada, Y., Wakasa, Y., Takagi, H., Takaiwa, F. and Fukushima, A. (2018) Efficacy of oral immunotherapy with a rice-based edible vaccine containing hypoallergenic Japanese cedar pollen allergens for treatment of established allergic conjunctivitis in mice. *Allergology international official journal of the Japanese Society of Allergology* **67**, 119–123.
- Fuller, R. S., Brake, A. J. and Thorner, J. (1989) Intracellular targeting and structural conservation of a prohormone-processing endoprotease. *Science (New York, N.Y.)* **246**, 482–486.
- Gaich, G., Chien, J. Y., Fu, H., Glass, L. C., Deeg, M. A., Holland, W. L., Kharitononkov, A., Bumol, T., Schilske, H. K. and Moller, D. E. (2013) The effects of LY2405319, an FGF21 analog, in obese human subjects with type 2 diabetes. *Cell metabolism* **18**, 333–340.
- Gälman, C., Lundåsen, T., Kharitononkov, A., Bina, H. A., Eriksson, M., Hafström, I., Dahlin, M., Amark, P., Angelin, B. and Rudling, M. (2008) The circulating metabolic regulator FGF21 is induced by prolonged fasting and PPARalpha activation in man. *Cell metabolism* **8**, 169–174.
- Gelvin, S. B. (2000) AGROBACTERIUM AND PLANT GENES INVOLVED IN T-DNA TRANSFER AND INTEGRATION. *Annual review of plant physiology and plant molecular biology* **51**, 223–256.
- Gelvin, S. B. (2003) Agrobacterium-mediated plant transformation: the biology behind the "gene-jockeying" tool. *Microbiology and molecular biology reviews MMBR* **67**, 16-37, table of contents.
- Gendron, F.-P., Mongrain, S., Laprise, P., McMahon, S., Dubois, C. M., Blais, M., Asselin, C. and Rivard, N. (2006) The CDX2 transcription factor regulates furin expression during intestinal epithelial cell differentiation. *American journal of physiology. Gastrointestinal and liver physiology* **290**, G310-318.
- Gengenbach, B. B., Keil, L. L., Opdensteinen, P., Müschen, C. R., Melmer, G., Lentzen, H., Bührmann, J. and Buyel, J. F. (2019) Comparison of microbial and transient expression (tobacco plants and plant-cell packs) for the production and purification of the anticancer mistletoe lectin viscumin. *Biotechnology and bioengineering* **116**, 2236–2249.
- Gengenbach, B. B., Müschen, C. R. and Buyel, J. F. (2018) Expression and purification of human phosphatase and actin regulator 1 (PHACTR1) in plant-based systems. *Protein expression and purification* **151**, 46–55.
- Ghasemi, A., Jeddi, S. and Kashfi, K. (2021) The laboratory rat: Age and body weight matter. *EXCLI journal* **20**, 1431–1445.

- Giannetti, A. M., Snow, P. M., Zak, O. and Björkman, P. J. (2003) Mechanism for multiple ligand recognition by the human transferrin receptor. *PLoS biology* **1**, E51.
- Gimeno, R. E. and Moller, D. E. (2014) FGF21-based pharmacotherapy--potential utility for metabolic disorders. *Trends in endocrinology and metabolism: TEM* **25**, 303–311.
- Giragossian, C., Vage, C., Li, J., Pelletier, K., Piché-Nicholas, N., Rajadhyaksha, M., Liras, J., Logan, A., Calle, R. A. and Weng, Y. (2015) Mechanistic investigation of the preclinical pharmacokinetics and interspecies scaling of PF-05231023, a fibroblast growth factor 21-antibody protein conjugate. *Drug metabolism and disposition: the biological fate of chemicals* **43**, 803–811.
- Giralt, M., Gavalda-Navarro, A. and Villarroja, F. (2015) Fibroblast growth factor-21, energy balance and obesity. *Molecular and Cellular Endocrinology* **418**, 66–73.
- Giritch, A., Marillonnet, S., Engler, C., van Eldik, G., Botterman, J., Klimyuk, V. and Gleba, Y. (2006) Rapid high-yield expression of full-size IgG antibodies in plants coinfecting with noncompeting viral vectors. *Proceedings of the National Academy of Sciences of the United States of America* **103**, 14701–14706.
- Gleba, Y., Klimyuk, V. and Marillonnet, S. (2005) Magniffection--a new platform for expressing recombinant vaccines in plants. *Vaccine* **23**, 2042–2048.
- Goetz, R., Beenken, A., Ibrahimi, O. A., Kalinina, J., Olsen, S. K., Eliseenkova, A. V., Xu, C., Neubert, T. A., Zhang, F., Linhardt, R. J., Yu, X., White, K. E., Inagaki, T., Kliewer, S. A., Yamamoto, M., Kurosu, H., Ogawa, Y., Kuro-o, M., Lanske, B., Razzaque, M. S. and Mohammadi, M. (2007) Molecular insights into the klotho-dependent, endocrine mode of action of fibroblast growth factor 19 subfamily members. *Molecular and cellular biology* **27**, 3417–3428.
- Goetz, R. and Mohammadi, M. (2013) Exploring mechanisms of FGF signalling through the lens of structural biology. *Nature reviews. Molecular cell biology* **14**, 166–180.
- Gómez-Sámano, M. Á., Grajales-Gómez, M., Zuarth-Vázquez, J. M., Navarro-Flores, M. F., Martínez-Saavedra, M., Juárez-León, Ó. A., Morales-García, M. G., Enríquez-Estrada, V. M., Gómez-Pérez, F. J. and Cuevas-Ramos, D. (2017) Fibroblast growth factor 21 and its novel association with oxidative stress. *Redox biology* **11**, 335–341.
- Gregory, J. and Barany, S. (2011) Adsorption and flocculation by polymers and polymer mixtures. *Advances in colloid and interface science* **169**, 1–12.
- Grisan, S., Polizzotto, R., Raiola, P., Cristiani, S., Ventura, F., Di Lucia, F., Zuin, M., Tommasini, S., Morbidelli, R., Damiani, F., Pupilli, F. and Bellucci, M. (2016) Alternative

use of tobacco as a sustainable crop for seed oil, biofuel, and biomass. *Agronomy for Sustainable Development* **36**, 55.

Hall, D. R., Hadden, J. M., Leonard, G. A., Bailey, S., Neu, M., Winn, M. and Lindley, P. F. (2002) The crystal and molecular structures of diferric porcine and rabbit serum transferrins at resolutions of 2.15 and 2.60 Å, respectively. *Acta crystallographica. Section D, Biological crystallography* **58**, 70–80.

Hassan, S., van Dolleweerd, C. J., Ioakeimidis, F., Keshavarz-Moore, E. and Ma, J. K.-C. (2008) Considerations for extraction of monoclonal antibodies targeted to different subcellular compartments in transgenic tobacco plants. *Plant biotechnology journal* **6**, 733–748.

Hayden, C. A., Streatfield, S. J., Lamphear, B. J., Fake, G. M., Keener, T. K., Walker, J. H., Clements, J. D., Turner, D. D., Tizard, I. R. and Howard, J. A. (2012) Bioencapsulation of the hepatitis B surface antigen and its use as an effective oral immunogen. *Vaccine* **30**, 2937–2942.

Hecht, R., Li, Y.-S., Sun, J., Belouski, E., Hall, M., Hager, T., Yie, J., Wang, W., Winters, D., Smith, S., Spahr, C., Tam, L.-T., Shen, Z., Stanislaus, S., Chinookoswong, N., Lau, Y., Sickmier, A., Michaels, M. L., Boone, T., Véniant, M. M. and Xu, J. (2012) Rationale-Based Engineering of a Potent Long-Acting FGF21 Analog for the Treatment of Type 2 Diabetes. *PloS one* **7**, e49345.

Hensel, G., Floss, D. M., Arcalis, E., Sack, M., Melnik, S., Altmann, F., Rutten, T., Kumlehn, J., Stoger, E. and Conrad, U. (2015) Transgenic Production of an Anti HIV Antibody in the Barley Endosperm. *PloS one* **10**, e0140476.

Hentze, M. W., Muckenthaler, M. U. and Andrews, N. C. (2004) Balancing acts: molecular control of mammalian iron metabolism. *Cell* **117**, 285–297.

Hernández-Velázquez, A., López-Quesada, A., Ceballo-Cámara, Y., Cabrera-Herrera, G., Tiel-González, K., Mirabal-Ortega, L., Pérez-Martínez, M., Pérez-Castillo, R., Rosabal-Ayán, Y., Ramos-González, O., Enríquez-Obregón, G., Depicker, A. and Pujol-Ferrer, M. (2015) Tobacco seeds as efficient production platform for a biologically active anti-HBsAg monoclonal antibody. *Transgenic research* **24**, 897–909.

Herzog, R. W., Sherman, A., Kwon, K.-C., Chang, W.-J. and Daniell, H. (2017) Lettuce Plants Expressing High Levels of Factor VIII Antigen in the Chloroplast for Oral Tolerance in Hemophilia a. *Blood* **130**, 362.

Hoefkens, P., Smit, M. H. de, Jeu-Jaspars, N. M. de, Huijskes-Heins, M. I., Jong, G. de and van Eijk, H. G. (1996) Isolation, renaturation and partial characterization of recombinant

human transferrin and its half molecules from *Escherichia coli*. *The international journal of biochemistry & cell biology* **28**, 975–982.

Holler, C., Vaughan, D. and Zhang, C. (2007) Polyethyleneimine precipitation versus anion exchange chromatography in fractionating recombinant beta-glucuronidase from transgenic tobacco extract. *Journal of chromatography* **1142**, 98–105.

Holler, C. and Zhang, C. (2008) Purification of an acidic recombinant protein from transgenic tobacco. *Biotechnology and bioengineering* **99**, 902–909.

Holtz, B. R., Berquist, B. R., Bennett, L. D., Kommineni, V. J. M., Muniguntti, R. K., White, E. L., Wilkerson, D. C., Wong, K.-Y. I., Ly, L. H. and Marcel, S. (2015) Commercial-scale biotherapeutics manufacturing facility for plant-made pharmaceuticals. *Plant biotechnology journal* **13**, 1180–1190.

Horsch, R. B., Fry, J. E., Hoffmann, N. L., Wallroth, M., Eichholtz, D., Rogers, S. G. and Fraley, R. T. (1985) A Simple and General Method for Transferring Genes into Plants. *Science (New York, N.Y.)* **227**, 1229–1231.

Hou, H.-W., Bishop, C. A., Huckauf, J., Broer, I., Klaus, S., Nausch, H. and Buyel, J. F. (2022) Seed- and leaf-based expression of FGF21-transferrin fusion proteins for oral delivery and treatment of non-alcoholic steatohepatitis. *Frontiers in plant science* **13**, 998596.

Houdelet, M., Galinski, A., Holland, T., Wenzel, K., Schillberg, S. and Buyel, J. F. (2017) Animal component-free *Agrobacterium tumefaciens* cultivation media for better GMP-compliance increases biomass yield and pharmaceutical protein expression in *Nicotiana benthamiana*. *Biotechnology journal* **12**.

Huang, J., Ishino, T., Chen, G., Rolzin, P., Osothprarop, T. F., Retting, K., Li, L., Jin, P., Matin, M. J., Huyghe, B., Talukdar, S., Bradshaw, C. W., Palanki, M., Violand, B. N., Woodnutt, G., Lappe, R. W., Ogilvie, K. and Levin, N. (2013) Development of a novel long-acting antidiabetic FGF21 mimetic by targeted conjugation to a scaffold antibody. *The Journal of pharmacology and experimental therapeutics* **346**, 270–280.

Huebbers, J. W. and Buyel, J. F. (2021) On the verge of the market - Plant factories for the automated and standardized production of biopharmaceuticals. *Biotechnology advances* **46**, 107681.

Huggenvik, J. I., Craven, C. M., Idzerda, R. L., Bernstein, S., Kaplan, J. and McKnight, G. S. (1989) A splicing defect in the mouse transferrin gene leads to congenital atransferrinemia. *Blood* **74**, 482–486.

- Hui, H., Farilla, L., Merkel, P. and Perfetti, R. (2002) The short half-life of glucagon-like peptide-1 in plasma does not reflect its long-lasting beneficial effects. *European journal of endocrinology* **146**, 863–869.
- Inagaki, T., Dutchak, P., Zhao, G., Ding, X., Gautron, L., Parameswara, V., Li, Y., Goetz, R., Mohammadi, M., Esser, V., Elmquist, J. K., Gerard, R. D., Burgess, S. C., Hammer, R. E., Mangelsdorf, D. J. and Kliewer, S. A. (2007) Endocrine regulation of the fasting response by PPARalpha-mediated induction of fibroblast growth factor 21. *Cell metabolism* **5**, 415–425.
- Inagaki, T., Lin, V. Y., Goetz, R., Mohammadi, M., Mangelsdorf, D. J. and Kliewer, S. A. (2008) Inhibition of growth hormone signaling by the fasting-induced hormone FGF21. *Cell metabolism* **8**, 77–83.
- Ito, S., Kinoshita, S., Shiraishi, N., Nakagawa, S., Sekine, S., Fujimori, T. and Nabeshima, Y. I. (2000) Molecular cloning and expression analyses of mouse betaklotho, which encodes a novel Klotho family protein. *Mechanisms of development* **98**, 115–119.
- Itoh, N. (2014) FGF21 as a Hepatokine, Adipokine, and Myokine in Metabolism and Diseases. *Frontiers in endocrinology* **5**, 107.
- Itoh, N., Nakayama, Y. and Konishi, M. (2016) Roles of FGFs As Paracrine or Endocrine Signals in Liver Development, Health, and Disease. *Frontiers in cell and developmental biology* **4**, 30.
- Itoh, N. and Ornitz, D. M. (2011) Fibroblast growth factors: from molecular evolution to roles in development, metabolism and disease. *Journal of biochemistry* **149**, 121–130.
- Iyori, M., Nakaya, H., Inagaki, K., Pichyangkul, S., Yamamoto, D. S., Kawasaki, M., Kwak, K., Mizukoshi, M., Goto, Y., Matsuoka, H., Matsumoto, M. and Yoshida, S. (2013) Protective efficacy of baculovirus dual expression system vaccine expressing *Plasmodium falciparum* circumsporozoite protein. *PloS one* **8**, e70819.
- Jaeger, G. de, Scheffer, S., Jacobs, A., Zambre, M., Zobell, O., Goossens, A., Depicker, A. and Angenon, G. (2002) Boosting heterologous protein production in transgenic dicotyledonous seeds using *Phaseolus vulgaris* regulatory sequences. *Nature biotechnology* **20**, 1265–1268.
- Jimenez, V., Jambrina, C., Casana, E., Sacristan, V., Muñoz, S., Darriba, S., Rodó, J., Mallol, C., Garcia, M., León, X., Marcó, S., Ribera, A., Elias, I., Casellas, A., Grass, I., Elias, G., Ferré, T., Motas, S., Franckhauser, S., Mulero, F., Navarro, M., Haurigot, V., Ruberte, J. and Bosch, F. (2018) FGF21 gene therapy as treatment for obesity and insulin resistance. *EMBO molecular medicine* **10**.

- Kang, H., Park, Y., Lee, Y., Yoo, Y.-J. and Hwang, I. (2018) Fusion of a highly N-glycosylated polypeptide increases the expression of ER-localized proteins in plants. *Scientific reports* **8**, 4612.
- Keinicke, H., Sun, G., Mentzel, C. M. J., Fredholm, M., John, L. M., Andersen, B., Raun, K. and Kjaergaard, M. (2020) FGF21 regulates hepatic metabolic pathways to improve steatosis and inflammation. *Endocrine connections* **9**, 755–768.
- Kempe, K., Rubtsova, M. and Gils, M. (2009) Intein-mediated protein assembly in transgenic wheat: production of active barnase and acetolactate synthase from split genes. *Plant biotechnology journal* **7**, 283–297.
- Kesik-Brodacka, M. (2018) Progress in biopharmaceutical development. *Biotechnology and applied biochemistry* **65**, 306–322.
- Khan, I. and Daniell, H. (2021) Oral delivery of therapeutic proteins bioencapsulated in plant cells: preclinical and clinical advances. *Current opinion in colloid & interface science* **54**.
- Kharitononkov, A. and Adams, A. C. (2014) Inventing new medicines: The FGF21 story. *Molecular metabolism* **3**, 221–229.
- Kharitononkov, A., Beals, J. M., Micanovic, R., Striffler, B. A., Rathnachalam, R., Wroblewski, V. J., Li, S., Koester, A., Ford, A. M., Coskun, T., Dunbar, J. D., Cheng, C. C., Frye, C. C., Bumol, T. F. and Moller, D. E. (2013) Rational design of a fibroblast growth factor 21-based clinical candidate, LY2405319. *PloS one* **8**, e58575.
- Kharitononkov, A. and DiMarchi, R. (2017) Fibroblast growth factor 21 night watch: advances and uncertainties in the field. *Journal of internal medicine* **281**, 233–246.
- Kharitononkov, A., Dunbar, J. D., Bina, H. A., Bright, S., Moyers, J. S., Zhang, C., Ding, L., Micanovic, R., Mehrbod, S. F., Knierman, M. D., Hale, J. E., Coskun, T. and Shanafelt, A. B. (2008) FGF-21/FGF-21 receptor interaction and activation is determined by betaKlotho. *Journal of cellular physiology* **215**, 1–7.
- Kharitononkov, A., Shiyanova, T. L., Koester, A., Ford, A. M., Micanovic, R., Galbreath, E. J., Sandusky, G. E., Hammond, L. J., Moyers, J. S., Owens, R. A., Gromada, J., Brozinick, J. T., Hawkins, E. D., Wroblewski, V. J., Li, D.-S., Mehrbod, F., Jaskunas, S. R. and Shanafelt, A. B. (2005) FGF-21 as a novel metabolic regulator. *The Journal of clinical investigation* **115**, 1627–1635.
- Kharitononkov, A., Wroblewski, V. J., Koester, A., Chen, Y.-F., Clutinger, C. K., Tigno, X. T., Hansen, B. C., Shanafelt, A. B. and Etgen, G. J. (2007) The metabolic state of diabetic monkeys is regulated by fibroblast growth factor-21. *Endocrinology* **148**, 774–781.

Kim, B.-J., Zhou, J., Martin, B., Carlson, O. D., Maudsley, S., Greig, N. H., Mattson, M. P., Ladenheim, E. E., Wustner, J., Turner, A., Sadeghi, H. and Egan, J. M. (2010) Transferrin fusion technology: a novel approach to prolonging biological half-life of insulinotropic peptides. *The Journal of pharmacology and experimental therapeutics* **334**, 682–692.

Kimple, M. E., Brill, A. L. and Pasker, R. L. (2013) Overview of affinity tags for protein purification. *Current protocols in protein science* **73**, 9.9.1-9.9.23.

Kinal, H., Park, C. M., Berry, J. O., Koltin, Y. and Bruenn, J. A. (1995) Processing and secretion of a virally encoded antifungal toxin in transgenic tobacco plants: evidence for a Kex2p pathway in plants. *The Plant cell* **7**, 677–688.

Knights, V. and Cook, S. J. (2010) De-regulated FGF receptors as therapeutic targets in cancer. *Pharmacology & therapeutics* **125**, 105–117.

Knödler, M., Opdensteinen, P., Sankaranarayanan, R. A., Morgenroth, A., Buhl, E. M., Mottaghy, F. M. and Buyel, J. F. (2023) Simple plant-based production and purification of the assembled human ferritin heavy chain as a nanocarrier for tumor-targeted drug delivery and bioimaging in cancer therapy. *Biotechnology and bioengineering* **120**, 1038–1054.

Kohli, N., Westerveld, D. R., Ayache, A. C., Verma, A., Shil, P., Prasad, T., Zhu, P., Chan, S. L., Li, Q. and Daniell, H. (2014) Oral delivery of bioencapsulated proteins across blood-brain and blood-retinal barriers. *Molecular therapy the journal of the American Society of Gene Therapy* **22**, 535–546.

Kumar, M., Tomar, M., Potkule, J., Verma, R., Punia, S., Mahapatra, A., Belwal, T., Dahuja, A., Joshi, S., Berwal, M. K., Satankar, V., Bhoite, A. G., Amarowicz, R., Kaur, C. and Kennedy, J. F. (2021) Advances in the plant protein extraction: Mechanism and recommendations. *Food Hydrocolloids* **115**, 106595.

Kurosu, H., Choi, M., Ogawa, Y., Dickson, A. S., Goetz, R., Eliseenkova, A. V., Mohammadi, M., Rosenblatt, K. P., Kliwer, S. A. and Kuro-o, M. (2007) Tissue-specific expression of betaKlotho and fibroblast growth factor (FGF) receptor isoforms determines metabolic activity of FGF19 and FGF21. *The Journal of biological chemistry* **282**, 26687–26695.

Kurosu, H., Ogawa, Y., Miyoshi, M., Yamamoto, M., Nandi, A., Rosenblatt, K. P., Baum, M. G., Schiavi, S., Hu, M.-C., Moe, O. W. and Kuro-o, M. (2006) Regulation of fibroblast growth factor-23 signaling by klotho. *The Journal of biological chemistry* **281**, 6120–6123.

Kusnadi, A. R., Nikolov, Z. L. and Howard, J. A. (1997) Production of recombinant proteins in transgenic plants: Practical considerations. *Biotechnology and bioengineering* **56**, 473–484.

- Kwon, K.-C. and Daniell, H. (2015) Low-cost oral delivery of protein drugs bioencapsulated in plant cells. *Plant biotechnology journal* **13**, 1017–1022.
- Kwon, K.-C. and Daniell, H. (2016) Oral Delivery of Protein Drugs Bioencapsulated in Plant Cells. *Molecular therapy the journal of the American Society of Gene Therapy* **24**, 1342–1350.
- Kwon, K.-C., Nityanandam, R., New, J. S. and Daniell, H. (2013) Oral delivery of bioencapsulated exendin-4 expressed in chloroplasts lowers blood glucose level in mice and stimulates insulin secretion in beta-TC6 cells. *Plant biotechnology journal* **11**, 77–86.
- Kwon, K.-C., Sherman, A., Chang, W.-J., Kamesh, A., Biswas, M., Herzog, R. W. and Daniell, H. (2018) Expression and assembly of largest foreign protein in chloroplasts: oral delivery of human FVIII made in lettuce chloroplasts robustly suppresses inhibitor formation in haemophilia A mice. *Plant biotechnology journal* **16**, 1148–1160.
- Kyndt, T., Quispe, D., Zhai, H., Jarret, R., Ghislain, M., Liu, Q., Gheysen, G. and Kreuze, J. F. (2015) The genome of cultivated sweet potato contains *Agrobacterium* T-DNAs with expressed genes: An example of a naturally transgenic food crop. *Proceedings of the National Academy of Sciences of the United States of America* **112**, 5844–5849.
- LaBrecque, D. R., Abbas, Z., Anania, F., Ferenci, P., Khan, A. G., Goh, K.-L., Hamid, S. S., Isakov, V., Lizarzabal, M., Peñaranda, M. M., Ramos, J. F. R., Sarin, S., Stimac, D., Thomson, A. B. R., Umar, M., Krabshuis, J. and LeMair, A. (2014) World Gastroenterology Organisation global guidelines: Nonalcoholic fatty liver disease and nonalcoholic steatohepatitis. *Journal of clinical gastroenterology* **48**, 467–473.
- Laeger, T., Baumeier, C., Wilhelmi, I., Würfel, J., Kamitz, A. and Schürmann, A. (2017) FGF21 improves glucose homeostasis in an obese diabetes-prone mouse model independent of body fat changes. *Diabetologia* **60**, 2274–2284.
- Lawrence, C. M., Ray, S., Babyonyshev, M., Galluser, R., Borhani, D. W. and Harrison, S. C. (1999) Crystal structure of the ectodomain of human transferrin receptor. *Science (New York, N.Y.)* **286**, 779–782.
- Lee, C., Kim, H.-H., Choi, K. M., Chung, K. W., Choi, Y. K., Jang, M. J., Kim, T.-S., Chung, N.-J., Rhie, H.-G., Lee, H.-S., Sohn, Y., Kim, H., Lee, S.-J. and Lee, H.-W. (2011) Murine immune responses to a *Plasmodium vivax*-derived chimeric recombinant protein expressed in *Brassica napus*. *Malaria journal* **10**, 106.
- Lee, K.-Y., Kim, D.-H., Kang, T.-J., Kim, J., Chung, G.-H., Yoo, H.-S., Arntzen, C. J., Yang, M.-S. and Jang, Y.-S. (2006) Induction of protective immune responses against the challenge of *Actinobacillus pleuropneumoniae* by the oral administration of transgenic tobacco plant

expressing ApxIIA toxin from the bacteria. *FEMS immunology and medical microbiology* **48**, 381–389.

Li, H., Bao, Y., Xu, A., Pan, X., Lu, J., Wu, H., Lu, H., Xiang, K. and Jia, W. (2009) Serum fibroblast growth factor 21 is associated with adverse lipid profiles and gamma-glutamyltransferase but not insulin sensitivity in Chinese subjects. *The Journal of clinical endocrinology and metabolism* **94**, 2151–2156.

Li, H., Fang, Q., Gao, F., Fan, J., Zhou, J., Wang, X., Zhang, H., Pan, X., Bao, Y., Xiang, K., Xu, A. and Jia, W. (2010) Fibroblast growth factor 21 levels are increased in nonalcoholic fatty liver disease patients and are correlated with hepatic triglyceride. *Journal of hepatology* **53**, 934–940.

Li, H. and Qian, Z. M. (2002) Transferrin/transferrin receptor-mediated drug delivery. *Medicinal research reviews* **22**, 225–250.

Li, S.-A., Watanabe, M., Yamada, H., Nagai, A., Kinuta, M. and Takei, K. (2004) Immunohistochemical localization of Klotho protein in brain, kidney, and reproductive organs of mice. *Cell structure and function* **29**, 91–99.

Lico, C., Chen, Q. and Santi, L. (2008) Viral vectors for production of recombinant proteins in plants. *Journal of cellular physiology* **216**, 366–377.

Lindbo, J. A. (2007) High-efficiency protein expression in plants from agroinfection-compatible Tobacco mosaic virus expression vectors. *BMC biotechnology* **7**, 52.

Liu, Y., Wang, H.-Y., Shao, J., Zaro, J. L. and Shen, W.-C. (2020) Enhanced insulin receptor interaction by a bifunctional insulin-transferrin fusion protein: an approach to overcome insulin resistance. *Scientific reports* **10**, 7724.

Lu, X., Jin, X., Huang, Y., Wang, J., Shen, J., Chu, F., Mei, H., Ma, Y. and Zhu, J. (2014) Construction of a novel liver-targeting fusion interferon by incorporation of a *Plasmodium* region I-plus peptide. *BioMed research international* **2014**, 261631.

Lundåsen, T., Hunt, M. C., Nilsson, L.-M., Sanyal, S., Angelin, B., Alexson, S. E. H. and Rudling, M. (2007) PPARalpha is a key regulator of hepatic FGF21. *Biochemical and biophysical research communications* **360**, 437–440.

Ma, J. K., Hiatt, A., Hein, M., Vine, N. D., Wang, F., Stabila, P., van Dolleweerd, C., Mostov, K. and Lehner, T. (1995) Generation and assembly of secretory antibodies in plants. *Science (New York, N.Y.)* **268**, 716–719.

Ma, J. K.-C., Drossard, J., Lewis, D., Altmann, F., Boyle, J., Christou, P., Cole, T., Dale, P., van Dolleweerd, C. J., Isitt, V., Katinger, D., Lobedan, M., Mertens, H., Paul, M. J., Rademacher, T., Sack, M., Hundleby, P. A. C., Stiegler, G., Stoger, E., Twyman, R. M.,

- Vcelar, B. and Fischer, R. (2015) Regulatory approval and a first-in-human phase I clinical trial of a monoclonal antibody produced in transgenic tobacco plants. *Plant biotechnology journal* **13**, 1106–1120.
- Ma, Y., Jin, X.-B., Chu, F.-J., Bao, D.-M. and Zhu, J.-Y. (2014) Expression of liver-targeting peptide modified recombinant human endostatin and preliminary study of its biological activities. *Applied microbiology and biotechnology* **98**, 7923–7933.
- Maa, Y.-F. and Hsu, C. C. (1996) Aggregation of recombinant human growth hormone induced by phenolic compounds. *International Journal of Pharmaceutics* **140**, 155–168.
- Maclean, J., Koekemoer, M., Olivier, A. J., Stewart, D., Hitzeroth, I. I., Rademacher, T., Fischer, R., Williamson, A.-L. and Rybicki, E. P. (2007) Optimization of human papillomavirus type 16 (HPV-16) L1 expression in plants: comparison of the suitability of different HPV-16 L1 gene variants and different cell-compartment localization. *The Journal of general virology* **88**, 1460–1469.
- Mamedov, T., Musayeva, I., Acsora, R., Gun, N., Gulec, B., Mammadova, G., Cicek, K. and Hasanova, G. (2019) Engineering, and production of functionally active human Furin in *N. benthamiana* plant: In vivo post-translational processing of target proteins by Furin in plants. *PloS one* **14**, e0213438.
- Mantamadiotis, T., Papalexis, N. and Dworkin, S. (2012) CREB signalling in neural stem/progenitor cells: recent developments and the implications for brain tumour biology. *BioEssays news and reviews in molecular, cellular and developmental biology* **34**, 293–300.
- Margolin, E., Oh, Y. J., Verbeek, M., Naude, J., Ponndorf, D., Meshcheriakova, Y. A., Peyret, H., van Diepen, M. T., Chapman, R., Meyers, A. E., Lomonossoff, G. P., Matoba, N., Williamson, A.-L. and Rybicki, E. P. (2020) Co-expression of human calreticulin significantly improves the production of HIV gp140 and other viral glycoproteins in plants. *Plant biotechnology journal* **18**, 2109–2117.
- Marillonnet, S., Thoeringer, C., Kandzia, R., Klimyuk, V. and Gleba, Y. (2005) Systemic Agrobacterium tumefaciens-mediated transfection of viral replicons for efficient transient expression in plants. *Nature biotechnology* **23**, 718–723.
- Markan, K. R., Naber, M. C., Ameka, M. K., Anderegg, M. D., Mangelsdorf, D. J., Kliewer, S. A., Mohammadi, M. and Potthoff, M. J. (2014) Circulating FGF21 is liver derived and enhances glucose uptake during refeeding and overfeeding. *Diabetes* **63**, 4057–4063.
- Mason, A. B., Byrne, S. L., Everse, S. J., Roberts, S. E., Chasteen, N. D., Smith, V. C., MacGillivray, R. T. A., Kandemir, B. and Bou-Abdallah, F. (2009) A loop in the N-lobe of human serum transferrin is critical for binding to the transferrin receptor as revealed by

mutagenesis, isothermal titration calorimetry, and epitope mapping. *Journal of molecular recognition JMR* **22**, 521–529.

Mason, A. B., Miller, M. K., Funk, W. D., Banfield, D. K., Savage, K. J., Oliver, R. W., Green, B. N., MacGillivray, R. T. and Woodworth, R. C. (1993) Expression of glycosylated and nonglycosylated human transferrin in mammalian cells. Characterization of the recombinant proteins with comparison to three commercially available transferrins. *Biochemistry* **32**, 5472–5479.

Mason, A. B., Woodworth, R. C., Oliver, R. W., Green, B. N., Lin, L. N., Brandts, J. F., Tam, B. M., Maxwell, A. and MacGillivray, R. T. (1996) Production and isolation of the recombinant N-lobe of human serum transferrin from the methylotrophic yeast *Pichia pastoris*. *Protein expression and purification* **8**, 119–125.

Matsubara, M., Kanemoto, S., Leshnowar, B. G., Albone, E. F., Hinmon, R., Plappert, T., Gorman, J. H. 3. and Gorman, R. C. (2011) Single dose GLP-1-Tf ameliorates myocardial ischemia/reperfusion injury. *The Journal of surgical research* **165**, 38–45.

Menassa, R., Zhu, H., Karatzas, C. N., Lazaris, A., Richman, A. and Brandle, J. (2004) Spider dragline silk proteins in transgenic tobacco leaves: accumulation and field production. *Plant biotechnology journal* **2**, 431–438.

Meng, F., Cao, Y., Khoso, M. H., Kang, K., Ren, G., Xiao, W. and Li, D. (2021) Therapeutic effect and mechanism of combined use of FGF21 and insulin on diabetic nephropathy. *Archives of biochemistry and biophysics* **713**, 109063.

Menkhaus, T. J., Bai, Y., Zhang, C., Nikolov, Z. L. and Glatz, C. E. (2004) Considerations for the recovery of recombinant proteins from plants. *Biotechnology progress* **20**, 1001–1014.

Menzel, S., Holland, T., Boes, A., Spiegel, H., Bolzenius, J., Fischer, R. and Buyel, J. F. (2016) Optimized Blanching Reduces the Host Cell Protein Content and Substantially Enhances the Recovery and Stability of Two Plant-Derived Malaria Vaccine Candidates. *Frontiers in plant science* **7**, 159.

Merlin, M., Gecchele, E., Arcalis, E., Remelli, S., Brozzetti, A., Pezzotti, M. and Avesani, L. (2016) Enhanced GAD65 production in plants using the MagnICON transient expression system: Optimization of upstream production and downstream processing. *Biotechnology journal* **11**, 542–553.

Moravec, T., Schmidt, M. A., Herman, E. M. and Woodford-Thomas, T. (2007) Production of *Escherichia coli* heat labile toxin (LT) B subunit in soybean seed and analysis of its immunogenicity as an oral vaccine. *Vaccine* **25**, 1647–1657.

- Moustafa, K., Makhzoum, A. and Trémouillaux-Guiller, J. (2016) Molecular farming on rescue of pharma industry for next generations. *Critical reviews in biotechnology* **36**, 840–850.
- Mraz, M., Bartlova, M., Lacinova, Z., Michalsky, D., Kasalicky, M., Haluzikova, D., Matoulek, M., Dostalova, I., Humenanska, V. and Haluzik, M. (2009) Serum concentrations and tissue expression of a novel endocrine regulator fibroblast growth factor-21 in patients with type 2 diabetes and obesity. *Clinical endocrinology* **71**, 369–375.
- Mullard, A. (2020) FDA rejects NASH drug. *Nature reviews. Drug discovery* **19**, 501.
- Nahampun, H. N., Bosworth, B., Cunnick, J., Mogler, M. and Wang, K. (2015) Expression of H3N2 nucleoprotein in maize seeds and immunogenicity in mice. *Plant cell reports* **34**, 969–980.
- Nakayama, K. (1997) Furin: a mammalian subtilisin/Kex2p-like endoprotease involved in processing of a wide variety of precursor proteins. *The Biochemical journal* **327**, 625–635.
- Nandi, S., Kwong, A. T., Holtz, B. R., Erwin, R. L., Marcel, S. and McDonald, K. A. (2016) Techno-economic analysis of a transient plant-based platform for monoclonal antibody production. *mAbs* **8**, 1456–1466.
- Nausch, H., Hausmann, T., Ponndorf, D., Hühns, M., Hoedtke, S., Wolf, P., Zeyner, A. and Broer, I. (2016) Tobacco as platform for a commercial production of cyanophycin. *New biotechnology* **33**, 842–851.
- Nausch, H., Mikschofsky, H., Koslowski, R., Meyer, U., Broer, I. and Huckauf, J. (2012a) Expression and subcellular targeting of human complement factor C5a in *Nicotiana* species. *PloS one* **7**, e53023.
- Nausch, H., Mikschofsky, H., Koslowski, R., Meyer, U., Broer, I. and Huckauf, J. (2012b) High-level transient expression of ER-targeted human interleukin 6 in *Nicotiana benthamiana*. *PloS one* **7**, e48938.
- Nishimura, T., Nakatake, Y., Konishi, M. and Itoh, N. (2000) Identification of a novel FGF, FGF-21, preferentially expressed in the liver. *Biochimica et biophysica acta* **1492**, 203–206.
- Nochi, T., Takagi, H., Yuki, Y., Yang, L., Masumura, T., Mejima, M., Nakanishi, U., Matsumura, A., Uozumi, A., Hiroi, T., Morita, S., Tanaka, K., Takaiwa, F. and Kiyono, H. (2007) Rice-based mucosal vaccine as a global strategy for cold-chain- and needle-free vaccination. *Proceedings of the National Academy of Sciences of the United States of America* **104**, 10986–10991.
- Ogawa, Y., Kurosu, H., Yamamoto, M., Nandi, A., Rosenblatt, K. P., Goetz, R., Eliseenkova, A. V., Mohammadi, M. and Kuro-o, M. (2007) BetaKlotho is required for metabolic activity

of fibroblast growth factor 21. *Proceedings of the National Academy of Sciences of the United States of America* **104**, 7432–7437.

Opdensteinen, P., Clodt, J. I., Müschen, C. R., Filiz, V. and Buyel, J. F. (2018) A Combined Ultrafiltration/Diafiltration Step Facilitates the Purification of Cyanovirin-N From Transgenic Tobacco Extracts. *Frontiers in bioengineering and biotechnology* **6**, 206.

Opdensteinen, P., Dietz, S. J., Gengenbach, B. B. and Buyel, J. F. (2021a) Expression of Biofilm-Degrading Enzymes in Plants and Automated High-Throughput Activity Screening Using Experimental *Bacillus subtilis* Biofilms. *Frontiers in bioengineering and biotechnology* **9**, 708150.

Opdensteinen, P., Lobanov, A. and Buyel, J. F. (2021b) A combined pH and temperature precipitation step facilitates the purification of tobacco-derived recombinant proteins that are sensitive to extremes of either parameter. *Biotechnology journal* **16**, e2000340.

Ornitz, D. M. and Itoh, N. (2015) The Fibroblast Growth Factor signaling pathway. *Wiley interdisciplinary reviews. Developmental biology* **4**, 215–266.

Oulion, S., Bertrand, S. and Escriva, H. (2012) Evolution of the FGF Gene Family. *International journal of evolutionary biology* **2012**, 298147.

Owen, B. M., Ding, X., Morgan, D. A., Coate, K. C., Bookout, A. L., Rahmouni, K., Klierer, S. A. and Mangelsdorf, D. J. (2014) FGF21 acts centrally to induce sympathetic nerve activity, energy expenditure, and weight loss. *Cell metabolism* **20**, 670–677.

Ozyigit, I. I. and Yucebilgili Kurtoglu, K. (2020) Particle bombardment technology and its applications in plants. *Molecular biology reports* **47**, 9831–9847.

Pacini, L., Jenks, A. D., Lima, N. C. and Huang, P. H. (2021) Targeting the Fibroblast Growth Factor Receptor (FGFR) Family in Lung Cancer. *Cells* **10**.

Parkkinen, J., Bonsdorff, L. von, Ebeling, F. and Sahlstedt, L. (2002) Function and therapeutic development of apotransferrin. *Vox sanguinis* **83 Suppl 1**, 321–326.

Perrimon, N. and Bernfield, M. (2000) Specificities of heparan sulphate proteoglycans in developmental processes. *Nature* **404**, 725–728.

Phan, H. T., Hause, B., Hause, G., Arcalis, E., Stoger, E., Maresch, D., Altmann, F., Joensuu, J. and Conrad, U. (2014) Influence of elastin-like polypeptide and hydrophobin on recombinant hemagglutinin accumulations in transgenic tobacco plants. *PloS one* **9**, e99347.

Phan, H. T., van Pham, T., Ho, T. T., Pham, N. B., Chu, H. H., Vu, T. H., Abdelwhab, E. M., Scheibner, D., Mettenleiter, T. C., Hanh, T. X., Meister, A., Gresch, U. and Conrad, U. (2020) Immunization with Plant-Derived Multimeric H5 Hemagglutinins Protect Chicken against Highly Pathogenic Avian Influenza Virus H5N1. *Vaccines* **8**.

- Qi, J., Ye, X., Li, L., Bai, H. and Xu, C. (2018) Improving the specific antitumor efficacy of ONC by fusion with N-terminal domain of transferrin. *Bioscience, biotechnology, and biochemistry* **82**, 1153–1158.
- Queiroz, L. N., Maldaner, F. R., Mendes, É. A., Sousa, A. R., D'Allastta, R. C., Mendonça, G., Mendonça, D. B. S. and Aragão, F. J. L. (2019) Evaluation of lettuce chloroplast and soybean cotyledon as platforms for production of functional bone morphogenetic protein 2. *Transgenic research* **28**, 213–224.
- Ridgley, L. A., Falci Finardi, N., Gengenbach, B. B., Opdensteinen, P., Croxford, Z., Ma, J. K.-C., Bodman-Smith, M., Buyel, J. F. and Teh, A. Y.-H. (2023) Killer to cure: Expression and production costs calculation of tobacco plant-made cancer-immune checkpoint inhibitors. *Plant biotechnology journal* **21**, 1254–1269.
- Rosen, E. D., Sarraf, P., Troy, A. E., Bradwin, G., Moore, K., Milstone, D. S., Spiegelman, B. M. and Mortensen, R. M. (1999) PPAR gamma is required for the differentiation of adipose tissue *in vivo* and *in vitro*. *Molecular cell* **4**, 611–617.
- Rossi, L., Dell'Orto, V., Vagni, S., Sala, V., Reggi, S. and Baldi, A. (2014) Protective effect of oral administration of transgenic tobacco seeds against verocytotoxic *Escherichia coli* strain in piglets. *Veterinary research communications* **38**, 39–49.
- Rossi, L., Di Giancamillo, A., Reggi, S., Domeneghini, C., Baldi, A., Sala, V., Dell'Orto, V., Coddens, A., Cox, E. and Fogher, C. (2013) Expression of verocytotoxic *Escherichia coli* antigens in tobacco seeds and evaluation of gut immunity after oral administration in mouse model. *Journal of veterinary science* **14**, 263–270.
- Roush, D. J. and Lu, Y. (2008) Advances in Primary Recovery: Centrifugation and Membrane Technology. *Biotechnol Progress* **24**, 488–495.
- Rühl, C., Knödler, M., Opdensteinen, P. and Buyel, J. F. (2018) A linear epitope coupled to DsRed provides an affinity ligand for the capture of monoclonal antibodies. *Journal of chromatography* **1571**, 55–64.
- Ruhlman, T., Ahangari, R., Devine, A., Samsam, M. and Daniell, H. (2007) Expression of cholera toxin B-proinsulin fusion protein in lettuce and tobacco chloroplasts--oral administration protects against development of insulinitis in non-obese diabetic mice. *Plant biotechnology journal* **5**, 495–510.
- Ruhlman, T., Verma, D., Samson, N. and Daniell, H. (2010) The role of heterologous chloroplast sequence elements in transgene integration and expression. *Plant physiology* **152**, 2088–2104.

- Sainsbury, F., Thuenemann, E. C. and Lomonossoff, G. P. (2009) pEAQ: versatile expression vectors for easy and quick transient expression of heterologous proteins in plants. *Plant biotechnology journal* **7**, 682–693.
- Salgado, J. V., Goes, M. A. and Salgado Filho, N. (2021) FGF21 and Chronic Kidney Disease. *Metabolism: clinical and experimental* **118**, 154738.
- Sanyal, A., Charles, E. D., Neuschwander-Tetri, B. A., Loomba, R., Harrison, S. A., Abdelmalek, M. F., Lawitz, E. J., Halegoua-DeMarzio, D., Kundu, S., Noviello, S., Luo, Y. and Christian, R. (2019) Pegbelfermin (BMS-986036), a PEGylated fibroblast growth factor 21 analogue, in patients with non-alcoholic steatohepatitis: a randomised, double-blind, placebo-controlled, phase 2a trial. *Lancet (London, England)* **392**, 2705–2717.
- Schaller, A. and Ryan, C. A. (1994) Identification of a 50-kDa systemin-binding protein in tomato plasma membranes having Kex2p-like properties. *Proceedings of the National Academy of Sciences of the United States of America* **91**, 11802–11806.
- Seidah, N. G. and Chrétien, M. (1999) Proprotein and prohormone convertases: a family of subtilases generating diverse bioactive polypeptides. *Brain research* **848**, 45–62.
- Shamloul, M., Trusa, J., Mett, V. and Yusibov, V. (2014) Optimization and utilization of *Agrobacterium*-mediated transient protein production in *Nicotiana*. *Journal of visualized experiments JoVE*.
- Shapiro, J., Sciaky, N., Lee, J., Bosshart, H., Angeletti, R. H. and Bonifacino, J. S. (1997) Localization of endogenous furin in cultured cell lines. *The journal of histochemistry and cytochemistry official journal of the Histochemistry Society* **45**, 3–12.
- Sharma, M., Premkumar, M., Kulkarni, A. V., Kumar, P., Reddy, D. N. and Rao, N. P. (2021) Drugs for Non-alcoholic Steatohepatitis (NASH): Quest for the Holy Grail. *Journal of clinical and translational hepatology* **9**, 40–50.
- Shenoy, V., Kwon, K.-C., Rathinasabapathy, A., Lin, S., Jin, G., Song, C., Shil, P., Nair, A., Qi, Y., Li, Q., Francis, J., Katovich, M. J., Daniell, H. and Raizada, M. K. (2014) Oral delivery of Angiotensin-converting enzyme 2 and Angiotensin-(1-7) bioencapsulated in plant cells attenuates pulmonary hypertension. *Hypertension (Dallas, Tex. 1979)* **64**, 1248–1259.
- Shil, P. K., Kwon, K.-C., Zhu, P., Verma, A., Daniell, H. and Li, Q. (2014) Oral delivery of ACE2/Ang-(1-7) bioencapsulated in plant cells protects against experimental uveitis and autoimmune uveoretinitis. *Molecular therapy the journal of the American Society of Gene Therapy* **22**, 2069–2082.

- Siddiqui, S. A., Sarmiento, C., Truve, E., Lehto, H. and Lehto, K. (2008) Phenotypes and functional effects caused by various viral RNA silencing suppressors in transgenic *Nicotiana benthamiana* and *N. tabacum*. *Molecular plant-microbe interactions MPMI* **21**, 178–187.
- Silva, M. J., Eekhoff, J. D., Patel, T., Kenney-Hunt, J. P., Brodt, M. D., Steger-May, K., Scheller, E. L. and Cheverud, J. M. (2019) Effects of High-Fat Diet and Body Mass on Bone Morphology and Mechanical Properties in 1100 Advanced Intercross Mice. *Journal of bone and mineral research the official journal of the American Society for Bone and Mineral Research* **34**, 711–725.
- Singhal, G., Kumar, G., Chan, S., Fisher, F. M., Ma, Y., Vardeh, H. G., Nasser, I. A., Flier, J. S. and Maratos-Flier, E. (2018) Deficiency of fibroblast growth factor 21 (FGF21) promotes hepatocellular carcinoma (HCC) in mice on a long term obesogenic diet. *Molecular metabolism* **13**, 56–66.
- Sonoda, J., Chen, M. Z. and Baruch, A. (2017) FGF21-receptor agonists: an emerging therapeutic class for obesity-related diseases. *Hormone molecular biology and clinical investigation* **30**.
- Staiger, H., Keuper, M., Berti, L., Hrabe de Angelis, M. and Häring, H.-U. (2017) Fibroblast Growth Factor 21-Metabolic Role in Mice and Men. *Endocrine reviews* **38**, 468–488.
- Steere, A. N., Byrne, S. L., Chasteen, N. D. and Mason, A. B. (2012) Kinetics of iron release from transferrin bound to the transferrin receptor at endosomal pH. *Biochimica et biophysica acta* **1820**, 326–333.
- Steiner, D. F. (1998) The proprotein convertases. *Current opinion in chemical biology* **2**, 31–39.
- Steinlein, L. M., Graf, T. N. and Ikeda, R. A. (1995) Production and purification of N-terminal half-transferrin in *Pichia pastoris*. *Protein expression and purification* **6**, 619–624.
- Stoger, E., Fischer, R., Moloney, M. and Ma, J. K.-C. (2014) Plant molecular pharming for the treatment of chronic and infectious diseases. *Annual review of plant biology* **65**, 743–768.
- Su, J., Sherman, A., Doerfler, P. A., Byrne, B. J., Herzog, R. W. and Daniell, H. (2015a) Oral delivery of Acid Alpha Glucosidase epitopes expressed in plant chloroplasts suppresses antibody formation in treatment of Pompe mice. *Plant biotechnology journal* **13**, 1023–1032.
- Su, J., Zhu, L., Sherman, A., Wang, X., Lin, S., Kamesh, A., Norikane, J. H., Streatfield, S. J., Herzog, R. W. and Daniell, H. (2015b) Low cost industrial production of coagulation factor IX bioencapsulated in lettuce cells for oral tolerance induction in hemophilia B. *Biomaterials* **70**, 84–93.

Sun, L., Ghosh, I., Paulus, H. and Xu, M. Q. (2001) Protein trans-splicing to produce herbicide-resistant acetolactate synthase. *Applied and environmental microbiology* **67**, 1025–1029.

Suzuki, A. and Diehl, A. M. (2017) Nonalcoholic Steatohepatitis. *Annual review of medicine* **68**, 85–98.

Suzuki, M., Uehara, Y., Motomura-Matsuzaka, K., Oki, J., Koyama, Y., Kimura, M., Asada, M., Komi-Kuramochi, A., Oka, S. and Imamura, T. (2008) betaKlotho is required for fibroblast growth factor (FGF) 21 signaling through FGF receptor (FGFR) 1c and FGFR3c. *Molecular endocrinology (Baltimore, Md.)* **22**, 1006–1014.

Szczepańska, E. and Gietka-Czernel, M. (2022) FGF21: A Novel Regulator of Glucose and Lipid Metabolism and Whole-Body Energy Balance. *Hormone and metabolic research = Hormon- und Stoffwechselforschung = Hormones et métabolisme* **54**, 203–211.

Talukdar, S., Zhou, Y., Li, D., Rossulek, M., Dong, J., Somayaji, V., Weng, Y., Clark, R., Lanba, A., Owen, B. M., Brenner, M. B., Trimmer, J. K., Gropp, K. E., Chabot, J. R., Erion, D. M., Rolph, T. P., Goodwin, B. and Calle, R. A. (2016) A Long-Acting FGF21 Molecule, PF-05231023, Decreases Body Weight and Improves Lipid Profile in Non-human Primates and Type 2 Diabetic Subjects. *Cell metabolism* **23**, 427–440.

Tanaka, N., Takahashi, S., Zhang, Y., Krausz, K. W., Smith, P. B., Patterson, A. D. and Gonzalez, F. J. (2015) Role of fibroblast growth factor 21 in the early stage of NASH induced by methionine- and choline-deficient diet. *Biochimica et biophysica acta* **1852**, 1242–1252.

Taverner, A., MacKay, J., Laurent, F., Hunter, T., Liu, K., Mangat, K., Song, L., Seto, E., Postlethwaite, S., Alam, A., Chandalia, A., Seung, M., Saberi, M., Feng, W. and Mrsny, R. J. (2020) Cholix protein domain I functions as a carrier element for efficient apical to basal epithelial transcytosis. *Tissue barriers* **8**, 1710429.

Thevis, M., Loo, R. R. O. and Loo, J. A. (2003) Mass spectrometric characterization of transferrins and their fragments derived by reduction of disulfide bonds. *Journal of the American Society for Mass Spectrometry* **14**, 635–647.

Tokuhara, D., Yuki, Y., Nochi, T., Kodama, T., Mejima, M., Kurokawa, S., Takahashi, Y., Nanno, M., Nakanishi, U., Takaiwa, F., Honda, T. and Kiyono, H. (2010) Secretory IgA-mediated protection against *V. cholerae* and heat-labile enterotoxin-producing enterotoxigenic *Escherichia coli* by rice-based vaccine. *Proceedings of the National Academy of Sciences of the United States of America* **107**, 8794–8799.

- Tusé, D., Tu, T. and McDonald, K. A. (2014) Manufacturing economics of plant-made biologics: case studies in therapeutic and industrial enzymes. *BioMed research international* **2014**, 256135.
- Verma, D., Moghimi, B., LoDuca, P. A., Singh, H. D., Hoffman, B. E., Herzog, R. W. and Daniell, H. (2010) Oral delivery of bioencapsulated coagulation factor IX prevents inhibitor formation and fatal anaphylaxis in hemophilia B mice. *Proceedings of the National Academy of Sciences of the United States of America* **107**, 7101–7106.
- Verwoerd, T. C., Dekker, B. M. and Hoekema, A. (1989) A small-scale procedure for the rapid isolation of plant RNAs. *Nucleic acids research* **17**, 2362.
- Verzijl, C. R. C., Van De Peppel, Ivo P, Struik, D. and Jonker, J. W. (2020) Pegbelfermin (BMS-986036): an investigational PEGylated fibroblast growth factor 21 analogue for the treatment of nonalcoholic steatohepatitis. *Expert opinion on investigational drugs* **29**, 125–133.
- Voinnet, O., Pinto, Y. M. and Baulcombe, D. C. (1999) Suppression of gene silencing: a general strategy used by diverse DNA and RNA viruses of plants. *Proceedings of the National Academy of Sciences of the United States of America* **96**, 14147–14152.
- Wally, J., Halbrooks, P. J., Vonnrhein, C., Rould, M. A., Everse, S. J., Mason, A. B. and Buchanan, S. K. (2006) The crystal structure of iron-free human serum transferrin provides insight into inter-lobe communication and receptor binding. *The Journal of biological chemistry* **281**, 24934–24944.
- Wang, C., Hennessey, J. A., Kirkton, R. D., Wang, C., Graham, V., Puranam, R. S., Rosenberg, P. B., Bursac, N. and Pitt, G. S. (2011a) Fibroblast growth factor homologous factor 13 regulates Na⁺ channels and conduction velocity in murine hearts. *Circulation research* **109**, 775–782.
- Wang, W., Tai, F. and Chen, S. (2008) Optimizing protein extraction from plant tissues for enhanced proteomics analysis. *Journal of separation science* **31**, 2032–2039.
- Wang, X., Su, J., Sherman, A., Rogers, G. L., Liao, G., Hoffman, B. E., Leong, K. W., Terhorst, C., Daniell, H. and Herzog, R. W. (2015) Plant-based oral tolerance to hemophilia therapy employs a complex immune regulatory response including LAP⁺CD4⁺ T cells. *Blood* **125**, 2418–2427.
- Wang, Y., Chen, Y.-S., Zaro, J. L. and Shen, W.-C. (2011b) Receptor-mediated activation of a proinsulin-transferrin fusion protein in hepatoma cells. *Journal of controlled release official journal of the Controlled Release Society* **155**, 386–392.

- Wang, Y., Shao, J., Zaro, J. L. and Shen, W.-C. (2014a) Proinsulin-transferrin fusion protein as a novel long-acting insulin analog for the inhibition of hepatic glucose production. *Diabetes* **63**, 1779–1788.
- Wang, Y., Wei, Z., Fan, J., Song, X. and Xing, S. (2023) Hyper-expression of GFP-fused active hFGF21 in tobacco chloroplasts. *Protein expression and purification* **208-209**, 106271.
- Wei, W., Dutchak, P. A., Wang, X., Ding, X., Wang, X., Bookout, A. L., Goetz, R., Mohammadi, M., Gerard, R. D., Dechow, P. C., Mangelsdorf, D. J., Kliewer, S. A. and Wan, Y. (2012) Fibroblast growth factor 21 promotes bone loss by potentiating the effects of peroxisome proliferator-activated receptor γ . *Proceedings of the National Academy of Sciences of the United States of America* **109**, 3143–3148.
- Weichert, N., Hauptmann, V., Helmold, C. and Conrad, U. (2016) Seed-Specific Expression of Spider Silk Protein Multimers Causes Long-Term Stability. *Frontiers in plant science* **7**, 6.
- Wente, W., Efanov, A. M., Brenner, M., Kharitonov, A., Köster, A., Sandusky, G. E., Sewing, S., Treinies, I., Zitzer, H. and Gromada, J. (2006) Fibroblast growth factor-21 improves pancreatic beta-cell function and survival by activation of extracellular signal-regulated kinase 1/2 and Akt signaling pathways. *Diabetes* **55**, 2470–2478.
- Wessling-Resnick, M. (2018) Crossing the Iron Gate: Why and How Transferrin Receptors Mediate Viral Entry. *Annual review of nutrition* **38**, 431–458.
- Widera, A., Norouziyan, F. and Shen, W.-C. (2003) Mechanisms of TfR-mediated transcytosis and sorting in epithelial cells and applications toward drug delivery. *Advanced drug delivery reviews* **55**, 1439–1466.
- Wilbers, R. H. P., Westerhof, L. B., van Raaij, D. R., van Adrichem, M., Prakasa, A. D., Lozano-Torres, J. L., Bakker, J., Smant, G. and Schots, A. (2016) Co-expression of the protease furin in *Nicotiana benthamiana* leads to efficient processing of latent transforming growth factor- β 1 into a biologically active protein. *Plant biotechnology journal* **14**, 1695–1704.
- Wilken, L. R. and Nikolov, Z. L. (2012) Recovery and purification of plant-made recombinant proteins. *Biotechnology advances* **30**, 419–433.
- Wingfield, P. (2001) Protein precipitation using ammonium sulfate. *Current protocols in protein science* **Appendix 3**, Appendix 3F.
- Woo, Y. C., Xu, A., Wang, Y. and Lam, K. S. L. (2013) Fibroblast growth factor 21 as an emerging metabolic regulator: clinical perspectives. *Clinical endocrinology* **78**, 489–496.

- Xiao, Y., Kwon, K.-C., Hoffman, B. E., Kamesh, A., Jones, N. T., Herzog, R. W. and Daniell, H. (2016) Low cost delivery of proteins bioencapsulated in plant cells to human non-immune or immune modulatory cells. *Biomaterials* **80**, 68–79.
- Xie, T. and Leung, P. S. (2017) Fibroblast growth factor 21: a regulator of metabolic disease and health span. *American journal of physiology. Endocrinology and metabolism* **313**, E292–302.
- Xin, P., Xu, X., Deng, C., Liu, S., Wang, Y., Zhou, X., Ma, H., Wei, D. and Sun, S. (2020) The role of JAK/STAT signaling pathway and its inhibitors in diseases. *International immunopharmacology* **80**, 106210.
- Xu, J., Lloyd, D. J., Hale, C., Stanislaus, S., Chen, M., Sivits, G., Vonderfecht, S., Hecht, R., Li, Y.-S., Lindberg, R. A., Chen, J.-L., Jung, D. Y., Zhang, Z., Ko, H.-J., Kim, J. K. and Véniant, M. M. (2009) Fibroblast growth factor 21 reverses hepatic steatosis, increases energy expenditure, and improves insulin sensitivity in diet-induced obese mice. *Diabetes* **58**, 250–259.
- Yamamoto, T., Hoshikawa, K., Ezura, K., Okazawa, R., Fujita, S., Takaoka, M., Mason, H. S., Ezura, H. and Miura, K. (2018) Improvement of the transient expression system for production of recombinant proteins in plants. *Scientific reports* **8**, 4755.
- Yan, M., Dongmei, B., Jingjing, Z., Xiaobao, J., Jie, W., Yan, W. and Jiayong, Z. (2017) Antitumor activities of Liver-targeting peptide modified Recombinant human Endostatin in BALB/c-nu mice with Hepatocellular carcinoma. *Scientific reports* **7**, 14074.
- Yang, S.-J., Carter, S. A., Cole, A. B., Cheng, N.-H. and Nelson, R. S. (2004) A natural variant of a host RNA-dependent RNA polymerase is associated with increased susceptibility to viruses by *Nicotiana benthamiana*. *Proceedings of the National Academy of Sciences of the United States of America* **101**, 6297–6302.
- Yigzaw, Y., Piper, R., Tran, M. and Shukla, A. A. (2006) Exploitation of the adsorptive properties of depth filters for host cell protein removal during monoclonal antibody purification. *Biotechnology progress* **22**, 288–296.
- Yilmaz, Y., Eren, F., Yonal, O., Kurt, R., Aktas, B., Celikel, C. A., Ozdogan, O., Imeryuz, N., Kalayci, C. and Avsar, E. (2010) Increased serum FGF21 levels in patients with nonalcoholic fatty liver disease. *European journal of clinical investigation* **40**, 887–892.
- Ying, L., Li, N., He, Z., Zeng, X., Nan, Y., Chen, J., Miao, P., Ying, Y., Lin, W., Zhao, X., Lu, L., Chen, M., Cen, W., Guo, T., Li, X., Huang, Z. and Wang, Y. (2019) Fibroblast growth factor 21 Ameliorates diabetes-induced endothelial dysfunction in mouse aorta via activation of the CaMKK2/AMPK α signaling pathway. *Cell death & disease* **10**, 665.

- Yong, J. M., Mantaj, J., Cheng, Y. and Vllasaliu, D. (2019) Delivery of Nanoparticles across the Intestinal Epithelium via the Transferrin Transport Pathway. *Pharmaceutics* **11**.
- Younossi, Z., Tacke, F., Arrese, M., Chander Sharma, B., Mostafa, I., Bugianesi, E., Wai-Sun Wong, V., Yilmaz, Y., George, J., Fan, J. and Vos, M. B. (2019) Global Perspectives on Nonalcoholic Fatty Liver Disease and Nonalcoholic Steatohepatitis. *Hepatology (Baltimore, Md.)* **69**, 2672–2682.
- Younossi, Z. M., Koenig, A. B., Abdelatif, D., Fazel, Y., Henry, L. and Wymer, M. (2016) Global epidemiology of nonalcoholic fatty liver disease-Meta-analytic assessment of prevalence, incidence, and outcomes. *Hepatology (Baltimore, Md.)* **64**, 73–84.
- Yu, Y., Jiang, L., Wang, H., Shen, Z., Cheng, Q., Zhang, P., Wang, J., Wu, Q., Fang, X., Duan, L., Wang, S., Wang, K., An, P., Shao, T., Chung, R. T., Zheng, S., Min, J. and Wang, F. (2020) Hepatic transferrin plays a role in systemic iron homeostasis and liver ferroptosis. *Blood* **136**, 726–739.
- Yuki, Y., Mejima, M., Kurokawa, S., Hiroiwa, T., Takahashi, Y., Tokuhara, D., Nochi, T., Katakai, Y., Kuroda, M., Takeyama, N., Kashima, K., Abe, M., Chen, Y., Nakanishi, U., Masumura, T., Takeuchi, Y., Kozuka-Hata, H., Shibata, H., Oyama, M., Tanaka, K. and Kiyono, H. (2013) Induction of toxin-specific neutralizing immunity by molecularly uniform rice-based oral cholera toxin B subunit vaccine without plant-associated sugar modification. *Plant biotechnology journal* **11**, 799–808.
- Yuki, Y., Nojima, M., Hosono, O., Tanaka, H., Kimura, Y., Satoh, T., Imoto, S., Uematsu, S., Kurokawa, S., Kashima, K., Mejima, M., Nakahashi-Ouchida, R., Uchida, Y., Marui, T., Yoshikawa, N., Nagamura, F., Fujihashi, K. and Kiyono, H. (2021) Oral MucoRice-CTB vaccine for safety and microbiota-dependent immunogenicity in humans: a phase 1 randomised trial. *The Lancet. Microbe* **2**, e429-e440.
- Yun, Y.-R., Won, J. E., Jeon, E., Lee, S., Kang, W., Jo, H., Jang, J.-H., Shin, U. S. and Kim, H.-W. (2010) Fibroblast growth factors: biology, function, and application for tissue regeneration. *Journal of tissue engineering* **2010**, 218142.
- Zeltins, A. (2013) Construction and characterization of virus-like particles: a review. *Molecular biotechnology* **53**, 92–107.
- Zeng, W., Wu, C., Wang, J., Cao, L., Jin, X., Zhu, J. and Lu, X. (2017) Toxicologic evaluations of recombinant liver-targeting interferon IFN-CSP: Genotoxicity and tегenіcratoіty. *Regulatory toxicology and pharmacology RTP* **89**, 13–19.

- Zhang, D., Nandi, S., Bryan, P., Pettit, S., Nguyen, D., Santos, M. A. and Huang, N. (2010) Expression, purification, and characterization of recombinant human transferrin from rice (*Oryza sativa* L.). *Protein expression and purification* **74**, 69–79.
- Zhang, X., Yeung, D. C. Y., Karpisek, M., Stejskal, D., Zhou, Z.-G., Liu, F., Wong, R. L. C., Chow, W.-S., Tso, A. W. K., Lam, K. S. L. and Xu, A. (2008) Serum FGF21 levels are increased in obesity and are independently associated with the metabolic syndrome in humans. *Diabetes* **57**, 1246–1253.
- Zhao, L., Niu, J., Lin, H., Zhao, J., Liu, Y., Song, Z., Xiang, C., Wang, X., Yang, Y., Li, X., Mohammadi, M. and Huang, Z. (2019) Paracrine-endocrine FGF chimeras as potent therapeutics for metabolic diseases. *EBioMedicine* **48**, 462–477.
- Zhen, E. Y., Jin, Z., Ackermann, B. L., Thomas, M. K. and Gutierrez, J. A. (2016) Circulating FGF21 proteolytic processing mediated by fibroblast activation protein. *The Biochemical journal* **473**, 605–614.
- Zimmermann, J., Saalbach, I., Jahn, D., Giersberg, M., Haehnel, S., Wedel, J., Macek, J., Zoufal, K., Glünder, G., Falkenburg, D. and Kipriyanov, S. M. (2009) Antibody expressing pea seeds as fodder for prevention of gastrointestinal parasitic infections in chickens. *BMC biotechnology* **9**, 79.
- Zischewski, J., Sack, M. and Fischer, R. (2016) Overcoming low yields of plant-made antibodies by a protein engineering approach. *Biotechnology journal* **11**, 107–116.
- Zupan, J., Muth, T. R., Draper, O. and Zambryski, P. (2000) The transfer of DNA from *agrobacterium tumefaciens* into plants: a feast of fundamental insights. *The Plant journal for cell and molecular biology* **23**, 11–28.

Acknowledgements

This thesis is dedicated to those who have helped me. Without them, I think I would not have been able to complete this thesis alone. I sincerely thank them.

First of all, I want to thank Prof. Inge Broer for giving me the opportunity to study for a PhD at the Faculty of Agricultural and Environmental Sciences of the University of Rostock and allowing me to have a fixed PhD income to ensure that I can concentrate on my research without any distractions. In particular, I want to thank her for her guidance and great support, scientific input and constructive feedback during my doctoral studies. I also want to thank Dr. Jana Huckauf for her timely help during my doctoral period, which enabled me to successfully complete my doctoral thesis. And I want to thank her for the care, support and encouragement she gave me.

Secondly, I want to thank Prof. Johannes F. Buyel for giving me the opportunity to study in the field of plant molecular agriculture at the Fraunhofer Institute for Molecular Biology and Applied Ecology IME. I want to thank him for his helpful comments, both in group meeting discussions and in the journal publication, which helped me improve my doctoral thesis.

I want to express special thanks and praise to my day-to-day supervisor Dr. Henrik Nausch, who always devotes a lot of time, energy and patience to coaching me. His knowledge and scientific rigor kept my reports, journal, and thesis of high standard. Special thanks to him for always guiding me when I was confused and giving me the motivation to move forward. He also gave me a lot of care, support, and encouragement. Without him, this thesis would not have been completed. I want to express my most sincere thanks to him again!

In addition, I want to thank my FGF21 project partners Prof. Susanne Klaus, Dr. Christopher A Bishop and Nancy Gahner, with whom I enjoyed fruitful discussions. I want like to thank Adjunct Professor Rima Menassa for being the reviser of my 2021 PhD outline and for her helpful suggestions at the PhD Seminar. Another "thank you" goes to PhD coordinator Dr. Birgit Orthen for her very direct proofreading and positive motivation during my PhD, which raised the bar for the Fraunhofer IME PhD program.

Furthermore, I appreciate the huge and comprehensive support of Sonja Konopka and Kerstin Thoss from the University of Rostock for their work in stable transformation, greenhouse and cloning vectors as well as Dirk Scheffler, Jörg Schuphan and Andreas Wagner from the Fraunhofer IME for their support and technical assistance in the lab and in the greenhouse.

Declaration of independence / Eidesstattliche Erklärung

Hiermit erkläre ich durch eigenhändige Unterschrift, die vorliegende Dissertation selbstständig verfasst und keine anderen als die angegebenen Quellen und Hilfsmittel verwendet zu haben. Die aus den Quellen direkt oder indirekt übernommenen Gedanken sind als solche kenntlich gemacht. Die Dissertation ist in dieser Form noch keiner anderen Prüfungsbehörde vorgelegt worden.

Ort, Datum

Curriculum Vitae

Hsuan-Wu Hou, M.Sc.

Date of birth 05.10.1988 in Hsinchu, Taiwan

Experience

- | | |
|-------------------|------------------------------------------------------------------------------------------------------------------------------------------------------------------------------------------------------------------------------------------------------------------------------------------------------------------------------------------------------------------------------------------------------------------------------------------------------------------------------------------------------------------|
| 09/2019 - Today | PhD Student

Fraunhofer-Institut für Molekularbiologie und Angewandte Oekologie IME
Department of Bioprocess Engineering, Germany

- Focus on downstream processing (DSP) of biopharmaceuticals (adaptation non-chromatographic and chromatographic purification methods to remove host cell proteins, such as ÄKTA IMAC, etc.) |
| 07/2018 - 09/2019 | PhD Student

Universität Rostock
Department of Agrobiotechnology, Germany

- Terminate the duration to 07/2018 - 09/2019 (the PhD degree, granted by the Universität Rostock will be added under education)
- Add some key to upstream production (USP) of biopharmaceuticals (design and cloning of expression vectors, establishing expression conditions, etc.) |
| 03/2017 - 03/2018 | Research Assistant

Academia Sinica
Institute of Molecular Biology, Taiwan

- Focus on reprogramming cancer cells through understanding of their metabolic signatures under glucose-/amino acid-deprivation (single cell dynamics, establishing deprivation mediums, etc.) |
| 02/2016 - 02/2017 | Research Assistant

National Chung Hsing University
Institute of Molecular Biology, Taiwan

- Continue master thesis (antibacterial activity of bacteriophage lytic membrane proteins and bacteria identification) |
| 08/2015 - 10/2015 | Visiting Guest

Universität Rostock
Department of Agrobiotechnology, Germany

- Lab match to have a PhD position (experimental support and finishing PhD proposal writing) |
| 09/2011 - 09/2014 | Master Thesis Student

National Chung Hsing University
Institute of Molecular Biology, Taiwan

- Focus on upstream production (USP) and downstream processing (DSP) of bacteriophage lytic membrane proteins in <i>Escherichia coli</i> (design and cloning of expression vectors, establishing expression and purification conditions such as sucrose density gradient fractionation and size-exclusion chromatography and protein-protein interactions and M13 bacteriophage production) |

Education	
2018 - Present	PhD's degree Fraunhofer-Institut für Molekularbiologie und Angewandte Oekologie IME Department of Bioprocess Engineering, Germany Universität Rostock Department of Agrobiotechnology, Germany - Title of Thesis "Comparing Seed-based Stable and Leaf-based Transient Expression for Production of Fibroblast Growth Factor 21-Transferrin fusion protein"
2011 - 2014	Master's degree National Chung Hsing University Institute of Molecular Biology, Taiwan - Title of Thesis "Expression and Functional Characterization of ORF151 (Rz) and ORF106 (Rz1) of <i>Xanthomonas fragariae</i> Bacteriocin"
2007 - 2011	Bachelor's degree Providence University Department of Cosmetic Science, Taiwan - Title of Thesis "Cloning and Expression of Human Elastase"
Course	
10/2021	Good Scientific Practice
05/2021	Living and working in Germany - Intercultural training for international PhD students and researchers
05/2021	Academic Presentation Skills
05/2021	Academic Writing
02/2021	Productivity, Project and Time Management for Scientists
Language	
English	Negotiable
German	Basic communication skills
Mandarin	First language

place, date

List of publications in scientific journals and presentations at conferences

Hsuan-Wu Hou, M.Sc.

Publication

09/2022 **Hou, H.W.**, Bishop, C.A., Huckauf, J., Broer, I., Klaus, S., Nausch, H., Buyel, J.F. (2022).
Seed- and leaf-based expression of FGF21-transferrin fusion proteins for oral delivery and treatment of non-alcoholic steatohepatitis. *Frontiers in Plant Science* 13: 998596; 10.3389/fpls.2022.998596.

Poster presentation

09/2019 **Botanik-Tagung - International Conference of the German Society for Plant Sciences**
Universität Rostock
- Title of Poster " Targeted delivery of FGF21 to the liver *in planta* bioencapsulation"

Conference talk

12/2021 **11th Fraunhofer IME PhD Seminar**
Fraunhofer-Institut für Molekularbiologie und Angewandte Oekologie IME
Department of Bioprocess Engineering, Germany
- Title of Seminar "Comparing seed-based stable and leaf-based transient expression for the production of the FGF21-Transferrin fusion protein"

12/2020 **10th Fraunhofer IME PhD Seminar**
Fraunhofer-Institut für Molekularbiologie und Angewandte Oekologie IME
Department of Bioprocess Engineering, Germany
- Title of Seminar "Transient expression of FGF21-Tf seems to be affected by the stability of the linker region"

11/2019 **9th Fraunhofer IME PhD Seminar**
Fraunhofer-Institut für Molekularbiologie und Angewandte Oekologie IME
Department of Bioprocess Engineering, Germany
- Title of Seminar "Tobacco SL632 as an expression platform using FGF21 and GFP as model proteins"

place, date